The role of the osteoclast during endochondral ossification in a rat fracture model

Michelle Maree McDonald

Submitted for the degree of
Doctor of Philosophy

The Orthopaedic Research and Biotechnology Department, The Children's Hospital Westmead

The University of Technology Sydney

May 2007

orthopaedic research
and biotechnology

Certificate of authorship

I certify that the work in this thesis has not previously been submitted for a degree nor has it been submitted as part of requirements for a degree as fully acknowledged within the text.

I also certify that the thesis has been written by me, any help that I have received in my research work and the preparation of the thesis itself has been acknowledged. In addition, I certify that all information sources and literature used are indicated in the thesis.

Signature of Candidate

Acknowledgements and Dedication

Many people have contributed to this thesis. Principal amongst these is my mentor and co-supervisor Associate Professor David Little, without whom this thesis may never have been completed. His scientific insight, encouragement and commitment to the project have been inspirational. Professor Little has provided extensive support and advice above and beyond that expected of a mentor or supervisor. My gratitude towards Professor Little extends beyond a debt that could ever be repaid. I am extremely thankful for his consistent belief in me. He has instilled in me a desire to continue learning and exploring the world of science that I would have never imagined possible.

I would like to thank my principal supervisor Dr Tamara Sztynda for her patience, support and infinite advice over the past 4 years. Dr Sztynda has motivated me to rise to each challenge I have faced. Her enthusiasm for research is inspiring and her implausible attention to detail has left a great impression on me. Dr Sztynda is a teacher with no boundaries whom I have enjoyed learning from for many years. I aspire to teach others in the future half as well as she does.

The Children's Hospital at Westmead has provided me with all the necessary infrastructure support to complete my experimental work and I am extremenly grateful to the institute.My colleagues here have been a valuable support system; in particular I would like to thank Dr Aaron Schindeler, for his patience and guidance when teaching a typical histologist about the world of cell culture and for instilling some of his extensive knowledge on scientific writing in me. To Dr Negin Amanat, thank you for all your engineering expertise and perserverence when teaching me. To the lab staff, thank you all for your friendly words of support. In particular, I would like to thank Kathy Mikulec and Alyson Morse and Helen Chapman for their extremely competent technical help which allowed me to focus and complete this enormous task. To Rachel Peat for assiting with the completion of this thesis and friendly advice.

The Mechanical Engineering department at Sydney University provided the equipment that allowed me to perform mechanical testing, and the Electron Microscopy unit provided access to microCT equipment for analysis. Staff from the Bone Program at the Garvan Institute, were also instrumental in supporting this work. Finally, the staff at the Institute of Medical and Veterniary Science in Adelaide assisted this work by performing some back scatter electon analysis on my samples.

To my parents, family and friends, I would like to express my gratitude to you all for your eternal belief in me and encouragement to keep at it, even when times got very hard. I finally finished my book and in doing so I've proven my nerd status in the family.

To my fiancé Paul, you are the reason I continue to push myself to climb mountains in life, I know you will always be behind me to catch me if I fall. Thank you for opening my mind and heart to a life of endless possibilities.

Finally, to my two loving grandmothers, Grandma Morris, who passed away in January 2006 and Nan O'Donnell, who passed on in February 2007. I know you will be smiling down on me with the pride and love that only Grandmothers know. Thank you for believing in me, to you both I dedicate this, the first PhD thesis in the families.

Table of contents

List of Illustrations

Abbreviations

ALN	Alendronate
αvβ3	Alpha V beta 3
ANOVA	Analysis of Variance
ATP	Adenosine triphosphate
bFGF	Basic fibroblastic growth factor
BMC	Bone mineral content
BMD	Bone mineral density
BMU	Bone remodelling unit
BP	Bisphosphonate
BPs	Bisphosphonates
BV/TV	Bone volume/ total volume (%)
ClC-7	Chlorine channel - 7
Col X	Collagen type X
CSF-1	Colony stimulating factor-1
CMC	Carboxymethyl cellulose
CTX	C-terminal telopeptide cross-links
DEPC	Diethylpolycarbonate
DEXA	Dual energy X-ray Absorbtiometry
DMSO	Dimethyl sulfoxide
ECM	Extracellular matrix
EDTA	Ethlyenediaminetetra Acetic Acid (disodium salt)
ELISA	Enzyme-linked immunosorbent assay
FBS	Foetal Bovine Serum
FPPS	Farensyl diphosphate synthase

GTP	Guanosine triphosphate
HD	High dose
HS	Heperan sulfate
HSPG	Heperan sulfate proteoglycans
ia/ia	Incisor absent rat
ICTP	Cross-linked carboxyterminal telopeptide of type I collagen
Ihh	Indian hedgehog
IV	Intravenous
KO	Knockout
LD	Low dose
M-CSF	Macrophage colony stimulating factor
µCT	Micro computerised tomography.
Mins	Minutes
MMA	Methylmethacrylate
MMP	Matrix metalloproteinase
MMP-9	Matrix metalloproteinase 9
MMP-13	Matrix metalloproteinase 13
mRNA	Messenger ribonucleic acid
N-BP	Nitrogen containing Bisphosphonate
NLM	Normal littermate
Oc	Osteocalcin
oc/oc	osteosclerotic mouse
OI	Osteogenesis Imperfecta
op/op	osteopetrotic mouse
OPG	Osteoprotegerin

OPN	Osteopontin
OVX	Ovariectomised
PBS	Phosphate buffered saline
P-C-P	Phosphorous-carbon-phosphorous
PCNA	Proliferating cell nuclear antigen
PECAM	Proliferating endothelial cell adhesion marker
PFA	Paraformaldehyde
PLGA	Poly L-lactide-co-glycolide
Ptc	Patched 1
PTH	Parathyroid hormone
PTHrP	Parathyroid hormone related protein
QCT	Quantitative computerised tomography
RANK	Receptor-activator of nuclear factor kappa beta
RANKL	Receptor-activator of nuclear factor kappa beta ligand
RNA	Ribonucleic acid
ROI	Region of Interest
RT	Room temperature
SC	Subcutaneous
SD	Standard deviation
SE	Standard error
Tb.N	Trabecular number
Tb.th	Trabecular thickness
TGFβ	Transforming growth factor beta
tl/tl	Toothless rat
TRAP	Tartrate resistant acid phosphatase

VEGF	Vascular endothelial growth factor
wt/het	wild type / heterozygous
ZA	Zoledronic Acid

Abstract

Bisphosphonates (BPs) are the most common treatment for osteoporosis, due to their powerful ability to inhibit osteoclastic bone resorption. They are also being investigated to augment callus production during fracture healing, however, concerns exist as to the effects of BPs during both initial fracture union and hard callus remodelling. Endochondral ossification during fracture repair is a critical process leading to initial union, and is assumed to be dependent on osteoclast function. Hard callus remodelling, known to be dependent on osteoclast function, is important to the completion of bone repair.

The role of osteoclasts during initial endochondral fracture union was investigated using the BP zoledronic acid (ZA) and in a genetic model of osteoclast inactivity, the incisor absent (*ia/ia)* rat. In addition, the effect of differing ZA treatment regimes on hard callus remodelling was investigated using both Bolus and Weekly ZA dosing. A Bolus of 0.1mg/kg ZA or 5 Weekly doses of 0.02mg/kg ZA or Saline were administered commencing 1 week post surgery in a rat femoral fracture model. Femoral fractures were also produced in *ia/ia* rats. Examinations were performed up to initial union and throughout callus remodelling.

ZA treatment did not alter the rate of endochondral fracture union. All fractures united by 6 weeks, with no difference in the percentage of cartilaginous callus between treatment groups at any time point. Fracture union was achieved by 3 weeks in both *ia/ia* and control rats, again with no difference in the percentage of cartilaginous callus.

In contrast, marked differences in hard callus were evident in the ZA treated groups. ZA increased callus bone mineral content, volume and importantly increased callus strength. Bolus ZA treatment did not delay the commencement of hard callus remodelling at 4 weeks post fracture, whereas this was delayed in the Weekly ZA group. By 12 and 26 weeks Bolus ZA had the same callus content of remodelled neo-cortical bone as Saline, however Weekly ZA had significantly less than saline at these times. These extensive delays in hard callus remodelling with Weekly ZA dosing produced a fracture callus of inferior material properties.

In conclusion, neither ZA treatment nor the absence of active osteoclasts in *ia/ia* rats delayed endochondral fracture union. Thus, this study confirms the redundancy of osteoclasts in this process. Bolus ZA treatment was superior to Weekly ZA dosing; hard callus remodelling proceeded, producing a strong fracture callus with improved material properties. This study supports the use of less frequent ZA doses during fracture repair.

1 Introduction

1.1 Bone Biology

1.1.1 Background

The skeleton requires constant maintenance of its mechanical properties in order to provide the structural framework for the body. This is achieved through continual skeletal remodelling, replacing old bone with new.

Two major bone cells are important as effectors of remodelling, the osteoclast and the osteoblast. Osteoclasts are responsible for resorption of bone matrix whilst osteoblasts synthesise new bone matrix. Remodelling is a highly controlled process with both osteoblast and osteoclast activity closely regulated by a number of factors and signalling pathways. Most of these are provided by the local environment in response to mechanical loading, combined with an overlay of systemic control. In addition, direct communication between osteoclasts and osteoblasts provides a mechanism that maintains the homeostatic balance between bone resorption and formation. It is the uncoupling of these two events that result in pathological bone diseases such as osteoporosis (Cimaz and Biggioggero, 2001).

The osteocyte, being the most abundant cell in mature bone, is thought to be responsible for modulation of remodelling through mechano-chemical transduction mechanisms. Osteocytes arise from osteoblasts that became incorporated within newly laid down matrix and encased within spaces called lacunae. Through cytoplasmic connections via canaliculi in the bone matrix, osteocytes perform intercellular communication in response to mechanical and chemical signals from their surrounding environment in order to modulate bone remodelling and maintain skeletal integrity (Knothe Tate *et al.*, 2004).

Bone formation encompasses three different processes; endochondral ossification, intramembranous ossification and appositional bone formation, which are all essential for skeletal development, growth, maintenance and repair. Endochondral ossification entails bone formation from a template of cartilaginous matrix. Intramembranous ossification entails bone formation through direct transformation of mesenchymal cells into bone forming cells, occurring without a cartilage framework. Lastly, appositional bone formation is the formation of new bone directly onto an existing bone template (Mao and Nah, 2004).

1.2 Development and regulation at the growth plate

Skeletal development commences in foetal development and involves both endochondral and intramembranous ossification. Much of the skeleton including the long bones, are formed primarily through the conversion of cartilage templates into ossified structures. In contrast, flat bones, such as the skull, are formed without a cartilage enlage, utilising intramembranous ossification (Mao and Nah, 2004, Ferretti *et al.*, 2006).

1.2.1 Long bone and physis formation

Endochondral ossification occurs from embryonic long bone formation throughout skeletal maturation until the cessation of growth. Responsible for the origin of foetal long bones, this process is also the source for longitudinal growth. As shown in Figure 1.1 long bones arise from the initial condensation of mesenchymal cells that differentiate into chondrocytes (Kronenberg, 2003). With a matrix rich in collagen type II and proteoglycan, the central chondrocytes hypertrophy and begin to secrete type X collagen. Adjacent perichondral cells differentiate into osteoblasts and form a peripheral bone collar. The hypertrophic chondrocytes attract new blood vessel formation as they mineralise their matrix and then undergo programmed cell death, or apoptosis, allowing development of the primary spongiosa through recruitment of osteoblasts through the intruding vascular supply.

The chondrocytes at either end of this central area of primary spongiosa continue to proliferate and thus lengthen the bone as the bone collar becomes the perichondral or cortical bone shell. The primary spongiosa formed in the metaphysis provides structural support for the cartilage of the growth plate. This primary trabecular bone contains central remnants of the calcified cartilage matrix from the hypertrophic chondrocytes. As it is remodelled into the secondary spongiosa these remnants are removed and the trabecular bone becomes sparser. Finally this secondary spongiosa is resorbed to form the bone marrow cavity, the main site for haematopoiesis in post-natal life.

At either end of the newly formed limb, secondary centres of ossification form through a similar process of chondrocyte hypertrophy, vascularisation and mineralisation. These areas of ossification become the epiphyses of the long bone, separated from the metaphysis and bone marrow cavity by the growth plate or physis (Figure 1.1),(Kronenberg, 2003).

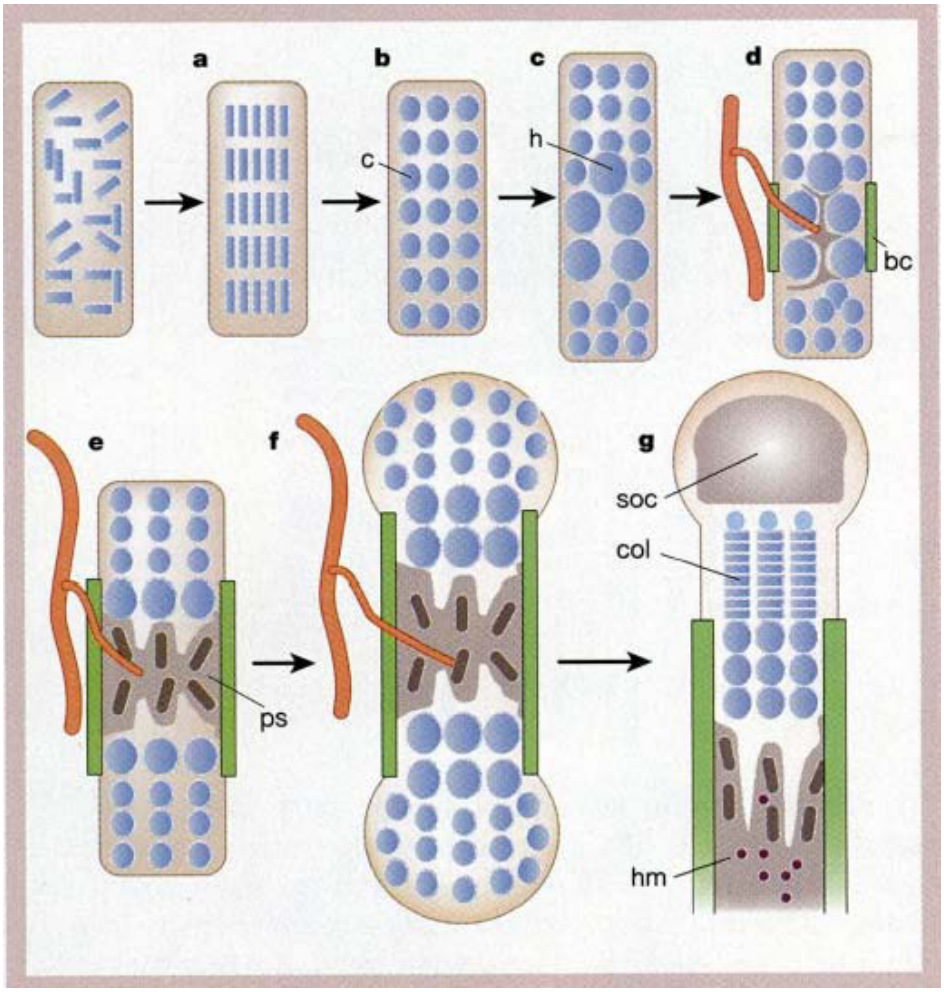

Figure 1.1. *Schematic depiction of the formation of long bones*.
Endochondral bone formation. **a**, Mesenchymal cells condense. **b,** Cells of condensations become chondrocytes (c). **c**, chondrocytes at the centre stop proliferation and become hypertrophic (h). **d,** Perichondral cells adjacent to (h) chondrocytes become osteoblasts, forming bone collar (bc). Hypertrophic chondrocytes direct the formation of mineralised matrix, attract blood vessels, and undergo apoptosis. **e**, Osteoblasts of primary spongiosa accompany vascular invasion, forming the primary spongiosa (ps). **f**, chondrocytes continue to proliferate, lengthening the bone. Osteoblasts of primary spongiosa are precursors of eventual trabecular bone; osteoblasts of bone collar become cortical bone. **g**, At the end of the bone, the secondary ossification centre (soc) forms. The growth plate below the soc forms orderly columns of proliferating chondrocytes (col). Haematopoietic marrow (hm) expands in marrow. Reproduced with permission of Nature Publishing Group (Kronenberg, 2003).

1.2.2 Chondrocyte development and maturation

The growth plate, or physis, consists entirely of cartilage and lies between the metaphysis and epiphysis of growing long bones. Three principal layers of cartilage cells (chondrocytes) exist at the growth plate; the resting zone, just under the epiphysis, followed by the proliferative and then the hypertrophic zones. Each different layer of chondrocytes is a direct product of the differentiation of chondrocytes from the previous layer. Chondrocytes of the resting zone are irregularly scattered in a bed of

proteoglycan matrix, whereas chondrocytes in both the proliferating and hypertrophic zones lie in this matrix in longitudinal columns parallel to the growth axis (Figure 1.2). Resting zone chondrocytes are round, periarticular cells with a matrix rich in type II collagen and have been reported to serve as stem-like cells in the growth plate, coordinating the columnar organisation of the lower zones. They are also documented to inhibit differentiation of proliferating chondrocytes into hypertrophic chondrocytes (Abad *et al.*, 2002).

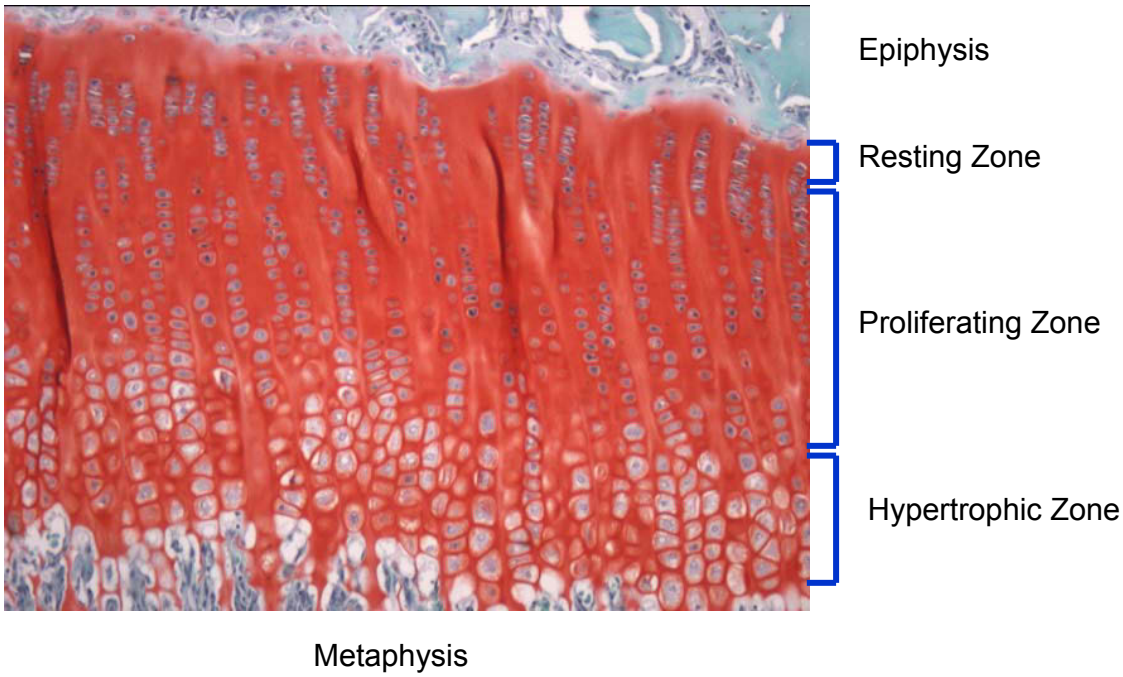

Figure 1.2 *Histological image of a mammalian growth plate, author's image.*
The three zones of chondrocytes within the growth plate include the resting zone, proliferating zone and the hypertrophic zone. These lie between the epiphysis and metaphysis of growing long bones. Staining with, Saffranin O, light green and haematoxylin shows the cartilage as red, the bone green and marrow cells purple. Original magnification x10.

The proliferating chondrocytes, with a matrix rich in type II collagen, demonstrate a flat yet columnar morphology and exhibit clearly defined polarity. They proliferate, forming the orderly columns that are particularly important in the directional lengthening of long bones (Wallis, 1996).

Finally, hypertrophic chondrocytes are a product of the ceased proliferation in the previous zone and their terminal differentiation. These cells no longer proliferate, and begin to enlarge; contributing to the longitudinal growth process. The hypertrophic chondrocyte matrix is now constituted mainly of type X collagen instead of type II. This alteration in matrix collagen permits mineralisation towards the end of the hypertrophic zone. The longitudinal septa between the chondrocytes mineralises whilst the transverse septae remain un-mineralised (Figure 1.3). Apoptosis of these terminal

cells occurs in concert with vascularisation following degradation of the transverse septae, creating a path for infiltrating bone forming cells which lay down new bone on the calcified cartilage template to form the primary spongiosa (Abad *et al.*, 2002).

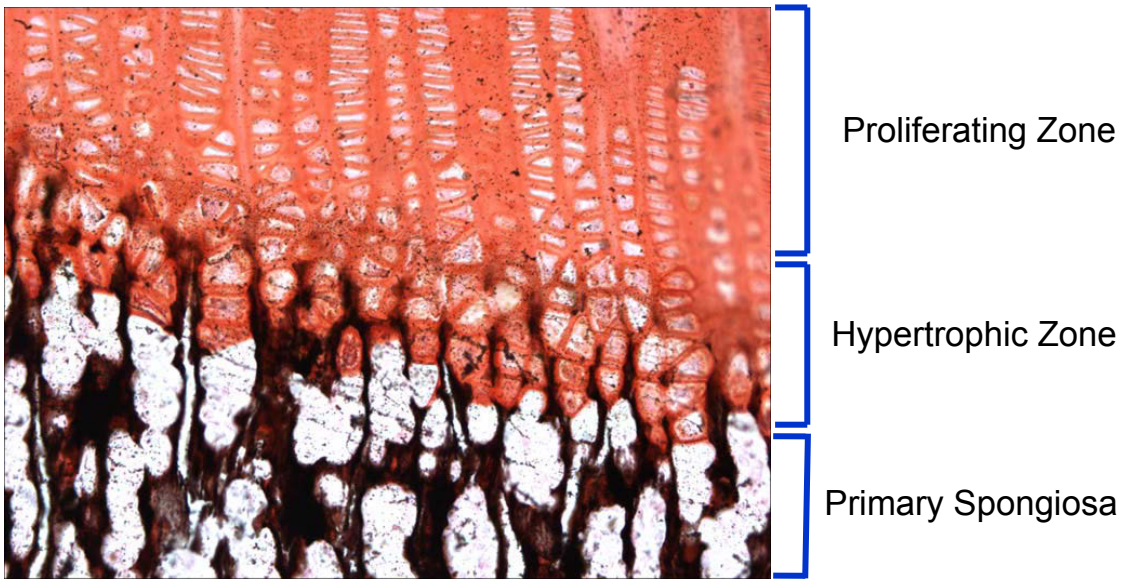

Figure 1.3 *Histology image of a mammalian growth plate demonstrating mineralisation of cartilage septa*, *author's image*
A section of growth plate showing the hypertrophic chondrocyte zones mineralised matrix and subsequent metaphyseal bone formation. Von Kossa, Saffranin O stain, showing cartilage as red and mineral deposition as black. Note the longitudinal septa of the hypertrophic chondrocytes are mineralised and the transverse septa remain un-mineralised. Original magnification x 10.

1.2.3 Paracrine regulation of the growth plate

Knowledge of the regulation of this highly complex and orderly process has lead to the understanding of how the discrete boundaries exist between the cell populations. Two major regulatory proteins have been described, parathyroid hormone related protein (PTHrP) and indian hedgehog (Ihh) (Juppner, 2000). PTHrP is produced in cells of the perichondrium and the periarticular or resting zone, the receptors for which are situated on proliferating chondrocytes where PTHrP acts to keep them in the proliferative pool (Kronenberg *et al.*, 1998). Mice deficient in PTHrP and or PTH/PTHrP receptor develop skeletal deformities due to reduced chondrocyte proliferation and subsequent premature differentiation of proliferative chondrocytes into hypertrophic cells, shortening the columnar proliferative zone of the growth plate (Kobayashi *et al.*, 2002). On the other hand, an increase in PTHrP signalling results in lengthening of the columnar proliferating zone (Wang *et al.*, 1993). PTHrP is therefore suggested to be a negative regulator in the switch from proliferative to pre-hypertrophic chondrocytes.

Indian hedgehog (Ihh) is a protein that has been located within the zone of transition from pre-hypertrophic to hypertrophic chondrocytes (Chung *et al.*, 2001). Over expression of the gene encoding Ihh results in growth plates that completely lack a hypertrophic zone and which continue as cartilaginous tissue without mineralisation and subsequent bone formation (Vortkamp *et al.*, 1996). Chondrocytes in mice over expressing the Ihh gene do not produce the type X collagen rich matrix, providing further evidence of reduced chondrocyte hypertrophy. The proliferating zone therefore persists in these growth plates suggesting that the Ihh protein blocks the transition to a hypertrophic state. Mice deficient in Ihh protein show an increase in hypertrophic chondrocytes due to their premature departure from the proliferating pool, as a result these mice also lack growth plate PTHrP protein expression (Kronenberg, 2003).

An additional interesting property of the protein Ihh is its control over osteoblast differentiation during endochondral bone development. Through binding to its receptor Patched-1 (Ptc) on perichondral cells it stimulates their differentiation into osteoblasts who produce the bone collar (St Jacques *et al.*, 1999). This transformation always occurs in the bone collar adjacent to the Ihh protein producing pre-hypertrophic zone of the growth cartilage. It has been suggested that the perichondrium is both the target of Ihh secretion and thus regulation of chondrocyte differentiation. Since the perichondral cell protein Ptc responds strongly to this protein in the region adjacent to the Ihh expressing chondrocyte zone, it is assumed it plays a role in the negative feedback loop between Ihh protein and PTHrP at the periarticular region (Vortkamp *et al.*, 1996).

The diagram in Figure 1.4 clearly explains the paracrine regulation of growth plate chondrocyte proliferation and hypertrophy (Kronenberg, 2003). Cells that are committed to hypertrophy, i.e. pre-hypertrophic, produce the protein Ihh, sending a signal to the perichondrium and up to the resting cartilage to increase PTHrP production. The PTHrP activates receptors in the proliferative zone, maintaining cellular proliferation and delaying their differentiation. As these cells progress further from the PTHrP rich resting zone they are able to differentiate into pre-hypertrophic chondrocytes and then hypertrophic chondrocytes. Once hypertrophic, these chondrocytes no longer produce Ihh protein therefore induce a negative effect on further chondrocyte proliferation through PTHrP (Wallis, 1996, Stevens and Williams, 1999).

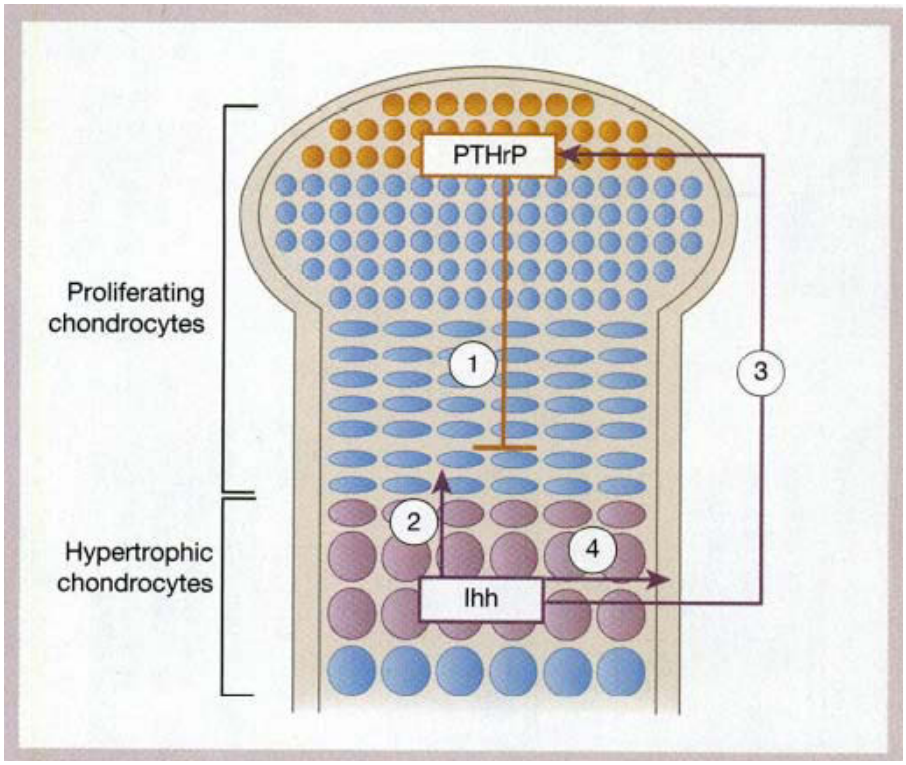

Figure 1.4 *Schematic representation of paracrine regulation of growth plate cartilage maturation.*
Indian hedgehog (Ihh)/parathyroid hormone related protein (PTHrP) negative-feedback loop. PTHrP is secreted from perichondral cells and chondrocytes at the ends of long bones (1). PTHrP acts on receptors on proliferation chondrocytes to keep the chondrocytes proliferating and, thereby, to delay the production of Ihh. When the source of PTHrP production is sufficiently distant, then Ihh is produced. The Ihh acts on its receptor on chondrocytes to increase the rate of proliferation (2) and, through a poorly understood mechanism, stimulate the production of PTHrP at the ends of bones (3). Ihh also acts on perichondral cells to convert these cells into osteoblasts of the bone collar (4).
Reproduced with permission from (Kronenberg, 2003).

1.2.4 Growth cartilage calcification

Calcification of cartilage matrix is the next coordinated stage in endochondral ossification at the growth plate. As the hypertrophic chondrocytes can no longer divide they increase in size, reducing their extracellular matrix. Type X collagen dominates this extracellular matrix as type II collagen has been progressively degraded, increasing the concentration of proteoglycan aggregates. This altered extracellular matrix is able to mineralise as hypertrophic chondrocytes at the terminal end of the physis take on many osteoblast-like characteristics. These include; increased alkaline phosphatase activity and expression of osteonectin and type I collagen (Alini *et al.*, 1992, Kodama *et al.*, 1993, Kirsch *et al.*, 1997).

Importantly, mineralisation of the hypertrophic chondrocyte matrix only occurs in the longitudinal septa of the cartilage matrix whereas the transverse septa remain un-mineralised. Thus, as the terminal chondrocytes die by programmed cell death the

transverse septa are degraded by cells of the ingrowing blood vessels. The longitudinal calcified remnants of the longitudinal septa remain as a scaffold for new bone formation by infiltrating osteoblasts (Roach and Clarke, 1999). This newly formed bone is referred to as the primary spongiosa of the metaphysis. Trabecular bone contained within this primary spongiosa consists of mineralised chondral remnants covered by woven bone laid down by osteoblasts. Subsequent removal of this primary bone occurs by invading osteoclasts, either remodelling it into more lamellar type bone, called secondary spongiosa, or simply removing it altogether to form the bone marrow cavity (Murakami *et al.*, 1994).

It is the crucial stage of cartilage matrix resorption, and its invasion by vessels that is not completely understood and therefore requires further investigation. Although numerous cell types have been suggested to be involved in this process, these associations are based mainly on observations that these cell types are present at this site of tissue resorption. The cells thought to be associated with this process include: osteoclasts, tartrate resistant acid phosphatase (TRAP) positive mononucleated pre-osteoclasts, vascular endothelial cells and even chondrocytes themselves (Lewinson and Silbermann, 1992, Roach and Clarke, 2000, Deckers *et al.*, 2002, Kawana and Sasaki, 2003, Yamazaki and Sasaki, 2005). However the necessity for the activity of all these cell populations during endochondral ossification has not been confirmed, in particular, the specific role of the osteoclast at the osteochondral junction is ill-defined.

1.2.5 Vascularisation of calcified cartilage

1.2.5.1 Early theories of vascularisation

The importance of the contribution of angiogenesis to the erosion of transverse cartilaginous septa and subsequent progression of endochondral ossification was investigated in detail in the early 1960's (Irving, 1964). Cartilage of the growth plate survives in an avascular environment until metaphyseal blood vessels meet the layer of terminal hypertrophic chondrocytes at the chondro-osseous junction. These vessels have been described as running vertically between the longitudinal bars of calcified cartilage, which form the framework of metaphyseal bone formation. At the site of the most distal transverse intercellular partition of growth cartilage the vessels terminate as sinusoidal like loops (Kirsch *et al.*, 1997). Vascular architectural analysis of the rat growth plate revealed that the microvascular structure involves a progressive division of vessels from the main metaphyseal artery into smaller branches until they terminate in a bulb-like fashion at the transverse septa (Arsenault, 1987). Because these septa remain un-mineralised, they are easily eroded by the invading vascular endothelial

cells, and the adjacent empty chondrocyte lacunae are then entered by the ingrowing vessel. These infiltrated lacunae attract cells of the osteoblast lineage which then proceed to line the mineralised cartilage septa with new bone (Kirsch *et al.*, 1997).

Later in 1967, further investigations of growth plate cartilage resorption concluded that capillaries mediate the resorption of un-mineralised cartilage (Schenk *et al.*, 1967). Mineralised cartilage resorption on the other hand was mediated by what these authors referred to as chondroclasts. Chondroclasts are described by Schenk's group as morphologically identical to osteoclasts and capable of resorption of the mineralised cartilage scaffold. Support for the theory that the transverse cartilaginous septa remains un-mineralised whilst two thirds of the longitudinal septa mineralise completely, also arose from the work of Schenk and his group (Schenk *et al.*, 1968). In addition they suggested that the degree of mineralisation within the longitudinal septal walls increases progressively as the junction between the chondral matrix and the infiltrating ossification is reached.

The fundamental role of neovascularisation in the process of endochondral ossification, without the need for chondroclast resorption was later confirmed. Detailed analysis of the ultrastructure of these vessels revealed that their morphological characteristics allowed them to perform their important roles in metaphyseal bone formation. These specialised vessels were suggested to regulate the size of the hypertrophic chondrocyte zone as they erode un-mineralised transverse septa, creating a path for the progression of metaphyseal osteoprogenitor cells towards the calcified cartilage matrix (Hunter and Arsenault, 1990).

A further investigation aiming to understand the relationship between chondroclasts and invading capillaries during erosion was performed in the rat mandibular condyle. It was recognised through this study that a difference exists between endochondral ossification at this anatomical site to that of the growth plate of long bones (Lewinson and Silbermann, 1992). The entire matrix of the hypertrophic chondrocytes in the mandibular condyle is mineralised, leaving no un-mineralised septa for capillary invasion.

In this case the chondroclast is seen to precede the vascular invasion, engulfing the mineralised matrix and allowing infiltration of osteoprogenitor cells into the evacuated chondrocyte lacunae. It may be possible that this process is similar to that occurring during fracture repair. If this is so then the osteoclast or chondroclast may be essential to the process.

1.2.6 Recent theories - Growth factors and angiogenesis

1.2.6.1 Vascular endothelial growth factor

Recent investigations have unveiled a new understanding of the regulators of angiogenesis in the growth plate. Providing proliferative or inhibitory properties, these regulators are expressed in the different cartilaginous zones of the growth plate (Gerber and Ferrara, 2000). Inactivation of vascular endothelial growth factor (VEGF) in growing mice resulted in almost complete suppression of vascular invasion into the terminal cells and thus an expanded hypertrophic chondrocyte zone. A reduction in chondroclast recruitment was also noted with consequent impairment of trabecular bone formation. Thus the gradient of VEGF found only in the matrix of hypertrophic chondrocytes was proven essential to the directional growth and cartilage invasion of the metaphyseal blood vessels (Mori *et al.*, 1988). Widening of the growth plate due to retarded vascularisation as seen in these VEGF deficient mice, implies that vascular invasion is the switch regulating chondrocyte apoptosis and cartilage removal. Furthermore, a marked increase in the height of the hypertrophic chondrocyte zone and a decrease in vascular infiltration was demonstrated in mice deficient in specific VEGF isoforms (Maes *et al.*, 2002). Thus angiogenesis is a major requirement for normal long bone development and growth. Moreover these mice exhibited a decrease in expression of matrix metalloproteinase 9 (MMP-9), a marker for cartilage resorption, implying decreased degradation of cartilage matrix.

1.2.6.2 Matrix metalloproteinase's (MMPs)

Matrix metalloproteinase's (MMPs) are expressed by chondroclasts, osteoclasts and blood vessel endothelial cells and are capable of cleaving components of the extracellular matrix such as collagen. This is clearly depicted in Figure 1.5 showing the secretion of MMPs into the extra cellular matrix (ECM) by endothelial cells of advancing vessels (Rundhaug, 2003). MMP driven proteolysis of the extracellular matrix allows cellular migration and release of stored signalling molecules such as VEGF and transforming growth factor beta (TGFβ), thus it is essential to the process of vascular invasion.

Matrix metalloproteinase-13 (MMP-13) production during foetal development is potent and specific to hypertrophic chondrocytes during endochondral ossification, suggesting a role in the degradation of type II collagen, a major component of proliferating cartilage. MMP-13 breaks down type II collagen about 6-fold more effectively than both type I and III collagen (Knauper *et al.*, 1996). As MMP-13 is

capable of type II collagen degradation, it therefore acts in the hypertrophic zone to denature the type II collagen of the proliferating chondrocyte matrix to allow for expression of type X collagen matrix in these terminal cells. Type X collagen matrix allows for mineralisation of the cartilage matrix and subsequent vascular invasion (Wu *et al.*, 2002). The denatured type II collagen can then be broken down by invading MMP-9 secreting vascular cells (Yamagiwa *et al.*, 1999). MMP-13 has also been located in osteoblasts, mononuclear bone lining cells and periosteal cells during endochondral ossification. This implies a potential role for MMP-13 in the breaking down of type I collagen in bone extracellular matrix, even though it is less effective here than during type II collagen degradation (Johansson *et al.*, 1997).

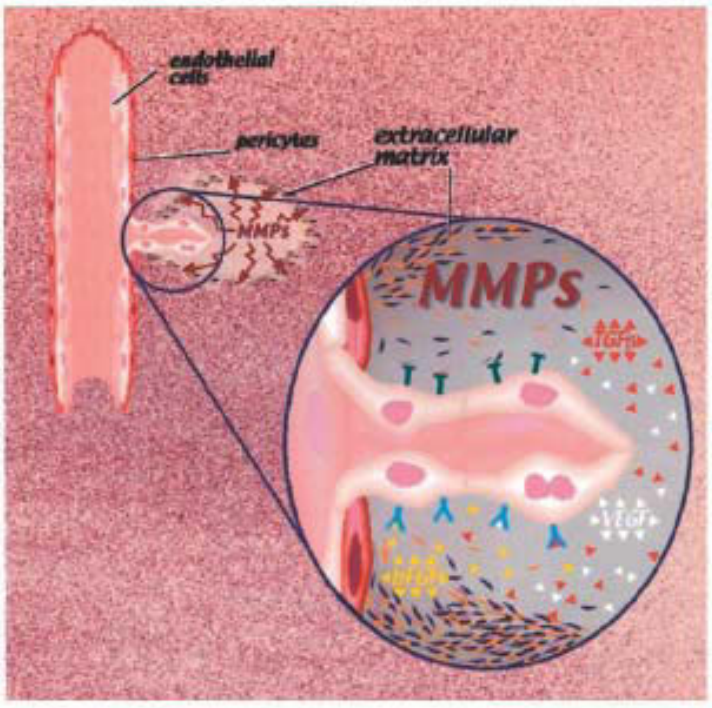

Figure 1.5 *Schematic Diagram of the role of MMPs in angiogenesis*.
Angiogenic factors such as vascular endothelial growth factor (VEGF) and basic fibroblastic growth factor (bFGF) (coloured triangles) secreted by inflammatory cells bond to their respective receptors (Y-shaped receptors) on the surface of endothelial cells. This activates MMP secretion, altered integrin expression and proliferation of the endothelial cells. As MMPs degrade the ECM, additional matrix bound VEGF and bFGF are released. In addition TGFβ and hidden integrin binding sites are exposed, potentiating signalling by the growth factor receptors. TGFβ induces further MMP secretion and is a chemo attractant for inflammatory cells and pericytes. MMPs also facilitate endothelial cell migration by removing by removing adhesion sites and cleaving cell-matrix receptors.
Reproduced with permission from Clinical Cancer Research (Rundhaug, 2003).

MMP-9 or gelatinase B, has highly specific degrading activity for collagens IV, V and XI and denatured type II collagen, and demonstrates specific localisation at sites of active tissue remodelling and neovascularisation (Vu *et al.*, 1998). By generating a mouse model deficient in MMP-9 (MMP-9 null mice) Vu and colleagues provided evidence of its importance in the process of endochondral ossification.

Investigation of the MMP-9 deficiency identified it's specificity in regulating cartilage vascularisation. A delay in endochondral ossification was caused by the lack of MMP-9 in the null mice (Vu *et al.*, 1998). The absence of MMP-9 lead to delayed hypertrophic chondrocyte apoptosis, vascularisation and ossification, thereby leading to abnormal accumulation of hypertrophic chondrocytes. Further, analysis into the angiogenic properties of MMP-9 in this study revealed a direct function in growth plate vascularisation, although it is not yet clear whether its function is to release angiogenic activators or inactivate angiogenic inhibitors (Vu *et al.*, 1998).

Discrete localisation of MMP-9 has been demonstrated at the transverse septum, the border between the last terminal hypertrophic chondrocyte and the invading vessels (Lee *et al.*, 1999). MMP-9 is not only present at this border but also shows high degradative activity. This was demonstrated by the localisation of the proteinase within debris in this region composed of type II collagen fibrils in various stages of digestion. It had been previously shown that MMP-9 is not synthesised by hypertrophic chondrocytes (Lee *et al.*, 1999). Thus the attack on the growth plate by MMP-9 must be launched from outside the cartilage, either from the invading vessels which exhibit high concentrations of MMP-9, or from synthesising endothelial cells. From their work Lee and colleagues (1999) proposed that MMP-9 performs the completion of the type II collagen fibril digestion of the cartilage matrix in the transverse septa. Again, they showed that MMP-9 deficiency only delayed angiogenesis, as it was not completely abrogated, therefore other factors must also be involved in regulating this process.

The theory of MMP-9 regulating the release of extracellular matrix (ECM) angiogenic factors was later supported by a study confirming that MMP-9 specifically regulated proteolysis of un-mineralised cartilage. Through the degradation of the cartilage ECM, MMP-9 triggered the release of VEGF (Engsig *et al.*, 2000). As a chemo attractant for endothelial cells VEGF plays an important role in vascularisation. Through blocking the function of VEGF, the impairment of growth plate invasion seen in MMP-9 null mice is mimicked (Gerber *et al.*, 1999). Further, it was shown that VEGF is also a chemo attractant for osteoclast precursors whilst also exhibiting direct effects on mature osteoclasts. The release of VEGF is important to all stages of endochondral ossification at the growth plate, especially for vascular invasion (Vu *et al.*, 1998, Engsig

et al., 2000, Zhou *et al.*, 2000, Nagai and Aoki, 2002, Lin *et al.*, 2002, Deckers *et al.*, 2002).

Deficiency in either MMP-13 or MMP-9 does not produce permanent changes at the growth plate, with phenotypes resolving by approximately 12 weeks of age in both models (Stickens *et al.*, 2004). These two proteases work in concert to cleave initial fibrillar collagen and then degrade the denature fragments. However, in the absence of one of these proteases, the other clearly compensates, resolving the growth plate phenotype. In the absence of both MMP-9 and MMP-13 on the other hand, the growth plate morphology is dramatically altered. A more severe lengthening and disorganisation of the chondral matrix is evident (Figure 1.6), and is not resolved as seen for the single knock-out models. This suggests a definite synergy between these two proteases in the regulation of endochondral bone formation, highlighting their importance to the process.

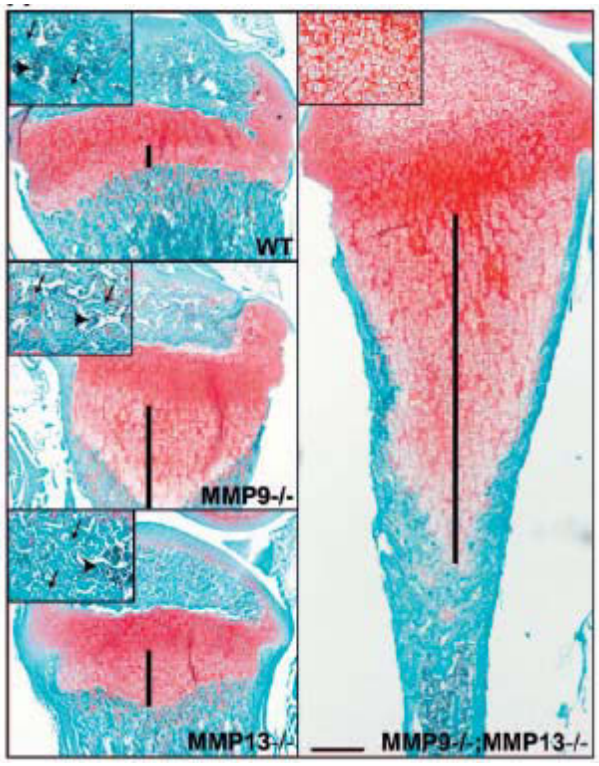

Figure 1.6. *Image of histological section showing the differences in growth plate morphology in WT, MMP-9 KO, MM-13 KO and MMP-9;MMP-13 double KO mice.*
Saffranin O staining of 2-week old tibiae from all genotypes. Increased hypertrophic zones are noted in both MMP-9 and MMP-13 KO samples but a dramatically expanded zone can be observed in the MMP-9;MMP-13 double KO tibia. Length is depicted by the black bars.
Reproduced with permission of the Company of Biologists (Stickens *et al.*, 2004).

1.2.6.3 The current understanding of the activity of osteoclasts and chondroclasts at the chondro-osseous junction

Osteoclastic resorption has commonly been associated with the degradation and removal of chondrocyte matrix during endochondral ossification (Bronckers *et al.*, 2000, Gerstenfeld *et al.*, 2003, Odgren *et al.*, 2003b, Wang *et al.*, 2004b). However the assumption that these resorptive cells are pivotal to this process arises mainly from their localisation at the sites of cartilage removal and their resorptive capabilities. An alternate hypothesis to this was raised by Schenk *et al,* (1967) some time ago by describing a new cell, the chondroclast (Schenk *et al.*, 1967). These cells are of the macrophage lineage and are commonly TRAP positive, so are often described as osteoclasts. But their role may not be in mineralised cartilage resorption as suggested by Schenk and group, but may be more so in the removal of un-mineralised cartilage. One author noted that the TRAP positive chondroclast showed characteristics that differentiated it from the osteoclast (Nordahl *et al.*, 1998). Firstly, the chondroclast is localised closer to the invasion front of the chondro-osseous junction than the osteoclast, suggesting a more pertinent role in cartilage degradation. In addition, where the chondroclast was found adjacent to cartilage matrix, it did not posses the ruffled border and clear zone that are so well known as osteoclastic characteristics. In agreement with this observation, Kawana and colleagues in 2003 demonstrated similar observational findings in osteoprotegerin (OPG) knock-out mice (Kawana and Sasaki, 2003). By removing this negative regulator of osteoclast differentiation, these mice exhibited extensive increased osteoclast and chondroclast populations, which produced an osteoporotic phenotype. The trabecular bone of the primary spongiosa was effectively destroyed in these mice by the increased osteoclast recruitment. This led to active bone formation directly on the growth plate cartilage remnants that remained, which were then rapidly resorbed by osteoclasts. The growth plates in these mice were also damaged as the enhanced chondroclast population invaded the chondral matrix. The morphology of the TRAP positive cells at the forefront of the cartilage infiltration demonstrated no ruffled border formation unlike those TRAP positive cells resorbing bone. Hence it was concluded that although TRAP positive and multi-nucleated, the chondroclasts resorbing the un-mineralised cartilage matrix were actually un-differentiated osteoclasts or pre-osteoclasts.

Nevertheless, since these TRAP positive MMP-9 secreting chondroclasts are in such close proximity to endothelial cells and perivascular cells at the forefront of vascularisation, their role may only be as angiogenic activators, making the endothelial cells the true cell responsible for un-mineralised cartilage resorption (Vu *et al.*, 1998).

1.2.6.4 Elimination of osteoclast/chondroclast activity from the vascularisation of chondral matrix

Recent investigations into mammalian cartilage resorption at the growth plate have been focused on the process of angiogenesis. Interference with vascular infiltration at the chondro-osseous junction disrupts the orderly process of cartilage mineralisation and consequent resorption and replacement by new bone. Although the osteoclast/chondroclast is undoubtedly important to the process of calcified cartilage removal, using new analytical techniques and eliminating the activity of these cells using animal models, recent investigations have revealed that chondroclasts and osteoclasts are not essential to the progression of blood vessel invasion and subsequent bone formation at the chondro-osseous junction (Deckers *et al.*, 2002, Sawae *et al.*, 2003).

Deckers and colleagues in 2002 dissociated angiogenesis and osteoclastogenesis during endochondral ossification using three *in vivo* models of suppressed osteoclastic resorption. One model consisted of treatment of neonatal mice with the drug clodronate. Clodronate is a first generation bisphosphonate (BP) that is metabolised into toxic adenosine triphosphate (ATP) analogues in mitochondria, inducing apoptosis of osteoclasts, thus it demonstrates strong anti-resorptive properties. Complete abolishment of osteoclast function with clodronate treatment, at a dose of 160μM/kg per day for 5 to 7 days, did not affect the process of angiogenesis and subsequent cartilage removal either in primary endochondral ossification of the tail vertebrae or at the growth plates of these neonatal mice. Furthermore, two parallel models of suppressed resorption; osteoclast deficient (c-fos knockout) mice and osteopetrotic (*op/op*) mice also showed a similar phenotype with normal angiogenesis at the growth plate. Both these mouse models exhibit a mutation in stimulating factors required for the production of a macrophage cell colony. Both mouse models completely lack osteoclast and chondroclast populations. Hence, this group concluded that vascular invasion at the chondro-osseous junction during endochondral ossification at the growth plate can occur in the absence of normal osteoclastic function as well as the complete absence of a macrophage cell colony. Through specific analyses it was also proposed that diminished osteoclast activity had no effect on the invasion of the vascular endothelial cells.

A recent study in new born rat femoral growth plates revealed a complete absence of ED-1 (a confirmed antibody marker of monocyte, macrophage lineage cells) positive macrophages and TRAP positive osteoclasts at the erosive front at the chondro-osseous junction (Figure 1.7), (Sawae *et al.*, 2003). Instead these cells were localised

behind this invading front where they were lining type I collagen mineralised bone matrix or remnants of septal cartilage. Those osteoclasts located near cartilage remnants however did not demonstrate ruffled border or clear zone formation, suggesting they are either not actively resorbing or are able to resorb un-mineralised cartilage matrix without this characteristic transformation. The cells at the very front of the erosion were in fact CD-34 positive capillary endothelial cells. CD-34 is a confirmed marker of vascular endothelial cells. It was thereby concluded, through this extensive morphological study, that the first step in cartilage-bone replacement is the degradation of un-mineralised chondrocytic transverse septum by vascular endothelial cells. Once the lacunae are open, invading osteoblasts deposit a thin layer of bone on the remaining mineralised longitudinal septa to form the primary spongiosa. Simultaneously, osteoclasts also invade the region from the metaphyseal side to begin remodelling the primary trabecular bone.

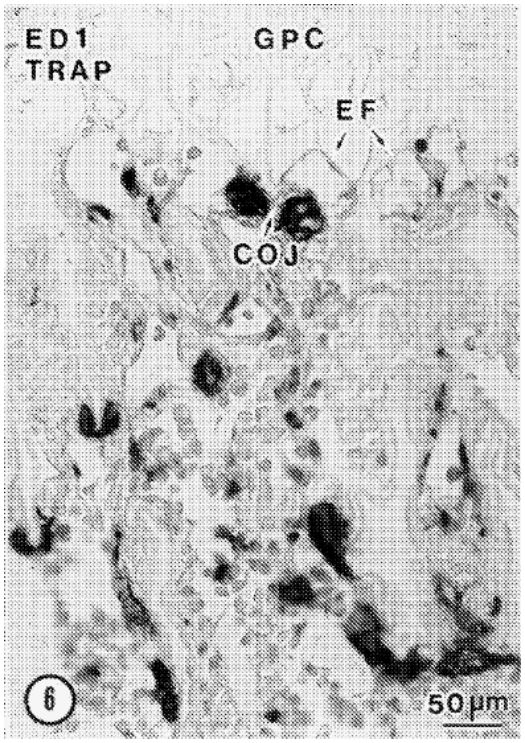

Figure 1.7. *Image of histology section showing localisation of macrophages at the chondro-osseous junction.* Double staining of ED1 and TRAP. ED-1-positive monocytes/macrophages are seen at the chondro-osseous junction (COJ), but they are distant from the erosive front (EF) of the transverse septal cartilage. (GPC) growth plate cartilage. Reproduce by permission of Oxford University Press (Sawae *et al.*, 2003).

As mentioned previously, MMPs are required by endothelial cells to degrade this cartilage matrix; thus the results from the *in vivo* work by Deckers' group, 2002, suggest bisphosphonates (BPs) do not inhibit MMP activity at the doses used. This is in contrast to *in vitro* data that suggests that BPs can reduce MMP-9 activity by 50% at a concentration of around 150µM (Boissier *et al.*, 2000). Approximately 20% of a

subcutaneous dose of clodronate is distributed to bone (Monkkonen *et al.*, 1990), thus from the 160μmol/kg per day dose of clodronate used by Deckers and group, a concentration of approximately 32μmol/kg of clodronate may be reached at the sites of bone formation daily. If no effect of bisphosphonate treatment is seen on the process of cartilage degradation and invasion by vascular endothelial cells at these doses, then clearly MMP activity has not been affected.

It is of great interest to consider the findings of these investigations in relation to the process of endochondral ossification during fracture repair. If osteoclasts are not essential to this process at the growth plate and if the same processes are in fact recapitulated during skeletal repair, then it is reasonable to hypothesise that osteoclasts may also be redundant to endochondral ossification during fracture repair.

1.3 The mechanism of endochondral fracture repair

1.3.1 General overview

The process of fracture repair is a complex series of events that in many ways replicate the processes of bone formation at the growth plate. Fracture repair is initiated by the activation of an inflammatory cell response to the injury of the bone and its surrounding soft tissue. A haematoma develops at the site of injury and released cytokines attract inflammatory cells. The recruitment and proliferation of undifferentiated mesenchymal cells from the surrounding tissue follows, resulting in a cellular blastema which becomes the foundation for the subsequent healing process (Bruder *et al.*, 1994). Inhibition of the initial inflammatory response by treatment with cyclo-oxygenase 2 (Cox-2) inhibitors has been shown to significantly delay the process of repair following blastema formation (Simon *et al.*, 2002).

Mesenchymal cells within the blastema begin to differentiate into immature chondrocytes and proliferate. These new chondrocytes form the fibrocartilaginous callus, often referred to as the soft callus, by laying down the extracellular matrix. This provides stability to the fracture site allowing for the next stages of repair to take place. At the same time periosteally derived mesenchymal cells, directly adjacent to the fracture site, differentiate into osteoblasts and begin to form woven bone matrix, known as intramembranous ossification. Direct appositional bone formation further bolsters the intramembranous external or hard callus (Einhorn, 1998, Einhorn, 2005).

The chondrocytes of the soft callus differentiate into hypertrophic chondrocytes which undergo endochondral ossification in a similar manner to that seen at the growth plate. The chondrocyte matrix is progressively mineralised and infiltrated by blood vessels, creating marrow spaces allowing for new bone formation by osteoblasts on the calcified cartilage scaffold. This adds to the already formed peripheral hard callus

(Bolander, 1992). Extensive remodelling of the woven primary bone callus created through both endochondral and intramembranous ossification, takes place from as soon as the new bone is formed. Osteoclastic resorption has been shown to commence in the periosteal callus as early as 2 weeks post fracture, increasing to a maximum in all areas of callus by 9 weeks in a sheep fracture model (Schell *et al.*, 2006). This resorption is always coupled with new bone formation by osteoblasts, remodelling the woven bone to form a new cortical shell. Concurrently, the old cortex is progressively removed and the site is remodelled until it resembles its original cortical structure (Vortkamp *et al.*, 1998).

These stages of fracture healing are shown in a rodent model by histological sections in Figure 1.8. The blue stained area is the avascular cartilage soft callus that is replaced by red woven bone tissue through endochondral ossification. Remodelling leads to the formation of a new cortex and removal of the old, until the structure resembles the original undamaged site.

Figure 1.8. *Histological sections demonstrating endochondral fracture healing. Author's image*
Alcian blue/picrosirius red stained fracture sections from mammalian samples demonstrate the complete removal of the blue cartilaginous soft tissue, its replacement with red bone tissue and the subsequent remodelling of the bone callus until it resembles its original structure. Original magnification x0.63.

1.3.2 Growth plate processes are recapitulated during fracture healing

1.3.2.1 Paracrine regulation

As the process of endochondral fracture union almost directly imitates that which is observed at the mammalian growth plate, it would be easy to speculate that the genetic signalling and expression of growth factors would also be similar. Analysis of murine fracture models revealed that a similar expression pattern of parathyroid hormone related protein (PTHrP) and indian hedgehog protein (Ihh) was exhibited to that described earlier in the growth plate (Vortkamp *et al.*, 1998). The PTH/PTHrP receptor was robustly localised in the differentiating chondrocytes of the 7 day callus, overlapping with Ihh protein expression. PTH/PTHrP receptors were detected in the less differentiated (proliferative) chondrocyte zone (towards the fibrous centre of the

fracture site). In addition the PTH/PTHrP receptor was localised in the area of ossification at the chondro-osseous junction where invading osteoblasts are forming the primary trabeculae of the primitive hard callus.

During the cartilaginous stage of repair at day 7, type X collagen and Ihh protein were co-localised. This was expected since pre-hypertrophic and hypertrophic chondrocytes during fracture had been shown to produce type X collagen, and that pre-hypertrophic chondrocytes express Ihh at the growth plate (Vortkamp *et al.*, 1998, Murakami and Noda, 2000). The type X collagen localisation was extended to the edge of the cartilaginous callus where there was ossification of hypertrophic chondrocyte matrix, clearly much further from the fracture site than Ihh production was found. During the later phases of fracture repair, when the cartilaginous callus had been removed, neither type X collagen nor Ihh were evident. Taken together, the expression patterns of the PTH/PTHrP receptor and Ihh protein during fracture repair clearly reflects that seen in the metaphysis in developing long bones.

The low level of PTHrP secretion in discrete regions of immature or resting chondrocytes in the fracture callus may be a result of the reduction in Ihh production from the hypertrophic chondrocytes. It could be suggested that this may be a mechanism which in fact differentiates fracture repair from bone development. As mentioned earlier, PTHrP is up regulated in response to increased Ihh signals through the perichondrium (bone collar) of growing long bones. Without this conduction mechanism during fracture repair PTHrP may only be produced in small amounts for a short period of time in the condensed resting chondrocytes. The low level of PTHrP in the zone of proliferative chondrocytes produced a reduced signal which failed to keep the chondrocytes in the proliferative pool, resulting in a larger soft callus composed of hypertrophic chondrocytes. Without the negative feed back loop that is provided by the perichondral bone at the growth plate, there might not be a continuous stimulation of chondrocyte proliferation. The soft callus content of proliferative chondrocytes therefore reduces throughout the repair process. This theory is supported by the fact that the cartilaginous callus is completely removed during fracture healing. Failure of the conduction of Ihh signalling to the resting chondrocytes and subsequent PTHrP up regulation may inhibit further chondrocyte proliferation thus allowing for hypertrophy, ossification and removal of the entire cartilaginous matrix. In order to provide evidence to support this hypothesis the stages of cartilaginous callus removal during fracture repair would require close examination analysis to detect the proliferation of chondrocytes, the cells that manufacture type II collagen instead of type X collagen.

Expression patterns of proliferating cell nuclear antigen (PCNA) in rat femoral fractures confirmed that proliferation of chondrocytes peaked at 7 days post fracture,

with a gradual decrease to day 21. Thus, proliferation of chondrocytes only occurred in the early stages of repair, whilst PTHrP expressing undifferentiated chondrocytes persisted. Without Ihh up regulation of PTHrP, no further proliferation was induced (Huk *et al.*, 2003).

1.3.2.2 Matrix metalloproteinase (MMP) activity

The initial stages of endochondral ossification, namely vascular invasion and degradation of cartilaginous matrix, depend upon the actions of MMPs. At least two MMPs have been shown to be involved in this process at the growth plate; MMP-13 regulates remodelling of the hypertrophic cartilage matrix (Johansson *et al.*, 1997) and MMP-9 regulates chondrocyte apoptosis and angiogenesis (Vu *et al.*, 1998). VEGF, a strong activator of angiogenesis, is activated by MMP-mediated cartilage matrix degradation at the growth plate (Gerber *et al.*, 1999). As the process governed by these proteases and growth factors also must occur during fracture callus endochondral ossification, MMPs and VEGF therefore play an important role during fracture repair.

MMP-13 expression during fracture repair has been restricted to hypertrophic chondrocytes and immature osteoblasts throughout the repair process (Yamagiwa *et al.*, 1999). MMP-13 positive cells were located adjacent to the chondro-osseous junction of the remodelling callus. Further analysis led to the suggestion that due to its enzymatic properties and site specificity during fracture healing, the primary role of MMP-13 was to initiate the cartilage matrix degradation in order to resorb and remodel the soft callus (Yamagiwa *et al.*, 1999). These results were further confirmed by other groups (Uusitalo *et al.*, 2000). With the capacity to cleave type II collagen in cartilage matrix, MMP-13 provides denatured type collagen II fibres that can be further degraded by MMP-9, thus it plays an important role in the process of cartilage degradation at the chondro-osseous junction. Therefore, as expected, endochondral fracture repair in the MMP-13 knockout mice was in fact delayed with increased persistence of cartilage callus at day 14 post fracture. This outcome confirmed the importance of this protease during both endochondral growth and repair (Kosaki *et al.*, 2007).

MMP-9 is secreted throughout the process of skeletal regeneration, in a similar manner to MMP-13 (Colnot *et al.*, 2003). During the inflammatory period of repair, days 3-4 post injury, abundant MMP-9 coding mRNA expression and protein has been demonstrated in mesenchymal and inflammatory cells. Throughout the early stage of the soft (cartilaginous) callus phase, MMP-9 was located in chondro/osteoclasts interposed between the hypertrophic cartilage and the newly forming bone. During the

hard callus phase of days 10-21 post fracture, the cartilaginous callus is replaced by vascularised bony callus. At 14 days MMP-9 positive cells were found within the hypertrophic cartilage callus localised to sites of vascular invasion. Strong MMP-9 expression was noted in osteoclasts that were degrading the new bone matrix during the remodelling phase, post day 14. MMP-9 clearly plays an important role here since it was demonstrated in contained areas throughout the entire repair process.

MMP-9 expression in fracture repair is also similar to that shown during endochondral ossification at the growth plate, as previously discussed (section 1.2.6.2). Discrete localisation of MMP-9 was demonstrated at the border of the chondro-osseous junction, indicating its involvement in the degradation of the un-mineralised transverse septa which allowed for the progression of the all important vascular invasion (Lee *et al.*, 1999).

Consistent with expression analysis of MMP-9 throughout fracture healing, MMP-9 deficient mice displayed compromised fracture healing (Colnot *et al.*, 2003). By day 14 post fracture, the wild type mouse fracture calluses were undergoing degradation of the cartilaginous callus, whereas the MMP-9 deficient mouse fracture calluses showed reduced degradation, with 3 times more cartilaginous callus content than wild-type mice at this stage. This was due to retention of hypertrophic chondrocytes. Normal calluses consisted completely of vascularised bone by day 21, whereas the mutant calluses still exhibited cartilaginous islands. By the remodelling phase at day 28, however, both normal and mutant mouse fracture calluses were composed of bone. The MMP-9 deficient repair defect was therefore eventually reversible, suggesting that other proteases may compensate for the deficiency in the latter stage. Notably, this fracture morphology showed a resemblance to that previously seen at the growth plate, with a significantly expanded growth plate that resolved over time (Vu *et al.*, 1998). The defect in MMP-9 null mice was shown to be limited only to the process of hypertrophic cartilage degradation, as chondrocyte maturity in the fracture callus was not affected. Osteocalcin (Oc), a documented marker of osteogenesis was found to be down regulated in the fracture callus of MMP-9 null mice, revealing that intramembranous ossification was also altered (Colnot *et al.*, 2003).

Although MMP-9 deficient mice showed no defect in chondrocyte maturity in their healing fractures it was postulated that they may exhibit delayed vascularisation (Jamsa *et al.*, 2002). Using immunolocalisation it was shown that very few endothelial cells had accumulated at the periphery of the cartilaginous callus in MMP-9 deficient mice when compared to wild type. This suggested a marked delay in angiogenesis of the cartilaginous callus in the mutant mice. The mechanism behind this delay in

vascular invasion was revealed to be a decrease in the bioavailability of functional VEGF. Although the expression of VEGF was higher in the MMP-9 null mouse callus (higher content of hypertrophic chondrocytes) its bioavailabilty was limited by the reduction in cartilage matrix cleavage and thus activation of VEGF activity. By treating both wild type and MMP-9 deficient mice with exogenous VEGF this theory was validated as the chondrocyte phenotype in the MMP-9 null fracture callus was rescued. The amount of hypertrophic cartilage was reduced and the synthesis of vascularised bone matrix enhanced. Thus, an interaction between MMP-9 and VEGF in the regulation of callus vascularisation and remodelling has been suggested.

1.3.2.3 Angiogenesis

Examination of the microvascular invasion during endochondral fracture repair revealed a morphological understanding of the importance of vascularisation to this process (Mark *et al.*, 2004). Electron microscopic analysis of vascular casts and histological sections throughout endochondral healing clarified the necessity of angiogenesis to fracture healing. At 2 weeks post fracture, blood vessels were shown branching only from the external soft tissue into the inter-cortical region of the fracture defect, terminating at the boundary of the avascular hypertrophic cartilage zone. Three and 4 weeks post fracture specimens showed a similar pattern with vessels from both the external region and the marrow cavity penetrating further into the fracture site, as the avascular cartilage was removed. By 6 weeks post fracture vessels no longer branched from the external soft tissue, instead originated only from the marrow canal, with some vessels crossing the fracture defect.

Finally by 12 weeks post fracture in this study, normal vascularity of the region was demonstrated with numerous marrow canal vessels crossing the fracture sites. Immunohistochemistry demonstrated capillaries lined with laminin positive basement membranes contained endothelial cells adjacent to hypertrophic chondrocyte matrix at the invasion front. Perivascular cells were commonly located near these vessels, participating in the degradation of the chondral matrix. Following the invasion front, precursor like cells differentiated into osteoblasts which proceed to lay down bone matrix on the remaining mineralised chondral matrix. This process is depicted in the schematic drawing created by these authors in Figure 1.9, (Mark *et al.*, 2004). The stimulus for such aggressive vascular infiltration during endochondral repair stems from the expression of VEGF by the hypertrophic chondrocytes. It is important to note that these authors make no mention of the presence of osteoclasts during this process, even excluding them from their explanatory schematic. It is clear these investigators

believe angiogenesis drives the progressive removal of chondral matrix during bone repair.

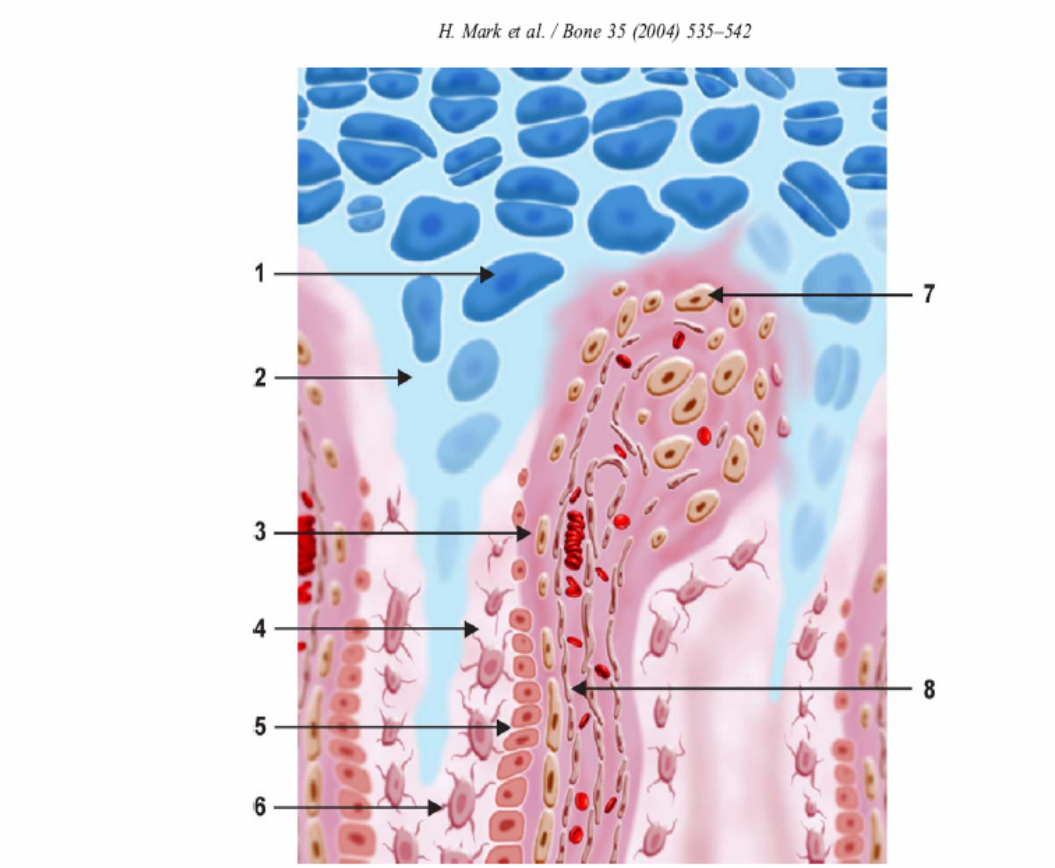

Figure 1.9 *Schematic drawing of vascular invasion during endochondral ossification in healing fractures.* The hypertrophic chondrocytes (1) and mineralised cartilage matrix (2) are formed into cylindrical structures. The endothelial cells (8) form capillary sprouts, here with palisading erythrocytes inside lumen. At the tip of the sprout, perivascular cells (7) are participating in both degradation of the chondroid matrix, and, continuing formation of the capillary sprouts. Behind the tip, precursor-like cells (3) are located seemingly differentiating into active enlarged cells from capillary sprouts that participate in degradation and invasion of the mineralised cartilage matrix. Accompanying precursor and endothelial cells differentiate into osteoblasts that successively replace the cartilage with bone. Adapted with permission from (Mark *et al.*, 2004).

The localisation of VEGF during fracture repair has been shown to have similar temporal and spatial patterns as that described during bone growth. Immunohistochemical localisation in a rat fracture model found VEGF protein in primitive chondroblasts as early as 5 days post fracture, as well as the hypertrophic chondrocytes of the fracture callus (Tatsuyama *et al.*, 2000). Further, more specialised analysis demonstrated strong VEGF expression in the early phase of fracture healing, with a decrease after day 5 post fracture (Pufe *et al.*, 2002). It was concluded that VEGF was stimulated during the initial inflammatory phase of fracture repair in order to initiate fracture healing through stimulation of angiogenesis. Human studies have also shown that large amounts of VEGF are found in the fracture haematoma in the very early stages of fracture repair (Street *et al.*, 2000).

The activity of a soluble, neutralising VEGF receptor (Flt-IgG) was later examined in a model of endochondral bone formation. Inhibition of VEGF in this model resulted in a delay in the vascular invasion and replacement of cartilaginous callus with bone responsible for the transition from soft callus to hard callus (Street *et al.*, 2002). This work also revealed a difference between fracture repair and the growth plate, with the haematoma and inflammatory reaction of the very early stage of fracture repair shown to provide the major source of VEGF. Without this early response and subsequent increased production of VEGF, the angiogenic stimulus would be attenuated and the fracture callus would remain avascular and hypoxic. The role of the haematoma and the inflammatory reaction in this process distinguishes fracture repair from the growth plate, as the stimulus for mesenchymal cell proliferation and differentiation differs between the two sites. Ferguson *et al*. commented on this difference in 1999 when considering the two processes. As described earlier, the process of mesenchymal cell condensation initiates the course of skeletogenesis, with numerous transcription factors and growth factors defining the population of cells acting to establish the cartilaginous template. Whether such a process occurs during the early stage of fracture repair has not been defined. Mesenchymal cells do aggregate at the fracture site but this is primarily in response to growth factors and cytokines produced from the inflammatory haematoma/blastoma. While the origin of these cells has also not yet been identified, the periosteum or the surrounding soft tissue has been implicated, as the removal of each has been shown to delay repair, but not completely prevent it (Park *et al.*, 2002). The subsequent differentiation of the condensed mesenchymal cells into a cartilaginous phenotype is also an undefined process. The succeeding cartilage maturation, mineralisation, vascularisation and removal during fracture repair have been demonstrated to follow those processes at the growth plate (Ferguson *et al.*, 1999).

It is becoming apparent that angiogenesis is a major contributor to skeletal repair (Hausman *et al.*, 2001) as well as for skeletal development (Maes *et al.*, 2002). Rat femoral fractures treated with a potent inhibitor of angiogenesis, TNP-470, were found to have severely impaired healing (Hausman *et al.*, 2001). TNP-470 functions by inhibiting a specific isoform of methionine aminopeptidase, blocking the proliferation of vascular cells *in vitro.* Both intramembranous and endochondral ossification were disturbed by the lack of angiogenesis, as well as a defect in the early formation of fracture blastema. In the early fracture site of treated rats, rather than a normal blastema, a dense fibrous tissue was found, characteristic of fracture non unions that have failed to undergo chondrogenesis. Thus a vascular supply is required in the early stages to provide the required stimulatory growth factors and initiators of

chondrogenesis. Normal formation of periosteal bone adjacent to the fracture gap was missing at day 7 following fracture. In control rats during days 14 to 21, the formed cartilaginous callus began to mature and was replaced by vascularised bone callus. At these time points in treated rats, the fracture site consisted mainly of fibrous tissue with only a few chondrocyte-like cells located near the interfaces with woven bone. Periosteal driven woven bone formation remained minimal at this time.

It was concluded that angiogenesis was important to all stages of fracture repair with even the early inflammatory stage showing impairment with angiogenesis inhibitory treatment (Hausman *et al.*, 2001). It appeared that a cartilaginous callus was replaced by a fibrous callus, prompting the conclusion that angiogenesis in early healing is required for normal formation of chondrogenic callus. Interference with other regulatory bone repair processes such as; growth factors, proteases, anabolic stimuli and resorption, result only in delays of the healing process, not its complete inhibition. Angiogenesis therefore represents a key factor driving fracture repair.

However, it has been shown that angiogenesis and osteoclastogenesis at the growth plate are two dissociated events: without osteoclast activity angiogenesis was able to proceed normally, leaving endochondral ossification at the growth plate undisturbed (Deckers *et al.*, 2002). Since angiogenesis appears to be the main driving force behind fracture healing, it could be reasonably proposed that inhibiting osteoclast activity at the site of fracture repair would have no adverse effects on the process of endochondral repair.

1.3.2.4 Hard callus remodelling requires osteoclastic resorption

Remodelling of the hard callus formed through endochondral fracture union is the final stage in the completion of skeletal repair. Encompassing both osteoclastic resorption and new bone formation by osteoblasts, remodelling is a complex coupled process (Einhorn, 1998). The woven bone that forms the primary hard callus has inferior intrinsic material properties to lamellar bone due to the organisation of it's matrix components (Currey, 2003). Woven bone is often laid down rapidly and contains fine fibred collagen with almost random orientation. In contrast, lamellar bone has a more precise structure and as it is laid down more slowly. The collagen fibres of lamellar bone are in thicker bundles and oriented in a lamellar plane, often with specific direction.

Mineralisation of these two types of bone tissue is also different (Hollinger and Wong, 1996). The membranes of chondrocytes and osteoblasts from woven bone undergo exocytosis to form matrix vesicles. These vesicles accumulate hydroxyapatite crystals, rupturing to release the crystals, which coalesce with adjacent vesicle

contents and mineralise the matrix. On the other hand Lamellar bone mineralisation occurs without matrix vesicles, the mineral being deposited by osteoblasts along the collagen fibrils of the organic osteoid matrix of bone. It is due to these differences in matrix components and the mechanical stimulus response to replace woven bone with lamellar bone that woven bone is considered mechanically inferior. The remodelling of woven bone into superior lamellar bone is therefore an important aspect of fracture healing, returning structural integrity to the injured limb.

The necessity of osteoclastic resorption is hence paramount to this remodelling process. Resorption of callus hard tissue has been demonstrated to commence as early as 2 weeks after fracture in a sheep fracture model, increasing in activity throughout the repair process (Schell *et al.*, 2006). A significant impact on this process is therefore exhibited by the inhibition of resorption. Both therapeutic intervention studies (Li *et al.*, 1999, Li *et al.*, 2001, Mori, 2003, Li *et al.*, 2000a, Lu *et al.*, 2004, Cao *et al.*, 2006), and models of osteoclast dysfunction (Marks, Jr. and Schmidt, 1978) demonstrate extensive inhibition of hard callus remodelling. These will be discussed in further detail in section 1.4.4.

1.3.3 Animal models of fracture repair

A suitable model for examining the effects of anti-resorptive treatment on fracture repair should involve a level of mechanical instability as to ensure the presence of endochondral ossification. It has been widely documented that the mechanical environment of a fracture plays an important role in determining the repair process (Goodship *et al.*, 1993). If a fracture is fixed with complete stability (zero tissue strain) it will heal only through intramembranous ossification, with very little or no cartilaginous phase. This model of fracture repair is less commonly employed clinically due to the implications of stress shielding osteopenia, bone weakening in response to disuse (Gardner *et al.*, 1998). Of more clinical relevance is fracture fixation that allows for a certain amount of instability without compromising the fracture site. In less stable fractures, repair occurs through endochondral ossification with development of a soft cartilaginous callus that provides the stability required for the progression of repair without causing stress shielding osteopenia (Bonnarens and Einhorn, 1984, Mark *et al.*, 2004a). As such, it is this model that is widely used to investigate fracture repair and therefore is the basis of the model to be used in this investigation.

A rat model of fracture repair was developed with fixation by way of an intramedullary rod which allowed for full movement but also maintained axial alignment of the bone (Bonnarens and Einhorn, 1984). This model utilised a technique that

creates a closed mid shaft fracture without disruption of the surrounding tissue. This is in contrast to an osteotomy or open fracture that involves surgical disruption of surrounding soft tissues and periosteum. Park and colleagues in 1999, investigated open and closed models and found substantial differences between the two (Park *et al.*, 1999). With the same external rigid fixation, the open osteotomy model showed inferior biomechanical properties to the closed fracture in the early stages of repair. This may be owing to the impaired periosteal callus formation described in the early phases. Callus size at this point was also reduced in the osteotomy model, due to the stripping of the periosteum and damage to the surrounding soft tissue, the production of the blastema is delayed. Washing of the site with saline also delayed the early repair stage, growth factor stimulators and bone marrow cells were rinsed away with the haematoma. Thus, with removal of the protective periosteum and initial injury response mechanism, the open osteotomy fracture provides a more challenging healing environment and a delay in repair is seen (Nunamaker, 1998).

Since this study is focusing on the roles of certain bone cells in normal bone repair, a simple model was desirable. As a result of these considerations the closed model of fracture repair with internal fixation, as described by Bonnarens & Einhorn (1984), was utilised in this examination, investigating the role of the osteoclast in bone growth and repair.

1.4 Osteoclast activity during skeletal growth and repair

1.4.1 The cell biology of the osteoclast

The osteoclast is a highly specialised cell that is essential for the resorption of both the inorganic and organic components of bone matrix, dentine and calcified cartilage. The osteoclast is a multi-nucleated cell formed by the fusion of mononuclear precursor cells derived from hemopoietic stem cells. This cell has very unique functional characteristics, including specific differentiation, adhesion to calcified surfaces, acidification of resorption lacunae and phagocytosis of bone components.

Following receptor-activator of nuclear factor kappa beta ligand (RANKL) stimulated differentiation into TRAP positive multi-nucleated cells osteoclasts attach to bone surfaces where they undergo cytodifferentiation into mature osteoclasts. The mature osteoclast is a phagocytic cell capable of dissolving the inorganic hydroxyapatite component of bone tissue and then digesting the remaining organic collagen matrix, Figure 1.10 (Boyle *et al.*, 2003).

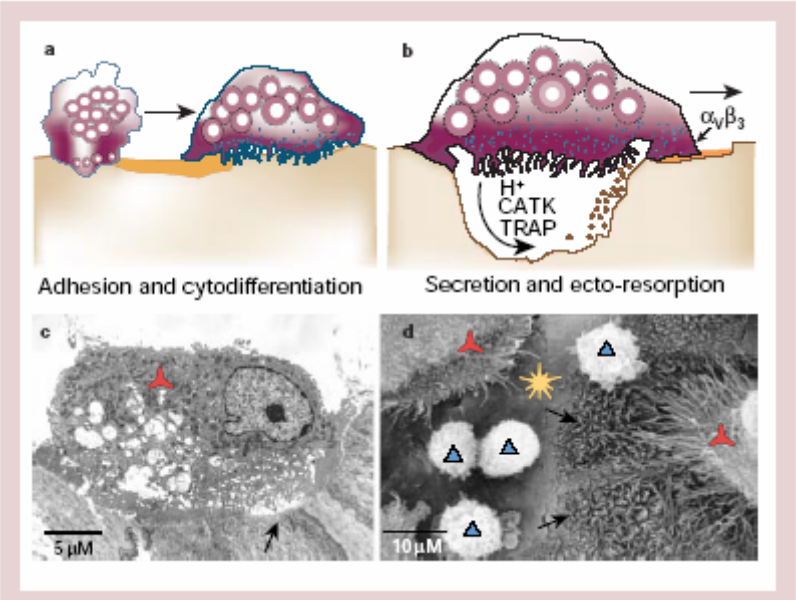

Figure 1.10. *Diagram of the two main stages of osteoclastic resorption, adhesion and cytodifferentiation and subsequent resorption.*
Activation of bone resorption. A, Multinucleated polykaryons are recruited by the action of CSF-1 and RANKL, which then adhere to bone and undergo cytodifferentiation into a mature osteoclast. b, RANKL stimulates osteoclast activation by inducing secretion of protons and lytic enzymes into a sealed resorption vacuole formed between the basal surface of the osteoclast and the bone surface. Acidification of this compartment by secretion of protons leads to the activation of TRAP and cathepsin K, which are the two main enzymes responsible for the degradation of bone mineral and collagen matrices. c, Transmission electron micrograph of an activated mouse osteoclast with a visible ruffled border in a resorption lacunae on the periosteal femoral cortical bone surface. Red propeller, osteoclast; black arrow, a resorption pit. d, Scanning electron micrograph of human osteoclasts generated *in vivo* on cortical bone slices from CSF-1 and RANKL-treated peripheral blood mononuclear cells. Re propellers, osteoclasts; black arrows, a resorption pit where the normally smooth lamellar bone surface has been resorbed to expose collagen bundles; yellow star, non-resorbed bone surface; blue triangles, mononuclear cells (potential osteoclast precursors)
Reproduce with permission from (Boyle *et al.*, 2003).

Osteoclastic resorption is achieved through numerous extracellular processes which firstly require adhesion of the cell to the bone surface (Farina and Gagliardi, 1999). Interactions between the osteoclast surface vitronectin receptor and the surface integrin alpha v beta 3 (αvβ3) and osteopontin on the bone surface produce a strong bond and allow polarisation of the cell and the formation of the resorption zone. At the boundaries of the adhered cell membrane, cytoplasmic clear zones form which contain no organelles but are rich in F-actin fibres. This transformation creates an actin-ring surrounding the resorption zone and produces a sealed external zone between the cell and the bone surface often referred to as the resorption lacuna. Between the clear zones within the resorption zone, the membrane of the cell forms from extensive convolutions, creating the characteristic osteoclast ruffled border.

The ruffled border membrane exhibits a high concentration of proton pumps that cause active exchange of positive ions from the cytoplasm into the resorption lacuna, acidifying it to commence demineralisation of the bone matrix. The proton pump specific to these cells belongs to the vacuolar ATPase+ family and is capable of pumping protons from the cytoplasm into the vacuolar lumen creating an electrical potential that forces exchange of positive ions across the membrane (Farina and Gagliardi, 1999). At the same time, chloride channels on the resorptive membrane allow for passive transport of chloride ions to maintain electroneutrility of the cell (Schaller *et al.*, 2004). Both these membrane constituents drive the processes necessary for the resorption of bone by osteoclasts. Further, cytoplasmic lysosomes that have migrated to the ruffled border area fuse with the membrane and release their proteolytic contents including TRAP (Singh *et al.*, 1974), the cysteine proteinase cathepsin K (Garnero *et al.*, 1998) and the collagenase's or matrix metalloproteinase's (MMPs) (Sato *et al.*, 1998).

TRAP is vastly expressed in osteoclasts and is of such specificity to these cells it is commonly used as an osteoclast-specific marker (Angel *et al.*, 2000). TRAP is a lysosomal phosphatase excreted into the resorption vacuole where it is highly active in the acidic environment. These actions include: dephosphorylation of the bone matrix proteins osteopontin and bone sialoprotein; two important proteins involved in osteoclast attachment to bone (Ek-Rylander *et al.*, 1994), and the final destruction of the matrix degradation products (Hollberg *et al.*, 2005). Shown at high concentrations in the transcytosolic vesicles, TRAP is capable of generating caustic reactive oxygen species that destroy collagen as it is transported through the osteoclast and released at the non-resorbing surface.

As expected from these findings, mice deficient in TRAP show a marked reduction in osteoclast function resulting in a mild osteopetrotic phenotype and long bone growth deformities (Hayman *et al.*, 1996). The skeletal defects in these mice stem from the disruption of the formation of the ruffled border and intracellular vesicular transport, confirming a function for TRAP in the modulation of intracellular transport (Hollberg *et al.*, 2002). Clearly TRAP plays an important function in osteoclastic regulation of skeletal homeostasis.

Cathepsin K is a proteolytic enzyme produced by osteoclasts and is capable of degrading type I collagen fibres which make up 90% of the organic bone matrix (Henriksen *et al.*, 2006). Once the acid driven demineralisation of bone occurs, cathepsin K commences degradation of the remaining organic matrix. In mice lacking this protease, bone resorption is partially impaired, confirming cathepsin K's essential role in osteoclastic bone resorption (Roth, 1976). Cathepsin K deficiency also leads to

the mild osteopetrotic human condition known as pyknodysostosis (Yamashita and Dodds, 2000). Examination of murine specimens lacking cathepsin K has shown extensive amounts of un-mineralised organic bone matrix remain in the resorption pits, revealing a specific function of this cathepsin in organic matrix degradation. A special characteristic of this enzyme is its ability to work optimally in acidic environments, particularly at a pH of 5.5 such as that produced in the osteoclastic resorption zone (Garnero *et al.*, 1998). This activity at low pH is what differentiates cathepsin K activity from the MMPs.

The collagenase's known as matrix metalloproteinase's (MMPs), including MMP-9, MMP-12 and MMP-13, have previously been described as important during bone growth (1.2.5) and repair (1.3.2.3) but they also play a pertinent role alongside cathepsin K in organic bone matrix resorption. Since the various MMP deficient mice do not exhibit reduced bone resorption, as is seen in the cathepsin K deficient mice, clearly none of the MMPs mentioned have been shown to be rate limiting to bone resorption. Even so, they have certainly been associated with the processes of osteoclastic inorganic bone matrix resorption (Hou *et al.*, 2004). There is some conflict in the literature as to the extent of MMP secretion by osteoclasts, with some authors suggesting MMP-9 is released by osteoclasts into the resorption lacunae where it acts to degrade organic matrix (Lowery *et al.*, 1999). Further, MMP-9 antisense oligonucleotide inhibition of osteoclastic resorption reduced dentine resorption pit formation in culture by 53% (Ishibashi *et al.*, 2006). It was suggested by these authors that MMP-9 was required for the preceding degradation of the organic matrix, allowing deeper resorption. Other authors disagree with this and believe instead that MMP-9 is not active in the resorption lacunae, especially considering that the pH here is acidic and therefore not optimal for MMP activity (Delaisse *et al.*, 2003). MMP-9 localisation in the resorption lacunae is yet to be confirmed thus its role in bone matrix degradation remains exclusive to cell migration (Sato *et al.*, 1998). When osteoclasts were cultured on collagen coated dentine discs in the presence of a non-specific MMP inhibitor, resorption was reduced, suggesting that osteoclast specific MMPs may be required for resorption in the presence of collagen on bone surfaces.

A less controversial MMP, MMP-13, which is not produced by osteoclasts, has been localised under the ruffled border of osteoclasts on bone surfaces (Nakamura *et al.*, 2004). MMP-13 is produced by both osteocytes and osteoblast lineages at sites of resorption. Here MMP-13 appears to initiate bone resorption by degrading the thin layer of un-mineralised matrix covering the bone surface prior to resorption, allowing attachment of the osteoclast to the bone surface. It is also said to play a role in the progression of bone resorption, smoothing off the resorption pit before new bone is

produced. This process is responsible for the smooth reversal lines (cement lines) seen on light microscopy sections of bone. These pertinent roles of MMP-13 in resorption have been confirmed by the fact that it is the only MMP that has been shown to have some rate limiting role in bone resorption. In a study looking at the calvarium resorption in MMP-13 deficient mice it was shown that bone was resorbed more slowly than in wild type mice (Inada *et al.*, 2004). It has been suggested that in the absence of cathepsin K, MMP-13 actively compensates in the degradation of organic bone matrix (Everts *et al.*, 1998). The osteopetrotic phenotype of the cathepsin K deficient mouse is not severe suggesting that a significant level of tissue remodelling has occurred in these mice, which could be through MMP-13 activity. Additional support for this theory arises from the observation that cross-linked carboxyterminal telopeptide of type I (ICTP) collagen fragments typically produced by MMPs are increased in the serum of cathepsin K deficient patients at the expense of the cathepsin K produced C-terminal telopeptide cross-link (CTX) fragment (Garnero *et al.*, 2003).

The potent degrading mixture of cysteine proteinases, phosphatases and collagenase's active in the acidic osteoclast resorption lacunae efficiently breaks down both inorganic and organic bone matrices of bone. The products of this degradation are transported into the osteoclast by endocytosis and subsequently released on the other side of the cell in a specialised region known as the functional secretory domain (Mulari *et al.*, 2003). Thus this transocytosis of degradation products allows for continual resorption without release of the sealed resorption zone. Motility is an additional specialised characteristic of the osteoclast as it is achieved without release of the sealed zone. Instead, the "resorption in motion" these cells are noted for is achieved through reorganisation of the sealed zone during movement (Helfrich *et al.*, 1996). This process however is not well understood at the molecular level. Migration of osteoclasts to resorptive surfaces has been explored and MMP-9 has been proposed to be involved in this process. Indications of this hypothesis came from the fact that MMP inhibitors completely prevented the formation of the marrow cavity in neonatal long bones (Blavier and Delaisse, 1995). Osteoclasts remained in the surrounding mesenchyme without migrating through the developing bone collar. The conclusion that this result was due to migration and not resorption was reinforced by the fact that potent anti-resorptive intervention did not prevent this migration.

Whether the MMPs involved in this process were of osteoclastic origin was explored using highly purified osteoclasts seeded onto collagen coated membranes. Cells were able to migrate, however, when an MMP inhibitor was added migration was prevented. Of the MMPs secreted by osteoclasts, only MMP-9 and 14 deficiencies led to significant reductions in osteoclast migration into the diaphyseal cores. This

identified these two MMPs as critical to osteoclast migration. They degraded the un-mineralised bone matrix, allowing osteoclast migration and attachment to bone surfaces, thereby initiating resorption (Sato *et al.*, 1998). Migrating osteoclasts have been shown to exhibit unique characteristics compared to actively resorbing osteoclasts. They are rounded and do not polarize unlike those osteoclasts actively resorbing, suggesting that movement through un-mineralised matrix does not involve normal osteoclast resorptive function. Instead MMP-9 is utilised by the osteoclast, secreting it to degrade the surrounding matrix allowing migration without the need for attachment, polarization, and acidification. Moreover MMP-9 has been proven to degrade type IV collagen which is the main constituent of blood vessel basement membrane. This indicates that MMP-9 may also facilitate the transit of pre-osteoclasts and osteoclasts from the blood to resorptive sites (Jemtland *et al.*, 1998). MMP-9 is also greatly involved in the process of endochondral ossification during bone growth and repair as described previously (1.2.5 and 1.3.2.3).

1.4.2 Regulation of osteoclast formation and activity.

As mentioned previously osteoclastogenesis is powerfully regulated by a number of cytokines and growth factors including tumour necrosis factor (TNF), macrophage colony stimulating factor (M-CSF) , receptor-activator of nuclear factor kappa beta ligand (RANKL) and its receptor RANK. TNF is strongly associated with osteoclastogenesis through numerous pathways. Firstly it induces a number of pro-osteoclastic cytokines such as M-CSF which promotes proliferation and differentiation of early osteoclast precursors. Further TNF indirectly stimulates bone resorption through effects on osteoblasts (Kimble *et al.*, 1997). RANK (receptor activator of NFκB) is a member of the TNF receptor family and is expressed on the surface of osteoclasts. Here it interacts with its ligand RANKL to stimulate osteoclast differentiation. Osteoprotegerin (OPG) is a secreted protein which functions as a competitive blocker of the RANKL/RANK binding thus acts to inhibit osteoclast differentiation. Both RANKL and OPG are secreted by stromal cells and osteoblasts and are closely regulated by numerous systemic and local factors in order to control osteoclast activity (Hofbauer *et al.*, 2000, Kostenuik, 2005).

Systemically, osteoclast formation is stimulated by the release of cytokines and circulating growth factors, whereas in the local bone microenvironment both the ECM and local osteoblasts play a pertinent role in osteoclast recruitment and activity. The ECM protein osteopontin (OPN) is known to be present in numerous non-mineralised tissues however it was originally isolated from bone where it carries out a functional

role in controlling mineralisation and remodelling. OPN deficient mice demonstrate changes in the mineral crystalinity throughout development such that the mineral content and crystal size are increased compared to wild type mice, producing a subtle osteopetrotic phenotype (Boskey *et al.*, 2002, Aitken *et al.*, 2004). Although the mechanism of this change is attributed to the fact that OPN may modulate mineralisation of bone tissue, it is more likely a result of reduced remodelling by osteoclasts, even though osteoclast number is not reduced in these mice. Osteoclast migration and adherence to bone surfaces is essential for correct resorption and is facilitated through the binding of the osteoclast surface integrin αVβ3 to OPN (Reinholt *et al.*, 1990). In addition to local OPN, osteoblasts stimulate osteoclastogenesis both directly by releasing factors such as M-CSF and RANKL and indirectly through mediating PTH and 1,25-dihydroxvitamin D3 levels which in turn modulate OPG and RANKL expression. Cell-to-cell contact is required for all of the abovementioned osteoblastic regulation mechanisms of osteoclastogenesis. Therefore osteoblasts play a key role in not only bone formation but also in the regulation of bone resorption. This is true not only for stimulation of osteoclast formation but also their function. In fact, it has been proposed that osteoblasts and osteoblast like bone lining cells are directly associated with bone resorption.

Firstly, it was noted by Wesolowski *et al.* 1995, that when highly purified osteoclasts were cultured on dentine, resorption pits failed to form, however when osteoblasts were added to the culture system resorption pits appeared. It was also proposed that osteoblast-like bone lining cells initiate osteoclastic resorption by removing a thin un-mineralised layer that covers bone surfaces allowing osteoclastic access to the mineralised surface. This was shown to be achieved through degradation using MMPs and provides further mechanism for the indirect control of resorption by osteoblasts. In addition, analysis by both (Everts *et al.*, 2002) and (Mulari *et al.*, 2004) have shown that osteoblast-like cells complete the bone resorption process by entering the resorption lacunae after the osteoclast and removing or “cleaning out” the remaining collagen fibrils that are left protruding from the lacunae. This process utilizes MMPs to degrade the remaining organic matrix, clearing the site and allowing for the first stage of new bone formation. These osteoblast-like cells then proceed to lay down a new layer of organized collagenous matrix providing the scaffold for mineralisation and completion of new bone formation.

1.4.3 The role of the osteoclast in bone growth and remodelling

Due to their specialised cellular structure and function osteoclasts are essential to normal bone homeostasis as they are the only cell type capable of mineralised tissue removal. Stimulation of osteoclast resorption arises from many systemic and local factors, previously described.

In section 1.2.1 I discussed long bone development and growth through a process termed endochondral ossification which involves mineralisation, invasion and removal of a cartilage template and its replacement with bone. The role of the osteoclast in this process is not yet completely elucidated; therefore conflicting ideas on the level of its involvement exist. Analysis of growth in numerous osteoclast mutant animal models has fuelled confusion, with some models exhibiting extreme growth dysfunction and others appearing normal. This will be discussed further in section 1.4.5.2. However, it remains undisputed that the osteoclast plays a pivotal role in the removal of the primary spongiosa bone formed through endochondral ossification, where it is the principal resorbing cell. On the other hand, the role of the osteoclast in the invasion and removal of the un-mineralised cartilage template remains unclear with some authors considering the mature osteoclast also to be the primary resorbing cell during this process whilst others do not (Lewinson and Silbermann, 1992, Vu *et al.*, 1998, Nordahl *et al.*, 1998, Deckers *et al.*, 2002, Kawana and Sasaki, 2003, Yamazaki and Sasaki, 2005). Clearly this conflict in opinions arises from the fact that the understanding of this process is not yet comprehensive. Therefore this investigation aims to provide the underlying evidence needed to clarify the role of the osteoclast in endochondral ossification.

During both post natal growth and after cessation of bone growth, maintenance of optimal skeletal architecture is achieved through continuous bone turnover. Bone resorption is one of two key processes essential to achieving this level of bone homeostasis, the other being bone formation. Through constant turnover the skeleton is completely replaced every 10 years, removing old strained bone matrix and replacing it with new. Therefore, optimal bone resorption through regulated osteoclast function is necessary throughout life (Parfitt, 2002). Undoubtedly, osteoclast activity is rate limiting to normal bone turnover and this has been demonstrated extensively through various genetic manipulation models and pharmaceutical intervention studies (Weinstein and Manolagas, 2000, Blair *et al.*, 2002, Dai *et al.*, 2004, Li *et al.*, 2006).

By resorbing bone tissue through the processes mentioned above, osteoclasts are a part of what is termed a bone modelling unit (BMU) which includes both osteoclast and osteoblasts acting in concert to remove old bone and replace it with

new. These units are continually active at a basal level until a stimulus, either local or systemic, produces a change (Parfitt, 2002). Signals that enhance bone remodelling arise from the local micro-environment, primarily through the osteocytes which are able to determine the fate of their surrounding matrix by transmitting signals through their connective system of canaliculi to the surrounding marrow spaces. These signals initiate either bone resorption in response to tissue damage such as fatigue micro-cracks, or bone formation in response to mechanical loading. Each of these responses is coupled to an opposing response such that a micro crack stimulates bone resorption which then stimulates new bone formation to replace the removed damaged tissue (Knothe Tate *et al.*, 2004)

Normal homeostatic levels of bone turnover vary amongst the population but as long as the resorption and formation processes are well balanced, skeletal integrity is maintained. It is not until imbalances occur that the skeleton is compromised, this is unfortunately the case for a large cohort of bone diseases such as osteoporosis and osteopetrosis (Helfrich, 2003). Diseases linked to osteoclast abnormalities have been well explored through various animal models and such work has enabled the progression of a deeper understanding of the role of osteoclasts during skeletal development, maintenance and repair.

1.4.4 The role of the osteoclast in bone repair

As described previously in section 1.3 there are two main stages of tissue remodelling during fracture repair, firstly initial union through endochondral ossification and secondly hard callus remodelling. The role of the osteoclast during the latter, hard callus remodelling, is clear and well understood. The involvement of these cells during endochondral fracture union on the other hand remains controversial.

Briefly, endochondral fracture union encompasses a multitude of events that proceed to firstly form a stabilising avascular cartilaginous callus which is then invaded and resorbed as it is replaced by ossified hard callus (see section 1.3 for further detail). It is the process of invasion and resorption of the soft cartilage callus that provides a level of perplexity in understanding osteoclastic activity during this early fracture repair stage. Due to their commonly noted activity during early fracture repair (Schell *et al.*, 2006) and localisation at the invading front of the chondro-osseous junction, osteoclasts have been assumed to be key players in this process. Conflicting data have been produced on the height of activity and localisation of osteoclasts here, many authors showing clear localisation of osteoclasts, others demonstrating vascular endothelial cells at the invasion front (Sawae *et al.*, 2003, Takahara *et al.*, 2004).

Although their localisation has been examined the exact necessity of osteoclast activity in this process has not been confirmed. Investigations have been performed in mice lacking osteoclast activity such as that performed by (Flick *et al.*, 2003) in the RANK knockout and osteopetrotic (*op/op*) mice in addition to administration of recombinant OPG to inhibit RANKL activity in normal mice. OPG administration throughout the fracture repair process inhibited osteoclast development and activation such that callus osteoclast number was significantly reduced. Endochondral fracture union was achieved at the same rate as control mice. Moreover, the *op/op* osteopetrotic mice, demonstrating a complete absence of active osteoclasts, showed an equivalent rate of endochondral fracture union to their normal littermates. In contrast, the RANK knockout mice again with reduced osteoclast activity showed a significant delay in this process with only 33% of fracture united by 28 days. Further analyses by these authors lead them to suggest this delay could be related to reduced bone formation and blood supply at the fracture site in these RANK knockout mice. Such conflicting results however provide reason for the confusion regarding the osteoclasts involvement here, whilst also justifying the need for an additional detailed examination to clarify this issue. The work outlined in this thesis describes a group of studies aimed to do precisely that.

Hard callus remodelling is an important process during the later stages of fracture healing, the purpose of which is to remodel the callus until it resembles the original bone structure. In contrast to initial union, the role of the osteoclast during hard callus remodelling is clear and unchallenged. Clearly osteoclasts are crucial to this process and their inactivation either biologically or pharmacologically would therefore lead to considerable delays in remodelling of the ossified callus.

In a mutant rat model of osteopetrosis, the incisor absent (*ia/ia*) rat, see section 1.4.6 for more details, whose osteoclast function is remarkably reduced, hard callus remodelling during fracture healing, is significantly hindered. The significantly larger hard callus compared to their normal littermates persists up to 6-7 weeks post fracture (Marks, Jr. and Schmidt, 1978). Furthermore, in normal animals, administration of the potent anti-osteoclastic group of drugs, bisphophonates, results in extensive increases in callus size and severe delays in callus remodelling (Li *et al.*, 1999, Li *et al.*, 2000a, Li *et al.*, 2001, Mori, 2003). As a result of the impact bisphosphonates have on the process of hard callus remodelling, these and other anti-resorptive drugs commonly used for the treatment of osteoporosis have been considered in a negative light in regards to final fracture healing (Cao *et al.*, 2002, Cao *et al.*, 2006). It is becoming obvious however that by discretely controlling dose frequencies of these drugs we may

be able to minimise their negative effects on hard callus remodelling. This will be discussed in detail in section 1.5.3.

1.4.5 Animal models of defective osteoclastogenesis

Disruption of the balance between bone formation and bone resorption can lead to either; (a) too little bone, *osteoporosis,* or (b) too much bone, either *osteopetrosis,* caused by decreased resorption or *osteosclerosis*, caused by increased formation. This review will focus on osteopetrosis.

Osteopetrosis is a human skeletal condition caused by an increase in bone matrix **retention** as a result of decreased bone resorption. This accumulation of bone interferes with marrow cavity formation and causes abnormal development of the external shape of long bones. This disease is diagnosed radiologically by apparent areas of dense bone in the metaphyseal regions of long bones and poor definition of medullary canals. Differing degrees of reduced osteoclast activity are the primary cause of this disease and define the three main classifications of this human disease, infantile malignant, intermediate mild and adult onset. Treatment of osteopetrosis in humans has been hindered by the large variation in response to therapy in this population. Within each classification the response to therapeutic intervention varies, suggesting the aetiology within this disease may not be the same (Lazner *et al.*, 1999).

Due to reduced remodelling in this disease, patients develop what is referred to as brittle bones, increasing their susceptibility to low-energy fracture. Response to fractures in the osteopetrotic population has not been thoroughly explored. One case review published by (de Palma *et al.*, 1994) suggested that fracture callus formation appeared normal however long term callus remodelling was significantly hindered. In addition, the new bone appeared very immature with cartilaginous remnants remaining as long as 1 year post-fracture and without the organised haversian system normally seen in repaired bone. This area of immature bone would be far more susceptible to refracture due to its inferior mechanical properties. Thereby, it is imperative that the understanding of this disease is improved to allow for successful therapeutic intervention.

Developing an understanding of osteopetrosis has been aided greatly by the existence of a large number of osteopetrotic animal models. These animal models exhibit radiographic sclerotic bone and commonly show inhibition of tooth eruption. These models include the osteopetrotic (*op/op*) mouse, the osteosclerotic mouse (oc/oc), the RANKL knockout mouse, the RANK knockout mouse, the toothless (tl/tl) rat, the osteopetrotic (*op/op*) rat and the incisor absent (*ia/ia*) rat, (Li *et al.*, 2000b,

Tuukkanen *et al.*, 2000, McLean and Olsen, 2001) and finally the cathepsin K knockout mouse (Saftig *et al.*, 1998). In addition, pharmacological intervention can also model this disease by inhibiting or stimulating key osteoclast modulators. These include OPG, cathepsin K inhibitors and bisphosphonates, each of these will be discussed in section 1.4.7

1.4.5.1 Animal models of osteoclast dysfunction

Based on their primary defects, the numerous spontaneously occurring animal models of osteopetrosis can be categorised into two groups. Either they exhibit a defect in the osteoclast or its precursor, or they have a defect in the bone microenvironment. The *ia/ia* rat and the oc/oc mouse which show apparent phenotypic reversal after bone marrow transplantation belong to the first group where the primary defect is in the precursor or osteoclast population (Lazner *et al.*, 1999). The *op/op* mouse and the tl/tl rat however belong to the latter group, as neither has been shown to recover from their phenotype after bone marrow transplant therapy. In addition to these naturally occurring mutations, there are also many engineered models of osteopetrosis. These include the RANKL knockout and OPG knockout mice which have defects in the ligands secreted by osteoblasts or stromal cells that interact with RANK on osteoclasts to stimulate osteoclast formation and activation, RANKL being a positive regulator and OPG a negatively regulator in this process (Kosetnuik et al., 2005). The RANK knockout mouse however carries a primary defect within its osteoclast population (Li *et al.*, 2000b). Furthermore, as the knowledge base of osteoclast biology and function broadens, so does the development of genetically engineered mouse models of osteoclast dysfunction. Such models have further added to the field of bone biology and include the αVβ3 integrin deficient mouse, the cathepsin K knockout mouse, the TRAP deficient mouse and the chlorine channel knockout mouse.

1.4.5.1.1 Naturally occurring mutant animal models

op/op mouse

The *op/op* mouse, or more recently called csf1^{op,} exhibits a deficiency of macrophage colony stimulating factor (M-CSF) or colony stimulating factor 1 (CSF-1) thus demonstrates almost a complete absence of both osteoclast and macrophage populations. CSF-1 is an osteoblast-derived osteoclast-inducing signal that is essential to osteoclast differentiation from fused precursor mononuclear cells. This extremely osteopetrotic mouse demonstrates extensive skeletal abnormalities including short

stature and low body weight due to developmental growth defects; however the epiphyseal growth plates appear normal. The defect in these mice was confirmed when *op/op* mouse macrophage progenitor cells were cultured in the presence of exogenous CSF-1 and they showed normal macrophage production, thus *in vivo* these mice lack this essential stimulatory factor (Wiktor-Jedrzejczak *et al.*, 1990).

The only form of rescue for these mice was achieved by implanting a diffusion chamber of CSF-1 producing cells into the peritoneal cavity for 1 month in 6 month old *op/op* mice. Although this did not completely rescue the osteopetrotic phenotype in these rats it did result in an 80-fold increase in the peritoneal macrophage population and the production of a small TRAP positive cell population in the marrow cavities, such a population was non existent prior to CSF-1 treatment (Wiktor-Jedrzejczak *et al.*, 1990). One interesting observation in these mice is that the few osteoclasts produced demonstrated normal morphology with ruffled border formation and normal resorptive activity.

To date no human equivalent mutation of the *op/op* mouse has been detected, indicating that this animal model of osteopetrosis however has not been extensively explored as. Further, this mouse mutation demonstrates a spontaneous recovery in the first few months after birth. Both these issues render this model of little value to exploring the human disease of osteopetrosis. However, the *op/op* mouse has been utilised frequently as a model of osteoclast absence, providing an avenue to explore the role of the osteoclast in bone growth and repair. Of extreme relevance to this topic is the work performed by Deckers *et al*. in 2002 utilised the *op/op* mouse in a study examining the effect of reduced osteoclast activity on both vertebral primary endochondral ossification and growth plate endochondral ossification on tibia and tail vertebrae. The *op/op* mouse showed normal angiogenesis into cartilage tissue and its subsequent removal and ossification, the authors concluding that in the absence of osteoclasts the process of endochondral ossification during vertebral growth is normal.

Furthermore, endochondral fracture repair also proceeded normally in these mice; complete union was achieved at the same rate as their wild type litter mates, Flick *et al.* 2003, also suggesting that osteoclast function is not required for endochondral fracture repair. Unfortunately, these fracture experiments were performed in 12 week old *op/op* mice which may have begun to recover from their phenotype and therefore demonstrate normalised osteoclast activity. In osteopetrotic models that display any phenotypic recovery it is essential to examine endochondral ossification within the time period of maximal osteoclast dysfunction.

Toothless (tl/tl) Rat

Similar to the *op/op* mouse the toothless rat has a mutation for loss of function in the CSF-1 gene resulting in significant reductions in osteoclast differentiation from precursor cells. These rats exhibit a more severe osteopetrotic phenotype than the *op/op* mice and do not show signs of phenotype recovery (Van Wesenbeeck *et al.*, 2002). Tooth eruption is completely inhibited in these rats due to the lack of resorption of the overlying alveolar bone. In addition to the dense osteopetrotic bone, tl/tl rats exhibit a distinct chondrodysplasia not seen in most osteopetrotic models. This dysplasia takes the form of a centrally thickened growth plate with reduced hypertrophic chondrocyte mineralisation and disorganised chondrocyte columns (Seifert, 1996).

It was suggested that reduced angiogenesis was the cause for this abnormality as when CSF-1 was administered to tl/tl rats; angiogenesis was stimulated along with osteoclast differentiation and resorption activity. Again CSF-1 administration provides the only avenue for phenotype rescue in these mutants (Aharinejad *et al.*, 1995). To date no fracture experiments have been performed in the *tl/tl* rat. Due to the possibility of angiogenic deficiencies in this model, interpretation of results from fracture experiments would be difficult.

Osteosclerotic (oc/oc or Tcrig1^{oc}) mouse

The osteosclerotic mouse is another resultant natural mutation model of osteopetrosis. The defect lies in the osteoclast itself, with no effect on osteoclast differentiation from precursor cells. A mutation in a gene encoding the osteoclast specific vacuolar proton pump renders these cells unable to resorb bone, leading to extensive osteopetrosis or osteosclerosis and delayed tooth eruption. The reduction in resorption leads to a compensatory increase in osteoclast number, however all osteoclasts produced are inactive. Growth retardation, long bone thickening and failure of marrow cavity formation are evident in these mice and they only survive until 4 weeks of age.

Rescue of these mice with marrow cell transplantation had been unsuccessful until recently when (Johansson *et al.*, 2006) delivered neonatal haematopoietic stem cells to young oc/oc mice and showed reversal of the extreme phenotype. In addition to the osteopetrotic phenotype these mice exhibit growth plate abnormalities with disorganised chondrocyte columns and extension of the hypertrophic chondrocyte zone, evidence of delayed invasion and removal of un-mineralised cartilage. Furthermore, examination of collagen deposition revealed disordered expression of types I, II and X collagen in the lower hypertrophic zone, although chondrocyte mineralisation was not impaired. Similar to the toothless rat, this delayed resorption of

the lower epiphyseal growth plate has been attributed to a reduced angiogenic stimulus and not to the reduction in osteoclast resorptive activity. Reference is commonly made back to the *op/op* mouse which shows normal epiphyseal growth plates (Yamasaki *et al.*, 2001).

Incisor Absent (ia/ia) Rat

The severe phenotypes outlined in the abovementioned osteopetrotic models are a product of deficits in osteoclastogenesis and thus reduced osteoclast populations. In contrast, the incisor absent (*ia/ia)* rat does not exhibit reduced osteoclast numbers, in fact they exhibit an increased osteoclast population. This suggests that the mutation causing the osteopetrosis is at the level of osteoclast function not differentiation, with an increase in osteoclastogenesis as a compensatory mechanism. Hence a less severe phenotype has been demonstrated in this model compared to the tl/tl and *op/op* rats (Seifert *et al.*, 1993). It is this specific difference in phenotype that led me to utilise the *ia/ia* rat in my investigations into the effects of osteopetrosis on fracture repair. A more thorough review of the literature on this model follows in section 1.4.6

1.4.5.1.2 Engineered animal models of abnormal osteoclast formation.

Receptor activator of NFKB (RANK) knockout (KO) mouse

Turning to engineered models of osteopetrosis, the RANK KO mouse has provided a useful model to discretely examine the role of RANK in bone homeostasis. Genetic knockout of the gene encoding the RANK receptor in mice has been achieved to produce a model of complete RANK receptor abolishment. This results in an extreme bone phenotype which is obvious from birth. RANK KO mice are clearly runted with no tooth eruption by 3 weeks of age. In addition they exhibit the typical signs of extreme osteopetrosis with dense, shortened long bones without marrow cavities. The complete absence of TRAP positive osteoclasts in these mice confirms the critical role of RANK receptors in osteoclast formation from precursor cells. Haematopoietic spleen cells were isolated from these mice and cultured in the presence of RANKL to stimulate osteoclast differentiation. TRAP positive cells failed to form from the KO cultures, confirming the lack of RANK receptors on the precursor cells. Furthermore, transplantation of bone marrow cells from unaffected mice with normal RANK expressing osteoclast precursors rescued the osteopetrotic phenotype in these KO mice (Li *et al.*, 2000b).

One interesting finding from the extensive investigation of this mouse model is the changes observed in the long bone growth plates. RANK KO mice showed obvious

expansion of the long bone growth plates, in particular the hypertrophic chondrocyte zone, suggesting a defect in vascularisation and removal of the hypertrophic chondrocyte matrix during endochondral ossification. Moreover, in the KO mice that recovered from the osteopetrosis after transplantation with normal bone marrow cells, growth plate abnormalities were also rescued.

Such results would suggest the necessity of osteoclast differentiation to the process of endochondral growth. However, the RANK KO mouse demonstrated an extreme model of osteopetrosis from the early stages of development. Thereby this model carries numerous underlying developmental defects that could also be involved in this manifested growth plate phenotype. The authors of this work suggest that the underlying hyperparathyroidism, due to reduced resorption, resulted in increased serum parathyroid hormone (PTH) levels. PTH is known to act upon PTH/PTHrP receptors on the growth plate chondrocytes, forming part of a feed back loop controlling chondrocyte proliferation and differentiation during this process, detail described earlier in section 1.2.3). Thus the up-regulated serum PTH in these mice may be the causative factor of the abnormal growth plate phenotype (Li *et al.*, 2000b). It still remains to be considered whether the absence of osteoclast precursors in these mice may have also influenced this developmental process.

Since endochondral ossification during growth is disrupted in these RANK KO mice then it would be expected that endochondral fracture repair may also be abnormal. As demonstrated by Flick and co-authors in 2003, this is in fact the case, with endochondral fracture repair significantly delayed in the RANK KO mouse. The underlying cause of this delay was explored and numerous explanations put forward. Firstly, the underlying extreme osteopetrotic phenotype was considered an influencing factor. These animals were severely osteopetrotic, making it impossible to internally pin the fracture limbs, reducing the stability of the fractures. Further, analysis of bone formation markers, mineral apposition and bone formation rates were significantly reduced. An anabolic defect such as this could have certainly impaired the repair response. Lastly, the authors considered vascularisation of the fracture site and saw significant reductions in the number of vessels and ratio of vessel area to tissue area in the RANK KO mice. These abnormalities could be contributing factors to the delayed healing; however they do not rule out the influence that the absence of osteoclasts may have here.

Receptor activator of NfKB ligand (RANKL) knockout mouse

As described previously, RANKL is the ligand required to bind to the RANK receptor on osteoclast precursors to initiate their differentiation into mature osteoclasts.

Expressed highly by osteoblasts and stromal cells and regulated closely by numerous bone resorbing factors, RANKL has been considered the elusive osteoclast differentiation factor. Deletion of the gene encoding this ligand therefore has produced an important mouse model to study. RANKL KO mice exhibit retarded growth after weaning, presumably due to the failure of tooth eruption and subsequent poor nutrition. As early as two days after birth, an obvious osteopetrotic phenotype is present with the typical stunted, dense, abnormally shaped long bones, vertebrae and ribs (Odgren *et al.*, 2003). In comparison bones formed through intramembranous ossification such as the skull appear normal. Histology confirmed the complete absence of TRAP positive osteoclasts and retention of primary metaphyseal bone throughout the diaphyseal cavities.

Again, abnormalities of the growth plate were noted however they were not described as being expanded, just disorganised. This was different to the RANK KO mouse that showed delayed invasion of the hypertrophic zone and growth plate expansion. This difference could be explained by the results seen with hemopoietic cell cultures from the RANKL KO mice, where TRAP cell formation did not occur in the presence of normal colony stimulating factors, the addition of RANKL to the cultures produced TRAP positive cells from the isolated KO cells. This confirmed firstly that the RANKL absence is the primary defect in these mice, moreover it proves that the haematopoietic cell population in these mice is essentially normal, the defect lying in the stimulus from the surrounding osteoblast/stromal cell population (Kong *et al.*, 1999). Therefore, *in vivo*, the osteoclast precursor cell population is normal; they just do not receive the signal to differentiate into mature resorbing osteoclasts.

One could conclude from the differences seen in the RANK KO and the RANKL KO mice that osteoclast precursor cells may in fact be capable of resorbing un-mineralised cartilage matrix at the invasion front of the chondro-osseous junction of the growth plate. In the RANK KO mice the precursor cells may not be capable of differentiating to the stage of RANK expression, therefore are less mature than the precursor cell population of the RANKL KO mice.

Further evidence to suggest a difference in the process of endochondral ossification in the RANK KO and RANKL KO mice is their response to fracture repair. As discussed, RANK KO mice exhibit delayed endochondral fracture repair. However, in the same study, fracture repair proceeded normally in the presence of recombinant RANK:Fc. RANK:Fc is an engineered molecule capable of competitively binding RANKL and thus blocking the RANKL/RANK stimulation of osteoclastogenesis. It could be argued that the RANK:Fc compound does not produce the osteopetrotic phenotype of the RANKL KO mouse, however with such fracture experiments yet to be examined

in the RANKL KO mouse, this comparison still provides some insight into the differences seen (Flick *et al.*, 2003).

In foetal murine bone, expression of RANKL has been shown in high levels in mesenchymal cells adjacent to the cartilaginous limb, hypertrophic chondrocytes, and regions of primary ossification (Lacey *et al.*, 1998). This suggests that the degradation of chondrocyte matrix during endochondral ossification may lead to the release of this ligand, increasing its local concentration and subsequently increasing the local population of mature osteoclasts.

Osteoprotegerin (OPG) knock out mouse

Although the OPG knockout mouse is not a model of osteopetrosis, its phenotype is relevant to discuss here because of its close links with the RANKL/RANK stimulation of osteoclastogenesis. Since OPG negatively regulates osteoclastogenesis, the OPG knockout mouse exhibits increased osteoclastic resorption leading to severe osteoporosis. Trabecular bone in these mice is destroyed by increased resorption and the cortical bone in these mice is considerably disorganised and porous, resulting in reduced bone strength. Osteoblast activity is up-regulated in response to the increased resorption, however bone quality continues to decline.

Furthermore, the growth plates in these mice are also destroyed, producing growth retardation and again suggesting a role for osteoclast activity during long bone growth (Kawana and Sasaki, 2003). Since the metaphyseal trabecular bone is in fact produced to provide mechanical support for the growth plate, it could be suggested that the extensive growth plate destruction seen in these mice is due to a collapse of this support structure. This engineered mouse model has been implicated as a model of osteoporosis as it provides an environment of endogenous increased resorption that can be manipulated with therapeutic strategies aiming to treat increased resorption.

1.4.5.1.3 Engineered models of osteoclast dysfunction

AlphaVBeta3 Integrin Knockout mouse

AlphaVBeta3 (αVβ3) integrin is expressed on the surface of osteoclasts and serves as a binding site for osteoclasts to the bone surface via OPN. Such specialised binding capacity is required for osteoclastic resorption of bone tissue, thus this integrin is important to normal osteoclast function. The αVβ3 integrin deficient mouse exhibits normal skeletal development and growth, however around 4 months of age develops an osteopetrotic phenotype due to reduced resorption. Osteoclasts from these mice are unable to bind bone tissue therefore do not polarise and form actin rings, rendering them unable to resorb bone (McHugh *et al.*, 2000). These mice have provided a model

to closely examine the role of this integrin in osteoclast function and have led to the development of numerous antagonists or inhibitors of the αVβ3 integrin as a method of anti-resorptive therapy (Hutchinson *et al.*, 2003, Murphy *et al.*, 2005).

Osteopontin knockout mouse

Osteopontin (OPN) is a non-collagenous ECM protein highly expressed in bone tissue where it carries out a role regulating bone tissue mineralisation and remodelling (section 1.4.2). OPN KO mice therefore demonstrate abnormal mineralisation of bone tissue with increased mineral content and crystal size, suggesting OPN is an inhibitor of mineral formation (Boskey *et al.*, 2002). Other examinations of these mice indicate that the changes in tissue properties are also due to reduced resorption by osteoclasts. With a normal number of osteoclasts present in these mice, OPN is proposed to be involved in osteoclastic function, namely via adherence to bone by interacting with the cell surface integrin αVβ3, and subsequent resorption of bone (Shapses *et al.*, 2003). OPN deficient mice also demonstrate reduced endothelial cell vascularisation and osteoclastic resorption of ectopic bone discs implanted in muscle, indicating an additional role for OPN in endothelial cell migration (Asou *et al.*, 2001). Endochondral bone development and growth are normal in the OPN KO mouse suggesting that OPN may not be necessary to endochondral ossification (Rittling *et al.*, 1998).

Bone regeneration and remodelling in the OPN KO mouse on the other hand was significantly altered. Angiogenesis of the avascular cartilaginous callus was delayed, reducing the formation of the initial bony callus. Fracture union was achieved in the OPN KO mice, with significant reductions in hard callus remodelling, such that by 8 weeks post fracture, the OPN KO mice demonstrated a 46% increase in callus size compared to wild type mice (Duvall *et al.*, 2006). Taken together, these studies in the OPN deficient mice indicate an important role for OPN in both bone formation and resorption, particularly during bone regeneration.

Cathepsin K knockout mouse

Cathepsin K is a proteinase secreted by resorbing osteoclasts into the zone of resorption, where it acts to degrade the organic collagen matrix after demineralisation has taken place, (Xia *et al.*, 1999, Delaisse *et al.*, 2003). Generation of mice deficient in cathepsin K led to the clarification of its role in bone resorption. Retardation of long bone growth was not seen in these mice however from an early age they develop an osteopetrotic like phenotype demonstrated by dense metaphyseal bone in long bones. This osteopetrotic phenotype is not as severe as in the models previously discussed but is evidence enough to suggest bone resorption is reduced in these mice. The

human disease, Pyknodysostosis, is caused by deletion of the gene encoding cathepsin K, also resulting in a mild osteopetrotic phenotype (Lazner *et al.*, 1999).

A level of resorption does take place in these modified mice, apparent by the normal bone length and with reduced amount of resorption of dentine by cultured osteoclasts from these mutant mice. Histology of long bones revealed the formation of a broad fringe of demineralised bone matrix lining the bone surfaces of cathepsin K knockout mice. Clearly the osteoclasts have removed the mineral content of the tissue, but without the proteolytic activity of the cathepsin K are unable to complete the process of removing the remaining matrix. The osteoclasts are then unable to further demineralise the tissue, proceeding to a new bone surface to resorb. Further, growth plate analysis revealed normal morphology but increased height, suggesting a slight delay in endochondral ossification in these mice. This may imply that cathepsin K is required for un-mineralised cartilage resorption at the chondro-osseous junction (Saftig *et al.*, 1998).

More recently, numerous compensatory mechanisms for the cathepsin K deficiency were revealed in these mice. Firstly, in response to the decrease in bone tissue resorption, osteoclastogenesis was significantly up-regulated resulting in a 2-fold increase osteoclast number. Secondly, a number of proteases capable of acting in concert with cathepsin K were up-regulated, suggesting they act to compensate for the cathepsin K deficiency (Kiviranta *et al.*, 2001).

TRAP knock out mice.

Tartrate resistant acid phosphatase (TRAP) is not only used as a marker to localise osteoclasts or measure their activity, it is also a secreted iron protein that carries out a function within the resorption zone. As described briefly in section 1.4.1, TRAP has been associated with the dephosphorylation of the bone matrix proteins osteopontin and bone sialoprotein which are involved with adhering the cell to the bone surface (Ek-Rylander *et al.*, 1994). The TRAP knockout mouse has provided a model to further explore the role TRAP plays in osteoclastic resorption. Similar to other osteoclast mutant mouse models, an osteopetrotic phenotype is seen with dwarfed and deformed long bones, increased bone mineral content and reduced resorption activity of osteoclasts *in vivo*. Again, growth plate abnormalities in these mice were evident with disorganisation and expansion of the chondrocyte columns (Hayman *et al.*, 1996, Hollberg *et al.*, 2002). This suggests TRAP activity may be involved in the process of endochondral ossification.

Chloride channel knockout mouse.

As described previously, acidification of the osteoclast resorption lacunae is an essential step in the process of bone resorption. The osteoclast surface chloride channel 7 (ClC-7) has been implicated in the regulation of lacunae acidification. This was revealed when a mouse deficient in the gene encoding theses channels was generated and examined. Due to the role ClC-7 channels play in resorption, these mice exhibit osteopetrosis as a result of dysfunctional osteoclastic resorption. It was thereby concluded that ClC-7 provides a conduit for chlorine exchange at the ruffled border interface, driving the acidic environment required to demineralise the bone matrix (Kornak *et al.*, 2001).

Further, examination of osteoclasts in culture from ClC-7 deficient human patients showed that the acidification process is essential to both the inorganic and organic phases of bone resorption (Henriksen *et al.*, 2006). As a result of these investigation, inhibitors of chloride channels have been explored as potential therapeutic modalities for increased resorptive disease states (Schaller *et al.*, 2004).

1.4.6 The incisor absent (*ia/ia*) rat

1.4.6.1 Bone phenotype in the ia/ia rat

The most obvious phenotypic characteristic of the incisor absent rat is the failure of incisor tooth eruption, hence their designation. The teeth of the developing rat are encompassed by bone, thus bone resorption is essential for eruption of the first molars or incisors. In this osteopetrotic mutant such resorption does not occur, resulting in the absence of these teeth. Otherwise externally normal, the *ia/ia* rat develops a strong osteopetrotic phenotype demonstrated by sclerotic regions of bone in the metaphyseal zones of long bones, lack of an obvious marrow cavity and an abnormal long bone shape (Marks, Jr., 1973). This mutation is non-lethal and only the homozygous genotype is affected, all rats having a normal life span. The genetic mutation causing this phenotype has been localised to a 4.7-cM region on rat chromosome 10q32.1 (Van Wesenbeeck *et al.*, 2004).

It has been confirmed by numerous studies that the *ia/ia* rat phenotype is a result of reduced resorption (Symons, 2003). A study in young developing *ia/ia* rats by (Marks, Jr., 1973) has shown that bone resorption as a response to exogenous PTH injections was significantly reduced in *ia/ia* mutants. It was also shown that no difference existed between normal litter mates (NLM's) and *ia/ia* rats in bone formation, providing further evidence for a specific osteoclast function mutation in these osteopetrotic rats. Osteoclast number in the metaphyseal areas of *ia/ia* rat long bones

were shown to be twice that of NLM rats confirming this phenotype is not due to reduced osteoclast formation but more so osteoclast function. However, it has been suggested by some authors that between the ages of 30 and 50 days, the affected rats enter a period of spontaneous remission with complete recovery from the phenotype seen at 100 days of age. This recovery period however requires more discrete examination and will require consideration when designing fracture experiments with these rats.

Abnormalities in the bone matrix and mineral properties of the long bones in the *ia/ia* rat have been demonstrated when compared to NLMs (Boskey and Marks, Jr., 1985). Increased mineral contents (ash weight) have been verified in both immature (11 days) and mature (52 days) *ia/ia* rats. Metaphyseal bone analysis revealed that this increase was the result of accretion of mineral deposition on existing hydroxyapatite crystals with reduced new crystal formation. Not only was the mineral deposition of each crystal increased, seen as an increased ratio of calcium to phosphate, but also the apparent size of the matrix crystals was raised, suggesting imperfections in matrix structure. High hexosamine contents were also evident in these mutant rats representing the persistence of mineralised cartilaginous tissue, correlating with the histological observation of retained mineralised cartilaginous cores in the osteopetrotic bone. Together these findings and the elevation in the ratio of calcium to phosphate content suggested to these authors a complete absence in bone remodelling.

Altered mineral accumulation can lead to changes in mechanical properties in the skeleton (Ferretti *et al.*, 1996). Although it would be assumed that increased bone mineral density would always lead to improved mechanical strength, a study of numerous osteopetrotic rat mutant models revealed this may not necessarily be the case. Femora and tibiae from 2 week old *ia/ia* rats underwent quantitative computerised tomography (QCT) analysis to show significant increases in tibial metaphysis bone mineral content (BMC) and bone mineral density (BMD) over NLM's. Tibial diaphyses were also significantly reduced in total bone area and thus cross sectional polar moment of inertia, a measure of theoretical bone strength, suggesting reduced cortical thickness as confirmed on histological analysis. No differences in femoral diaphyseal mineral properties were noted. Mechanical evaluation revealed that although mineral content was increased in these bones, both femora and tibiae were significantly weaker (Tuukkanen *et al.*, 2000). Thus, in osteopetrosis, increased BMD does not strengthen bone, instead it increases bone fragility under bending forces. It is proposed that this reduction in strength can be attributed to the reduced material properties (brittleness) of the retained primary bone, compared to stronger secondary bone. In a study investigating anti-resorptive therapy it was inferred that increases in

BMD caused by suppression of bone remodelling can lead to the accumulation of micro damage and thus reduced mechanical properties of the bone (Mashiba *et al.*, 2001).

Limitations do however exist in the abovementioned study into the mechanical properties of *ia/ia* rat long bones. These include the fact that the focus of the 3-point bend mechanical testing was on the femoral and tibial diaphyses, which were not sites of significant increases in BMD in the *ia/ia* mutant rat. The diaphyses of these limbs, although showing thinned cortices, do not exhibit the large amounts of retained primary bone seen in metaphyseal bone; therefore this strength analysis is not a precise measurement of the extreme phenotypic characteristic of this osteopetrotic mutant. Examination of the mechanical properties of a discrete area of metaphyseal bone would provide superior evidence to support the hypothesis of reduced mechanical properties in osteopetrosis. Secondly, this investigation focused on immature *ia/ia* rats which exhibit extremely high amounts of immature bone. Mature rats from this population should be examined in the same manner to allow analysis after removal of some of this primitive bone.

Long bone growth may also be hindered in these *ia/ia* mutants however no close examination of growth plate morphology has been completed. Preliminary phenotypic analysis of these rats in our laboratory shows a decrease in long bone growth during development suggesting that reduced osteoclast function is associated with impaired bone growth. However, this may be attributed to a reduction in food consumption due to feeding alterations caused by the absence of the incisors. Discrete analysis of growth plate morphology in these rats is required to determine if any pathological changes occur during endochondral development. The central hypothesis of this thesis that osteoclasts are redundant in this process, would lead to the speculation that no disturbance of growth plate endochondral ossification would be seen in the *ia/ia* rats. This will therefore be closely examined in this investigation.

1.4.6.2 Osteoclast function in the ia/ia rat

An essential part of normal bone resorption is attachment of the osteoclast to the bone surface and formation of the resorbing membrane, the ruffled border. As outlined in Figure 1.11, this bone surface contact is made at a specialised area of the osteoclast membrane through binding of αvβ3 integrins to OPN on the bone surface. The cell then polarises with all binding integrins moving to the bone/cell interface forming what is called the organelle-free clear zone near the bone bound membrane of the cell, entirely surrounding the ruffled border. Bone tissue resorption occurs only after secretory vesicles release degrading enzymes at the bone surface, promoting formation of the finger-like expansions of the plasma membrane, known as the ruffled

border. Secretion of enzymes such as carbonic anhydrase from vesicles at the ruffled border produces the acidic environment required for bone matrix degradation (Reinholt *et al.*, 1999).

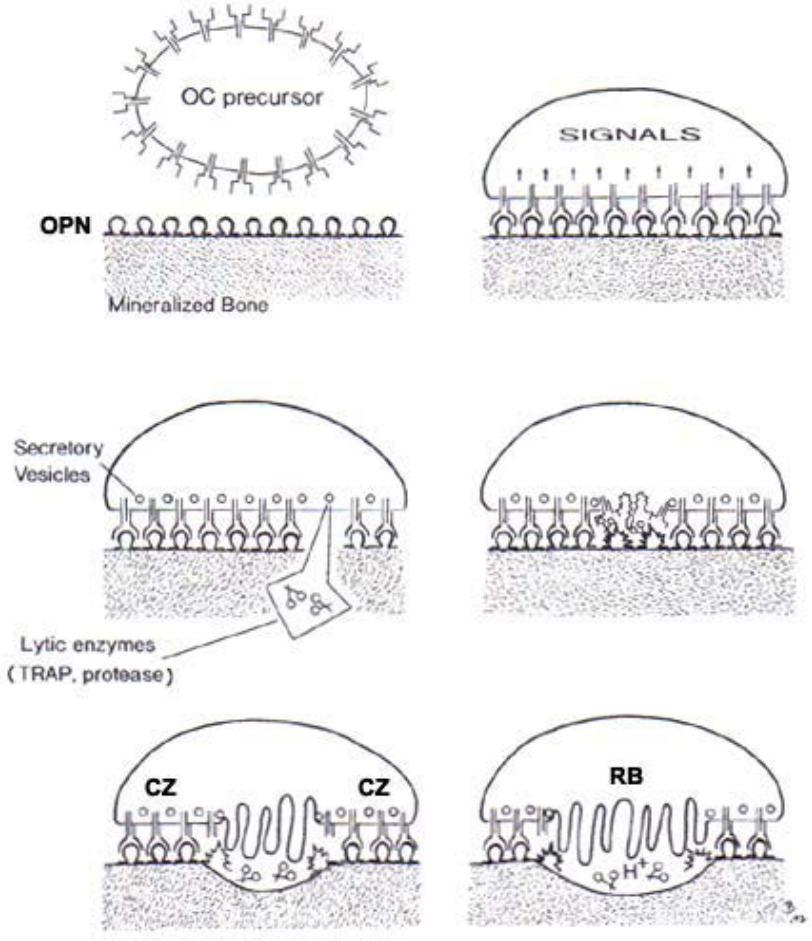

Figure 1.11 *Depiction of the stages leading to bone resorption*
αvβ3 integrins on the osteoclast surface bind OPN on the bone surface signalling polarisation of the osteoclast (OC) and concentration of binding integrins on the cell/bone interface.
Secretory vesicles migrate to cell/bone surface and release lytic enzymes (TRAP), proteases triggering formation of the clear zones (CZ) and ruffled border (RB) of the plasma membrane. This article was published in Experimental Cell Research, 251,(Reinholt *et al.*, 1999), Copyright Elservier.

Marks *et al,* in 1973, demonstrated that cytoplasmic acid phosphatase activity in *ia/ia* rat osteoclasts was double that of NLMs but lacked the increased concentration of activity at the bone-cell interface (ruffled border) as seen in NLM osteoclasts. Thus it was concluded that *ia/ia* osteoclasts were unable to secrete this essential enzyme, thereby reducing bone tissue degradation.

More recently it was revealed that not only do the *ia/ia* mutant osteoclasts develop a defective ruffled border at their surface of bone contact but they also show an increased clear zone (Reinholt *et al.*, 1999). Large cytoplasmic vesicles were all but

absent in mutant osteoclasts in comparison to the abundant vesicles seen in NLM osteoclasts. As previously reported TRAP activity was also altered in mutant cells, although they showed a 3 fold increase in total TRAP mRNA levels over normal littermates they did not demonstrate the high ruffled border concentration of NLM cells.

Osteopontin (OPN) has been associated with bone resorption due to its localisation on bone surfaces and demonstrated interaction with osteoclast membrane bound adhesion integrins (Reinholt *et al.*, 1990). OPN distribution in NLM showed increased intensities of the protein along surfaces near the clear zones of active resorbing osteoclasts, with reduced expression at the ruffled border/bone interface, whereas in *ia/ia* mutants OPN expression was seen as completely homogenous along bone surfaces(Reinholt *et al.*, 1999). It is suggested that this difference is caused by the lack of ruffled border formation and enzyme secretion of *ia/ia* mutant osteoclasts, inhibiting the alteration in OPN expression during resorption as seen in NLM osteoclasts.

Confirming the data on TRAP expression presented by Marks and colleagues in 1973, this recent investigation revealed a 3-fold increase in TRAP mRNA and a 6-fold increase in TRAP enzyme activity in *ia/ia* mutants compared to NLM's. Again it was concluded that since osteoclast numbers are 2 to 3-fold higher in *ia/ia* mutants, this increase in TRAP protein levels was not due to *de novo* synthesis of the protein, more likely the increases are attributed to the absence of TRAP secretion from mutant osteoclasts. Further to this, the reduced numbers of large intracellular phagocytic vesicles and increases in numbers of small secretory vesicles provide evidence for dysfunction of TRAP secretion and thus matrix resorption. Hence, osteoclast dysfunction has been recognised as the cause for the osteopetrotic phenotype observed in the incisor absent rat.

1.4.6.3 Fracture repair in the ia/ia rat

Radiological assessment of fracture healing in osteopetrotic patients has been described by some authors as pathological however others state that remodelling occurs normally but is markedly slowed. (de Palma *et al.*, 1994) With long bone fractures common in this diseased population, I believe a thorough understanding of the underlying pathology is necessary. The *ia/ia* rat has been utilised to examine fracture repair in osteopetrosis. Long bones of 1-2 week old *ia/ia* and NLM rats were fractured and followed for 2, 3, 4, 5 and 7 weeks post fracture. Callus size was not evidently different at 2 weeks but increased callus mineralisation was observed radiologically in *ia/ia* rats compared to NLMs. Callus remodelling had commenced at 3 weeks in NLMs with remodelling and reduction of callus size. On the other hand *ia/ia*

rat calluses had not changed. However, a slight reduction in callus size was seen in *ia/ia* rats by 4 weeks, although even at 5 weeks it still remained larger and more radio dense than the NLMs which had remodelled and reduced in size significantly at this stage. By 7 weeks *ia/ia* rat calluses remained large and very dense but some remodelling was apparent.

Histological analysis demonstrated that remodelling in normal calluses had resulted in union of fracture ends at 3 weeks, while fracture sites in *ia/ia* rats showed large amounts of dense irregular osteopetrotic bone (Schmidt *et al.*, 1977). Although numerous osteoclasts were seen in osteopetrotic calluses, large areas of this dense irregular bone remained up to 6 weeks post fracture. As seen in fracture calluses treated with anti-resorptive agents, hard callus remodelling is significantly delayed in the *ia/ia* rat due to diminished osteoclastic function. This study suggests that normal endochondral healing may occur in osteopetrotic patients with a delay in the hard callus removal.

This group then progressed to examine the effects of spleen cell transplantation in this *ia/ia* rat fracture model. As mentioned earlier in this review normal spleen cell transplantation into the *ia/ia* rat rescues the bone phenotype by providing a colony of normally functioning pre-osteoclast cells (Marks, Jr., 1976). This result confirmed that the dysfunction of the *ia/ia* rat osteoclasts was the primary cause for the reduced bone resorption phenotype. The transplantation method was repeated in the *ia/ia* fracture model to once again confirm the mutant osteoclast as responsible for the fracture pathology observed. Interestingly the cured osteopetrotic rats still showed signs of delayed fracture healing; however remodelling was far more advanced than in untreated *ia/ia* rats. Fractures sites in NLM rats were completely remodelled at 4 weeks post fracture; this was delayed to almost twice that time in untreated *ia/ia* rats which took till 9 weeks to remodel their calluses.

Transplant treated *ia/ia* rats showed accelerated healing with complete callus remodelling evident as early as 6 weeks post fracture. Although there was improvement with transplantation it did not return the fracture repair process to normal. It was suggested that this occurred because the fracture was induced only 3 days after spleen cell transplantation (Marks, Jr. and Schmidt, 1978). The previous study demonstrated that skeletal transformation from an osteopetrotic phenotype to normal took 2 weeks. A fracture produced at 2 weeks post treatment might heal normally, but this investigation is yet to be performed.

These important investigations into fracture repair in osteopetrotic rats however fail to examine the early stage of fracture repair, endochondral ossification; hence it is unclear if this early process is pathological in osteopetrosis. Without the normal

progression of cartilaginous tissue forming the primary spongiosa and subsequent remodelling of this tissue into lamellar bone, normal fracture repair would not occur in osteopetrotic patients. Assessment of endochondral fracture repair in *ia/ia* rats was therefore performed in this study to provide further knowledge towards understanding the pathology of fracture repair in osteopetrotic patients and more importantly elucidate the specific role of the osteoclast during the entire fracture repair process.

1.4.7 Pharmacological inhibition of osteoclast formation and activity

The underlying increase in bone resorption seen in many bone diseases and the outcomes from examining the many animal models of osteoclast dysfunction has prompted extensive research into potential therapeutic strategies aimed at manipulating osteoclast activity. Such research and development has led to the development of a group of "anti-resorptive" therapies. These include; recombinant OPG (Simonet *et al.*, 1997), cathepsin K inhibitors (Lark *et al.*, 2002), RANK:Fc (Flick *et al.*, 2003), monoclonal antibodies to RANKL, Denosumab (Bekker *et al.*, 2004), and bisphosphonates (Schindeler and Little, 2005).This exciting area of investigation has led to the successful utilisation of these interventions to treat many high bone turnover diseases, including osteoporosis.

1.4.7.1 Recombinant OPG

As outlined in the section 1.4.5.2, a deficiency of OPG leads to a severe osteoporotic phenotype caused by extensive increases in resorption. Due to the discrete control OPG exhibits over osteoclast formation, through blocking RANKL stimulation, it became a target of potential therapeutic intervention. Exogenous OPG administration results in large reductions in osteoclastic cells, hence significantly reducing bone resorption. Recombinant OPG dosing in normal mice resulted in a 3-fold increase in metaphyseal trabecular bone volume (Simonet *et al.*, 1997). Further, in osteoporotic ovariectomised rats, recombinant OPG treatment prevented the bone loss normally demonstrated by these rats (Shimizu-Ishiura *et al.*, 2002). These studies and many others led to the clinical application of recombinant OPG for the treatment of post menopausal osteoporosis with significant effects (Bekker *et al.*, 2001).

1.4.7.2 Cathepsin K inhibitor

Based on outcomes from knockout models, cathepsin K inhibition has been explored as a potential approach to anti-resorptive therapy. Firstly, non-specific cysteine protease inhibitors were used for their anti-resorptive properties to examine cathepsin inhibition, however these were not specific to cathepsin K and were inhibiting

other collagenase's like MMPs (Holliday *et al.*, 1997). Then an antisense oligodeoxynucleotide to cathepsin K was developed and shown to produce a 30-52% decrease in resorption pit size and depth on dentine slices by cultured rabbit osteoclasts, in a dose dependent-manner. These results were comparable to those achieved with non-specific cysteine protease inhibitors (Inui *et al.*, 1997). More recently however synthesized compounds, designed from X-ray co-crystal structures of peptide aldehydes bound to papain, that specifically inhibit cathepsin K have been developed and form a new era in potential anti-resorptive therapies on the pharmaceutical market (Yamashita and Dodds, 2000).

These new molecules have been tested in a wide range of animal models including rats and non-human primate models of postmenopausal bone loss. By preventing the bone loss usually exhibited by these modified models, these compounds have found their place as anti-resorptive therapies (Kleerekoper and Schein, 2001, Lark *et al.*, 2002, Kumar *et al.*, 2007). These studies have lead to numerous planned human clinical trials of these new improved compounds, in both the treatment of bone diseases such as osteoporosis as well as metastatic bone cancers (Kleerekoper and Schein, 2001).

Therapeutic intervention with cathepsin K inhibitors has raised numerous concerns regarding the bone specificity of these molecules. Cathepsin K expression has been observed in other tissue sites including, the thyroid, ovary and colon. This suggests that osteoclastic actions are not the only target of these compounds. As a result, recent work has aimed to produce cathepsin K inhibitor-polymer conjugates with moieties that directly target them to bone or joint sites (Wang *et al.*, 2004). Moreover, these compounds require daily administration, commonly by oral applications, compromising their efficacy in comparison to other clinically available potent anti-resorptive therapies like monthly injections of bisphosphonates. Consideration of the comparison of these molecules to bisphosphonates has been examined by our research group in models of bone repair. Daily oral doses of a small molecule cathepsin K inhibitor were unable to produce the same level of callus retention in a bone morphogenic protein (BMP) enhanced critical sized defect as a single intravenous dose of the bisphosphonate zoledronic acid (un-published data).

1.4.7.3 RANK:Fc

RANK:Fc is an engineered compound that acts in a similar manner to recombinant OPG. It has high affinity for competitively binding RANKL, preventing RANK/RANKL stimulation of osteoclastogenesis. It has been used to examine the effect of RANK signalling blockade during fracture repair in a mouse model. High dose

RANK:Fc eliminated osteoclasts in the fracture callus on day 14 but had no significant effects on the union of fracture sites. Although continuous therapy of RANK:Fc produced a large osteopetrotic callus devoid of osteoclastic resorption (Flick *et al.*, 2003).

1.4.7.4 RANKL inhibition (Denosumab)

RANKL inhibitors have been suggested to be capable of suppressing bone resorption to a greater extent than any other class of anti-resorptive drug. The fusion protein of OPG-Fc demonstrated a half life that required monthly dosing to maintain this high level of suppression of resorption (Kostenuik, 2005). Thus, a monoclonal antibody to RANKL, called denosumab, was produced as an alternative to recombinant OPG. Monoclonal antibodies have significantly longer half-lives than fusion proteins, hence a comparable dose of denosumab in post-menopausal women maintained suppression of resorption for more than six months (Bekker *et al.*, 2004), compared to just 45 days in similar patients given OPG-Fc (Bekker *et al.*, 2001). At this stage detailed histological analysis of the effects of denosumab and its anti-fracture efficacy await further long-term studies.

1.4.7.5 Bisphosphonates

Bisphosphonates (BPs) are the most commonly used anti-resorptive therapy to treat many bone diseases such as osteoporosis. There are many reasons for the successful implementation of this group of drugs. These reasons include; their high specificity for bone tissue due to their bone binding ability, their long half life of activity, minimal adverse effects and extensively researched and well understood mechanism of action.

As this group of drugs are utilised to explore the role of the osteoclast during fracture repair in this study a more detailed background follows.

1.5 Bisphosphonates

1.5.1 Mechanisms of bisphosphonate action

Bisphosphonates (BPs) are synthetic compounds characterised by a phosphate – carbon – phosphate (P-C-P) bond, which has a strong affinity for bone mineral. Analogues of the compound pyrophosphate, BPs contain a carbon atom in place of an oxygen atom, making them completely resistant to enzymatic breakdown *in vivo*.

Many different BPs have been developed with differences in their actions and potency as determined by their side chain configuration. The generic formula for BPs is

given below (Figure 1.12). R1, may vary but is often hydrogen (H) or hydroxide (OH), R2 on the other hand is the highly variable side chain. This offers the major source of variability between different bisphosphonates.

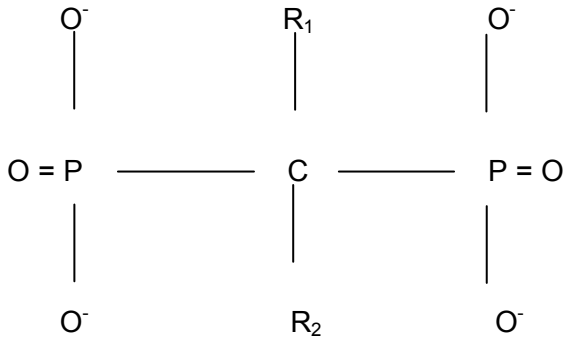

Figure 1.12. *Generic formula for a bisphosphonate*, Where (P) is phosphate, (O) is oxygen, C is carbon, R1 is either H or OH and R2 is a variable side chain. Reproduced with kind permission of Springer Science and Business Media (Kanis *et al.*, 1995).

Bisphosphonates inhibit bone resorption through a direct effect on osteoclast function and viability, whilst also exhibiting an indirect effect by inhibiting osteoblastic recruitment of osteoclasts (Licata, 1997). The direct effects of BPs on osteoclasts are well understood, particularly those of the new, more potent, nitrogen containing BPs. As demonstrated in table 1.1, the relative potencies of the available BPs have increased immensely as new molecules are developed. Etidronate, Clodronate and Tiludronate are all nitrogen lacking BPs, therefore exhibit low anti-resorptive potencies. The BPs listed in Table 1.1 however are nitrogen containing bisphosphonates (N-BPs) and thus exhibit high potency. This increase in potency with the addition of the nitrogen atom is due to the ability of the molecule to inhibit farensyl diphosphate synthase (FPPS) an enzyme of the mevalonate pathway. This inhibition of FPPS results in reduced prenylation of guanosine triphosphases (GTPases), such as Ras, in effect causing decreases in osteoclastogenesis, survival and function (Rogers *et al.*, 2000, Schindeler and Little, 2005). Thus N-BPs potently inhibit many aspects of osteoclast function, leading to retention of calcium in the skeleton due to reduced osteoclastic resorption. Subsequently this reduced resorption results in increased intestinal calcium absorption. In growing rats this has resulted in an increase in bone mass (Licata, 1997).

Table 1.1
Relative Anti-Resorptive Potencies of Bisphosphonates

Compound	Relative Potency
Etidronate	1
Clodronate	10
Tiludronate	10
Pamidronate	100
Alendronate	500-1,000
Risedronate	5,000-10,000
Ibandronate	10,000
Incandronate	1,000
Zoledronic Acid	20,000

Table 1.1 *Outlines the approximate relative potencies (to Etidronate) of bisphosphonates in inhibition of metaphyseal bone resorption in vivo*. (Fleisch, 1999).

More recently it has been shown that bisphosphonates can have direct effects on osteoblasts, perhaps through bFGF, (Sahni *et al.*, 1993, Giuliani *et al.*, 1998a). In vitro experiments have that pamidronate and zoledronic acid specifically up-regulate the production of new bone by osteoblasts, while etidronate does not (Reinholz *et al.*, 2000). However, new *in vivo* techniques for examining the effects of BP bound to a calcified matrix on osteoblasts suggest that osteoclastic resorption and release of the BP are required before osteoblast affects are seen (Schindeler and Little, 2005). This new technique offers a model that more closely resembles the processes that occur *in vivo*. This study suggests that the results seen in all *in vivo* examinations of the effects of BPs on osteoblasts without the presence of a calcified matrix are not clearly representative of the biological processes *in vivo*.

1.5.2 Bisphosphonates for the treatment of osteoporosis

Third generation N-BPs have been proven to be effective in osteoporosis. Their effectiveness has been attributed to their high specificity for bone and their anti-

osteoclastic activity. The overall result from treatment with N-BPs being an increase in net bone mass, reduced bone turnover and thus a reduction in the incidence of fracture (Rodan, 1997). The N-BP, alendronate (ALN), has been shown to be effective in increasing bone mass and reducing fracture rates in postmenopausal osteoporosis. A trial was performed using ALN and included 2027 women with osteoporosis and at least one vertebral fracture (Black *et al.*, 1996). Fifteen percent of control patients sustained new vertebral fractures whereas only 8% of women in the ALN treated group had fractures. Recently presented clinical trial results, of a once-yearly infusion of 5mg of zoledronic acid in post menopausal women, saw a 70% decrease in the occurrence of vertebral fractures and a 40% decrease in hip fractures (Black *et al.*, 2007).

1.5.2.1 Bisphophonates and mineralisation of bone

Mineralisation of bone tissue during bone formation occurs in two stages; firstly a primary mineral deposition occurs at the calcification front, followed by a slower progressive increase in deposition, commonly referred to as secondary mineralisation. The pathological bone turnover resulting in osteoporosis involves not only a decrease in the degree of secondary mineralisation, but also the premature removal of primary mineralised tissue before secondary mineralisation begins. BPs such as ALN have been used for many years to treat such pathological bone turnover. It was initially understood that BPs prevented resorption of existing bone tissue, thus preserving the bone architecture. However, more recently it has been revealed that BPs also allow for enhanced or prolonged secondary mineralisation (Boivin and Meunier, 2002a, Stepan *et al.*, 2003).

Secondary mineralisation occurs through preservation of mature basic multicellular units (BMUs) and an accompanying reduction in the formation of new BMUs. New BMUs are sites of new bone formation and are thus under-mineralised when compared to mature BMUs. Hence a higher ratio of mature to new BMUs leads to a higher level of mineralisation (Allen and Burr, 2007). In a study of ALN therapy in post menopausal osteoporotic women, the mean degree of mineralisation of bone was increased up to 11.4% compared to untreated controls. These results translate to significant increases in BMD at the sites measured and significant increases in bone strength (Boivin *et al.*, 2000).

With reduced bone resorption however comes the problem of reduced bone turnover, leading to the accumulation of micro damage in bone tissue. Bisphosphonate induced accumulation of micro damage has been well documented in both animal models, (Mashiba *et al.*, 2000, Bosch *et al.*, 2000, Miller *et al.*, 2007) and clinical

investigations (Stepan *et al.*, 2003, Nyman *et al.*, 2004). Due to reducing the number of active BMUs, BPs reduce the removal and repair of micro fractures, leading to their accumulation. To date however there has been little evidence to suggest the accumulation of such small scale tissue damage has a negative impact on the quality of the bone. In fact, most studies have shown increases in overall strength with no change in the intrinsic material properties of the bones. These results have been attributed to the enhanced degree of mineralisation produced by BP treatment (Bosch *et al.*, 2000, Miller *et al.*, 2007).

1.5.2.2 Potential complications of bisphophonate therapy

As the number of osteoporotic patients on chronic BP therapy increases so do new concerns about the possible negative effects BPs may have in these patients (Fleisch, 2001, Odvina *et al.*, 2005). Although fracture incidence is reduced with treatment it is not completely prevented, thus consideration must be given to treatment after a fracture occurs in these patients. Bisphosphonate inhibition of osteoclast function may interfere with the initial stages of the repair process thus questions have been raised as to whether patients should discontinue treatment during the course of repair (Odvina *et al.*, 2005). Even so, assessment of fracture healing, under the influence of high dose BP treatment of Osteogenesis Imperfecta, revealed no interference with fracture healing (Munns *et al.*, 2004, Pizones *et al.*, 2005).

If however it can be shown that the initial vital stages of fracture repair proceed normally in the presence of BP treatment, these concerns may be resolved. In fact, BP treatment can provide a positive effect on the modulation of fracture by increasing the net bone mass of the callus, consequently providing increased resistance to re-fracture (Amanat *et al.*, 2005). Delayed fracture repair has in fact been shown in a rat model of osteoporosis, suggesting that cessation of treatment in osteoporotic patients may indeed impair the process further (Namkung-Matthai *et al.*, 2001). Moreover, a recent study showed that ALN treatment in a rat non-union fracture model significantly increased the union rate over controls (Toro J, 2005).

1.5.2.3 Regimen options for bisphsphonate treatment

Frequency of BP dosing is an emerging area of concern when treating osteoporotic patients. As new more potent BPs emerge on to the market, opportunities arise for reducing the frequency of administration. The current treatment of the Australian population of osteoporosis sufferers is a weekly oral form of ALN. However new BPs, such as ibandronate and zoledronate, provide monthly oral or yearly intravenous administration. Comparisons of these new options to the weekly ALN have been performed, revealing improved patient compliance and reduced side effects whilst

maintaining equivalent levels of improvement in bone properties (Lindsay R *et al.*, 2006). The effects of BP treatment on fracture healing may also be influenced by the dosing regime. Weekly BP doses would increase the amount of newly formed fracture callus that the compound is to. Monthly or yearly BP doses on the other hand would only bind to the callus formed at the time of administration. Thus, to reduce the accumulation of BP in a fracture callus, less frequent BP dosing may be optimal when augmenting fracture healing. A single dose bound to a portion of callus bone, may prevent early resorption of primary callus but allow for remodelling to proceed following the achievement of union. One part of the study outlined by this thesis is designed to examine the theory that less frequent dosing of more potent BPs may be optimal in the augmentation of healing fractures.

1.5.3 Bisphosphonates and fracture repair

While not specifically used as a therapeutic strategy in normal healing fractures, many reports document increased callus size after BP administration during fracture repair.

The effect of Pamidronate on fracture repair in sheep was investigated with the aim of assessing its role in fractures around cancer metastases in patients already treated with BPs (Goodship *et al.*, 1994). Using a weekly dose of 0.5 mg/kg for 4 weeks pre operatively and 12 weeks post operatively, they noted an increase in mineralisation of the callus, but demonstrated subsequent decreases in hard callus remodelling. Torsional strength was also increased in the treated group. They concluded that Pamidronate used in the treatment of metastases may restore the integrity of the healing bone faster than in untreated individuals.

A series of experiments on the effects of Clodronate on fracture healing were performed by Nyman and colleagues. Firstly, rats given weekly clodronate 50 mg/kg subcutaneously regained equivalent tensile load capacity to that of the un-fractured bone, while calluses were remodelled to lamellar bone in both groups. clodronate produced calluses that were significantly heavier and contained more calcium than those in the control group at 2 months after fracture (Nyman *et al.*, 1996). Using a similar protocol, clodronate in rabbits led to increased callus formation and reduction in osteopenia under a rigid plate used to internally fix a fracture (Nyman *et al.*, 1993a). Lastly, a study in 1996 led them to conclude that after clodronate administration; the differentiation of osteoblasts into mature osteocytes was disturbed, producing abnormal bone structure around the osteocytes. In the clodronate-treated group, the amount of newly formed bone matrix appeared increased, but mineralisation of the bone matrix was

delayed. Spatial organisation of the trabecular bone was reduced compared to the control animals. However no delay occurred in the union of the bone segment by new bone with clodronate administration (Nyman *et al.*, 1993b).

Tarvainen and colleagues performed a study in denervated rats to assess the effects of Clodronate on fracture healing in an osteoporotic environment (Tarvainen *et al.*, 1994). Clodronate treatment did not affect the bending strength of healing callus of osteopenic rats at 2, 4, 8, or 12 weeks after fracture, but reduced the strength of healing callus in normal rats ($p < 0.05$) at 8 weeks. Radiological callus width increased in Clodronate-treated groups both in osteopenic (8 and 12 weeks, $p < 0.001$) and normal rats (8 weeks, $p < 0.05$) when compared with saline-treated groups. As previously shown, remodelling of the fracture callus was delayed with Clodronate.

ALN, a newer, more potent BP, was examined in fracture healing in beagle dogs, with the aim of highlighting any detrimental effects (Peter *et al.*, 1996). A 2 mg/kg/day dose was given for 9 weeks preceding fracture, 16 weeks after fracture, or both before and after fracture (25 weeks). They noted normal bone healing at the fracture site in all dogs. Conversely, ALN treatment during the fracture-healing period led to a 2-3 fold increase in calluses size at 16 weeks compared to those in dogs that received a placebo during the healing period. They described this result as a consequence of slower callus bone remodelling, an expected effect of the compound. Mechanical testing showed that both the ultimate load at failure and the flexural rigidity of both the fractured and contralateral intact bone were unaffected by treatment with ALN. The authors concluded that treatment with ALN before or during fracture healing, or both, resulted in no adverse effects on the union, strength, or mineralisation of bone in mature beagle dogs (Peter *et al.*, 1996).

Li and group aimed to test “whether bisphosphonates disturb the process of fracture healing”. Six doses of 0.01 or 0.1 mg/kg of incadronate was administered to rats over a period of two weeks prior to creating fractures using an open osteotomy technique. They showed increased callus formation in rat femoral fractures pre-treated with incandronate (Li *et al.*, 1999). As seen in Figure 1.13 continuation of therapy, 3 doses per week, for 16 weeks after fracture, increased callus formation even further, but the new bone did not remodel to form a cortical shell as seen in the pre-treated group. This delay in remodelling was offset by the increased volume of callus in the continual dose group, thereby still producing an improvement in the mechanical properties of the healing bone.

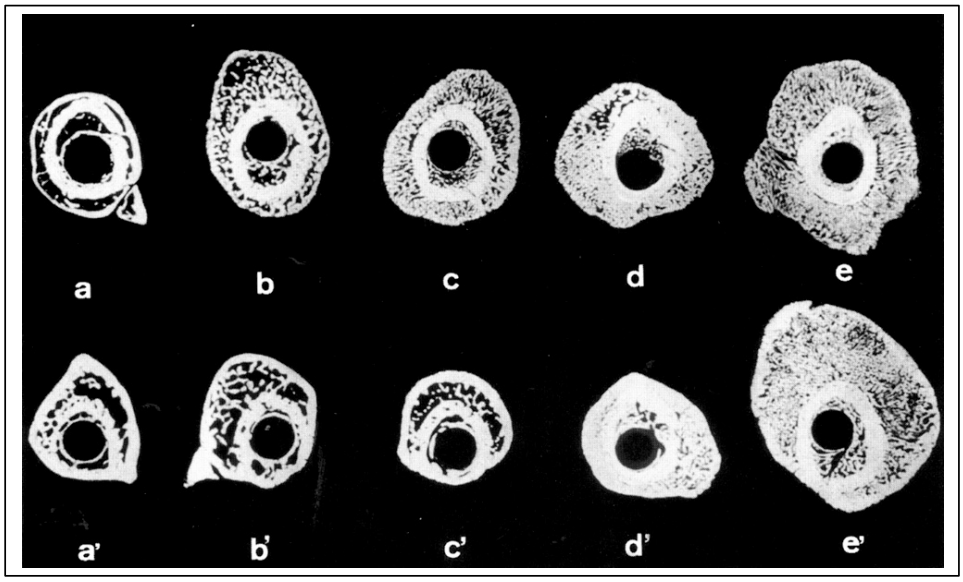

Figure 1.13 *Effect of incadronate on rat fracture healing.*

The top row are animals culled at six weeks, the second row were culled at 16 weeks. The groups are a) controls, b) pre-dosed with six doses of 0.01 mg/kg, c) pre-dosed with six doses of 0.1 mg/kg, d) pre-dosed and continued on 0.01 mg/kg three times per week, e) pre-dosed and continued on 0.1 mg/kg three times per week. There is an increased amount of immature callus at six weeks in all treated groups, and group e) at 16 weeks shows an enormous amount of new bone formation, but with no evidence of remodelling. Reproduced with permission from (Hadjiargyrou *et al.*, 2000).

More recently a study was published using the same doses of incadronate with the aim of assessing the early effects on fracture healing at two and four weeks (Li *et al.*, 2000a). Despite the illustrative cases showing increased callus formation (Figure 1.14), the histomorphometric measurements of callus area were only significantly different between the continuous high dose treated and control groups at four weeks. This lead Li and colleagues to conclude that: "*with respect to clinical usage, the present study suggests that bisphosphonates cannot be used clinically as agents to increase callus formation*".

Although this study was unable to demonstrate an early enhancement in callus formation it did answer one important question governing our work. By measuring the concentration of the BP in the fracture callus was at 2 and 4 weeks after fracture the authors provide important evidence for the recirculation of BP during the healing process. The incandronate concentration in the callus fell off over time, but was still detectable at 4 weeks post fracture in the group pre-dosed with the drug. This suggests that the effects on the callus were due to recirculation of the drug directly acting on the callus and not due to serum calcium balance changes.

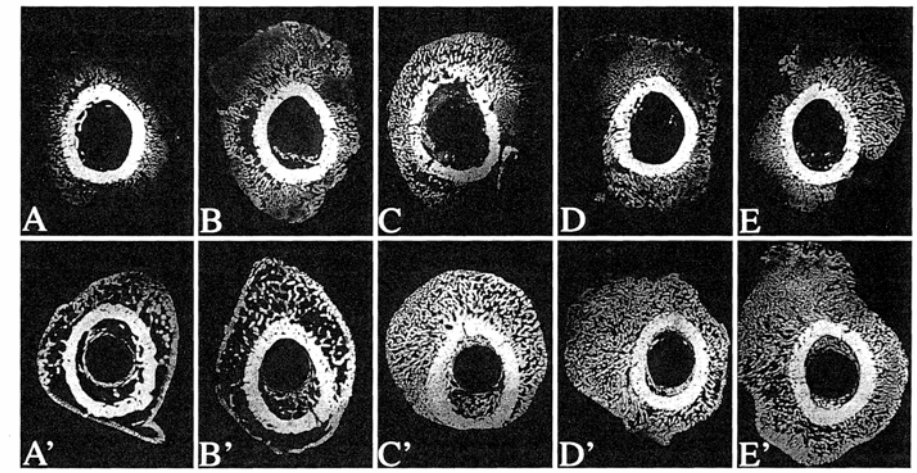

Figure 1.14. *Effect of incadronate on rat fracture healing.*

The top row are animals culled at two weeks, the second row were culled at four weeks. The groups are A) controls, B) pre-dosed with six doses of 0.01 mg/kg, C) pre-dosed with six doses of 0.1 mg/kg, D) pre-dosed and continued on 0.01 mg/kg three times per week, E) pre-dosed and continued on 0.1 mg/kg three times per week. Remodelling is absent in D and E. Although the treated group callus looks larger than controls in all groups, the authors state only E was significant, and only at 4 weeks. Reproduced with permission from (Li *et al.*, 2000a).

Clearly BP treatment during fracture healing has been thoroughly explored, however these experiments do not show the potential for increased bone formation with BPs. The conclusion that BPs cannot be used to increase callus formation is not justified by this data. The study of Peter *et al* and our own work refute this. Firstly, recent work by our group examining the timing of a single dose of zoledronic acid in a rat closed fracture model showed significant increases in mineralised callus size (Amanat *et al.*, 2007). Incadronate is felt to be 10 to 50 times less potent than zoledronic acid (J Green, Novartis Pharma AG, personal communication 2000) Therefore the efficacy of incandronate, even in the high dose group the experiments performed by Li et al, is up to 10 times lower than we anticipated in our fracture experiments. Likewise, higher doses did lead to increased callus area, however as these doses were given continuously, this could be due solely to the fact that the calluses did not remodel. My proposed protocol of comparing a single bolus dose at the 1 week post surgery against continuous weekly dosing commencing 1 week post surgery will explore this theory. The single dose should allow for remodelling to commence at the later time points whilst being potent enough to induce an increase in callus size in the earlier stages.

Finally, in a bone defect model, inhibition of bone repair was shown with extremely high doses of locally delivered pamidronate (Choi *et al.*, 2007). Using a poly L-lactide-co-glycolide (PLGA) carrier pamidronate was delivered locally in a rabbit calvarial bony defect model at total doses of 2mg and 3mg. At 2 weeks post surgery, reduced bone formation was noted in pamidronate groups compared to PLGA only and control

samples, with avascular necrosis evident only in pamidronate samples. By 4 weeks, pamidronate samples were infiltrated by inflammatory cells, not present in control samples. By 8 weeks pamidronate defects showed extensive avascular fibrotic tissue in with no sign of bone tissue, in contrast to control samples which were completely healed.

Although this study did not use a weight bearing long bone fracture model, the outcomes remain highly relevant to this investigation. By delivering the high pamidronate doses locally, these authors achieved local dose concentrations high enough to impede bone healing. This was suggested to be a result of anti-angiogenic, anti-MMP and local cellular cytotoxic effects of the high dose pamidronate. However, the authors confirmed a slow release of approximately 500µg of pamidronate per day from the PLGA carrier, ruling out cytotoxic effects on osteoblasts but not osteoclasts.

1.5.4 Bisphosphonates and bone growth

Bisphosphonate treatment appears to have a negative effect on the function of the growth plate. Studies have documented these effects in laboratory animals (Li *et al.*, 1999, McCarthy *et al.*, 2002, Evans *et al.*, 2003, Smith *et al.*, 2005), although the doses of BPs used in these studies are considerably high. In contrast to this, using increasing doses of the early generation BP, tiludronate, Murakami and group demonstrated no effect on growth plate height in young rats (Murakami *et al.*, 1994). Treatment with clinically relevant doses of clodronate also showed no undesirable effects on the vascular invasion and removal of the cartilaginous matrix in the growth plate, thus no disruption of growth. It was pointed out however, that an increase in metaphyseal primary spongiosa was evident due to reduced resorption (Deckers *et al.*, 2002).

Such changes in metaphyseal primary spongiosa with BP treatment are commonly reported (Amanat *et al.*, 2005), and are often associated with decreases in longitudinal growth (Little *et al.*, 2003b, Smith *et al.*, 2005). However, growth plate morphology is not often analysed in such studies. One study did set out to explore the exact effect of BPs in growing rats and demonstrated decreases of 16% and 19% in femoral length with high dose pamidronate and zoledronic acid (ZA) respectively. However, growth plate height in these samples remained unaffected, dissociating growth plate height and longitudinal growth under BP treatment (Pataki *et al.*, 1997). On the other hand, very high doses of the bisphosphonate ALN were examined on a mouse model of osteogenesis imperfecta (*oim*) and significant growth plate disruption was seen (Camacho *et al.*, 2001). This model replicates a human bone disorder caused by a defect in the gene encoding type I collagen. The phenotype of this disease

is variable with patients suffering varying degrees of impairment of bone structure and mineralisation. They commonly suffer from fractures due to osteoporosis from accelerated remodelling. BPs have therefore become a common treatment for this disease as it reduces the rate of remodelling, resulting in increased mineralised bone and thus reduced fractures.

The effects of long term BP treatment on the growth of osteogenesis imperfecta sufferers has raised much concern, leading to studies such as that performed by Evans *et al.* It was concluded in this study that doses of ALN greater than 2.5mg/kg/wk result in inhibition of growth through alteration of growth plate morphology. Enlargement of the growth plate in the treated samples, particularly the hypertrophic chondrocyte zone, is a sign of reduced vascular invasion and cartilage matrix resorption. This result might be explained by the inhibitory effects of BPs on MMPs at extremely high doses (section 1.5.5) The low dose group (0.125mg/kg/wk) showed no effect on overall growth and growth plate height in this model. This low dose represented clinical doses used to treat osteogenesis imperfecta patients (Evans *et al.*, 2003).

However, these concerns have not been duplicated in clinical studies in children. Brumsen *et al*, reporting their experience of 12 immature patients on long term bisphosphonate therapy, documented normal linear growth, and indeed catch-up growth occurred in those patients treated before puberty (Brumsen *et al.*, 1997). Moreover, in a study examining 3 years of pamidronate therapy in children with polyostotic fibrous dysplasia, Plotkin and colleagues documented stable height z-scores in all patients regardless of treatment (Plotkin *et al.*, 2003).

As suggested earlier, the cells responsible for driving endochondral ossification may exclude the mature resorbing osteoclast. Therefore, the anti-osteoclastic effects of a BP may not be the cause for the detrimental effects seen at the growth plate. Instead they may be due to anti-MMP effects or direct effects on chondrocytes themselves as suggested by some authors (Smith *et al.*, 2005).

1.5.5 Zoledronic acid and fracture repair

I have elected to explore the properties of zoledronic acid (Novartis) in fracture repair. Zoledronic acid (ZA) is being investigated as a more potent, hopefully even safer BP than those previously explored (pamidronate, clodronate). ZA is the most potent BP synthesised to date and whose chemical structure is shown in Figure 1.15. ZA has been approved in Australia for use in hypercalcemia of malignancy and is under development for use in the treatment of Paget's disease and osteoporosis. Due

to its relative anti-osteoclastic potency, ZA is administered clinically intra-venously on a quarterly to yearly basis for benign conditions, and monthly in cancer patients.

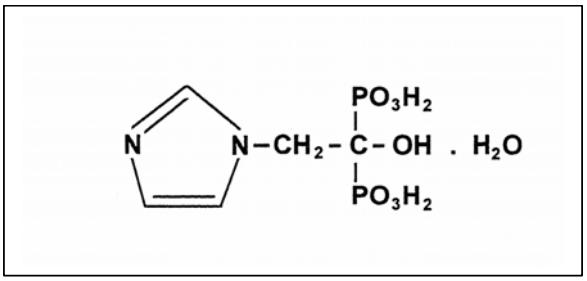

Figure 1.15 *The chemical structure of zoledronic acid.*

The potency of ZA is also beneficial in relation to MMP inhibition. Whilst investigating the effects of various BPs on metastatic bone formation Boissier *et al* concluded that all BPs are capable of anti-MMP activity. It was shown that increasing doses of clodronate, ibandronate and zoledronate (zoledronic acid) resulted in decreased MMP-9 activity, the mechanism of which was described (Boissier *et al.*, 2000). The 'bone-hook', common to the structure of all bisphosphonates, is responsible for their capability to bind to bone and also the chelation of divalent cations and thus the growth inhibition of calcium crystals. It was thus hypothesised that since the actions of MMPs is dependent on zinc (a divalent cation), BP inhibition would occur through similar chelation of zinc, thus reducing it's availability to MMPs. This was supported by the fact that the effect was completely reversed in the presence of zinc. It is due to this mechanism that a highly potent BP would have decreased MMP inhibitory effects.

Since each molecule of any BP carries this zinc chelating "bone hook" then the fewer the molecules circulating, the less zinc chelated and thus reduced inhibition. Therefore zoledronic acid used at low doses due to its high potency should not have the anti MMP effect that higher doses of less potent BPs would posses. Evidence to support this theory is supplied by Teronen *et al.* who specifically examined the MMP inhibitory effects of numerous BPs *in vivo* (Teronen *et al.*, 1999). Figure 1.16 summarises the results produced from this work and demonstrates obvious differences between the different BPs examined.

TABLE 1. The effects of various bisphosphonates on MMP activities, activation, production, and malignant cell invasion

Downregulation or inhibition of:	Clondronate	Pamidronate	Alendronate	Zolendronate	Nedrinate	Clodrinate	Tilundronate
MMP-1 activity	+++	+++					+++
MMP-2 activity	+++	+					
MMP-3 activity		+++	+++				+++
MMP-8 activity	+++	+++	+++				
MMP-9 activity	+++	+++	++				
MMP-12 activity			+++	+++			
MMP-13 activity		+++	+++				
MMP-14 activity	+++						
MMP-20 activity				+++			
U2-OS MMP-2 activation	+++						
MG63 MMP-2 activation	++						
MG63 MT1-MMP expression	+++						
MG63 MT1-MMP production	+++						
HT1080 cell invasion	+++		+++		+++	+++	
C8161 cell invasion	+++		+++		+++	+++	

Figure 1.16. *The effects of various BPs on MMP activities, activation, production, and malignant cell invasion.* Reproduced with permission from (Teronen *et al.*, 1999).

Earlier, less potent BPs such as clodronate, pamidronate and alendronate exhibit a broad inhibition of MMP activity, including MMP-9 and MMP-13. The more potent zoledronic acid on the other hand showed inhibitory effects only on MMP-12 and MMP-20. It is unclear from this study what exact concentration of each BP is required to produce this inhibition (Teronen *et al.*, 1999). ZA therefore offers a therapy with highly potent anti-osteoclastic effect and minimal inhibition of the MMPs. ZA thereby offers an avenue to closely explore the role of osteoclastic resorption during endochondral fracture repair without the concerns of concurrent inhibition of MMP driven resorption.

1.5.6 Bisphosphonate dosing regimes

As it is expected that ZA treatment will result in delayed remodelling of hard callus during fracture repair, two different dosing regimes will be investigated. All dosing will begin one week post fracture to allow for initial callus formation and stability to be achieved. Previous results from a pilot study in a similar closed model revealed that at 1 week post fracture a significant cartilaginous callus had formed (unpublished data). Since it is the remodelling of this soft callus into hard callus that we wish to investigate dosing will commence after cartilage callus formation. Also, since ZA has a high affinity for bone and we wish to enhance the concentration of the dose at the fracture site, we require bony callus for it to bind to. The fracture callus prior to the 1 week time point, consists mainly of fibro-cartilage tissue thus the ZA will not bind to and remain at the fracture site. Delaying the dose by 1 week allows for mineralised callus formation, providing a mechanism to enhance the dose localisation at the injury site.

A single dose of ZA will be administered subcutaneously 1 week post fracture and will be compared to the same total dose divided into weekly doses. It is hypothesised that at 6 weeks post fracture the single dose group should have increased hard callus remodelling over the continuously dosed group. The constant incorporation of ZA into the forming callus will further delay its resorption whereas the cessation of ZA dosing should allow for remodelling of the callus formed after the 1 week dosing time point. This is due to newly formed bone only having trace amounts of recirculating ZA to bind. The clinical relevance behind this dosing investigation is to provide evidence for both the safe use of BPs during fracture repair and also the cessation of BP treatment after initial repair to allow for complete callus remodelling.

1.6 Study hypotheses and conclusions

The investigations to be performed in this study aim to support the following hypotheses developed through this thorough review of the literature on endochondral ossification.

By inhibiting osteoclast function with the use of ZA in a rat fracture model it will be illustrated that resorbing osteoclasts are not essential to the process on endochondral ossification during the initial stages of fracture repair. If no effects are seen on the process then the study will also provide evidence for the safe use of BPs during periods of fracture repair. In fact, by providing a larger stronger callus without delaying the vital initial repair stages the potential use of BPs as an adjunctive therapy during fracture repair may be realised.

To approach this hypothesis with a non-pharmacological model of reduced osteoclastic resorption, endochondral fracture repair will also be explored in the osteopetrotic *ia/ia* rat. By demonstrating normal endochondral fracture union in the absence of resorbing osteoclasts in these rats, the outcome of the ZA experiment will be validated.

It is also believed that through analysis of the growth plate samples in both the ZA fracture study and the incisor absent rats, we will provide evidence to support the recent findings on the role of the osteoclasts during ossification at this site. Furthermore, this study may help clarify the effects of BPs on growth plate morphology at therapeutic doses.

The comparative dosing regimes analysed in this study will reveal pertinent information regarding the issue of continuous dosing versus a single bolus dose. From the results of similar investigations it is believed that a single bolus dose may be optimal over continual dosing. By providing a larger and stronger callus than normal but allowing normal hard callus remodelling to proceed, a single bolus dose could be

viewed as the most favourable regime. On the other hand, continual dosing may not allow hard callus remodelling to proceed, therefore hindering the process. This result may also be of interest in regards to osteoporotic patients on chronic BP treatment who sustain fractures. If no negative effects are seen by the bisphosphonates on the vital early stages of fracture repair then clinicians will be provided with evidence suggesting that continuation of treatment will not be detrimental. However, if the hypothesis that continual dosing in this model prevents the final remodelling stage of repair is realised, it may be suggestive that treatment should be ceased at this time.

This extensive investigation will provide new evidence in the area of endochondral ossification during skeletal growth and repair and may create avenues for new therapeutic approaches to fracture repair.

2 Justification of methods

2.1 Use of the Einhorn rat fracture model

2.1.1 Species selection

The rat has been a popular animal model for the study of fracture healing of both long bones (tibia, femur) and flat bones (skull) (Bonnarens and Einhorn, 1984, An *et al.*, 1994). As an adaptable small animal model that is still large enough to allow for reproducible mechanical testing, this species was utilised to explore fracture healing. Furthermore, as fracture healing is particularly sensitive to age, it was assessed in young rats in this study to achieve more rapid and reproducible healing (Nunamaker, 1998, Meyer, Jr. *et al.*, 2001). Wistar rats were used in this study examining fracture healing in normal rats.

2.1.2 The incisor absent rat

When examining the role of the resorbing osteoclast during endochondral ossification, pharmacological inhibition of these cells did not provide sufficient proof to confirm or refute the hypotheses. Accordingly, a model of biologically inhibited osteoclastic resorption was sought to complete this investigation. The incisor absent (*ia/ia*) rat offers such a model with extensive osteopetrosis due to a significant reduction in osteoclastic resorption of bone (section 1.4.6.1). Although a thorough phenotypic investigation was required before exploring endochondral fracture repair in these rats, they provided an outstanding opportunity to confirm the outcomes produced when BPs were used to block osteoclast resorption during endochondral fracture repair. All experimental animals were housed and cared for under the conditions of the animal facility they were located in (section 8.1.1).

2.1.3 Bonnarens and Einhorn Closed fracture model

A closed fracture model was chosen over an open osteotomy model for this study, due to the reduced negative impact on surrounding soft tissue. An open model involves surgical disruption of nearby muscle and periosteal tissue resulting in a delayed healing response with reduced callus size and mechanical strength when compared to the closed fracture model (Park *et al.*, 1999). Thus due to the focus of this study being the contribution of specific cells to normal fracture healing, a less complex, faster healing model was required. The closed model of fracture repair with internal fixation, as described by Bonnarens *et al* in 1984, was therefore utilised.

A model of the 3-point drop weight fracture apparatus was designed based on that described by Bonnarens *et al*, 1984 to produce clean internally fixed closed fractures (Figures 2.1 and 2.2, section 8.1.2). This technique allows for unrestricted post-operative movement whilst maintaining axial alignment of the fractured bone.

The technique required modification to adapt for the younger *ia/ia* utilised in this study. As the femora were smaller had the mutant osteopetrotic bone phenotype, a number of modifications to the fracture apparatus were required to produce clean, reproducible fractures (section 8.1.3.2).

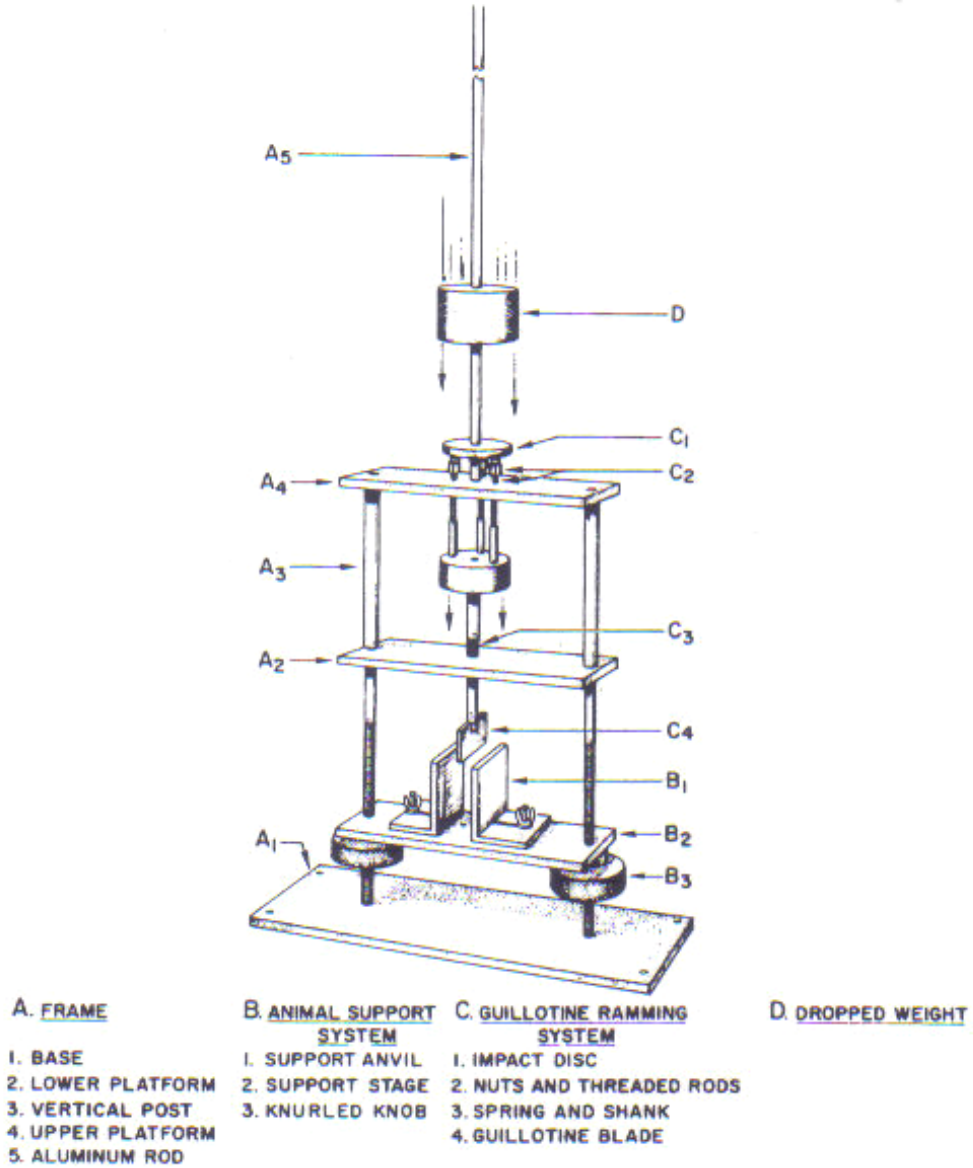

Figure 2.1 *Image of closed fracture apparatus sketch from Bonnarens and Einhorn used to develop apparatus used in this study*. Derived with permission from (Bonnarens and Einhorn, 1984). The femur is placed at the 3-point guillotine blade (C4) and support (B1) to produce a fracture by dropping the weight (D)

Figure 2.2 *Image of closed fracture apparatus used in experiments.*

This apparatus was developed based on that shown in figure 2.1 with some minor alterations. The femur was placed at the 3-point guillotine and the weight dropped to create fractures. This was used in studies outlined in chapters 3, 4, 5 and 6.

2.1.4 Fixation

The intra-medullary rod used in this model was a 1.1mm thick Kirschner wire which fits tightly in the medullary cavity to provide stable but non rigid fixation, with good fracture alignment (section 8.1.2).

As this study focused on the role of the osteoclast during endochondral fracture repair, a certain level of mechanical instability was required. High stability or rigid fixation of fractures has been established to induce healing through mainly intramembranous type bone formation, omitting the formation of an initial cartilaginous callus and thus its transformation into bone through endochondral ossification. Less stable fixation results in the production of a cartilage anlage to establish initial stability at the site, then proceeds through endochondral ossification to union. (Bonnarens and Einhorn, 1984, Goodship *et al.*, 1993, Mark *et al.*, 2004a). Therefore, the intramedullary pinning technique with minimal stability used in this study provided the perfect environment for normal endochondral fracture union to occur. It was important to ensure good alignment of all fracture sites to make mechanical testing of the samples feasible.

2.1.5 Exclusion criteria

As the production of fractures using the closed technique is not completely controlled, production of a clean transverse mid diaphyseal fracture was not 100 reproducible. As it is important to examine a homogenous experimental population, reproducibility of fractures was paramount. Using x-ray, each fracture was assessed for fragmentation, angulation and placement (section 8.1.2 and 8.1.3.2). An exclusion rate of approximately 10% was produced by this assessment, as those animals with fractures deemed as not acceptable were removed from further examination.

2.2 Fracture repair time course of analysis

2.2.1 Background on initial endochondral fracture union

Endochondral fracture repair involves production of an initial stabilising cartilage soft callus which is progressively removed and replaced by woven bone tissue until union is achieved (section 1.3.1). As the aim was to outline the role of the osteoclast during this process, a detailed assessment at numerous stages of endochondral repair was crucial.

2.2.2 Time points examined to assess initial endochondral repair

In order to ensure the process of endochondral fracture healing in the Wistar rats used in this experiment could be closely examined, 4 early time points were employed. Post fracture samples were harvested at 1, 2, 4, and 6 weeks, providing information from calluses containing a large amount of cartilage at 1 week, to complete union through removal of cartilage at 6 weeks (section 8.1.5). These time points were determined from the results obtained by other investigators using a similar closed fracture model (Bonnarens and Einhorn, 1984, Kokubu *et al.*, 2003, Meyer, Jr. *et al.*, 2001, Einhorn, 2005). In addition, open rat fracture studies which involve a greater extent of soft tissue damage performed previously by our research group demonstrated almost complete fracture union, as determined by x-ray, by 6 weeks (Amanat *et al.*, 2005, Jackson *et al.*, 2006).

2.2.3 Background on hard callus remodelling during fracture repair

The final process of fracture repair requires restructuring of the mineralised callus formed during endochondral repair until the site resembles the original whole bone structure. This entails the actions of both osteoclasts and osteoblasts acting in concert, remodelling the hard callus into compact lamellar bone to produce a new cortical structure to replace the damaged bone (section 1.3.3). It is well understood that

osteoclastic activity is essential to this process, as in the absence of bone resorption; hard callus remodelling is substantially hindered (sections 1.4.4 and 1.5.3). As fracture repair is a comprehensive process from injury through union to the re-establishment of the original structure, this examination would not be complete without assessing the effects of reduced osteoclast activity during the later remodelling phase.

2.2.4 Time points examined to assess hard callus remodelling

The phase of remodelling in the rat closed fracture model commences as early as 4 weeks post fracture. Evidenced by a reduction in callus size at this stage, osteoclastic resorption of the primary hard callus is occurring even prior to achievement of bony union. From 6 weeks onwards, the effects of extensive remodelling can be seen in the normal healing fracture, with little primary woven bone callus remaining after being remodelled into a new cortical shell. Inhibition of osteoclastic resorption however prevents this early remodelling such that by 6 weeks extensive amounts of this primary callus remain. Two further time points at 12 and 26 weeks post fracture were therefore employed to examine the rate of re-establishment of original bone structure with and without inhibition of resorption. Previous studies examining the effects of BPs and other anti-resorptive therapies on hard callus remodelling during fracture repair in rats have explored post fracture samples at 12 and 16 weeks (Tarvainen *et al.*, 1994, Li *et al.*, 1999, Cao *et al.*, 2002) However control samples in these studies did not show complete re-establishment of normal cortical bone structure, with hard callus still remaining (Figure 1.13). Thus, a later time point of 26 weeks post fracture was added to this investigation.

2.3 Selection of Bisphosphonate dosing regimes

2.3.1 Background on zoledronic acid

The anti-resorptive capacity of BPs comes from their ability to specifically bind bone tissue and inhibit its resorption by osteoclasts (section 1.5). A new generation of BPs have been released as new therapeutic agents in the class of anti-resorptives. These BPs contain a nitrogen atom and so are called N-BPs. Zoledronic Acid (ZA) belongs to this group of N-BPs and therefore exhibits more potent anti-resorptive effects than previous BP compounds, section 1.5.

2.3.2 Single dose compared to weekly dosing of ZA

As a result of its increased efficacy and potency, ZA offers the potential for reduced dosing levels and frequency. Currently used less potent BPs such as ALN, have been administered orally on a weekly basis with outstanding anti-resorptive efficacy. In a comparative study of once yearly ZA and weekly ALN doses in post-menopausal osteoporotic women, more rapid and greater reductions in resorption with yearly ZA were shown compared to weekly ALN (Lindsay R *et al.*, 2006). Furthermore, patient preference was strongly in favour of the yearly ZA, improving patient compliance. Therefore, improved potency and resulting reduced dosing frequency are emerging trends for current BP therapy. An understanding of how this extreme change in BP administration may affect fracture repair is essential. By comparing a single dose of ZA to divided weekly doses in this fracture repair investigation, the aim of my work was to outline new and exciting insights into the effects of different BP dosing regimens.

2.3.3 Determination of ZA dosage

BPs not only exhibit strong anti-osteoclastic effects, they have also been shown to demonstrate inhibitory effects on other cell types and processes, including osteoblasts and vascular cells that drive angiogenesis (Wood *et al.*, 2002, Reinholz *et al.*, 2002, Hamma-Kourbali *et al.*, 2003, Greiner *et al.*, 2006). BPs have also been implemented in the reduction of skeletal events related to malignant tumours, in particular bone metastases and multiple myeloma (Boissier *et al.*, 2000). However, the dose level required for such anti-angiogenic efficacy is far higher than the anti-osteoclastic dose levels. Treatment of cancer and bone metastases with intravenous (IV) ZA range in dose levels from 4mg to 16mg for a 50kg patient monthly (Chen *et al.*, 2002, Lipton *et al.*, 2002, Corey *et al.*, 2003). For the treatment of osteoporosis however doses of 4-5mg of IV ZA are given annually (Yang *et al.*, 2005, Lindsay R *et al.*, 2006).

As this study aims to examine the role of the osteoclast during endochondral fracture union and hard callus remodelling, only anti-osteoclastic ZA dose levels are required. Thus, based on the 5mg dose administered to an approximately 50kg elderly osteoporotic female, the dose of 0.1mg/kg formed the basis for the ZA dosing used in this examination. Previous studies performed by our group examining ZA during bone healing have successfully utilised this dose to enhance callus size and strength (Little *et al.*, 2003a, Little *et al.*, 2003b, Amanat *et al.*, 2007).

The dose levels that were therefore used were: the high dose groups of a single bolus dose of 0.1mg/kg or 5, weekly, divided doses of 0.2mg/kg, and the low dose

groups of a single bolus dose 0.025mg/kg and 5, weekly, divided doses of 0.005mg/kg (section 8.1.4.1). The high dose levels have increased clinical relevance in regards to the effects of anti-resorptive therapy such as ZA on both endochondral union and hard callus remodelling during fracture repair. The lower dose levels were employed only for the examination of the early phase of endochondral healing. This additional dosing level was included to allow consideration of lower ZA dosing regimens for the augmentation of initial fracture healing. Further, this lower ZA dose group was also added to provide further knowledge on the systemic effects of ZA treatment in growing rats.

2.3.4 Systemic effects of ZA treatment

The high bone specificity of BPs indicates that a systemic dose would distribute throughout the entire skeleton. Hence the anti-resorptive effects of BP dosing would be evident on a whole system level. In regards to treating a localised situation, such as a long bone fracture, other underlying effects of BPs should be considered. In this context, contralateral limbs and long bone growth plates were analysed in all growing rats receiving ZA in this study.

Systemic effects of BPs on long bones have been examined with a single subcutaneous (SC) dose of 3mg/kg of Pamidronate producing increases of approximately 10% in mid diaphyseal cortical bone BMC and Volume compared to saline (Amanat *et al.*, 2005). However, in young rats examining fracture repair under ZA treatment, Amanat et al showed no changes in the contra-lateral limb with a single IV dose of 0.1mg/kg Zoledronic Acid.

In a study investigating the effects of ZA in distraction osteogenesis in rabbits, 2 IV doses of 0.1mg/kg of ZA given 2 weeks apart produced a 12% increase in contra-lateral BMC in growing rabbits (Little *et al.*, 2003). Such changes would be expected due to the reduced resorption in these BP treated animals therefore close analysis of contralateral limbs were performed in all ZA treated specimens in the investigations for this thesis.

Of additional interest in all the abovementioned studies there were changes seen also at the metaphysis of the contralateral limbs. Pamidronate, as a single SC 3mg/kg dose, produced what the authors referred to as a “metaphyseal line” representing a region of retained primary spongiosa under the growth plate. Nevertheless, no mention was made as to whether the growth plates themselves were affected (Amanat *et al.*, 2005). Furthermore, this study investigated a single IV dose of 0.1mg/kg of carbon 14 (^{14}C) tagged ZA, allowing for examination of the systemic distribution of the drug. The metaphyseal bone formed at the time of dosing contained

large amounts of ZA, confirming systemic circulation of BPs and their effects on metaphyseal bone (Amanat *et al.*, 2007).

A closer examination of the retained primary metaphyseal bone in BP treated animals was performed by Smith and colleagues in 2005. Either a single IV dose, or two IV doses of 0.1mg/kg of ZA was administered to growing rabbits and produced the typical radio dense lines of retained primary metaphyseal bone. Histological examination of these lines showed they contained abundant remnants of calcified cartilage matrix surrounded by bone as seen immediately under the growth plate of untreated animals. There was a 3% decrease in longitudinal growth in these ZA treated limbs. This led to the authors examining the growth plate height which showed a 12% reduction in height in the single IV dose group and a 24% reduction in the double IV dose group when compared to saline controls. It was therefore suggested that the growth plate morphology had been disrupted, resulting in the metaphyseal lines of retained growth plate matrix and reduced growth (Smith *et al.*, 2005). Little *et al* also demonstrated reductions of approximately 5-8% in tibial length with two IV doses of ZA at 0.1mg/kg. However, the growth plate heights were not analysed in these samples.

Retardation of long bone growth is commonly associated with alterations at the growth plate, leading to speculation that BP may be affecting the growth plate in these studies. This point remains controversial with conflicting data from numerous studies. In contrast to the data mentioned above from Smith *et al* 2005, Evans and group (2003) saw an increase in growth plate height in ALN dosed osteogenesis imperfecta *(oim)* mice, (see section 1.5.4). It is with these conflicting outcomes in mind that analysis of the systemic effects of ZA in this body of work included both radiological analysis of mid diaphyseal bone from contralateral limbs along with histological analysis of long bone growth plates (sections 8.1.5 and 8.4)

2.4 Radiological Analysis

2.4.1 X-ray

X-ray analysis forms an important part of the investigations in this thesis. The surgical procedures performed to generate the fractures requires x-ray confirmation of correct intra-medullary pin placement and assessment of fracture quality. Fast acquisition of such confirmation was required to reduce anaesthesia times and hence reduce the impact on the research animals. Thus, a digital x-ray set up was used for both surgical x-rays and post harvest radiographic analysis, section 8.2.1. Post fracture samples were also x-rayed and assessed for radiological union as performed previously in fracture repair (Flick *et al.*, 2003, Makino *et al.*, 2005, Hak *et al.*, 2006).

In addition to fracture assessment, x-ray analysis was performed on samples used in the phenotype analysis of the *ia/ia* rat. This method allowed for rapid determination of the extensive osteopetrotic phenotype established by these rats and aided extensively in the selection of the time points to be analysed for determination of age of recovery in these animals.

2.4.2 Dual Energy X-ray Absorbtiometry (DEXA)

Dual energy x-ray absorbtiometry (DEXA) scans are an important non-invasive tool when examining phenotype changes in body composition. Using 2 dimensional x-rays combined with absorbance threshold analysis; DEXA scans are able to determine the mineral content and areal density of bone. These scans are commonly used to detect changes in bone area, BMC and areal BMD in either total body or individual limbs for both phenotype analysis (Phillips *et al.*, 2000) and assessment of bone repair mechanisms. (Eyres *et al.*, 1993, Maffulli *et al.*, 1997, Bauss *et al.*, 2004,(Kosaki *et al.*, 2007). Originally clinical DEXA instruments were adapted for small animals like rats with specialised software, useful only on animals greater than 200g in size. However recently the PIXImus (Lunar, Madison, WI) was designed to allow for detection of skeletal changes in small animals, namely mice, and were validated for use in rats (Soon *et al.*, 2006).

Although DEXA is not as accurate as 3 dimensional QCT scans, it does offer a fast and reproducible method of measuring density changes in a large region of interest. Due to the extensive changes in metaphyseal bone density observed on radiographs in the incisor absent (*ia/ia)* rats as described in chapter 5, it was determined that DEXA scans of this region would produce useful data to quantitate these differences (section 8.2.2).

2.4.3 Quantitative computerized tomography (QCT)

QCT offers a 3 dimensional data set of x-ray attenuation coefficients to provide analysis of mineralised tissue properties. QCT scans yield data for not only densitometric parameters including bone volume, BMC, volumetric BMD, but also geometrical measurements such as polar moment of inertia, along with periosteal and endosteal circumference of cortical bones. In addition, QCT can be utilised to distinguish between cortical and trabecular bone tissue. With an *ex vivo* precision of about 1%, as calculated by the co-efficient of variance, QCT offers an accurate assessment of skeletal elements (Gasser, 1995). Such accuracy has lead to the comparison of QCT scans to histological analysis of fracture repair, confirming it as a

tool to predict the mechanical stability of healing bones (Augat *et al.*, 1997). Further, QCT has been validated as a non-invasive estimate of rat femur bending strength (Ferretti *et al.*, 1996).

This investigation utilised QCT to assess mineralised tissue properties of fracture calluses throughout both initial healing and during the later stages of hard callus remodelling (section 8.2.3). BP treatment enhances BMC, volume and BMD at sites of skeletal repair (Little *et al.*, 2001b, Little *et al.*, 2001c, Little *et al.*, 2003b, Amanat *et al.*, 2005, Amanat *et al.*, 2007). Similar outcomes were produced in this study with differences between the two ZA dosing regimes. Further, QCT provided evidence for differences in hard callus remodelling through the dynamics of changing callus size as well as observational changes from the cross sectional images produced using the software package Scion image for Windows (Scion Incorporated, USA) (Figure 2.4a).

2.4.4 Micro computerised tomography.

Micro computerised tomography (μCT) is similar to QCT scans however demonstrates a much higher resolution of image acquisition. Due to this increased level of information very detailed 3 dimensional reconstructions of scan slices can be produced as seen in Figure 2.3.

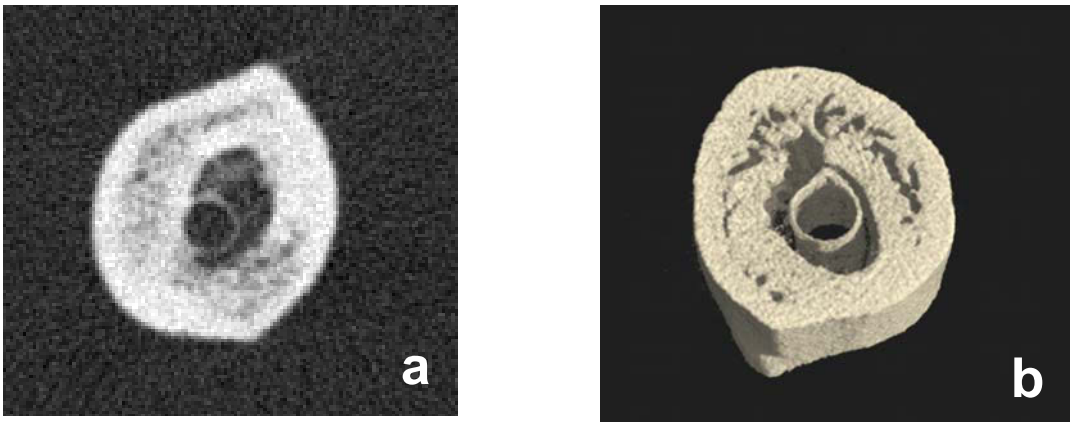

Figure 2.3 *Comparison of resolution and detail obtained from QCT and μCT scan of a fracture callus.*

(a) Example of a 2 dimensional image generated from a single cross sectional slices from a QCT scan of a fracture callus at 26 weeks post fracture. (b) Example of 3 dimensional image generated from numerous cross sectional slices from μCT scan of a fracture callus at 26 weeks post fracture. The μCT scan generates images of higher resolution and detail to allow production of useful 3 dimensional images, improving the understanding of the geometry of the bony callus.

These detailed images are generated from numerous slices, providing a 3 dimensional view of the callus geometry. Data acquisition from μCT scans are also more accurate than QCT, for both densitometric and geometric parameters, and with

increased software capabilities the generation of 3 dimensional data has also become available. Trabecular thickness and trabecular number have until now only been provided through laborious histomorphometric analysis. μCT however, provides a faster, more accurate way of generating this data, whilst also adding 3 dimensional parameters such as trabecular connectivity (Jiang *et al.*, 2000) and is commonly used to detect phenotypic skeletal changes in small animal models (Bouxsein *et al.*, 2005). This advanced 3 dimensional technique of analysing bone architecture has been compared to the conventional histological technique with outstanding correlation (Thomsen *et al.*, 2005). Thus it has provided a new, faster avenue for exploring bone structure. Although, when considering smaller changes in bone architecture, histological analysis remains more sensitive than μCT (Hordon *et al.*, 2006). Therefore this advance in skeletal analysis has not yet completely surpassed conventional methods.

The one main advantage of this technique however is the provision of high resolution information able to be transformed into 3 dimensional images. It is this aspect of μCT technology that is utilised in this investigation.

Micro CT was employed in this study to allow for 3 dimensional confirmation of histological findings from analysis of fractures at 26 weeks post fracture, see section 8.2.4. Due to the complexity of μCT scanning only one representative sample from each of the treatment groups at 26 weeks post fracture were scanned. Therefore, quantitative data was not generated from this analysis. Instead 3 dimensional images, similar to that seen in figure 2.3b, were generated for observational comparisons of hard callus remodelling to the end point.

2.5 Histological techniques

Although x-rays are used clinically to assess the progress of a healing bone, they do not provide all the information required to understand the exact stages of repair. The early soft cartilaginous callus is not mineralised therefore it is translucent on a radiograph. When this soft callus is removed by endochondral ossification, it is replaced with mineralised bone. The x-ray reveals a bridged fracture site at this stage and in this study this denoted radiological union. However, the formation of the cartilage soft callus and the process of its ossification cannot be clearly demonstrated radiologically, leading to the requirement of histological examination of fracture healing.

Histological analysis provides a detailed examination of bone samples at the tissue level. By incorporating both decalcified and un-decalcified histology in this investigation, detailed morphology and tissue properties were examined.

Assessment of fracture healing requires detailed morphology with definition of cell and matrix types. This was achieved through decalcified paraffin embedded histology and specialised staining techniques to differentiate between cartilage, fibrous and bone matrix, as outlined in sections 8.4.3 and 8.4.4.1. Growth plate analysis performed on contra-lateral femora in the fracture studies also employed decalcified histology with specific cartilage staining. Further, localisation of distinctive cell types can also be achieved through decalcified paraffin sections.

Un-decalcified resin histology on the other hand is specifically used to assess the mineral properties of the tissue components. This technique was applied to the bone phenotype assessment of the *ia/ia* rat, (section 8.4.2). With the knowledge that these rats exhibit extensive skeletal abnormalities it was determined that the combination of both resin and paraffin histology would improve the understanding of this phenotype. In addition, the MMP inhibitor MMI270 dose finding study required analysis of mineralisation at the growth plate to determine if any changes would be seen, hence both resin and paraffin histology were utilised, see chapter 6. Specialised staining techniques were then employed to determined the mineralisation of the tissue (section 8.4.4.2).

Differential staining of tissue types in the healing fracture samples, growth plates of contra-lateral femora and the *ia/ia* rat proximal tibial samples allowed for quantification of tissue areas to assess the healing process.

2.5.1 Histomorphometric analysis using BIOQUANT

Observational grading of union or grid point counting of tissue types on histological sections are techniques commonly used to provide outcome data to assess fracture repair (Kokubu *et al.*, 2003, Flick *et al.*, 2003, Makino *et al.*, 2005, Hak *et al.*, 2006). More recently however, with the expansion of computerised microscopy and image analysis, histomorphometric analysis has become increasingly accurate, leading to its use to quantitatively assess fracture healing (Jackson *et al.*, 2006, Kosaki *et al.*, 2007).

In order to evaluate both tissue type area in fracture calluses and mineralised tissue area in the proximal tibia in this study, an image analysis technique was employed. BIOQUANT Nova Prime image analysis connected to a digital QICAM camera and Leica microscope set up was used to examined initial endochondral fracture repair, hard callus remodelling and growth plate height and bone tissue volume in the proximal tibiae of the *ia/ia* rat (section 8.4.5). Endochondral repair was assessed as performed previously by our group (Jackson *et al.*, 2006), by measuring the area of

the callus containing avascular cartilage tissue compared to vascularised bone tissue on Saffranin O stained sections which differentially stains cartilage matrix (see section 8.4.5.2). A new technique was developed for this investigation to assess hard callus remodelling during fracture healing. This involved determining the area of callus that was remodelled into neo-cortical bone, compared to primary woven bone (see section 8.4.5.2).

In conjunction with endochondral fracture healing, growth plate height was examined to assess developmental endochondral ossification in samples from all fracture repair experiments (section 8.4.5.3). Finally, bone volume in the metaphysis of the proximal tibia of the *ia/ia* rats was assessed on von Kossa stained sections, as done previously, to determine the ratio of bone volume to total volume (BV/TV) (section 8.4.5.4) (Murakami *et al.*, 1994, Little *et al.*, 2003a, Misof *et al.*, 2005).

2.6 Analysis of serum markers of bone metabolism

Bone turnover can be monitored systemically by the assessment of metabolites produced through bone formation or resorption and released into the circulation. C-telopeptide cross links (CTX) is a fragment produced when type I collagen matrix of bone is degraded (Garnero *et al.*, 2003). Released into the circulation from resorbing osteoclasts, the levels of CTX can be measured from both serum and urine samples. Hence, when bone resorption is increased or reduced in response to pathological diseases or pharmacological intervention, CTX levels increase or decrease respectively.

This technique of systemically measuring resorption was employed in the investigation of the phenotype of the *ia/ia* rat (section 8.7). By measuring serum CTX levels in the *ia/ia* rat and comparing it to control levels, a clearer understanding of the recovering phenotype was realised in these rats. The reinstatement of normal osteoclast function *in vivo* may not immediately produce noticeable changes in the phenotype at the tissue level. However, a slight increase in osteoclast function due to recovery of these cells may produce a small but detectable increase in serum CTX levels. Thereby this method allowed for a more accurate assessment of functional recovery in the *ia/ia* rats.

2.7 Mechanical testing of fracture samples

Extensive increases in callus BMC and bone volume with BP treatment owing to reduced resorption are commonly seen in similar examinations of fracture repair (Goodship *et al.*, 1994, Li *et al.*, 1999, Amanat *et al.*, 2005). Often these increases

produce relative improvements in the mechanical strength of these bones, providing increased protection against re-fracture.

However, BP treatment has been related to defects in mineralisation of bone tissue as a result of reduced remodelling and at high dose levels BPs have even been suggested to have a negative impact on fracture callus strength (Lenehan *et al.*, 1985).

It is with this in mind that assessment of mechanical strength of fracture calluses was performed in this study. Using a previously described method of torsional mechanical testing (Amanat *et al.*, 2005), calluses both at the time of initial union, 6 weeks and by the completion of hard callus remodelling at 26 weeks post fracture were analysed.

2.7.1 Background on torsional mechanical testing technique

Torsional testing measures the mechanical properties of bone under going shear stress by twisting the bone with both ends rotated in opposing direction (Turner and Burr, 1993). One of two testing techniques recommended for testing rat long bones, torsional testing evaluates the resistance to common occurring clinical fractures. Torsional testing is therefore commonly employed when examining fracture callus strength (Schmidmaier *et al.*, 2002, Mark and Rydevik, 2005, Amanat *et al.*, 2005, Holstein *et al.*, 2006).

2.7.2 Test protocol

Both right and left femora were tested in torsion to provide data for both fracture callus strength and whole limb strength for comparison. External rotational forces at an angular displacement of 6 degrees/second, were applied to each bone such that, the twisting motion was performed in an opposite directions to the un-fractured femurs. This was to account for differences in bone structure between the two sides. Samples were tested using the technique outlined in section 8.5 at 6 and 26 weeks post fracture.

2.7.3 Outcome parameters

Torque and angular displacement were both recorded during the testing procedure. From these data outputs the following parameters were generated: peak torque to failure, stiffness and stress. Peak torque to failure describes the overall resistance of the bone to strain in torsion. Stiffness data, as calculated by the slope of the linear region of the torque versus angular displacement curve, provides a measure for the brittleness of the bone as a whole. Finally, stress, strain and Young's modulus were calculated to measure the material properties of the bone tissue, providing

information on the quality of the bone tissue matrix independent of the mass or geometry of the bone overall (see section 8.5.4). These final parameters were important to assess the differences in material properties between Weekly ZA and Bolus ZA resulting from delayed hard callus remodelling.

2.8 In vitro *studies*

2.8.1 Justification for *in vitro* examinations

To provide a thorough examination of the *ia/ia* rat phenotype, *in vitro* analysis was employed. With the abnormality in these rats localised to a particular cell population, it became apparent that discrete investigations of *ia/ia* rat osteoclasts were required.

The reduction in resorptive capabilities of the *ia/ia* rat osteoclasts produces an extreme skeletal phenotype at the tissue level in these rats (Marks, Jr., 1973). Rescue from this phenotype has been achieved by transplantation of normal hemopoietic cells, confirming the mutation is within this cell population. The change in tissue phenotype is a direct result of the change seen in the cell population, however the recovery does not manifest immediately. Changes in the proportions of normal osteoclasts were noted as early as 1 day post transplantation. On the other hand, histological, and radiographic evidence of bone resorption took a week or more to develop (Marks, Jr., 1976), (Marks, Jr. and Schneider, 1982). Hence, detection of cellular recovery in the *ia/ia* rats would precede evidence of recovery at the tissue level. This resulted in the need to discretely examine both the osteoclast population and tissue samples for signs of recovery. To date however there has been little work focusing on the *in vitro* activity of the mutant *ia/ia* osteoclasts. An *in vitro* examination of osteoclast differentiation and resorption was therefore performed as part of this thesis investigation.

2.8.2 Primary cell culture technique

Primary osteoclast cultures were obtained from bone marrow samples from both *ia/ia* and wild/type/heterozygote (wt/het) rats at 5, 9, 12 and 20 weeks of age. Using previously described techniques, a cell population containing osteoclast and pre-osteoclast cells was separated and stimulated to produce TRAP positive osteoclastic cells by culturing in the presence of RANKL and M-CSF, see section 8.6 (Schindeler and Little, 2005). Seeded on plastic for differentiation experiments and on calcium phosphate discs for resorption experiments, these cells were grown to maturity for 10 days.

These two techniques allowed for analysis of cellular differentiation, morphology of mature osteoclasts and resorptive activity of the cell populations. Using the Bioquant image analysis system, which was optimised for histological purposes, the changes in cell differentiation and resorption between the genotypes were quantified.

In addition to resorption analyses on calcium phosphate discs, resorption of human bone samples was also examined using these cell populations. This technique utilises the release of collagen breakdown products through resorption to measure resorptive activity.

Improving the level of analysis in the *ia/ia* rat phenotype investigation, by utilising both *in vivo* and *in vitro* examinations, has allowed for a more discrete determination of recovery age in these rats and thus enhancing the validity of the fracture experiments performed on these rats.

2.9 Dose finding study for the MMP inhibitor MMI270

2.9.1 Background on MMP activity during fracture healing

As this investigation is exploring the role of the osteoclast during endochondral ossification, with the hypothesis that they are not rate limiting to this process, thought must be given to the possible alternative cell populations that are indeed vital here. The actions of MMPs during endochondral ossification have been thoroughly explored. Of particular importance to this process are MMP-13 and MMP-9, with mice deficient in either or both of these MMPs demonstrating severe delays in endochondral growth and fracture repair (Vu *et al.*, 1998, Colnot *et al.*, 2003, Inada *et al.*, 2004, Kosaki *et al.*, 2007) (section 1.3.2.3). Clearly these studies implicate MMP secreting cells, including vascular endothelial cells, chondrocytes and chondroclasts, as rate limiting candidates to endochondral ossification. These developments thereby lead to the assessment of fracture repair in the absence of MMP activity.

2.9.2 MMI270, a broad spectrum MMP inhibitor in fracture repair

The compound MMI270 is a broad spectrum MMP inhibitor developed by Novartis Pharma as a potential anti-angiogenic compound for the treatment of metastatic cancers. Previous studies using this compound, and other compounds of similar nature, have been investigating its use to; prevent breast cancer induced osteolytic lesions (Winding *et al.*, 2002), perturb angiogenesis and glioma invasion in brain tumour models (Yoshida *et al.*, 2004), and treat cold injury induced brain oedema in rats (Kawai *et al.*, 2003). Clinical trials of this agent in anti-cancer therapy have also been performed (Levitt *et al.*, 2001). The potential negative effects of this anti-

angiogenic compound on endochondral ossification however have not been explored. By demonstrating delayed endochondral fracture healing under the influence of this agent, the results produced in the MMP-9 and MMP-13 knockout models will be confirmed and a new level of biological understanding of endochondral ossification will be revealed.

2.9.3 MMI270 dose finding study

A dose rate of 20mg/kg twice daily by SC administration was determined for MMI270 fracture studies from previous examinations using this compound in rats (Kawai *et al.*, 2003). Unfortunately this dose level was not sufficient to attenuate endochondral ossification in this study, hence normal fracture repair occurred. As a result, a dose finding study was then performed where increased doses of the agent were administered both orally and subcutaneously to growing rats and endochondral growth was assessed. The optimal dose level and mode of administration required to effect endochondral ossification was determined. This new dose level was then used in future fracture experiments aimed to examine the effects of MMP inhibition on endochondral repair.

2.10 Overall methodological aims

Together these experimental methods form the basis for a comprehensive investigation aiming to elucidate the role the osteoclast plays during endochondral fracture repair. Furthermore, additional analytical methods were included in this study to examine the role of the osteoclast during fracture hard callus remodelling as well as to provide evidence to reveal the main cells and processes that are required for normal endochondral repair.

3 Effects of zoledronic acid treatment on endochondral fracture union

3.1 Introduction

Endochondral ossification is a vital process during the initial stage of diaphyseal fracture repair. The cartilage, or chondral, soft callus that is formed following the inflammatory response must be removed and replaced by bone in order to achieve bony union. This is achieved through progressive mineralisation, vascular invasion, and removal of this chondral matrix. The resulting mineralised tissue then forms a template for new bone formation and thus bony callus production. As described in more detailed in section 1.3 of chapter 1, this highly regulated process has been well explored however it is not yet completely understood (Sundquist *et al.*, 1995, Deckers *et al.*, 2002, Sawae *et al.*, 2003, Takahara *et al.*, 2004).

A highly avascular network, cartilage matrix is formed at the fracture site through differentiation of precursor cells attracted to the site by inflammatory signals. This rapidly formed “soft” callus provides an initial form of non-rigid stability to the repair site, temporarily bridging the bone ends to maintain orientation and structure. Unique in purpose, endochondral fracture repair is unlike any other form of tissue repair, although the underlying mechanisms governing this process are somewhat familiar to that seen during bone growth. The chondrocytes that constitute the cartilage soft callus demonstrate a morphology and signal pattern that closely resembles that seen in growth plate chondrocytes. During longitudinal growth endochondral ossification occurs at specific sites of long bone ends to achieve bone growth. As described in more detail in chapter 1, section 1.2.2, chondrocytes at these locations proliferate, differentiate and hypertrophy in an organised fashion before they are invaded, mineralised and their matrix utilised to form the primary spongiosa of metaphyseal bone (Abad *et al.*, 2002). It has been demonstrated that during fracture healing this process is to some extent recapitulated, suggesting that the governing mechanisms underlying endochondral fracture repair are similar (Ferguson *et al.*, 1999). However, a distinctive characteristic of fracture healing is the production of a repair site that is devoid of scar tissue. This is due to the stable environment created by endochondral fracture union, allowing fusion of the original bone ends, whilst the resultant bony callus is remodelled until the site is close to the original structure.

Infiltration of the cartilage callus by a vascular network during endochondral fracture repair is the initiating step towards its replacement. As seen during long bone growth, the hypertrophic chondrocytes demonstrate properties that prepare the matrix

for removal. Firstly they are capable of matrix mineralisation and subsequent apoptotic cell death, signalling imminent cellular invasion. In addition the un-mineralised chondrocyte matrix is rich in VEGF which once released stimulates further angiogenesis. Finally, this un-mineralised matrix is degraded by invading cells, allowing progression of marrow cells into the avascular tissue mass. It is this step, the degradation of un-mineralised chondral matrix, that to date eludes complete understanding. It has been assumed that bone resorbing cells, osteoclasts, are responsible for this vital step owing to their phagocytic capabilities, and their proximity to the site. However, recent studies have dissociated osteoclast activity and angiogenesis during endochondral growth (Deckers *et al.*, 2002). It was therefore speculated that due to the high conservation of its mechanistic processes, endochondral fracture repair would proceed normally in the absence of osteoclast activity.

This chapter explores the hypothesis that osteoclast function is redundant to the process of endochondral ossification during fracture repair. If so, this heralds new developments in the understanding of bone repair and is likely to significantly influence strategies targeting the modulation and enhancement of fracture healing. The third generation N-BP, Zoledronic Acid (ZA), was utilised to potently inhibit osteoclast activity in a rat model of fracture repair.

3.2 Study Design

Assessment of initial endochondral ossification in this study was performed utilising a commonly used rat closed femoral fracture model in 9 week old male Wistar rats, as described in the appendix, section 8.1.2. ZA was used to inhibit normal osteoclast activity at 4 different dosing regimes. Two bolus doses were examined, either a single high dose of 0.1mg/kg (Bolus ZA HD) or a low dose of 0.025mg/kg (Bolus ZA LD) was administered subcutaneously 1 week post fracture. Further, two regimens of divided weekly dosing were also investigated, namely 5 weekly doses such of 0.02mg/kg (Weekly ZA HD) or 0.005mg/kg (Weekly ZA LD), such that the continual weekly dose groups received the same total dose as the corresponding single bolus dose. Control animals were given saline on a weekly basis, as were bolus dosed animals after the initial bolus dose at week 1 post fracture.

The division of the single dose into smaller weekly doses was incorporated into this study to model the different BP dosing regimens administered clinically as discussed in chapter 1 section 1.5.6, (Lindsay R *et al.*, 2006). To examine initial repair, samples were harvested at 2, 4, and 6 weeks post fracture from all treatment groups. Each treatment group contained 10 rats at each of the 3 time points analysed. In addition, 10 rats that received saline only were used to produce baseline data for callus morphology at 1 week post fracture (Table 3.1). A few treatment groups had more than 10 animals as extra rats were included to allow for experimental exclusions due to the nature of the closed fracture technique. As described in detail in the appendix, section 8.1.2, the closed fracture model has a reduced level of control over the position and quality of fracture production leading to exclusion of animals demonstrating fragmentation or poor positioning of the fracture site.

	Sample number per group			
Treatment Group	***1 week***	***2 weeks***	***4 weeks***	***6 weeks***
Saline	10	10	10	10
Bolus ZA Low Dose	-	10	10	10
Weekly ZA Low Dose	-	10	10	10
Bolus ZA High Dose	-	10	10	10
Weekly ZA High Dose	-	10	10	10

Table 3.1 *Sample numbers harvested from rats of each treatment group at 1, 2, 4 and 6 weeks post fracture.* Bolus ZA Low Dose 0.025mg/kg, Weekly ZA Low Dose 0.005mg/kg, Bolus ZA High Dose 0.1mg/kg, Weekly ZA High Dose 0.02mg/kg.

Radiographs were performed at the time of harvest to assess the stage of radiologically determined union. Detailed histological analysis was utilised to establish the rate of endochondral ossification up to 6 weeks when complete union was expected for this model.

Histomorphometric analysis was also performed on growth plates of the un-operated distal femora of all animals in the experiment. This was done in order to confirm that the results seen during endochondral ossification at the growth plate were consistent with those seen during repair. The growth plate thereby provided an internal confirmation for the analysis of endochondral ossification in the absence of osteoclast function.

3.3 Results

3.3.1 Radiological analysis of fracture union

X-rays of all fracture samples demonstrated the same rate of radiological fracture union for all treatment groups from 2 to 6 weeks post fracture. By 6 weeks 90% of all samples had achieved radiological union regardless of treatment (Table 3.2 and Figure 3.1).

Treatment		***2 weeks***	***4 weeks***	***6 weeks***
Saline	Not united	11	10	1
	United	0	0	9
	Total	11	10	10
Bolus ZA LD	Not united	10	8	1
	United	0	2	9
	Total	10	10	10
Weekly ZA LD	Not united	11	10	1
	United	0	0	9
	Total	11	10	10
Bolus ZA HD	Not united	10	11	1
	United	0	0	9
	Total	10	11	10
Weekly ZA HD	Not united	13	9	0
	United	0	1	10
	Total	13	10	10

Table 3.2 *X-ray grading of samples at 2, 4 and 6 weeks post fracture.* Samples were determined either united or not-united from radiographs for each treatment group at 2, 4 and 6 weeks post fracture. Bolus ZA Low Dose 0.025mg/kg, Weekly ZA Low Dose 0.005mg/kg, Bolus ZA High Dose 0.1mg/kg, Weekly ZA High Dose 0.02mg/kg.

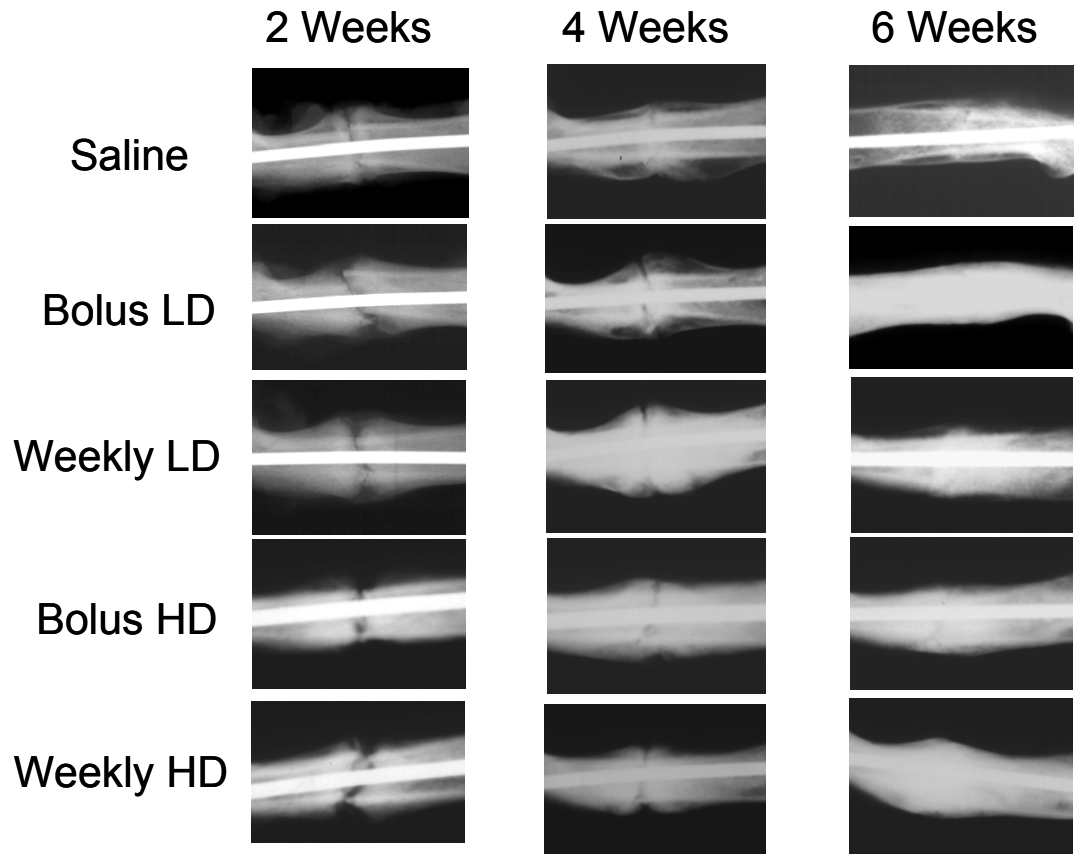

Figure 3.1 *Representative X-rays at each time point examined for each treatment group.* Ninety percent of samples achieved radiological union by 6 weeks. These images also demonstrate the larger, denser callus formed under the influence of ZA treatment. Each sample still contains the intramedullary rod in the marrow cavity. Bolus ZA Low Dose 0.025mg/kg, Weekly ZA Low Dose 0.005mg/kg, Bolus ZA High Dose 0.1mg/kg, Weekly ZA High Dose 0.02mg/kg.

3.3.2 Quantitative computerized tomographic (QCT) analysis of the fracture callus

Quantitative computerised tomography (QCT) analysis revealed profound effects on the fracture callus in ZA treated groups at all examined time points. All data means, standard deviations and statistical significances are outlined in Table 3.3, over page.

Fracture callus BMC at 2 weeks was significantly increased 21% and 20% compared to Saline in both Bolus ZA LD and Weekly ZA LD groups respectively, with statistical significance of $p<0.01$. In addition Weekly ZA HD produced a 13% increase in BMC compared to Saline at 2 weeks, with $p<0.05$ (Figure 3.2). On the other hand, callus Volume at 2 weeks was not affected by ZA treatment, all ZA groups showed no difference to Saline for this parameter (Figure 3.3). Such changes in BMC without corresponding increases in callus size produced significant increases in callus BMD with ZA treatment. Bolus ZA HD, Weekly ZA LD and Weekly ZA HD demonstrated increases of 13%, 10% and 14% respectively compared to Saline at 2 weeks ($p<0.01$).

By 4 weeks the enhanced effects of the ZA treatment had become more pronounced. Callus BMC was significantly increased 36% to 60% in all four of the ZA treatment groups compared to Saline with the Weekly ZA LD group exhibiting the largest change and statistical significances of $p<0.01$ for all groups. Further, Weekly ZA LD had an 18% larger callus BMC than Bolus ZA LD at this time ($p<0.01$) (Figure 3.2). Unlike at 2 weeks, callus volume by 4 weeks showed significant changes under the influence of ZA treatment. All ZA treatment groups produced increases of 31% to 55% in callus Volume compared to the Saline group ($p<0.01$), again with the Weekly ZA LD group showing the largest increase, and also demonstrating a 19% increase over the Bolus ZA LD group ($p<0.05$) (Figure 3.3). Since both callus BMC and volume had increased by 4 weeks, callus BMD showed a difference of only 7% in the Weekly ZA HD group compared to Saline, with a statistical significance of $p<0.05$.

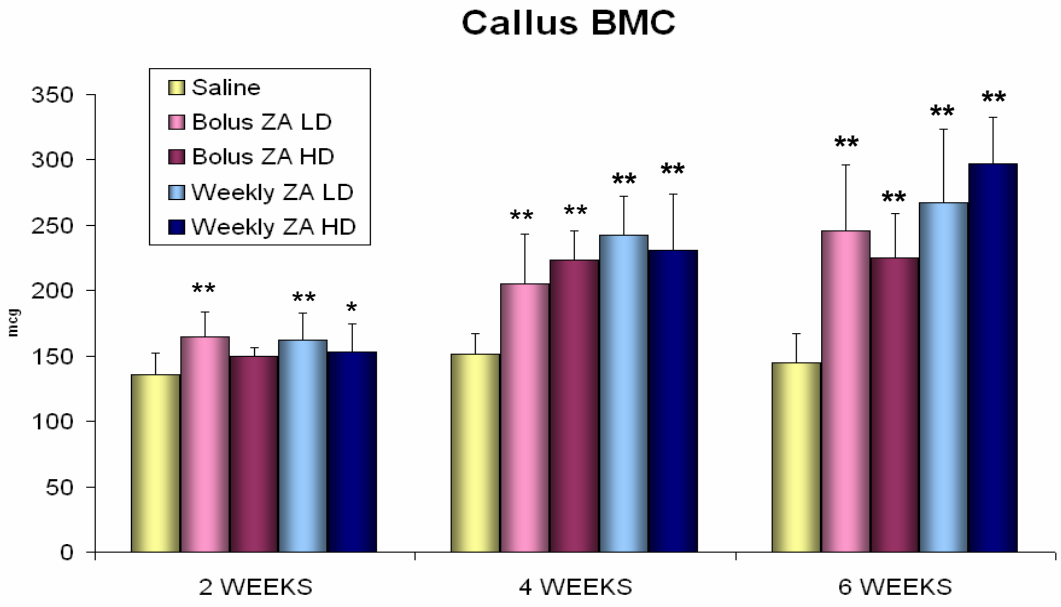

Figure 3.2. *Bar chart of Mean values for Callus BMC for all treatment groups at 2, 4 and 6 weeks post fracture.*
Error bars show standard deviations. 2 asterix (**) represents $p<0.01$ when compared to Saline, 1 asterix (*) represents $p<0.05$ when compared to Saline. ZA treatment produced up to 2-fold increases in callus BMC compared to Saline by 6 weeks post fracture.
Bolus ZA Low Dose 0.025mg/kg, Weekly ZA Low Dose 0.005mg/kg, Bolus ZA High Dose 0.1mg/kg, Weekly ZA High Dose 0.02mg/kg.

Treatment	*2 Weeks*				*4 Weeks*				*6 Weeks*			
Means	**N**	**BMC (mcg)**	**Volume (mm3)**	**BMD (mcg/cm3)**	**N**	**BMC (mcg)**	**Volume (mm3)**	**BMD (mcg/cm3)**	**N**	**BMC (mcg)**	**Volume (mm3)**	**BMD (mcg/cm3)**
Saline	9	135.3	197.6	684.7	10	151.2	182.5	828.6	10	145.2	157.4	922.7
Bolus ZA Low Dose	10	164.3**	224.3	732.6	10	205.0**	238.8**	858.4	9	245.4**	264.0**	929.7
Bolus ZA High Dose	10	149.4	193.1	773.5**	11	223.7**	257.6**	868.6	9	225.3**	241.2**	934.0
Weekly ZA Low Dose	11	162.1**	216.1	750.0**	10	242.6**^{aa}	283.3**^{a}	856.4	10	267.6** ^{o}	283.8**	942.8
Weekly ZA High Dose	12	153.2*	196.4	780.4**	9	231.1**	260.7**	886.2*	8	297.1** $^{a\ oo}$	314.4** ^{o}	945.0
Standard Deviations												
Saline	9	17.2	30.9	50.1	10	15.8	24.0	37.2	10	22.0	28.8	59.9
Bolus ZA Low Dose	10	19.8	36.2	59.1	10	38.3	53.4	55.2	9	50.5	80.5	97.8
Bolus ZA High Dose	10	6.8	16.4	71.6	11	21.8	36.1	34.9	9	34.0	49.6	56.6
Weekly ZA Low Dose	11	20.7	43.1	45.2	10	29.6	41.8	54.8	10	55.7	69.2	71.3
Weekly ZA High Dose	12	21.3	35.0	47.6	9	42.7	67.5	58.3	8	35.5	46.1	42.6

** $p<0.01$ when compared to Saline, ^{aa} $p<0.01$ when compared to Bolus ZA Low Dose, ^{o} $p<0.05$ when compared to Bolus ZA High Dose
* $p<0.05$ when compared to Saline, ^{a} $p<0.05$ when compared to Bolus ZA Low Dose, ^{oo} $p<0.01$ when compared to Bolus ZA High Dose

Table 3.3. *Quantitative computerise tomography data for fractured femurs for all treatment groups at 2, 4 and 6 weeks post fracture.*
Bone mineral content (BMC), Callus mineralised tissue volume (Volume) and volumetric bone mineral density (BMD). N – number of samples. Units are micrograms (mcg), millimetres cubed (mm3) and micrograms per millimetre cubed (mcg/mm3). Note the extensive changes in all parameters with ZA treatment. Bolus ZA Low Dose 0.025mg/kg, Weekly ZA Low Dose 0.005mg/kg, Bolus ZA High Dose 0.1mg/kg, Weekly ZA High Dose 0.02mg/kg.

Changes in fracture callus properties were most notable by the 6 week time point. By this stage callus BMC was significantly increased to between 55% and 105% in the ZA treatment groups, statistical significance of $p<0.01$. The Weekly ZA HD group demonstrated the largest increase in BMC at 6 weeks, and it was also significantly increased by 21% over Bolus ZA LD ($p<0.05$) and 32% over Bolus ZA HD ($p<0.01$) (Figure 3.2).

Callus volume was notably increased with ZA treatment by 6 weeks. Increases of 53% to 100% were demonstrated in all ZA treatment groups compared to Saline ($p<0.01$). The largest increases were seen in the Weekly ZA dose groups, both HD and LD. Callus volume was also increased by 30% in the Weekly ZA HD group compared to the Bolus ZA HD group ($p<0.05$) (Figure 3.3). Relative increases in callus BMC and volume with ZA by 6 weeks produced callus BMD values showing no differences between treatment groups.

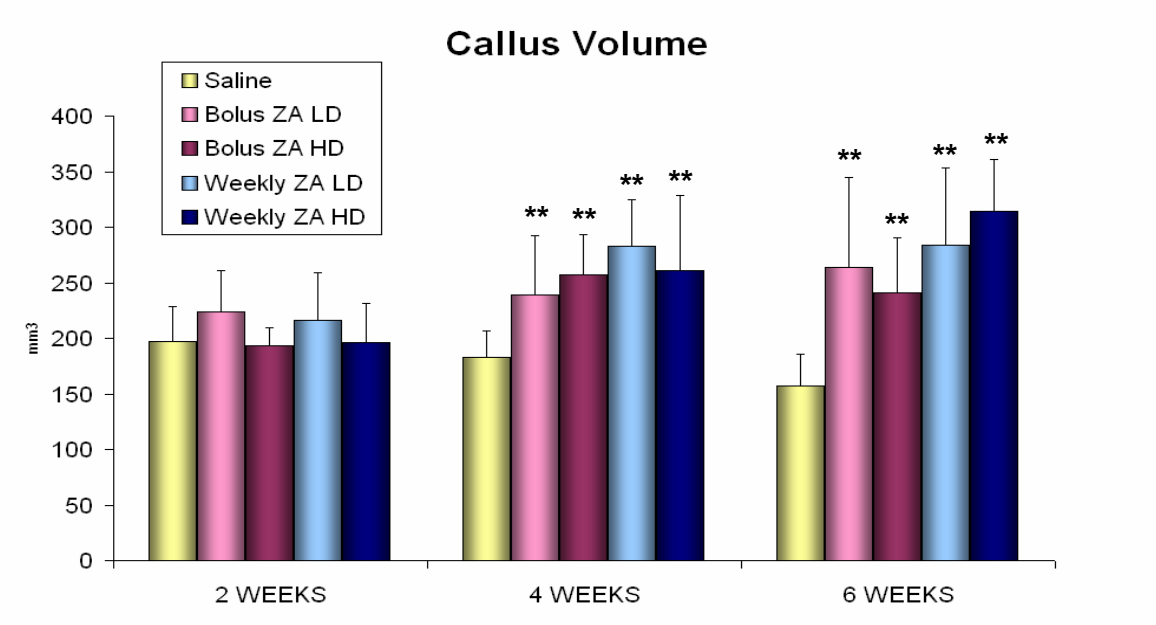

Figure 3.3. *Bar chart of mean values for callus volume for all treatment groups at 2, 4 and 6 weeks post fracture.*

Error bars show standard deviation. 2 asterix (**) represents $p<0.01$ when compared to Saline. ZA treatment produced increases of up to 2-fold in callus volume compared to Saline by 6 weeks post fracture. Bolus ZA Low Dose 0.025mg/kg, Weekly ZA Low Dose 0.005mg/kg, Bolus ZA High Dose 0.1mg/kg, Weekly ZA High Dose 0.02mg/kg.

3.3.3 Histological analysis of endochondral ossification

3.3.3.1 Histomorphometry of cartilage content

Histomorphometric analysis of callus sections at 1, 2, 4 and 6 weeks post fracture in this Wistar rat study revealed no significant difference between treatment groups in the percentage of the callus that was vascularised hard bone versus cartilaginous callus. Baseline 1 week post fracture data of fracture callus vascular tissue area was 60%, thus 40% of the callus contained avascular fibro-cartilaginous soft callus. At 2 weeks post fracture all groups showed 91% to 92% of the fracture callus as vascularised bone tissue, by 4 weeks this was increased to 97% to 99% and finally at 6 weeks 99-100% of the callus was vascularised primary bone callus in all treatment groups (Figures 3.4 and 3.5). When tested statistically, no significant differences were noted between dose groups at all times examined. Thus, the rate of removal of the avascular soft callus was the same in all treatment groups such that at 6 weeks all groups showed almost complete removal of this soft callus.

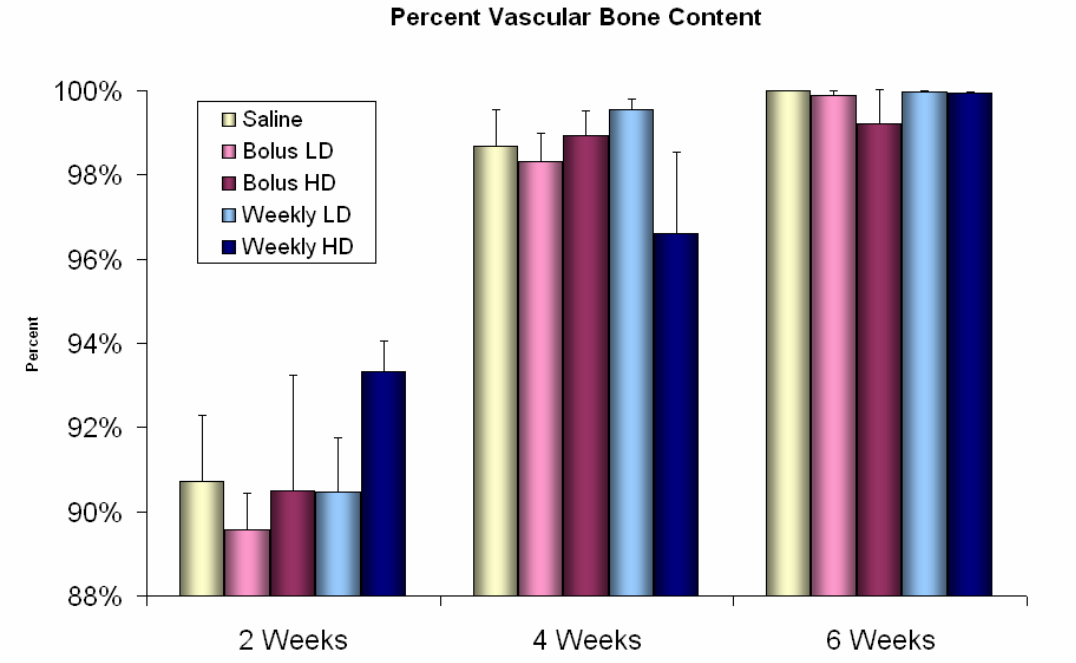

Figure 3.4 *Bar chart of mean values for percentage callus vascular bone content for all treatment groups at 2, 4 and 6 weeks post fracture.*
Error bars represent standard errors. No statistical differences were noted between treatment groups. Bolus ZA Low Dose 0.025mg/kg, Weekly ZA Low Dose 0.005mg/kg, Bolus ZA High Dose 0.1mg/kg, Weekly ZA High Dose 0.02mg/kg.

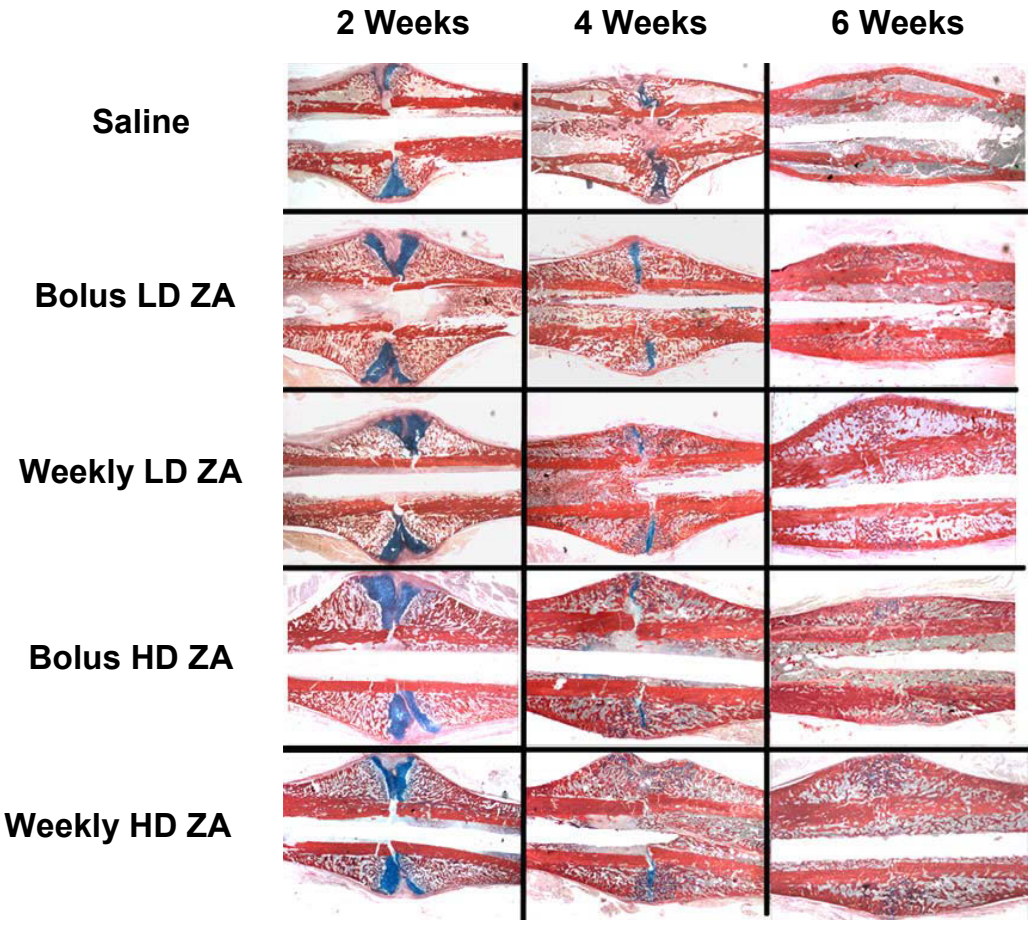

Figure 3.5. *Representative sections from Saline, Bolus LD and HD ZA and Weekly LD and HD ZA treated rats at 2, 4 and 6 weeks post fracture.*
Alcian Blue/Picrosirius red stain demonstrating the removal of the blue avascular cartilaginous callus and its replacement with red ossified callus. This occurred at the same rate in all samples regardless of treatment. Original magnification x 0.63. Bolus ZA Low Dose 0.025mg/kg, Weekly ZA Low Dose 0.005mg/kg, Bolus ZA High Dose 0.1mg/kg, Weekly ZA High Dose 0.02mg/kg.

3.3.4 Histological analysis of endochondral ossification during long bone growth

3.3.4.1 Histomorphometry of growth plate height during ZA influenced growth

Growth plate height measurements were performed on all un-operated distal femora as an internal control for the effects of systemic ZA on endochondral ossification. This analysis revealed no difference between controls and any treatment groups throughout the experimental period. At 2, 4, and 6 weeks post fracture, corresponding to 11 week, 13 weeks and 15 weeks of age, ZA treatment at either low or high dose and in either Bolus or Weekly regimens had no significant effect on the height of the growth plate (Figure 3.6). Figure 3.7 shows representative sections of the growth plates from each treatment group and time point examined for growth plate

height with no difference demonstrated between the treatment groups. This suggests that there was no impact from the ZA on the process of vascular invasion and chondrocyte removal during endochondral ossification during long bone growth in this study.

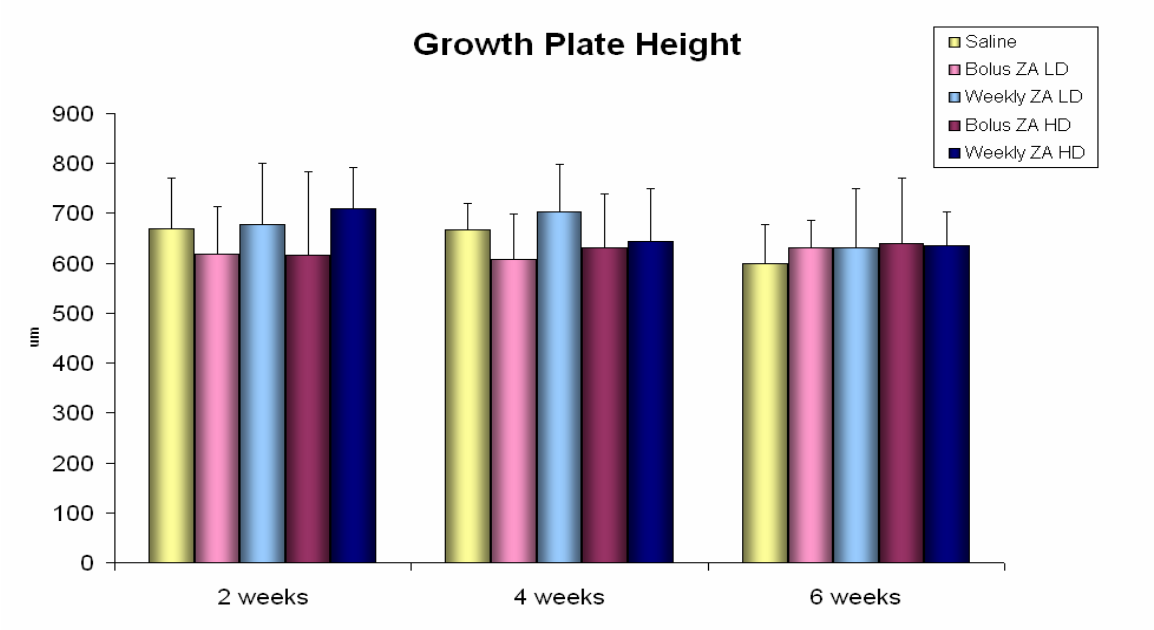

Figure 3.6 *Mean values for femoral growth plate height for all treatment groups at 2, 4 and 6 week post fracture time points*.
Error bars represent 1 standard deviation. Growth plate height was not different with ZA treatment compared to Saline at all time points. Bolus ZA Low Dose 0.025mg/kg, Weekly ZA Low Dose 0.005mg/kg, Bolus ZA High Dose 0.1mg/kg, Weekly ZA High Dose 0.02mg/kg.

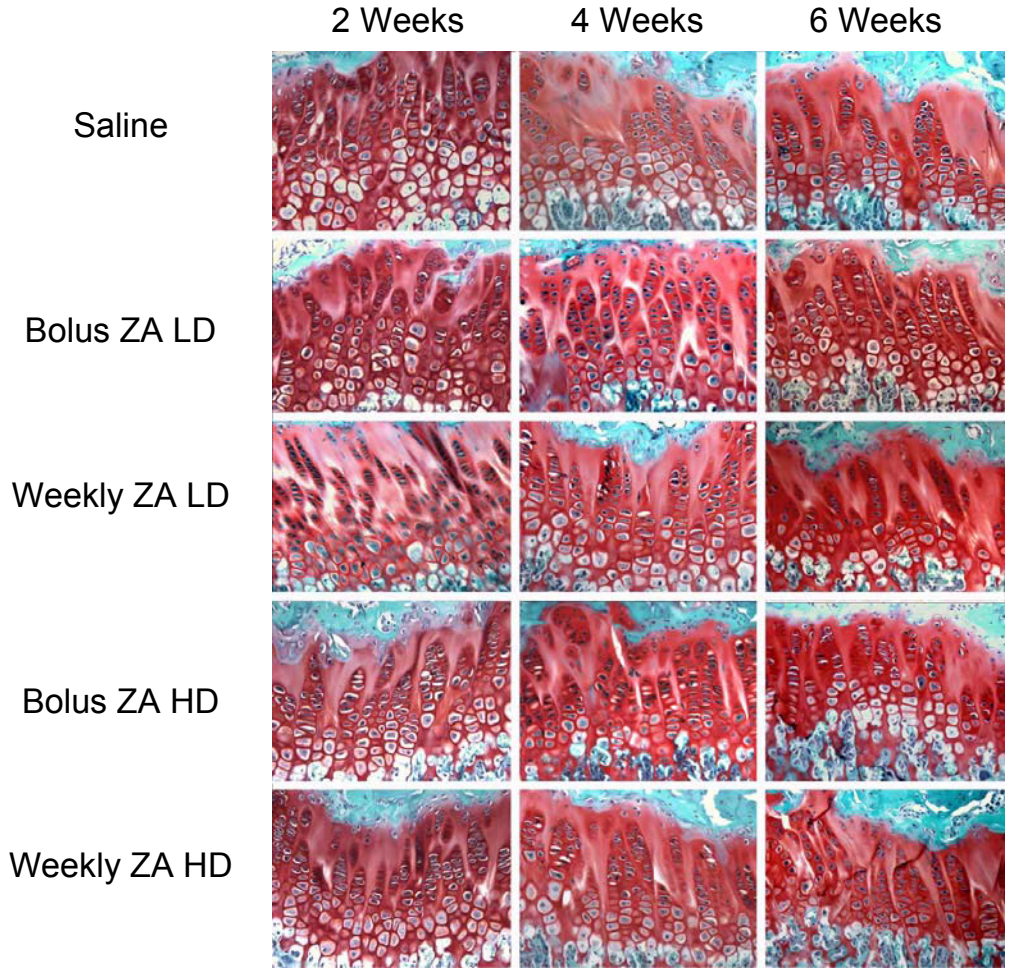

Figure *3.7* *Representative sections of growth plate from distal femurs of each treatment group at each time point examined.*
Saffranin O / light green stained sections. Growth plate cartilage is stained red and bone is stained green. These images demonstrate similar growth plate heights for all treatment groups at all time points examined. Original magnification X20.

3.4 Discussion

X-ray analysis of fractures to 6 weeks in this study provided the first evidence that the rate of initial endochondral fracture union was not affected with ZA treatment. By 6 weeks radiological examination showed bridging of the fracture sites had been achieved in at least 9 out of 10 samples in each treatment group (Figure 3.1). These x-ray images also illustrated that the amount mineralised callus was increased with ZA treatment and QCT scans confirmed these changes.

Increases in mean callus BMC was demonstrated in each of the ZA treatment groups compared to Saline from 2 to 6 weeks post fracture. Callus volume showed increases with ZA only at 4 and 6 weeks, with early changes in BMD at only the 2 week time point. By 6 weeks, BMC and callus volume were increased by up to two fold in the

Weekly ZA HD group suggesting significant retention of the hard callus formed in these calluses. Although not to the same magnitude, Bolus ZA also produced increases in callus BMC and volume compared to Saline, again with the largest increase seen at the 4 week time point in the Bolus ZA HD and at 6 weeks in the Bolus ZA LD (Figures 3.3 and 3.4). These increases in callus mineral properties were a result of primary bone retention due to reduced resorption and not related to increases in bone formation compared to control samples. Considering that the Bolus ZA doses were administered at 1 week after surgery, the resulting effects on callus retention were obvious even up to 6 weeks post fracture, especially so in the Bolus ZA LD group.

The mode of administration of ZA also had a significant impact on the resulting hard callus properties. By dividing the doses into 5 smaller weekly doses, providing the same total dosage of ZA but in a continuous administered form, the resulting net hard callus formed was further enhanced. Not only were the Weekly ZA calluses larger and contained more mineral than the Saline calluses, but as early as 4 weeks post fracture Weekly ZA LD calluses were also larger (19%) and had a higher BMC (18%) than that of the Bolus ZA LD calluses. By 6 weeks the Weekly ZA HD calluses showed a higher callus BMC than both Bolus ZA HD (32%) and Bolus ZA LD (21%) and were considerably larger (30%) than Bolus ZA HD calluses. Such differences in the effects between dose administrations were not evident at the 2 week time point when each group had received only one dose of ZA. These differences between dose administrations suggest that continuous weekly dosing of ZA produced an additive effect on the retention of bony callus up to 6 weeks, producing a larger more mineralised callus that may be more resistant to re-fracture. However, as previously demonstrated with BPs in fracture, this retention of primary callus may negatively impact the material properties of the callus (Monier-Faugere *et al.*, 1999). This issue will be addressed in chapter 5.

The most important outcome of this examination is the process of soft callus removal during fracture repair to achieve initial union. As hypothesised, the rate of endochondral fracture repair was not hindered with either bolus or weekly, high or low dose ZA treatment in this model, suggesting that osteoclastic function is not vital to this process. By quantifying the percentage of each callus that contained avascular cartilage callus and thus, the percentage of callus that had been vascularised and subsequently ossified, this study has demonstrated that ZA treatment had no effect on this process.

When ZA dosing commenced at 1 week following surgery, baseline data at this time showed that only 60% of the callus had been vascularised and thus mineralised, the remaining callus containing avascular fibro-cartilage or mesenchymal tissue. By 2

weeks the mean callus percentage of vascularised bone tissue had increased dramatically to approximately 90%, the remaining 10% was maturing avascular cartilage, regardless of treatment. Complete ossification was achieved by 6 weeks post fracture, with all avascular cartilaginous soft callus removed, in all treatment groups. Since ZA is a potent inhibitor of osteoclasts both *in vitro* (Schindeler and Little, 2005) and *in vivo* (Glatt *et al.*, 2004), then it is valid to conclude from these results that normal osteoclastic activity is not required to complete soft callus removal through endochondral ossification. Furthermore, confirmation of this result is provided by the growth plate analysis in this study where ZA treatment had no impact on the height of the growth plates; suggesting no adverse effects of this BP on the process of endochondral ossification at sites of long bone growth. This too reiterates the possibility that endochondral ossification is not limited by the activity of resorbing osteoclasts.

4 Endochondral fracture union in the osteoclast mutant incisor absent rat.

4.1 Introduction

The exact role of the osteoclast during endochondral ossification remains to be clarified as recent developments contradict the current paradigm. Until recently, due to their phagocytic capabilities, osteoclasts have been assumed to be the primary cell responsible for driving the degradation and replacement of avascular cartilage tissue during endochondral ossification (Lewinson and Silbermann, 1992). It is this process that ensures the removal of the initial soft cartilage callus of a fracture site, a vital stage in the formation of a bony hard callus, resulting in union. It was therefore logical to predict an essential role for the osteoclast in the initial stage of fracture healing. However Deckers *et al*. in 2002, have recently demonstrated that inhibition of osteoclast function during vertebral growth in mice had no effect on the process of endochondral ossification.

Furthermore, by inhibiting osteoclast function during fracture healing in a normal rat using the BP ZA, no effect was shown on cartilage removal (chapter 3). Such results have created a new school of thought regarding the putative central role the osteoclast may play at sites of endochondral ossification. However, the outcomes shown thus far in fracture repair were produced only through one mechanism of inhibiting osteoclast function, that of BP treatment. Considering that the work by the Deckers' group in 2002 demonstrated normal endochondral growth both under bisphosphonate treatment and in an animal model of reduced osteoclast activity, the *op/op* mouse, it was necessary to also examine fracture repair in a similar animal model.

BPs are known to specifically bind to mineralised tissue, including bone and calcified cartilage, where they act on osteoclasts actively resorbing these sites. On the other hand, un-mineralised tissue matrix such as cartilage is not bound by BPs. Thus it also remains to be clarified as to whether osteoclasts or pre-osteoclastic cells are still capable of resorbing the BP free un-mineralised cartilage matrix. In order to determine whether or not this is the case and to add to the work performed by Deckers and others 2002, this chapter examines fracture healing in a rat model of osteoclast inactivity, the incisor absent (*ia/ia)* rat.

The *ia/ia* rat demonstrates a spontaneous mutation that results in abnormal osteoclast function, chapter 1 section 1.4.6.1. Briefly, a genetic mutation of known but

very broad location, results in the development of osteoclasts that are unable to actively resorb bone tissue. In the non-resorbing state, the mutant cells appear morphologically similar to normal osteoclasts, however when they bind to a bone surface to initiate resorption they fail to polarise and form a ruffled border. Without this physiological membrane transformation, these cells are unable to demineralise and thus resorb bone tissue (Marks, Jr., 1973, Boskey and Marks, Jr., 1985, Seifert *et al.*, 1993, Reinholt *et al.*, 1999). With this functional deficiency these rats provide a model to further test our hypothesis that osteoclast activity is redundant during endochondral fracture repair.

Furthermore, the *ia/ia* rat model with its inactive osteoclast population allowed further analysis of hard callus retention. BP treatment resulted in retention of hard bony callus and thus an increase in callus size and mineral content, see chapter 5. The formation and remodelling of the hard bony callus during fracture healing in the *ia/ia* rat has been previously demonstrated by Schmidt and colleagues (Schmidt *et al.*, 1977). In a few words, fractures were performed in 2 week old rats and it was shown that the reduction in callus size seen 3 weeks post fracture in the control wt/het rats was not seen in the *ia/ia* rats. Moreover, even after 7 weeks the fracture calluses in the mutant rats remained largely un-remodelled.

One limitation of this *ia/ia* rat model is its tendency to spontaneously recover from its osteoclast mutation. The osteopetrotic phenotype that is strongly evident in these rats has been documented to resolve between 7-14 weeks of age (Marks, Jr., 1973). Although this has been investigated, the exact timing of the commencement of this recovery has not been thoroughly demonstrated. In order to ensure all fracture healing studies in this rat therefore occurred prior to this recovery, initial phenotypic investigations were performed on young and aged *ia/ia* rats to determine a more exact time frame for recovery. The results of this phenotype investigation are included in this chapter to demonstrate that the fracture repair experiments were performed exclusively within the period prior to recovery.

4.2 Study design

4.2.1 Phenotype analysis study

A colony of *ia/ia* rats and wildtype/heterozygous (wt/het) rats was produced from initial breeding stock kindly supplied by Neucom North-eastern Ohio Universities College of Medicine. In order to exactly determine the age when the rats recover from their osteoclastic defect, a detailed time scale analysis of the growing *ia/ia* rat was performed. At least 2 male rats from each genotype at 3, 5, 7, 9, 12 and 20 weeks of

age were used for this part of the study. Both *in vivo* and *in vitro* examinations were performed including: x-rays and DEXA scans to asses overall tissue mineral properties, histology to assess detailed tissue and cell properties and morphology, serum analysis of bone resorption markers and lastly primary osteoclast cell culture experiments to asses osteoclast differentiation and resorption *in vitro*. This extensive investigation allowed for a definitive determination of recovery in these rats, allowing for confident analysis of fracture healing during the period of osteoclast dysfunction.

4.2.2 Fracture study

Fracture repair examinations were performed once the initial phenotype study was complete and the age of recovery determined more precisely. The rat femoral closed fracture method was utilised again for this study (chapters 3 and 5, appendix) to create fractures in 5 week old rats. Modifications were required to this procedure to deal with the differences between the young 5 week old *ia/ia* rats and the 9 week old Wistar rats used in previous studies, (chapter 2 and appendix). Once optimised, fracture healing to union was assessed at 1, 2, and 3 weeks post fracture, these time points corresponding to 6, 7 and 8 weeks of age. Again radiological analysis was performed using x-ray and QCT to determine mineral tissue properties of fracture calluses. Further, detailed histological analysis, similar to that performed in chapter 3, was performed allowing for close examination of endochondral fracture union in these rats. In addition to analysis of fracture samples, examination of samples from all fracture experiment rats was performed to confirm that no signs of recovery were evident in these animals. This involved similar analysis to that performed in the phenotype study, with the addition of QCT scans, providing further understanding of the phenotype in these mutant *ia/ia* rats.

4.3 Results

4.3.1 The incisor absent rat bone phenotype

4.3.1.1 Radiological analysis

4.3.1.1.1 X-ray

Tibiae from male rats of both *ia/ia* and wild type genotypes at 3, 5, 7, 9 and 12 weeks of age were x-rayed for analysis. Radiographs revealed extensive phenotypic differences between mutant *ia/ia* rats and their normal littermates which included both homozygous positive (+/+) and heterozygous (-/+) rats (wt/het). Long bone growth appeared reduced in the mutant rats with an obvious reduction in tibial length (Figure

4.1). More importantly however is the obvious increased density of the metaphyseal bone tissue in *ia/ia* rats. Due to the lack of osteoclastic resorption, the primary spongiosa of the *ia/ia* long bones is not removed, producing a dense area of retained trabecular bone in this region.

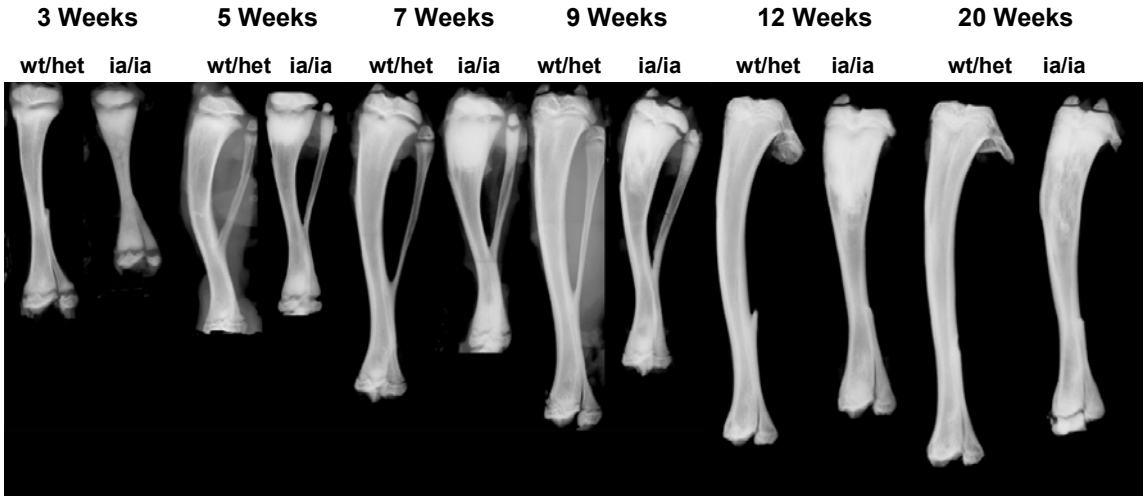

Figure 4.1. *Representative x-ray images of tibiae from both wt/het and ia/ia rats at each time point examined for phenotype analysis.*
Original magnification x 1.5. Note the obvious dense metaphyseal bone in the proximal region with signs of resorption evident by 12 weeks and extensive resorption by 20 weeks of age.

Femoral length was examined for all samples from radiographs. From 3 weeks of age, *ia/ia* rats demonstrated an 11-14% decrease in femur length compared to wt/het rats ($p<0.01$) Figure 4.2. The rate of change of femur length between 3 and 20 weeks of age was similar between genotypes, such that the magnitude of the difference remained the same. Importantly, after phenotypic recovery, the *ia/ia* rats did not catch up to wt/het rats in femoral length, suggesting that the reduction in femur length was not a result of osteoclast dysfunction.

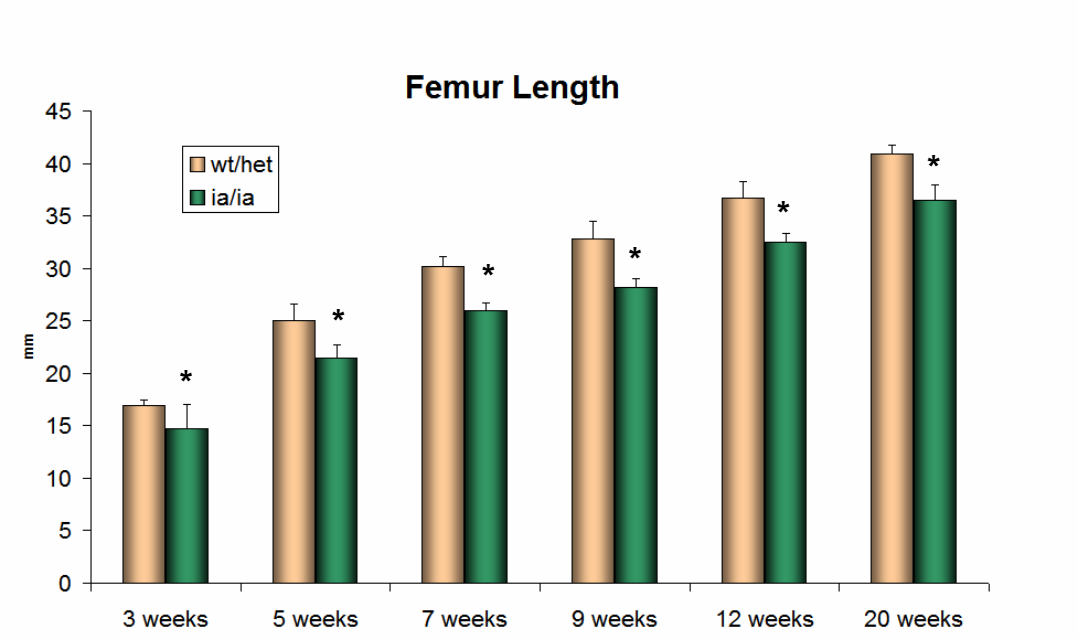

Figure 4.2. *Bar chart demonstrating mean femur length in ia/ia and wt/het rats.*
Error bars represent SD, *p<0.01 compared to wt/het. *ia/ia* rats demonstrated decreases in femur length of 11-14% compared to wt/het rats. Note the rate of femoral growth is similar between 3 and 20 weeks in both genotypes.

4.3.1.1.2 DEXA

DEXA scans were performed on all tibiae harvested for this phenotype analysis. Within the region of interest, mean values in the proximal tibial metaphysis were calculated for each genotype at each time point for BMC. The area analysed was the same in each sample thus the BMC values reflect exactly the same changes seen in BMD as an increase in mineral content in a given area directly increases the density of bone in that region.

When first measured at 3 weeks of age, a 63% increase in BMC was observed in the *ia/ia* mutant tibias compared to wt/het ($p<0.01$). By 5 weeks of age this had increased to a change of 109% ($p<0.05$), and 110% by 7 weeks ($p<0.01$). By 9 weeks of age the difference was increased further to 136% in the mutants compared to the wt/hets and by 12 weeks it had reached 220% ($p<0.05$). By 20 weeks however the *ia/ia* mutant samples showed a significant decline in the BMC in this region, resulting in only a 95% increase over wt/het samples by this age ($p<0.05$). Figures 4.2 and 4.3 clearly demonstrate these changes in metaphyseal bone properties, including BMD which reflects a similar trend as the BMC values, as the region of interest was kept constant. The wt/het rats show a slight, steady increase in mineral accrual during the

period of analysis, whereas the *ia/ia* mutant samples showed extensive increases up to 12 weeks of age with a significant drop by 20 weeks.

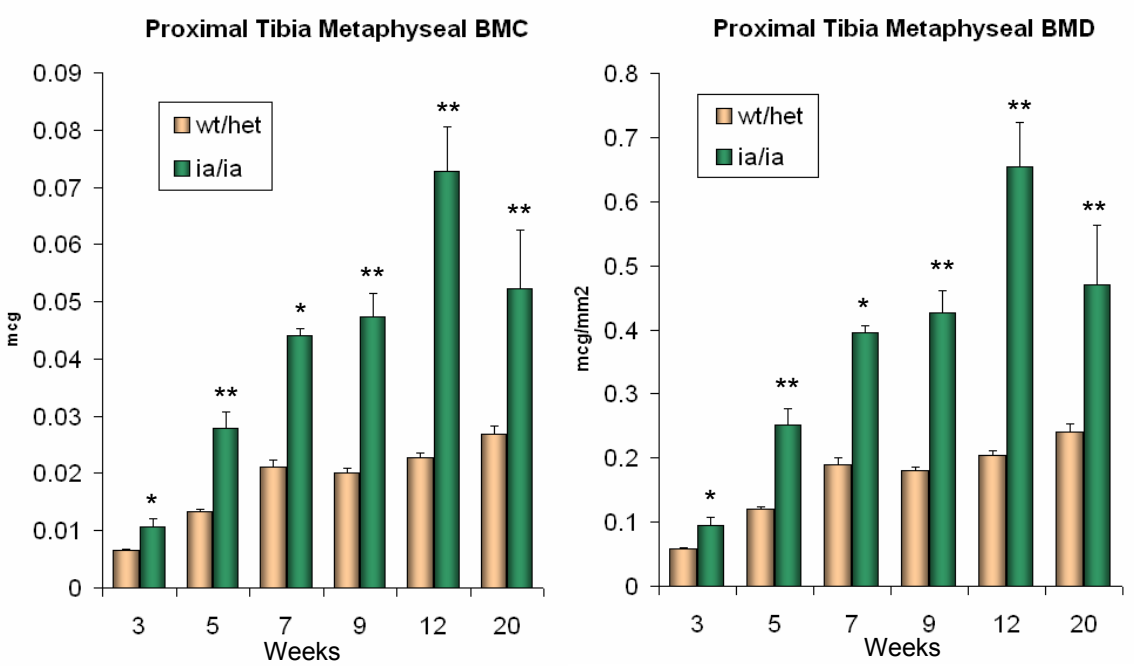

Figure 4.3 *Bar charts of mean values for proximal tibia BMC and BMD for ia/ia and wt/het rats from DEXA scan analysis.*
Error bars represent 1 standard deviation,1 asterix (*) represents p<0.01 when compared to wt/het, 2 asterix (**) represents p<0.05 when compared to wt/het. *ia/ia* rats demonstrated increases of up to 3 fold over wt/het rats in both BMC and BMD in this region. The *ia/ia* rat BMC increased steadily to 12 weeks with a significant reduction to 20 weeks of age. Weeks is the age of the rats at the time of harvest.

4.3.1.2 Histological analysis

4.3.1.2.1 Resin histology of proximal tibiae

The ratio of bone volume to total volume (BV/TV) was analysed in two regions of the proximal metaphysis as outlined in the methods appendix section 8.3.5.4. These regions were described as proximal metaphysis and distal metaphysis, corresponding to primary and secondary spongiosa respectively (Murakami *et al.*, 1994).

Proximal metaphyseal BV/TV

From 3 weeks of age male *ia/ia* rats showed a mean proximal metaphysis BV/TV ratio of 28% compared to only 11% in wt/het rats (p<0.01). By 5 weeks this had increased to 54% in *ia/ia* mutant male rats compared to just 20% in wt/het (p<0.01). From 7 weeks of age this mean proximal metaphyseal BV/TV ratio was maintained at a range of 47% to 61% at 20 weeks of age. On the other hand wt/het rats peaked in metaphyseal BV/TV ratio at 7 weeks with 22%, reducing slightly to 16% at 20 weeks

of age. Hence *ia/ia* mutant rats maintained a 1-fold increase in BV/TV in the proximal metaphysis over the wt/het rats throughout the time course of the phenotype examination. At 20 weeks of age this increase in *ia/ia* rats over wt/het reaching almost a 3-fold difference ($p<0.01$), (Figures 4.4 and 4.5).

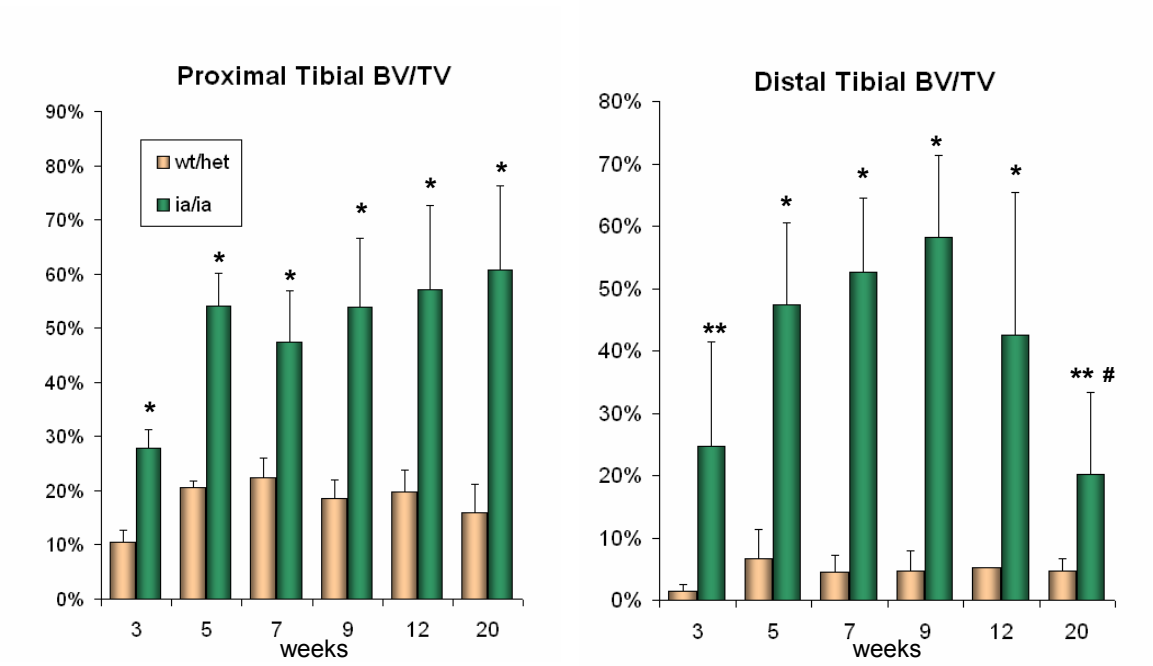

Figure 4.4. *Bar charts of mean proximal and distal metaphyseal BV/TV*.
Error bars represent 1 standard deviation, 1 asterix (*) represents $p<0.01$ when compared to wt/het, 2 asterix (**) represent $p<0.05$ when compared to wt/het, 1 hash (#) represents $p<0.05$ when compared to *ia/ia* 12 weeks. Note the changes in distal metaphyseal BV/TV from 12 weeks onwards. The *ia/ia* rats show a decrease in BV/TV in this region from 12 weeks of age, suggesting resorption is occurring in these rats. Weeks is age at time of harvest in weeks.

Distal metaphyseal BV/TV

The distal region of the tibial metaphysis usually contains only a small volume of trabecular bone tissue as demonstrated in the wt/het samples with only a 1% BV/TV in this region at 3 weeks, increasing to 7% at 5 weeks and then plateauing to 5% by 20 weeks of age. In contrast however the *ia/ia* rats showed a mean distal metaphyseal BV/TV of 25% at 3 weeks of age ($p<0.05$), increasing steadily to 58% at 9 weeks of age, such that at least a 10-fold increase is seen at 5 weeks, 7 and 9 weeks of age over wt/het distal metaphyseal BV/TV ($p<0.01$). However after 9 weeks a decrease in the *ia/ia* distal BV/TV is seen, dropping to 42% at 12 weeks and down further to 20% by 20 weeks ($p<0.05$) (Figure 4.4 and 4.5).

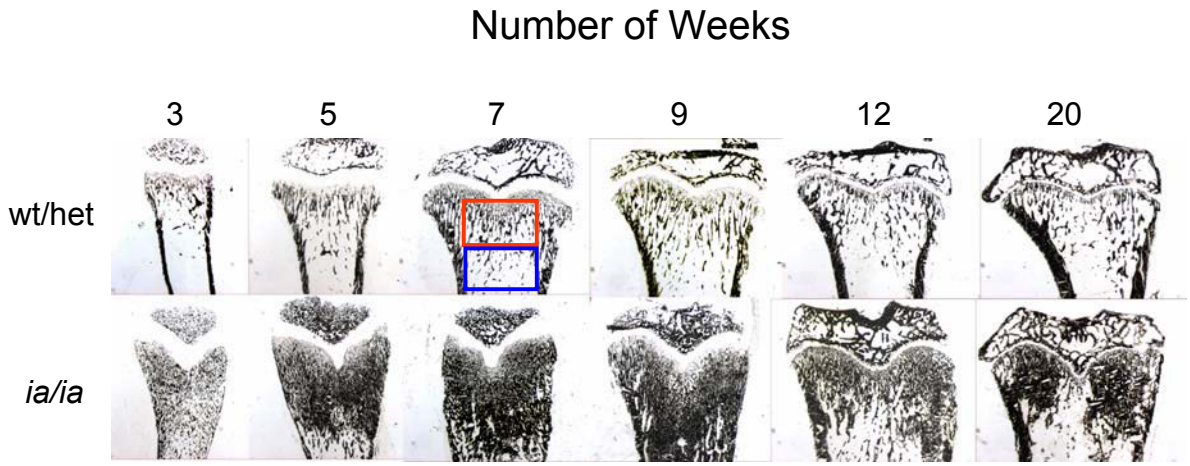

Figure 4.5 *Representative von Kossa stained sections at 3, 5, 7, 9, 12, and 20 weeks of age used for BV/TV analysis*.
Original magnification x 0.8. Von Kossa stained mineralised tissue black. Note the extensive increases in bone volume in the *ia/ia* samples compared to the wt/het samples and also the reduction in distal metaphyseal bone volume in the *ia/ia* rats from 12 weeks onwards. The red box indicates the region determined as the proximal metaphysis. The blue box indicates the region determined as the distal metaphysis.

4.3.1.3 Serum analysis of resorption markers

Serum levels of the bone degradation product CTX were measured in a cross sectional analysis in samples taken from both male wt/het and *ia/ia* rats at 3, 5, 7, 9, 12 and 20 weeks of age. Serum CTX concentrations were significantly reduced in the *ia/ia* rat samples compared to wt/het controls up to the 9 week age time point as shown in Figure 4.5. A 75% reduction was seen at 3 weeks of age in the *ia/ia* samples ($p<0.05$), this level of reduction was somewhat maintained with a 63% reduction at 5 weeks ($p<0.01$) and a 64% reduction at 7 weeks of age ($p<0.05$). By 9 weeks of age the reduction in serum CTX levels in the *ia/ia* samples compared to wt/het controls fell to just 28% ($p<0.05$) and by 12 weeks no statistical differences remained between the *ia/ia* samples and wt/het controls. Figure 4.6 also clearly demonstrates a pattern of high levels of CTX concentration during the early growth ages, with significant reductions after cessation of growth at 12 weeks of age in the wt/het rats. Although at lower levels than wt/het controls, this pattern is somewhat similar in the *ia/ia* mutant samples with higher levels of CTX during the early growth phase, reducing by 12 weeks of age.

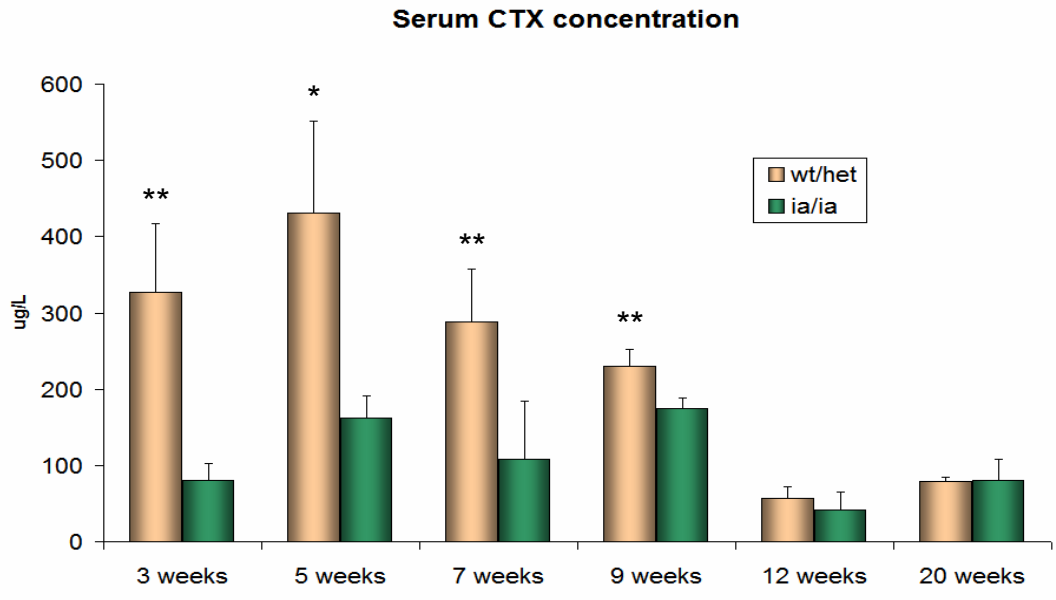

Figure 4.6 *Bar chart of mean values of serum CTX levels in ia/ia and wt/het rats at each time point examined*.
Error bars represent 1 standard deviation. 1 asterix (*) represents p<0.01 when compared to wt/het, 2 asterix (**) represents p<0.05 when compared to wt/het. *ia/ia* rat serum CTX levels began to normalise to the level of wt/het by 9 weeks of age with no differences seen from 12 weeks onwards.

4.3.1.4 In vitro primary osteoclast culture analysis

4.3.1.4.1 TRAP staining and cell morphology

Analysis of primary osteoclast cells in culture demonstrated some differences between *ia/ia* and wt/het rats at the cellular level. At most time points examined, the number of tartrate resistant acid phosphatase (TRAP) positive differentiated cells was not different between the two genotypes after culture of primary osteoclasts (Figures 4.7 a-b and 4.8 a), apart from the exception of a slight increase at 5 weeks in the *ia/ia* mutant cultures over wt/het ($p<0.05$). The morphology of the TRAP positive cells also did not appear different between the two genotypes at 5, 12 and 20 weeks of age. However at 9 weeks of age, the cultured cells from the *ia/ia* mutant rats demonstrated fewer large multinucleated TRAP positive cells than were seen in the wt/het cultures at this time point. Although there was no quantitative difference in the number of TRAP positive cells, their differentiation or fusion into large multinucleated cells appeared hindered. This observation was consistent throughout the samples examined at this

time point, this is shown in figure 4.7a. The *ia/ia* TRAP positive cells also did not appear to spread on the plastic culture wells the same as wt/het cells suggesting a reduced level of adherence to the plate surface.

At 12 weeks of age however, the primary osteoclasts responded once again like wt/het cells to the RANKL and M-CSF stimulation. The same number of TRAP positive cells had been produced, but also the morphology of the osteoclasts resembled those seen in wt/het cultures, they were well spread and multi-nucleated (Figure 4.7b and 4.8a). By 20 weeks again normal osteoclast differentiation and morphology was seen in the *ia/ia* mutant cultures (Figure 4.7b and 4.8a).

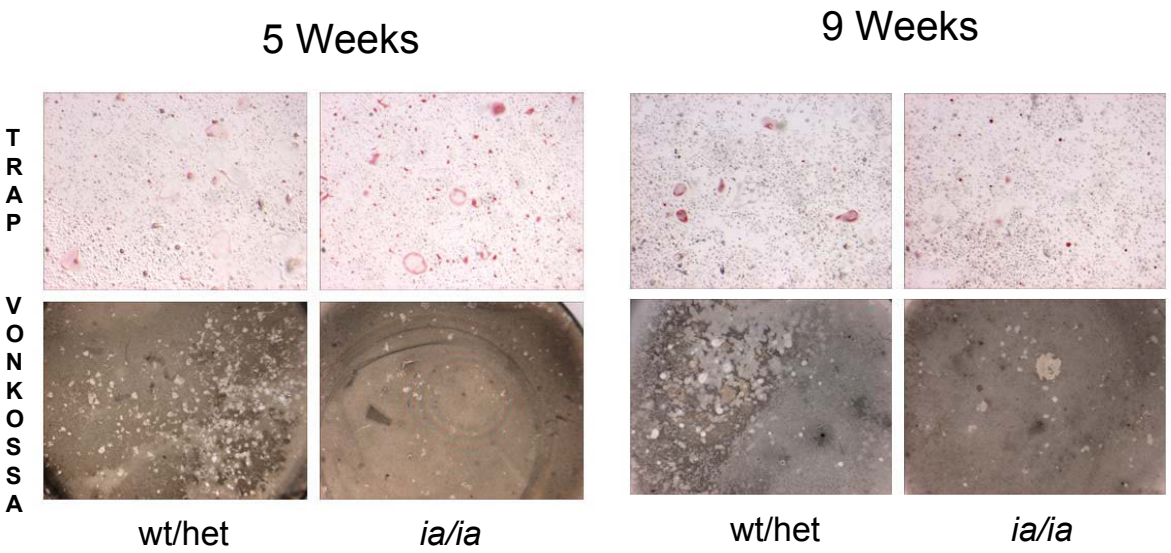

Figure 4.7a. *Representative images of osteoclast differentiation and resorption assays at 5 and 9 weeks of age.*
Top row, TRAP stain cells from wt/het and *ia/ia* cell cultures at 5 and 9 weeks of age, original x 3.2 magnification. Bottom row, von Kossa stained brown/black calcium phosphate discs from wt/het and *ia/ia* cell cultures at 5 and 9 weeks of age, original x 0.8 magnification. TRAP positive cells, stained red, appeared smaller and with reduced nuclei at 9 weeks of age in *ia/ia* compared to control. The same number of TRAP positive cells were seen at each time point in both genotypes but significantly reduced resorption was evident at both these time points in the *ia/ia* rat cultures.

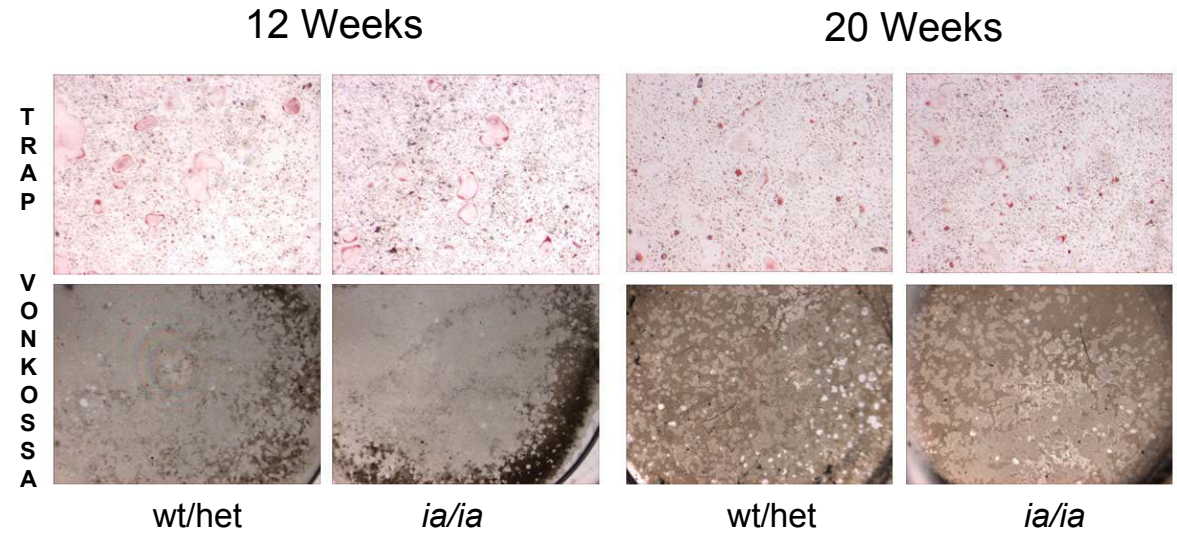

Figure 4.7b. *Representative images of osteoclast differentiation and resorption assays at 12 and 20 weeks of age.* Top row, TRAP stain cells from wt/het and *ia/ia* cell cultures at 12 and 20 weeks of age, original x 3.2 magnification. Bottom row, von Kossa stained brown/black calcium phosphate discs from wt/het and *ia/ia* cell cultures at 12 and 20 weeks of age, original x 0.8 magnification. The same number of TRAP positive cells, stained red, were seen at each time point in both genotypes. Resorption of the calcium phosphate discs was not different between genotypes at these later time points.

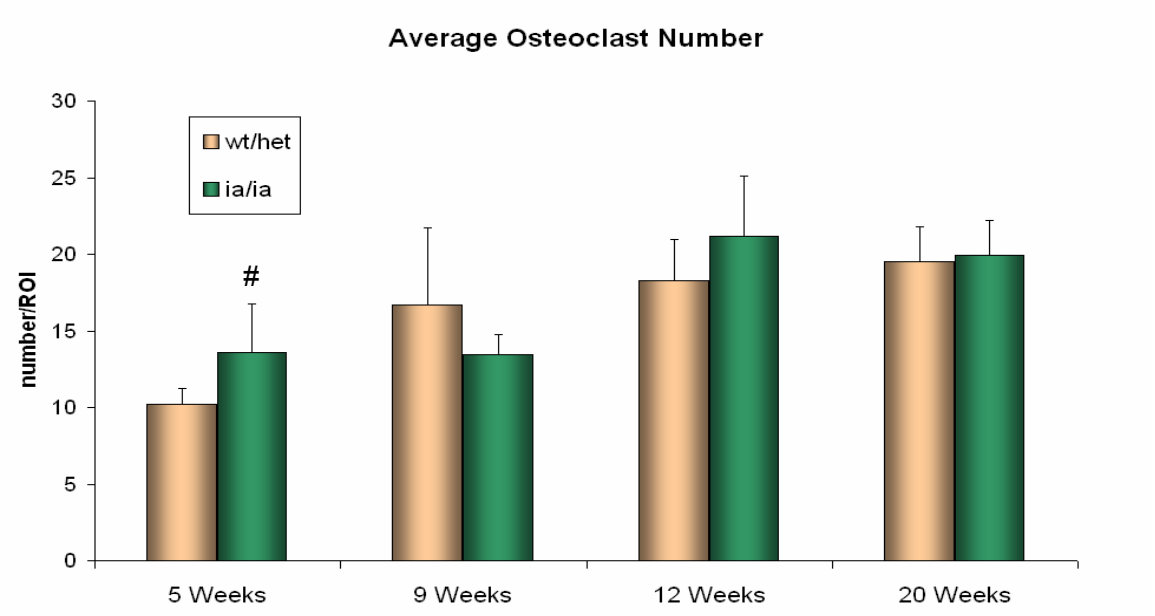

***Figure 4.8a**. Bar chart of mean osteoclast number per region of interest (ROI) in wt/het and ia/ia cell cultures at 5, 9, 12 and 20 weeks of age.*
Error bars represent 1 standard deviation. Hash (#) represents $p<0.05$ when compared to wt/het. A slight increase in TRAP positive cells was noted at 5 weeks of age in the *ia/ia* cultures.

4.3.1.4.2 Resorption assay

Calcium phosphate discs

When examining the resorptive capabilities of these cells an obvious difference arose between the two genotypes at the early ages. At 5 weeks of age, as seen clearly in figure 4.7a, after 10 days of culture with primary osteoclast cells, the von Kossa stained calcium phosphate discs showed significantly less resorption by the mutant cells. This difference was quantified to show that 27% of the disc area was resorbed by the cells in the wt/het samples, where as only 2% of the disc area was resorbed by the cells in the *ia/ia* cultures ($p<0.01$, Figure 4.8b).

By 9 weeks of age the difference in resorption between genotypes remained, again with 63% of the disc area resorbed in the wt/het cultures and only 17% resorption in the *ia/ia* cultures ($p<0.01$, Figure 4.7a and 4.8b).

At 12 weeks of age, there was a significant increase in the amount of calcium phosphate resorption, the wt/het cell cultures showed a significant increase in the area of resorption occurring, compared to 9 weeks of age, with 92% of the calcium phosphate being resorbed. The mutant *ia/ia* cells also showed an obvious increase in resorption with 71% of the disc area resorbed, reducing the difference between the two genotypes. By 20 weeks of age, no difference was evident in the level of resorption between both the wt/het and *ia/ia* cell samples, with 54% of the area resorbed in the wt/het and 59% for *ia/ia* samples (Figure 4.7b and 4.8b).

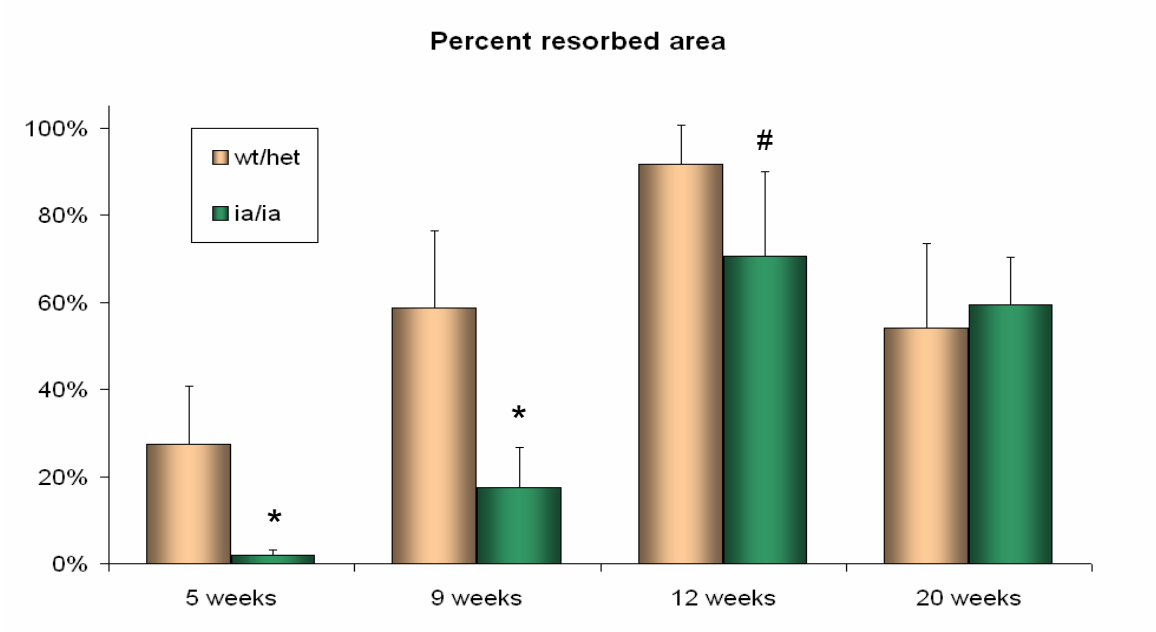

Figure 4.8b. *Bar chart of mean percent area of calcium phosphate disc resorbed for both wt/het and ia/ia cell cultures at 5, 9, 12 and 20 weeks of age.*
Error bars represent standard deviations. 1 asterix (*) represents $p<0.01$ when compared to wt/het, 1 hash (#) $p<0.05$ when compared to wt/het. Note large reductions in resorbed area at 5 and 9 weeks in the *ia/ia* osteoclast cultures with normalisation commencing by 12 weeks and completed by 20 weeks of age.

Human bone disc ELISA assay

The final *in vitro* method utilised to examine osteoclast function in the *ia/ia* rat was a cell culture system involving primary cell cultures in wells containing discs of human bone. These bone discs allow for discrete analysis of osteoclast resorptive capacity by the release of collagen degradation products into the cell media (section 8.6.3). Using an enzyme-linked immunosorbent assay (ELISA) kit specifically designed to detect these fragments, quantitative analysis was performed on media samples produced from cells grown in cultures in these wells from 5 and 12 weeks of age. Data produced from this analytical technique is presented in table 4.1 and although some trends for differences between the two genotypes were demonstrated, the experiment will need to be repeated to validate the data. This is because the negative control sample demonstrated a helical peptide concentration of 17.48µg/L which is higher than a large number of sample readings. Also, many of the sample readings produced large standard deviations, suggesting the technique requires optimisation. To improve the validity of results produced by this method, samples may have to be left longer on the bone discs prior to harvest to increase the detection

levels of the peptide. In addition, the cell plating density may need to be increased to enhance the osteoclast cell population and hence resorption levels. Figure 4.9 demonstrates TRAP positive cells in close proximity to human bone chips, confirming that resorbing cells were produced in the period of culture used in this experiment.

Time Point	***Genotype***	**5 Weeks**	**20 Weeks**
Day 0 to 14	*wt/het*	20.48 (12.02)	12.16 (2.53)
	ia/ia	14.63 (3.41)	10.72 (1.30)
Day 0 to 10	*wt/het*	16.17 (0.94)	15.03 (1.76)
	ia/ia	14.36 (5.33)	12.36 (1.70)
Day 6 to 14	*wt/het*	29.65 (18.50)	19.03 (5.46)
	ia/ia	16.83 (1.83)	22.47 (4.99)
Day 6 negative control	*wt/het*	36.76	17.00
	ia/ia	22.71	16.34
negative control	*Media*	17.48	17.48

Table 4.1. *Data values for helical peptide (a product of collagen degradation) concentrations from human bone disc culture experiment.*
Values are presented as mean and 1 standard deviation. Units are µg/L

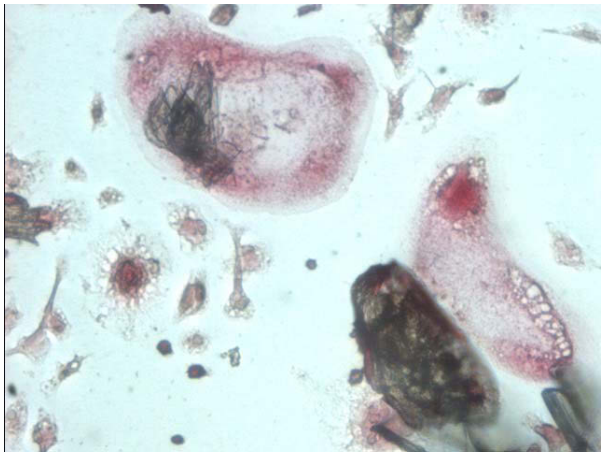

Figure 4.9. *Image of TRAP positive cells (red) from a wt/het sample on human bone discs (brown) in culture after media was removed for analysis*. These cells appear to be adhered to and resorbing the bone discs in this image.
Original magnification x 40.

4.3.2 Confirmation of osteopetrosis in fracture experiment rats

4.3.2.1 Radiological analysis

4.3.2.1.1 X-ray

As was seen on the x-ray analysis in the pilot phenotype analysis study (section 4.1) x-rays un-fractured tibia from the *ia/ia* rats used in the fracture experiments demonstrated continuous areas of radio dense metaphyseal bone compared to normal wt/het rats. This can be seen in the representative x-ray images of proximal tibia from both *ia/ia* and wt/het rats involved in the fracture experiments and is highlighted by an asterix in these images. (Figure 4.10) This difference was quantified using DEXA analysis.

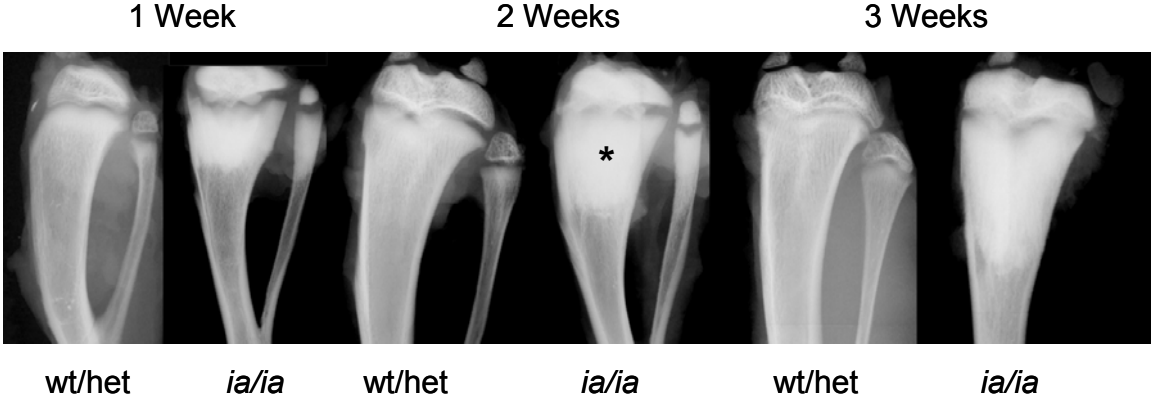

Figure 4.10. *Representative x-ray images of proximal tibia from wt/het and ia/ia samples from rats at the 1, 2, and 3 week time points of the fracture experiments*.
These images correspond to samples at 6, 7 and 8 weeks of age. Original magnification x 1.5. The asterix (*) illustrates the region of dense bone in the metaphysis of *ia/ia* rats that is not evident in wt/het samples.

4.3.2.1.2 Dual Energy X-ray Absorbtiometry (DEXA)

DEXA scans were performed on the contra-lateral proximal tibia of all rats used in the fracture experiments to confirm the persistence of the osteopetrotic phenotype. At the first harvest time point of 1 week *ia/ia* rats showed a 163% increase in BMC compared to wt/het rats in the proximal metaphysis of the tibia ($p<0.01$,) confirming the reduction in resorption in these rats. By 3 weeks this increase was reduced to 107% compared to wt/het rats ($p<0.01$). When considering the developmental changes over this period of time in these rats a 37% increase in BMC can be seen between the 1 and 3 week (6 and 8 weeks of age) time points in the wt/het rat proximal tibia. On the other hand the *ia/ia* mutant rats showed only an increase of 8% in BMC during this time (Figure 4.11). As this data were determined from 2 dimensional images using a constant area all BMD values reflect the exact changes seen in BMC.

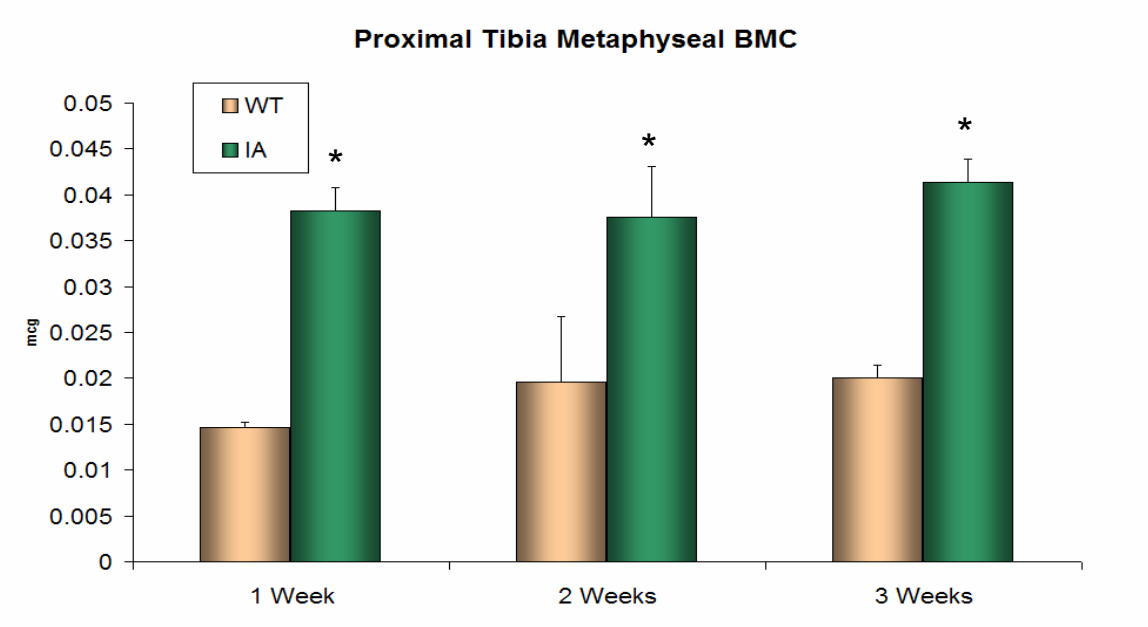

Figure 4.11 *Bar charts of mean proximal tibial metaphyseal BMC measured by DEXA in wt/het and ia/ia rats from fracture experiments at 1, 2, and 3 weeks post fracture*.
Error bars represent 1 standard deviation. Asterix (*) represents p<0.01 when compared to wt/het. The increased BMC remained constant throughout the experimental period. Units are micrograms (mcg).

4.3.2.2 Histology

Histological analysis of the proximal tibia collected from all rats involved in the fracture experiment confirmed that no recovery from the osteopetrotic phenotype had occurred in these experimental rats. Table 4.2 outlines all data determined from histomorphometric determinations of the proximal tibial metaphyseal area in all samples as performed for the phenotype analysis as described in section 4.3.1.2.

Parameter	***Genotype***	***1 Week***	***2 Weeks***	***3 Weeks***
Proximal BV/TV (%)	*wt/het*	27 (4)	26 (6)	30 (4)
	ia/ia	47 (7) *	45(8)*	48 (6)*
Distal BV/TV (%)	*wt/het*	7 (4)	9 (6)	15 (5)
	ia/ia	51 (16)*	52 (11)*	51 (19)*
Proximal Trabeculer Thickness (µm)	*wt/het*	73.6 (12.9)	72.7 (11.0)	80.1 (10.3)
	ia/ia	92.6 (19.7)†	91.3 (22.4)†	79.0 (11.8)
Distal Trabecular Thickness (µm)	*wt/het*	78.2 (13.5)	74.1 (18.5)	97.0(11.3)
	ia/ia	148.3 (56.7)*	125.2 (39.8)*	134.7 (56.7)
Proximal Trabecular Number (N/mm)	*wt/het*	3.7 (0.4)	3.6 (0.5)	3.7 (0.4)
	ia/ia	5.3 (0.6)*	5.2 (0.7)*	5.8 (0.9)*
Distal Trabecular Number (N/mm)	*wt/het*	1.0 (4.5)	1.1 (0.5)	1.5 (0.4)
	ia/ia	4.0 (1.22)*	4.5 (2.1)*	4.0 (2.1)*

*Mean (StD), * represents p<0.01 when compared to wt/het*
† represents p<0.05 when compared wt/het

Table 4.2 *Data generated from histomorphometric analysis of proximal tibial metaphysis in growing ia/ia and wt/het rats.* Note the significant increases in BV/TV, trabecular number and thickness in the *ia/ia* rats compared to wt/het at each time point examined.

The BV/TV of the proximal region of the tibial metaphysis in the wt/het rats was maintained between 26-30% throughout the 3 week period of the fracture experiment. The *ia/ia* rats showed significantly higher mean proximal BV/TV of 47% at 1 week post fracture, which was maintained at the 3 week end time point ($p<0.01$, Table 4.2, Figure 4.12). Distal metaphyseal BV/TV, increased in wt/het rats from 7% to 15% throughout the 3 week fracture experiment period. However, the *ia/ia* rats demonstrated a distal metaphyseal BV/TV of 51% at 1 week post fracture, almost a 6-fold increase over wt/het rats, maintaining this increased BV/TV to the end time point with a mean BV/TV of 51% ($p<0.01$, Table 4.2, Figure 4.12). The histological images in Figure 4.13 of the von Kossa stained sections used for this analysis reveal these differences showing extensive retention of primary metaphyseal spongiosa in the *ia/ia* rats throughout the fracture experimentation period, clearly confirming the maintenance of the osteopetrotic phenotype.

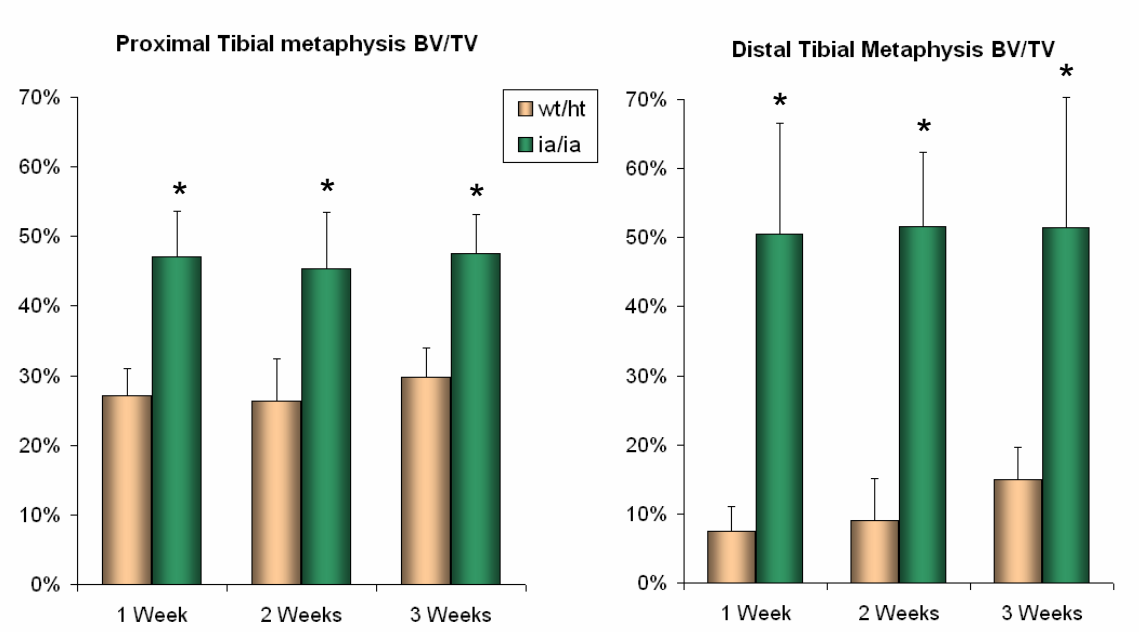

Figure 4.12 *Bar charts of mean values for tibial metaphyseal BV/TV of fracture samples for both ia/ia and wt/het genotypes at 1, 2 and 3 weeks post fracture.*
Error bars represent 1 standard deviation, Asterix (*) represents $p<0.01$ when compared to wt/het. Note the consistently increased BV/TV in both proximal and distal regions in the *ia/ia* rats compared to wt/het.

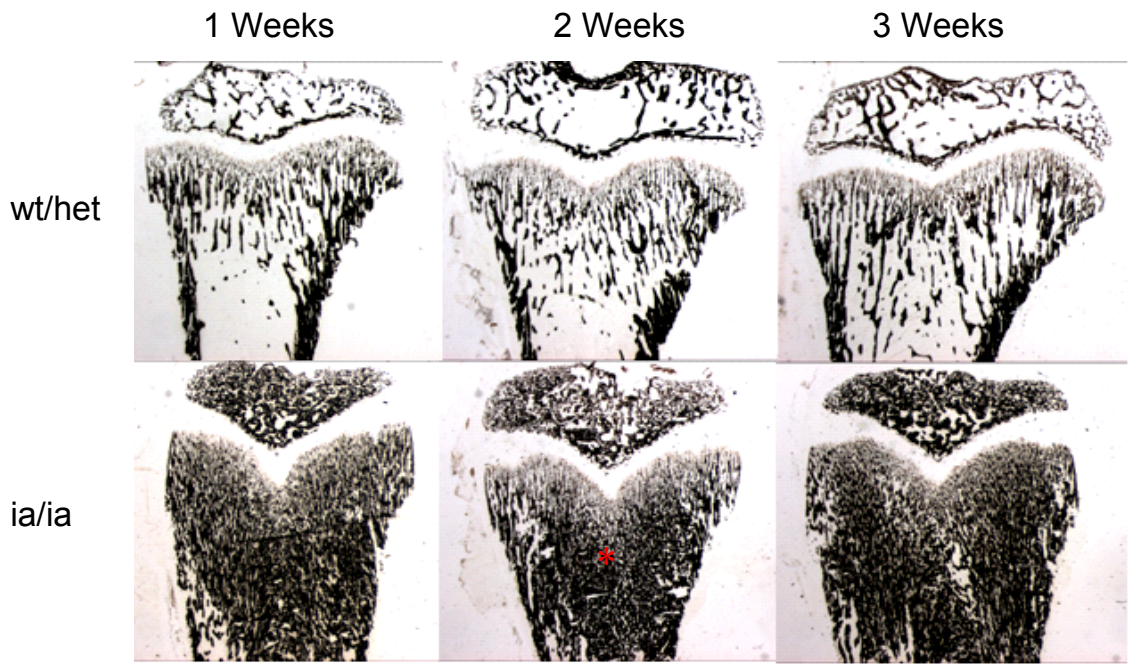

Figure 4.13. *Representative proximal tibia von Kossa stained sections of wt/het and ia/ia rat samples at 1, 2, and 3 weeks post fracture*.
Note the extensive increase in bone volume in the metaphyses of the *ia/ia* samples, shown as red asterix) compared to the wt/het controls. This increase is maintained throughout the fracture experiment period, and was due to increased trabecular thickness and number. Von Kossa stains mineralised tissue black. Original magnification x 1.0.

The mechanistic reasons behind the increased BV/TV in the *ia/ia* mutant rat samples can be explained by the morphological trabecular bone properties. As shown in Table 4.2 and Figures 4.14 and 4.15, both trabecular number ($p<0.01$) and thickness ($p<0.05$) were significantly increased over wt/het samples at the 1 and 2 week time points in the proximal metaphyseal region. However by the final 3 week time point trabecular thickness is no longer increased in the *ia/ia* samples compared to wt/het, but trabecular number remains 56% higher at this stage ($p<0.01$).

In the distal metaphyseal region, again we see significant increases in both trabecular number and thickness at 1 and 2 week time points ($p<0.01$). As seen in the proximal region, the distal metaphyseal trabecular thickness is no longer increased at 3 weeks in the mutant rats, however trabecular number remains 166% higher in the *ia/ia* mutants compared to wt/het at this time ($p<0.01$, table 4.2, Figure 4.14, Figure 4.15 and Figure 4.12). This normalization of trabecular thickness in the distal region in the *ia/ia* rats to the 3 week time point was a result of the wt/het rats increasing trabecular thickness to a level more similar to the *ia/ia* samples.

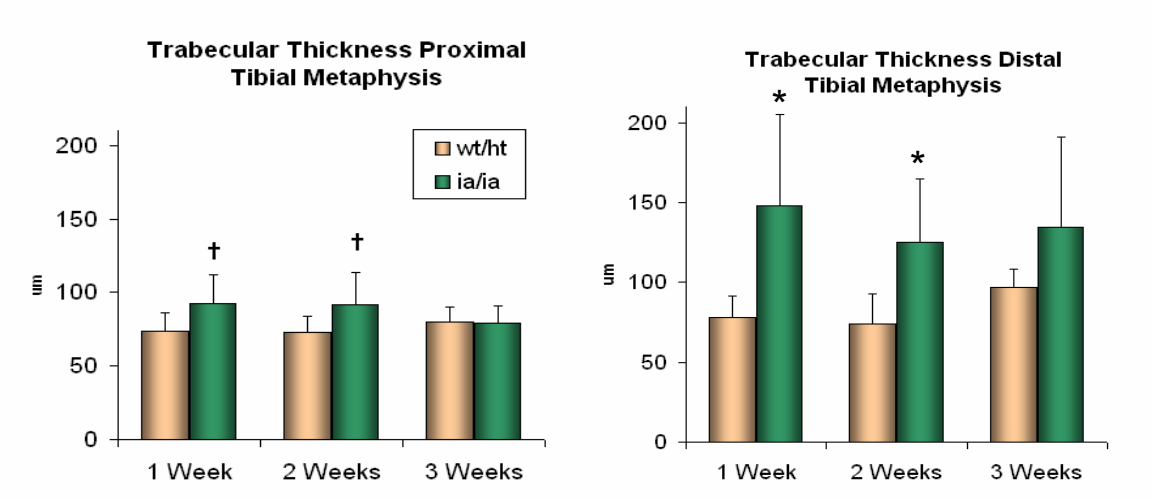

Figure 4.14 *Bar charts of mean values for tibial metaphyseal trabeculae thickness of fracture samples for both ia/ia and wt/het genotypes at 1, 2 and 3 weeks post fracture.*
Error bars represent 1 standard deviation, asterix (*) represents p<0.01when compared to wt/het. *ia/ia* rats showed increased trabecular thickness in both regions at 1 and 2 weeks compared to wt/het, with no increase seen by 3 weeks post fracture.

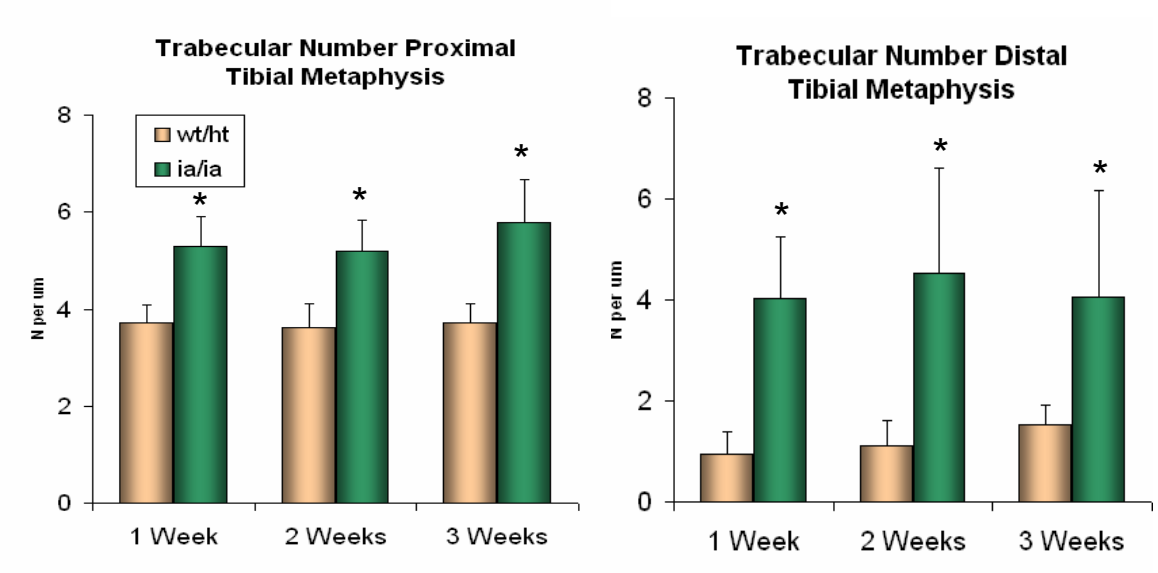

Figure 4.15 *Bar charts of mean values for tibial metaphyseal trabecular number of fracture samples for both ia/ia and wt/het genotypes at 1, 2 and 3 weeks post fracture*.
Error bars represent 1 standard deviation, asterix (*) represents p<0.01 when compared to wt/het. *ia/ia* rats showed increased trabecular thickness in both regions at all time points compared to wt/het.

4.3.3 Analysis of initial fracture repair in ia/ia rats

4.3.3.1 Radiological analysis

4.3.3.1.1 Radiological grading of fracture union.

Radiographs were graded as either united or not united based on bridging of the fracture site with radio opaque bone tissue (section 8.2.1)

No difference in the rate of radiologically determined union was seen throughout the healing process between the wt/het and mutant *ia/ia* rats. At 1 week post fracture there were no bridging of fracture sites in either genotype group. By 2 weeks however, 60% of wt/het rats and 50% of *ia/ia* rats demonstrated union, this difference was not significant by chi squared analysis, and by 3 weeks post fracture both genotypes demonstrated 100% union. (Figure 4.16)

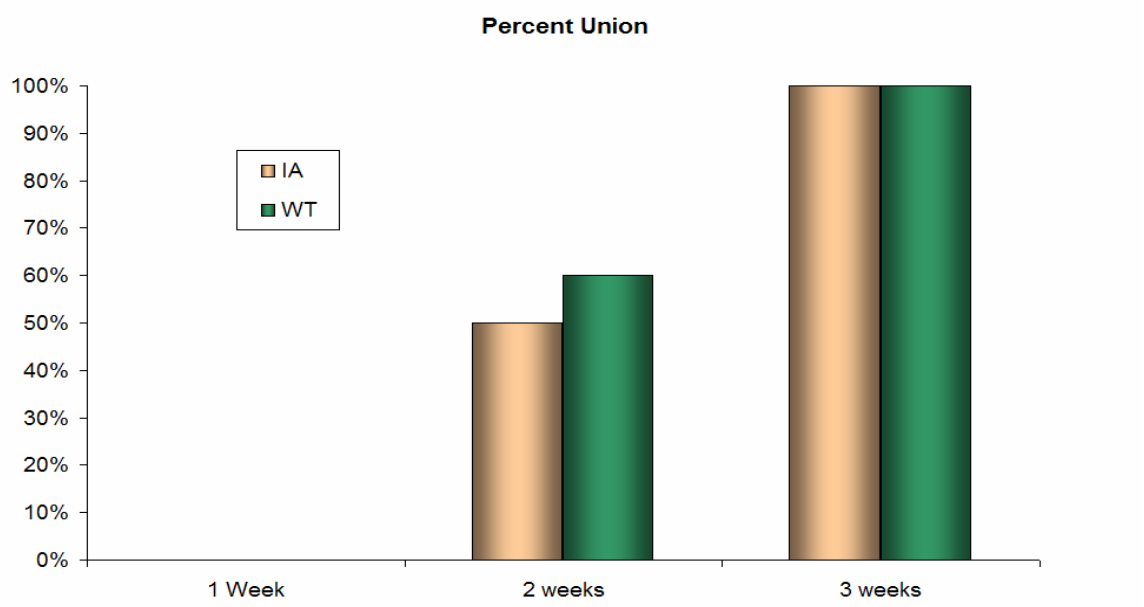

Figure 4.16. *Bar charts of percent union rates of both wt/het and ia/ia rats at 1, 2, and 3 weeks post fracture as assessed radiologically.*
Standard deviations could not be generated due to statistical analysis method used. No differences were seen in the rate of union between the two genotypes.

4.3.3.1.2 Quantitative computerized tomography (QCT) analysis of callus and contralateral limb.

Fracture site

Analysis of hard callus volume using QCT demonstrated significant changes in the BMC, Volume, BMD, periosteal circumference (circumference) and polar moment of inertia (moment of inertia) of the fracture callus in the mutant *ia/ia* rats compared to the wt/het controls. All raw data is outlined in Table 4.3 and is presented as mean and 1 standard deviation.

As early as 1 week post fracture, callus BMC was significantly increased by 23% in the *ia/ia* rats over wt/het controls ($p<0.01$). Mineralised callus volume had only increased by 13% at this early stage ($p<0.05$), thus the increased BMC also produced an 8% increase in callus BMD in the *ia/ia* rats compared to wt/het controls ($p<0.01$). The periosteal circumference of the callus and moment of inertia were not different between genotypes at this early healing stage.

By 2 weeks post fracture the differences in hard callus properties between genotypes were more pronounced, with callus BMC 58% higher in the *ia/ia* rats compared to wt/het controls ($p<0.01$). Callus volume had increased 41% over wt/het controls by this time, this increase in volume meant that the difference seen at 1 week in callus BMD no longer persisted at 2 weeks. Again the circumference of the callus was not different between genotypes at 2 weeks however the moment of inertia was 63% greater in the *ia/ia* rats than wt/het controls, although this did not reach statistical significance with a p value of 0.06, Table 4.3).

Lastly, by the final outcome time point of 3 weeks when union had been achieved in all samples, BMC was 132% higher in *ia/ia* calluses compared to wt/het controls ($p<0.01$). Further increases in callus volume were also noted with *ia/ia* rats showing a 124% increase over wt/het controls ($p<0.01$). Again callus BMD did not show any differences between genotypes at 3 weeks. Callus circumference was significantly increased 38% in *ia/ia* rats compared to controls by 3 weeks ($p<0.01$) leading to a 251% increase in polar moment of inertia ($p<0.01$, Table 4.3). These changes seen throughout the course of the fracture experiment are evident in the representative cross sectional CT scan images in Figure 4.17.

In addition to the quantitative data generated from QCT scans, the images produced using this technique, as shown in Figure 4.17, present an observational difference between the fracture calluses of *ia/ia* rats and their wt/het littermates. By 3 weeks post fracture, the wt/het calluses demonstrate a clearly defined neo-cortex, developed through remodelling of the hard callus. In contrast, *ia/ia* callus show no

signs of developing this neo-cortex at 3 weeks, suggestive of a delay in hard callus remodelling here.

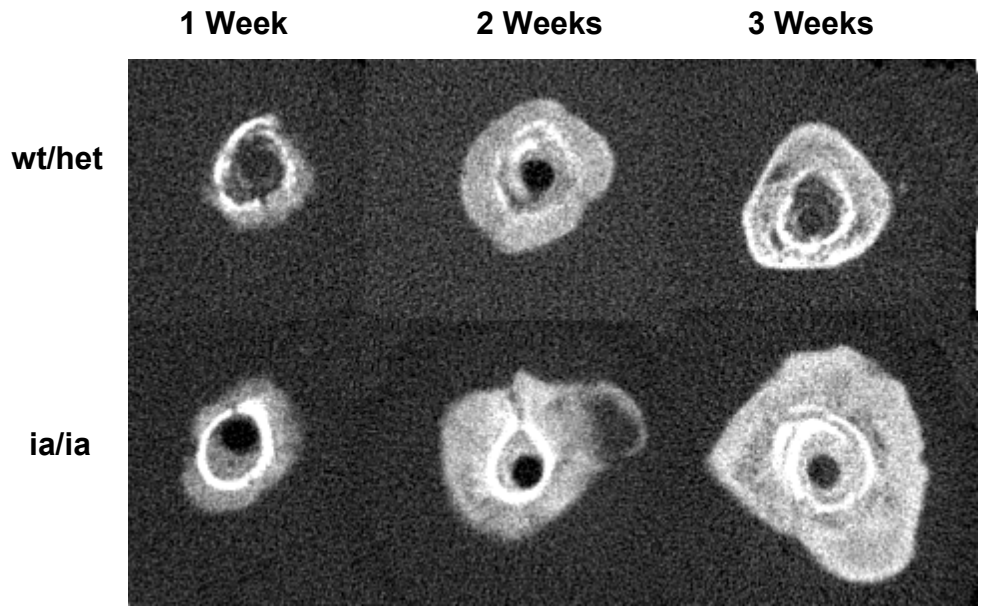

Figure 4.17. *Representative cross sectional QCT scan images of the central region of the fracture site of both wt/het and ia/ia fracture samples at 1, 2 and 3 weeks post fracture*.
Fracture calluses of *ia/ia* rats show a significant increase in callus mineralisation and size, shown as increased intensity and areas of white image, compared to wt/het calluses by 3 weeks post fracture. The wt/het samples show a slight decrease in size between 2 and 3 weeks, *ia/ia* calluses increasing further at this stage.

Operated (Right) Femora

Parameter	*Genotype*	*1 Week*	*2 Weeks*	*3 Weeks*
BMC (mcg)	*wt/het*	32.49 (3.67)	47.57 (10.47)	48.22 (7.48)
	ia/ia	40.09 (3.63)*	75.18 (15.95)*	112.00 (20.44)*
BMD (mcg/mm3)	*wt/het*	635.58 (32.92)	666.67 (123.70)	733.07 (106.79)
	ia/ia	683.49 (36.09)*	707.41 (69.20)	736.64 (47.95)
Volume (mm3)	*wt/het*	51.57 (8.39)	76.95 (28.37)	68.34 (16.96)
	ia/ia	58.48 (6.44)**	108.36 (25.64)†	152.97 (26.95)*
Polar Moment of Inertia (mm4)	*wt/het*	28.65 (12.23)	63.21 (41.24)	49.47 (20.51)
	ia/ia	30.71 (8.72)	103.17 (51.54)	173.52 (58.11)*
Periosteal Circumference (cm)	*wt/het*	11.93 (0.83)	14.62 (2.62)	14.12 (1.64)
	ia/ia	11.96 (0.89)	16.52 (2.54)	19.48 (1.66)*

Mean (SD) ** p<0.01 when compared to wt/het,*

**p<0.05 when compared to wt/het, †p<0.02 when compared to wt/het

Non-operated (Left) Femora

Parameter	*Genotype*	*1 Week*	*2 Weeks*	*3 Weeks*
BMC (mcg)	*wt/het*	19.07 (1.31)	25.78 (0.96)	30.93 (1.45)
	ia/ia	22.39 (2.95)*	27.86 (5.32)	32.17 (7.23)
BMD (mcg/mm3)	*wt/het*	909.58 (9.57)	985.42 (22.27)	1023.35 (26.59)
	ia/ia	843.02 (45.36)*	848.20 (23.03)*	837.82 (36.70)*
Volume (mm3)	*wt/het*	20.99 (1.29)	26.22 (1.09)	30.32 (1.08)
	ia/ia	27.80 (4.45)*	34.86 (6.15)*	40.45 (9.93)*
Polar Moment of Inertia (mm4)	*wt/het*	7.78 (1.18)	12.16 (1.81)	15.70 (1.59)
	ia/ia	13.31 (3.14)*	17.39 (4.78)*	21.88 (7.53)**

Mean (SD) ** p<0.01 when compared to wt/het,*

***p<0.05 when compared to wt/het*

Table 4.3 *Data generated from QCT scans of operated and non-operated femora of ia/ia and wt/het rats.*
SD 1 standard deviation. Units are micrograms (mcg), Micrograms per millimetre cubed (mcg/mm3) millimetres cubed (mm3) and millimetres to the poser of 4 (mm4).

Contralateral Limb

Analysis of the un-operated left femora revealed interesting data on the phenotypic changes observed in the long bones of mutant *ia/ia* rats. Three slices of 1 mm thickness and 2 mm apart were scanned in the mid diaphyseal region to cover a region comparable to that obtained on the right femora of the fracture region.

Mineralised callus properties of the comparable mid-shaft of *ia/ia* rats showed significant differences to that of the wt/het controls at the time points analysed in this study. The 1, 2 and 3 week post fracture outcome time points correspond to 6, 7 and 8 weeks of age respectively. The tissue in this diaphyseal region consists only of cortical bone thus these data represent any differences in cortical bone structure that develop in the growing *ia/ia* and wt/het rats due to the reduced level of resorption. All raw data values are presented in Table 4.3 as mean with 1 standard deviation.

Cortical BMC at 6 weeks of age showed a 20% increase in *ia/ia* rats compared to wt/het controls ($p<0.01$) however by 7 weeks of age this had reduced to an increase of just 8% ($p<0.01$) and by 8 weeks of age this difference in BMC no longer existed (Table 4.3). Cortical bone volume at 6 weeks was 36% higher in the *ia/ia* bones compared to wt/het controls, this percentage increase remaining constant up to 8 weeks of age ($p<0.01$). On the other hand, cortical BMD was significantly different between genotypes at 6, 7 and 8 weeks of age, however the changes were reductions in the *ia/ia* mutants compared to wt/het by 7%, 14% and 18% respectively ($p<0.01$). Thus, cortical mid diaphyseal bone in the mutant *ia/ia* rats showed a constant increase in cortical bone volume over the time course of the study but with reducing mineral content, resulting in a steady decrease in cortical bone BMD (Table 4.3).

4.3.3.2 Histological analysis of endochondral ossification

4.3.3.2.1 Histomorphometry of cartilage content

Quantification of callus properties on histological sections revealed important results. The area of each callus that contained avascular cartilage and mesenchymal tissue was not different between genotypes throughout the experimental period, (Figures 4.18-4.20). At 1 week post fracture both wt/het and mutant *ia/ia* rat calluses contained 85-88% vascularised bone tissue. By 2 weeks this was increased to 96-97% in both wt/het and *ia/ia* calluses, and by 3 weeks the avascular tissue was no longer present in either genotype such that all calluses were 100% vascular bone tissue (Figures 4.18 and 4.19). This result confirming that the process of endochondral fracture repair in these mutant rats proceeds at the same rate as in the normal littermates.

Interestingly, this quantitative analysis revealed a difference between the two genotypes in the area of vascularised bone tissue at 3 weeks post fracture. At this final outcome stage when all calluses were completely ossified, the mutant *ia/ia* rat calluses had a 61% larger total callus area than wt/het rats ($p<0.05$) (Figure 4.20). This result corresponds to data achieved from QCT scans presented in section 4.3.4.1.2. These results also demonstrate a delay in hard callus remodelling in the *ia/ia* rats. By 3 weeks wt/het calluses have shown a significant reduction in callus area, whereas *ia/ia* calluses continue to increase in size up to 3 weeks post fracture. Clearly, hard callus remodelling is not taking place in the mutant fracture sites.

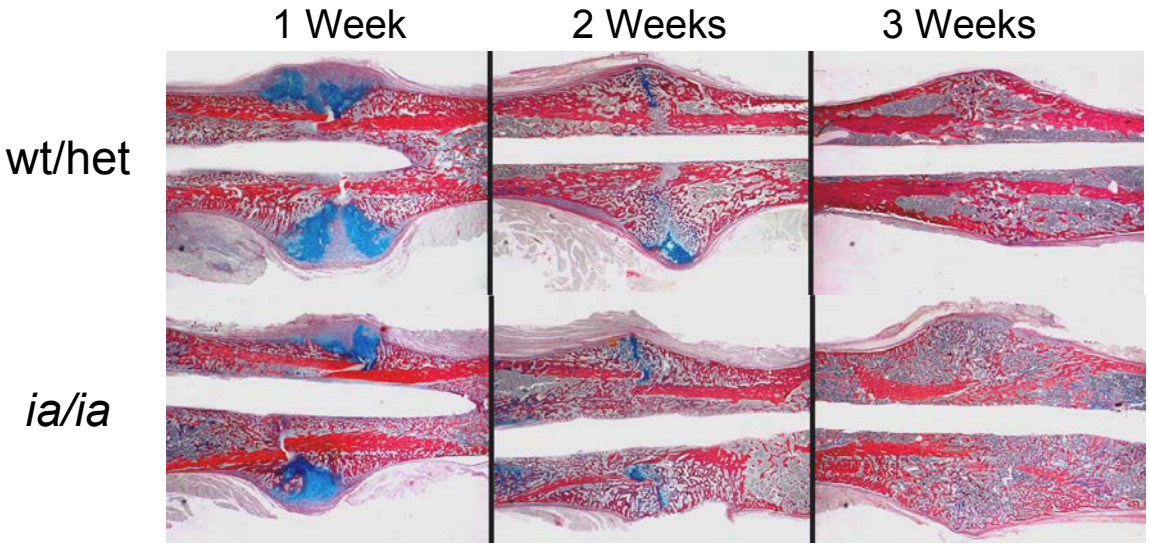

Figure 4.18. *Representative sections of wt/het and ia/ia samples at each time point examined demonstrating normal endochondral ossification.*
Alcian blue stained the cartilage blue and Sirius red stained the bone tissue red. Removal of the blue cartilage tissue and replacement with red ossified bone tissue is achieved at the same rate in both *ia/ia* and wt/het samples. Original magnification x 0.63.

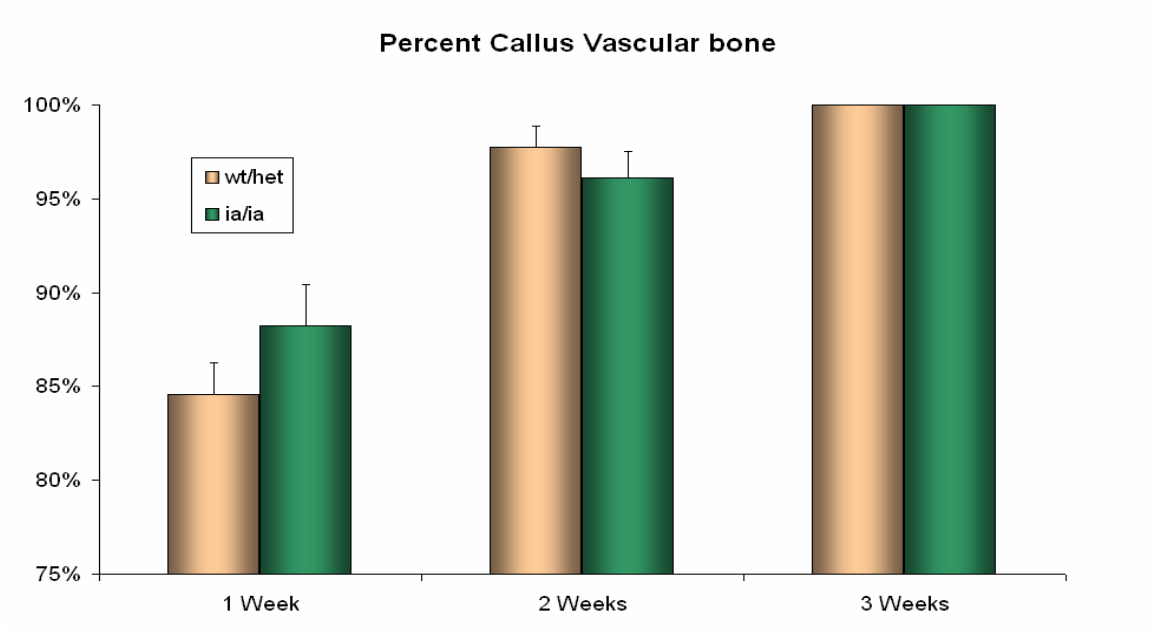

Figure 4.19. *Bar chart of mean percentage of callus containing vascular bone tissue for wt/het and ia/ia samples at 1, 2 and 3 weeks post fracture.*
Error bars represent 1 standard deviation. All samples showed 100% vascular bone content at 3 weeks. No differences were noted between the two genotypes at any time point examined.

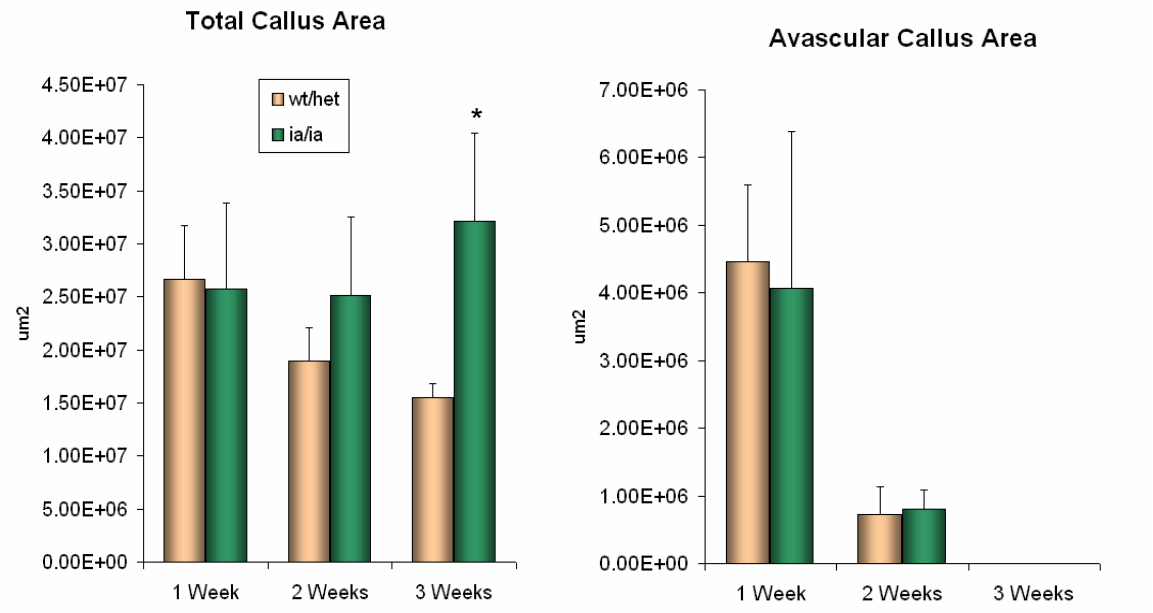

Figure 4.20. *Bar charts of mean total callus area and avascular callus area for both wt/het and ia/ia samples at 1, 2 and 3 weeks post fracture.*
Error bars represent 1 standard deviation, asterix (*) represents $p<0.05$ compared to wt/het. The total callus area was significantly increased in the *ia/ia* rats over wt/het at 3 weeks. No differences were seen in the area of avascular cartilage tissue. Micrometers (μm)

4.3.3.2.2 Histomorphometry of tibial growth plate height

Tibial growth plate height was not different between the two genotypes at each of the time points examined during the fracture experiments. At each of 6, 7 and 8 weeks of age *ia/ia* rats demonstrated equivalent mean growth plate height to their wt/het littermates (Figures 4.21 and 4.22).

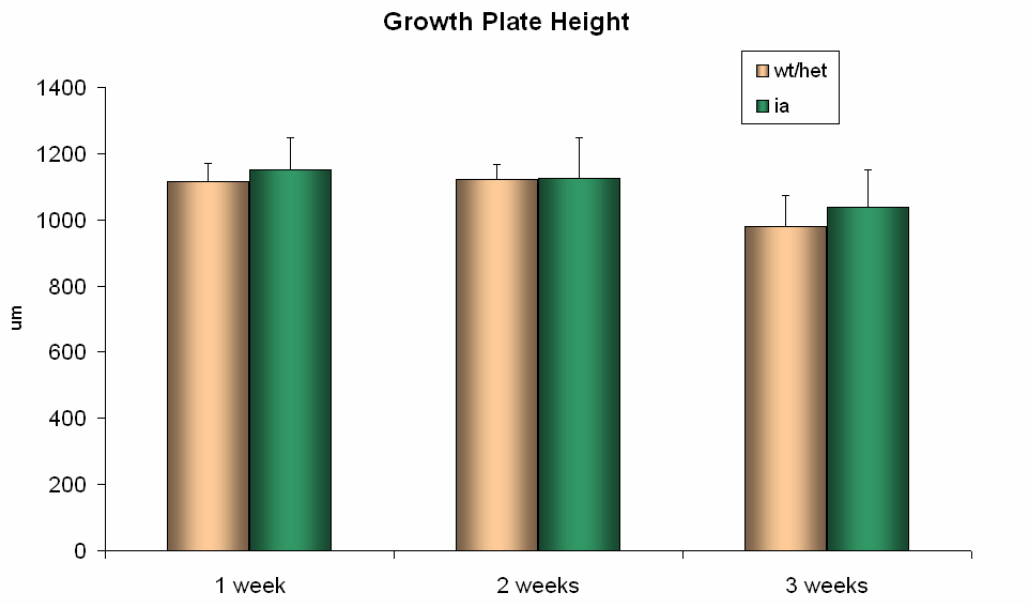

Figure 4.21. *Bar chart of mean growth plate height from the proximal tibia for both wt/het and ia/ia samples at the 1, 2 and 3 weeks post fracture time points.*
Error bars represent 1 standard deviation. No differences were seen between genotypes in growth plate height. Micrometers (μm)

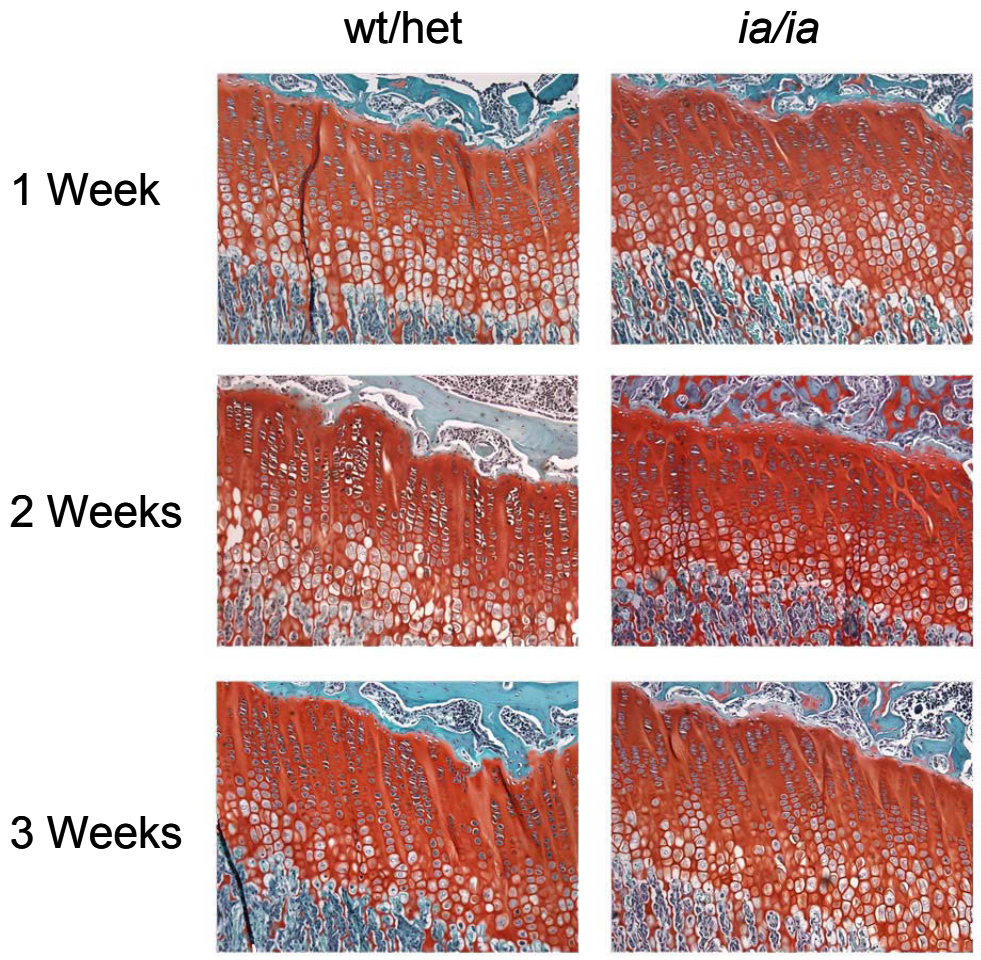

Figure 4.22. *Representative sections of proximal tibial growth plates from wt/het and ia/ia samples at 1, 2 and 3 weeks post fracture.*
Saffranin O/ light green stain, cartilage tissue of growth plate is stained red and bone is stained green. Original magnification x10. Average growth plate height was not different between genotypes.

4.4 Discussion

4.4.1 Recovery from osteopetrosis in the incisor absent rat.

Initial radiological analysis on x-rays revealed the distinctive skeletal abnormalities the *ia/ia* rat carries, as reported by previous authors (Marks, Jr., 1973). These include shortened limbs, with somewhat abnormal shape and formation, along with dense sclerotic metaphyseal bone, as demonstrated clearly in Figure 4.2. Furthermore, DEXA scans of this area of dense metaphyseal bone revealed quantitative increases in the amount and density of mineralised tissue retained in the tibial metaphases of these mutant rats. Histological examination of metaphyseal bone showed extensive retention of primary spongiosa in the mutant rats, and a dramatically increasing the BV/TV in the metaphyseal region, seen clearly in Figure 4.5.

The first evidence to suggest recovery of bone resorption in the mutant rats in the current study surfaced when the area of interest analysed by histology was divided into proximal and distal regions. These regions roughly correspond to primary spongiosa (proximal) and secondary spongiosa (distal). Up to 20 weeks of age the proximal metaphyseal BV/TV remained at around 60% in the mutant *ia/ia* rats suggesting no change in the level of resorption in this region up to this age. However, when looking at the distal area on the metaphysis, a region where the wt/het rats demonstrate a BV/TV of approximately 5%, the first signs of recovery of resorption became apparent in the *ia/ia* rats. Up to 9 weeks of age the distal BV/TV was maintained at approximately 50% in the *ia/ia* rats, however from 12 weeks onwards this began to decrease such that by 20 weeks BV/TV in this region had dropped to only 20%. This unmistakably demonstrates that at the tissue level, active resorption was taking place in these *ia/ia* samples from 12 weeks of age.

Further, serum CTX level analysis confirmed that recovery from the inactive resorption in these rats occurred at a similar time point. Corresponding to the histological analysis, measurement of serum CTX levels revealed a recovery from the decreased osteoclast resorption in the young *ia/ia* mutant rats to similar levels to wt/het by 12 weeks of age (Figure 4.9). However, as early as 9 weeks of age, the differences seen between the *ia/ia* and wt/het rats in serum CTX was reduced, dropping from 64% at 7 weeks to just 28% at 9 weeks. Thus, active resorption at 9 weeks of age in the *ia/ia* rats was of a more similar level to wt/het than that seen at earlier ages. Although, as histology demonstrates, the outcomes of this recovering resorptive activity at the tissue level do not manifest until a later age, i.e. 10-12 weeks.

Finally, *in vitro* culture of primary osteoclasts from growing *ia/ia* and wt/het rats provide the last line of evidence for confirmation of recovery by 12 weeks of age. Although a similar level of TRAP positive multinucleated cell differentiation was noted between the two genotypes at 5 weeks of age, the resorptive capacity of the *ia/ia* cells was greatly reduced at this age compared to wt/het cells. A significant reduction in resorption of the calcium phosphate substrate reflects that the TRAP positive cells that did form, were not able to resorb the substrate as efficiently as normal wt/het cells. Similarly, at 9 weeks of age no significant reduction in the number of TRAP positive cells was seen between the mutant *ia/ia* and wt/het cultures, however upon morphological analysis it became clear that the TRAP positive cells in the *ia/ia* cultures were less mature. The *ia/ia* TRAP positive cells appeared smaller and fewer cells were multinucleated compared to wt/het cells. It is unclear as to why this difference was evident at this time point as it was not obvious at any other time point examined. This time point was completed as the first *in vitro* experiment so the cells

may have been treated more vigorously than subsequent time points, leading to removal of more of the mature differentiating cells in the *ia/ia* populations that had not yet adhered well to the plastic surface. As a result subsequent *in vitro* experiments were treated less vigorously when the culture media was changed and these differences were not seen. This does suggests however that data from the 9 week age time point may be aberrant and require repetition. The resorption assay on calcium phosphate discs at this 9 week time point however can be included as it was not affected by excessive rinsing. As was noted at 5 weeks, *ia/ia* mutant cells at 9 weeks demonstrated a significantly reduced capacity of resorption of the calcium phosphate substrate compared to wt/het cells (Figure 4.7a and 4.8). These data corresponding to *in vivo* experimental outcomes that up to 9 weeks of age *ia/ia* rat osteoclasts exhibit an extreme deficiency in resorptive capabilities compared to wt/het rat osteoclasts.

By 12 weeks of age, in concert with *in vivo* data obtained, recovery of osteoclast function was demonstrated *in vitro*. Both wt/het and *ia/ia* primary osteoclast cultures saw significant increases in the number and size of TRAP positive multi-nucleated cells compared to 9 weeks of age, with no observable differences between the genotypes. More importantly, however, resorption of the calcium phosphate discs was not different between the genotypes at 12 weeks of age, with the *ia/ia* cells demonstrating extensive resorptive capabilities, comparable to wt/het cells, which remained evident up to 20 weeks of age (Figures 4.7b and 4.8).

In addition to resorption on calcium phosphate discs, human bone chips were also used. However data from this technique was not consistent and negative control values failed to validate the data obtained, thus this experiment requires repetition and further optimisation to determine if the trends seen were real results. From figure 4.9 it is apparent that the cells in these cultures were differentiated into TRAP positive cells, however a longer period of incubation in the wells before sample harvesting as well as increased initial cell plating density may be considered in the optimisation of this method in the future.

As a result of the extensive phenotype work it was determined that up to 9 weeks of age the *ia/ia* mutant rat exhibits extreme osteopetrosis due to an osteoclast population that is unable to resorb bone matrix. Between 9 and 12 weeks of age however this mutation begins to resolve and a new population of normally resorbing osteoclasts develops, driving the commencement of recovery from the osteopetrotic phenotype. Finally, subsequent fracture repair studies were performed with the knowledge that up to 9 weeks of age, the mutant rats exhibit osteoclasts with grossly deficient capability of bone matrix. For this reason 5 week old rats were chosen for subsequent fracture experiments.

4.4.2 Assessment of resorption activity in fracture experiment rats

Examination of tibia from each fracture experimental rat allowed for repetition and expansion of analysis performed in the initial phenotype study, and provided further confirmation that osteoclast function remained reduced throughout the course of the fracture experiments. DEXA scans and histology of the tibial metaphyses confirmed that the osteopetrotic phenotype was maintained in these rats until the end of the experiment. As demonstrated in the initial phenotype analysis, the dense region in the tibial metaphysis of the *ia/ia* rats seen on radiographs (Figure 4.10) was 163% higher in bone mineral content than wt/het controls at the first harvest time point of 1 week post fracture, 6 weeks of age. However, by 3 weeks post fracture, 8 weeks of age, this increase was only 107%.

The fact that the difference between the mutant and normal rats was reduced by the end time point implies that these rats are recovering from their reduced resorption. However when examining the data longitudinally it can be seen that during the 2 week period (6 to 8 weeks of age) both the wt/het and mutant rats show an increase in net mineral accrual with wt/het rats showing a larger mineral accrual of 37% compared to just 8% in *ia/ia* rats. The area of bone examined by this analytical method is within a 2.3cm distance directly below the growth plate. Since rats at this age have been shown to grow on average 2.5 cm per week for wt/het and 2 cm per week for *ia/ia* rats (data not presented in this thesis) the area of bone measured between 6 and 8 weeks is almost completely new bone. From this it could be suggested that the reduction in difference between the genotypes by 8 weeks of age is due to a bone formation deficit in the mutant rats and not a recovery of resorptive activity. However, analysis of this bone phenotype to date has failed to quantitatively demonstrate any changes in bone formation in the mutant *ia/ia* rats, thus this is an area that requires further investigation in this rat model of osteopetrosis. On the other hand this unexpected result may be explained by the limitations of the method of analysis. The DEXA scans do not allow for discrete separate analysis of trabecular and cortical bone, thus both types of bone are included in the data produced. The reduction in the rate of mineral accrual in the *ia/ia* rats therefore may be due to thinning of the cortical bone due to the reduced remodelling of bone in these rats. In fact, the *ia/ia* rat has been previously shown to develop thinner cortices than those of their wt/het littermates whilst showing extensive increases in metaphyseal trabecular bone (Tuukkanen *et al.*, 2000). This is supported further by the data produced from histological analysis of metaphyseal trabecular bone which showed up to 6-fold increases in metaphyseal BV/TV.

Analysis at the tissue level confirmed those results determined by original phenotype analysis with histology of the metaphyseal area of these samples revealing a 60-74% increase in proximal metaphyseal BV/TV and a 240-600% increase in distal metaphyseal BV/TV in *ia/ia* rats compared to wt/het over the entire period of analysis. Most importantly however, the distal metaphyseal BV/TV did not reduce over the this time in the *ia/ia* rats, staying constant at approximately 50%, further confirming that recovery of resorption was not taking place in these rats. Due to the larger sample size, further analysis was performed on these samples to determine the mechanism behind the increased BV/TV. It was confirmed that both trabecular number and thickness were increased at the earlier ages (6 and 7 weeks) in both proximal and distal regions in *ia/ia* samples. However by the end time point of 8 weeks, only trabecular number was increased in the *ia/ia* rats over wt/het in both distal and proximal regions, trabecular thickness normalising by this age. When considering the changes within each genotype during this growth period the *ia/ia* rats showed a slight decrease in trabecular thickness in the two regions whilst maintaining a relatively consistent trabecular number.

On the other hand, the wt/het samples showed a slight increase in trabecular thickness and trabecular number in both regions. These differences suggest that appositional bone formation on existing trabeculae may be reduced over time in the *ia/ia* rats in response to reduced resorption with the new trabeculae formed becoming thinner over time, particularly in the proximal region. However, the number of trabeculae formed appears un-affected, as these are initially formed through endochondral ossification, and then built-upon through appositional bone formation. Although the trabecular thickness normalised in the proximal region, the persistence of increased trabecular number allowed the BV/TV in *ia/ia* rats to maintain a significant increase over wt/het at 8 weeks, which is evident in figure 4.15.

4.4.3 Endochondral fracture repair in the *ia/ia* rat

The initial stages of fracture healing were examined from 1 to 3 weeks post fracture in young *ia/ia* rats, the outcome time point being 8 weeks of age. This was well within the period of osteoclast dysfunction, as determined in the first part of this chapter. At this young age, fractures heal at a faster rate than older rats thus a shorter healing period was used in this study than the ZA fracture study discussed in chapter 3. Radiographs revealed equivalent rates of healing with all fractures showing radiologically determined union at 3 weeks post fracture.

Histological analysis of fracture repair as performed previously and detailed in chapter 3, confirmed this result, with no difference in the percentage of each callus which contained avascular cartilage tissue between genotypes at any time point examined. This was such that by 3 weeks all samples exhibited complete removal of the un-mineralised cartilage soft callus and replacement with hard bone tissue. Therefore, the process of initial endochondral fracture union in the absence of functional osteoclasts proceeded normally, replicating the result enumerated in chapter 3 when ZA was administered to block osteoclast function during fracture repair. Thus, these data suggest that any role the osteoclast plays during initial endochondral fracture union is functionally redundant, and therefore it is not rate limiting to this process.

4.4.4 Endochondral ossification at the growth plate occurs normally in the *ia/ia* rat.

In conjunction to endochondral fracture union, endochondral growth was also assessed in the *ia/ia* rats and compared to normal wt/het littermates. Growth plate height was not significantly altered in the *ia/ia* rats at either 6, 7, or 8 weeks of age. Normal progression of endochondral ossification at sites of long bone growth in these mutant rats is therefore suggested by this outcome (Figure 4.22).

4.4.5 Hard callus remodelling in the incisor absent rat fracture callus.

As was shown by previous authors, the amount of mineralised bone in the fracture calluses was significantly increased in the mutant *ia/ia* rats. QCT scans revealed up to almost a 2.5-fold increase in mineralised callus tissue volume at 3 weeks in the *ia/ia* mutant rats compared to control calluses. When comparing the fracture calluses to the un-operated femora, the mutant *ia/ia* rats showed almost a 4-fold increase in mineralised tissue volume over the left intact limb. Control wt/het calluses on the other hand exhibited only a 2.2-fold increase in mineral tissue volume compared to their intact limbs. This confirmed what has been previously documented that hard callus remodelling is completely hindered in these young mutant rats (Schmidt *et al.*, 1977) (Marks, Jr. and Schmidt, 1978).

Between 2 and 3 weeks post fracture wt/het calluses did not increase in size, instead they actually showed a decrease of 11% in callus volume at this stage. Further, QCT scan images illustrate the development of a neo-cortex in the 3 week post fracture wt/het samples (Figure 4.18). Taken together, these outcomes confirm that remodelling of the primary hard callus formed through endochondral ossification

has occurred in the wt/het samples. Mutant *ia/ia* rat calluses on the other hand increased in volume by 41% between the 2 and 3 week time points, and showed no evidence of development of a neo-cortex on the cross sectional images, hence hard callus remodelling had not commenced in these samples. Taken together, these data offer strong evidence that osteoclast activity was completely absent in the *ia/ia* rats throughout the time course of the fracture healing experiment. Furthermore these outcomes correspond to those presented in chapter 5, suggesting that osteoclastic resorption is irrefutably essential to the remodelling of the hard callus formed during fracture healing.

In conclusion, this examination of phenotype recovery and fracture repair in the *ia/ia* rat has added to the prevailing understanding of bone development and repair in an osteoclast deficient environment. By pinpointing an age of recovery in these rats this work has provided important information for future investigations in this rat model of osteopetrosis. More importantly, the fact that endochondral fracture repair was unaffected in the absence of functional osteoclasts in these rats, compliments the work performed and discussed in chapter 3 of this thesis, adding to the building knowledge on the exact role osteoclasts play during endochondral development and repair.

5 A single bolus dose of zoledronic acid is superior to weekly dosing, enhancing hard callus size and strength with minimal delays in remodelling after fracture.

5.1 Introduction

BPs are a group of anti-catabolic drugs currently used as first-line treatment for osteoporosis. BPs have unique bone specific properties and exclusively target the resorptive activity of the osteoclast (Sato *et al.*, 1991). The advent of N-BPs has led to significant increases in both the potency and efficacy of these drugs. The result of such improvements in potency has lead to a reduction in the dosing frequency required to achieve equivalent anti-catabolic effects in osteoporotic patients (Thiebaud *et al.*, 1997).

As the number of osteoporotic patients on chronic BP therapy increases, so does the number of new concerns about the possible negative effects BPs may have in these patients, particularly with regard to fracture repair (Munns *et al.*, 2004, Odvina *et al.*, 2005). Although fracture incidence is markedly reduced with treatment, it is not completely prevented. Furthermore, new patients are commonly enrolled onto BP therapy after a fracture. Thus consideration must be given to the effects of BP treatment after a fracture occurs in these people.

Fracture repair occurs through two main phases of tissue remodelling or replacement. The initial stage of this process is termed endochondral ossification which involves the removal of an avascular cartilage callus and replacement with a hard callus comprising mainly of vascularised woven bone. This process leads to complete bridging of the fracture site to provide union. Secondly, the newly formed immature bone callus is remodelled into mature lamellar bone until the site resembles the original bone structure (Einhorn, 1998).

Concerns have been raised as to whether patients should discontinue BP treatment during the course of repair (Fleisch, 2001). It is feasible that BP inhibition of osteoclast function could interfere with the initial stages of the repair process and cause a delay in union. Furthermore, it has been shown that hard callus remodelling is grossly delayed by continuous BP treatment (Li *et al.*, 1999, Li *et al.*, 2001). Our group has performed extensive investigations into the effects of BPs on early fracture repair see chapter 3, and (McDonald MM, 2006). The focus of this chapter is on the later stage of hard callus remodelling during fracture repair.

BP treatment has been shown to increase the net bone mass of the hard callus (Li *et al.*, 1999, Li *et al.*, 2001. In addition, a reduction in dosing frequency of new, more

potent, BP analogues may reduce any negative effects implicated for these drugs during fracture healing (Monier-Faugere *et al.*, 1999).

Zoledronic Acid (ZA) is a N-BP that exhibits high anti-resorptive potency at low doses, permitting its use at such doses, less frequently. A single bolus 5mg dose of ZA has recently been shown to be superior to oral risedronate treatment for Paget's disease (Hosking *et al.*, 2006), and a single yearly dose therapy has anti-fracture efficacy in osteoporosis (Black *et al.*, 2007). A comparison of a single annual dose of ZA with weekly oral Alendronate (ALN), which is 2-4 times less potent than ZA, in post-menopausal osteoporotic women has shown that the single ZA dose produces more rapid and greater reductions in resorption than the weekly ALN (Lindsay R *et al.*, 2006). Finally, it has been demonstrated through a comparative trial that patient preference for BP dosing lies with a single yearly ZA infusion instead of weekly oral ALN for the treatment of post menopausal women with osteoporosis (Lindsay R *et al.*, 2006). Thus, the recent improvements made in BP potency has led to a reduction in dose frequency, and more importantly a positive effect on patient compliance. Such a reduction in dosing frequency may in fact improve the outcomes for BP treated patients who suffer a fracture during treatment or present with fractures prior to treatment.

Our previous studies have shown that a bolus dose of N-BPs increase callus size and strength in distraction osteogenesis (Little *et al.*, 2001a, Amanat *et al.*, 2005). Preceding fracture studies, that have modelled only continuous dosing regimens in line with oral modes of therapy, have shown increased callus size but delayed hard callus (Lenehan *et al.*, 1985, Nyman *et al.*, 1993b, Goodship *et al.*, 1994, Tarvainen *et al.*, 1994, Hyvonen *et al.*, 1994, Peter *et al.*, 1996, Nyman *et al.*, 1996, Madsen *et al.*, 1998, Li *et al.*, 1999, Adolphson *et al.*, 2000, Li *et al.*, 2000a, Li *et al.*, 2001, Koivukangas *et al.*, 2003, Bauss *et al.*, 2004). The intention of this study was to compare the effects of an equivalent post fracture weekly BP dosing to dosing only once, on initial strength at union. The aim was to examine the differences between these dosing regimes on callus retention and strength at union as well as the hard callus remodelling that occurs post union.

5.2 Study Design

The well described Bonnarens and Einhorn closed rat fracture model used in the previous study examining early fracture union, chapter 3, was again utilised in 9 week old male Wistar rats (Bonnarens and Einhorn, 1984). In addition the high dose ZA levels administered in chapter 3 were used in this experiment. The doses used were in the form of either a single bolus dose of 0.1mg/kg of ZA administered 1 week post fracture

or as 5 divided weekly doses of 0.02mg/kg, also administered from 1 week post surgery. For this study, samples from the high dose ZA and Saline control groups at 2, 4, and 6 weeks from the study outlined in chapter 3, were examined for the commencement of hard callus remodelling. In addition, two further time points at 12 and 26 weeks post fracture were added to assess the long term effects of the two different ZA dosing regimens on hard callus remodelling (Table 5.1). To add to the extensive radiological and histological analysis this study also included additional samples used to analyse the mechanical properties of the calluses. The sample allocations pre group are outlined in Table 5.1. This additional level of analysis was included to assess the overall structural integrity of the samples, an outcome measure which is commonly impacted upon by delays in hard callus remodelling. Mechanical testing produced data for the peak torque to failure of each callus as well as the stiffness of the bone, a measure of the brittleness of the callus. Finally, three dimensional μCT scans were employed to enhance the understanding of the effect that delays in hard callus remodelling can have on overall bone structure.

	Time Point				
Treatment Group	**2 Weeks**	**4 Weeks**	**6 Weeks**	**12 Weeks**	**26 Weeks**
Saline	10	10	25	10	25
Bolus ZA	10	10	25	10	25
Weekly ZA	10	10	25	10	25

Table 5.1. *Number of animals allocated to each treatment groups and harvest time point.*

Treatment groups included; Saline, Bolus ZA at a dose of 0.1mg/kg, delivered1 week post fracture and Weekly ZA at a dose of 0.02mg/kg again commencing 1 week post fracture. Each group contained 10 samples for histological analysis. At 6 and 26 weeks an extra 15 samples were used for mechanical testing. ZA – Zoledronic Acid.

5.3 Results

5.3.1 Radiographic analysis

5.3.1.1 Fracture union

Radiographic assessment of samples revealed that 96% of all fractures achieved complete union by 6 weeks regardless of treatment. These results are outline in table 5.2 which shows the number of samples either united or not united for each treatment group at 6, 12 and 26 weeks post fracture. X-rays demonstrated obvious fracture union by 6 weeks in the majority of samples with enhanced callus size and radio density with ZA treatment. These changes are evident in Figure 5.1 which shows representative x-ray images from each treatment group at the 6 week time point.

Treatment		*6 weeks*	*12 weeks*	*26 weeks*
Saline	Not united	1	0	0
	United	26	11	25
	Total	27	11	25
Bolus ZA	Not united	1	0	0
	United	24	11	25
	Total	25	11	25
Weekly ZA	Not united	1	0	0
	United	24	11	23
	Total	25	11	23

Table 5.2. *The number of fracture samples either united or not united as determined radiologically for each treatment group at 6, 12 and 26 weeks post fracture*. There was no difference in the number of united fractures at each time point between treatment groups. ZA – Zoledronic Acid

Figure 5.1. *Representative x-ray images of samples from each treatment group at 6 weeks demonstrating complete union at this stage.* Each fracture site shown is clearly united with bony callus at this stage, therefore ZA dosing did not delay radiological healing. Both Bolus ZA (0.1mg/kg) and Weekly ZA (0.02mg/kg) calluses show increased size and radio density of the fracture calluses. Original magnification x 1.5

5.3.1.2 Quantitative computerised tomography (QCT)

ZA treatment resulted in significant increases in mineralized callus size and content at all time points examined as measured by QCT. The changes seen are evident in figure 5.2 which contains representative images of cross sectional CT scan slices of fracture calluses for each treatment group at 4, 6, 12 and 26 weeks post fracture. For Bolus ZA and Weekly ZA treatment groups, respectively, callus BMC was significantly increased compared to Saline at 4 weeks (48% and 53%), 6 weeks (55%

and 105%), 12 weeks (37% and 71%) and 26 weeks (61% and 102%) with a high statistical significance of $p<0.01$. Similarly fracture callus volume was also significantly increased over Saline at 4 weeks (41% and 43%), 6 weeks (53% and 100%), 12 weeks (33% and 57%) and 26 weeks (62% and 109%) in both Bolus ZA and Weekly ZA treatment groups respectively. When tested statistically using one way ANOVA these increases were found to be of significance with $p <0.01$. These data are outlined in Table 5.3 showing mean and standard deviations for bone mineral content (BMC) and Volume of the calluses for each treatment group. Figure 5.3 illustrates these data in bar chart format, clearly demonstrating the significant increases in BMC and Volume with both Bolus and Weekly ZA treatment.

Fracture callus polar moment of inertia, a theoretical measure of callus strength, was also modulated with ZA therapy. At 6 weeks post fracture, increases in mean moment of inertia of 70% (Bolus ZA) and 156% (Weekly ZA) were noted when compared to control. By 26 weeks increases of 81% (Bolus ZA) and 171% (Weekly ZA) were seen. These increases with Bolus and Weekly ZA compared to Saline were tested statistically using one way ANOVA and produced p-values of <0.01. The mean data and standard deviations are presented in Table 5.3. Callus BMD did not vary between treatment groups at any time points examined from 6 weeks onwards (data not shown).

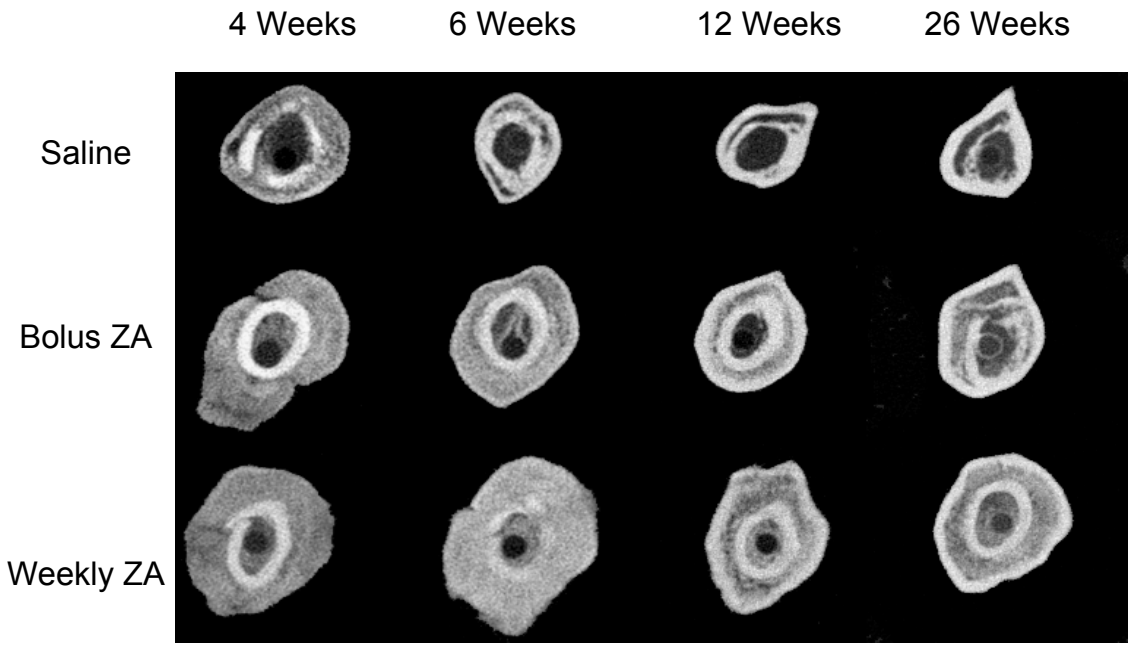

Figure 5.2. *Representative cross sectional images from QCT scans at the central region of the fracture site for each treatment group at 4, 6, 12 and 26 weeks post fracture*.

The enhanced callus size and density with ZA treatment is evident with larger cross sectional size and increased intensity of images. Moreover, evidence of extensive delays in hard callus remodelling are seen in the Weekly ZA samples with no reduction in size until after 6 weeks and

delayed formation of the neo-cortex seen at the periphery of the callus in both Saline and Bolus ZA samples at this time. Bolus ZA shows superior remodelling compared to Weekly ZA.

Table 5.3 *a and b Mean values and standard deviations (SD) for data generated from QCT scans of both operated (a) and non-operated (b) femurs for bone mineral content (BMC), Bone volume (Volume) and polar moment of inertia.*

a

Operated Femur

Parameter	Treatment Group	2 Weeks	4 Weeks	6 Weeks	12 Weeks	26 Weeks
BMC (mcg)	*Saline*	135.3 (17.19)	151.2 (15.79)	142.4 (19.05)	155.87 (14.54)	142.95 (23.16)
	Bolus ZA	149.38 (6.79)	223.74 (21.81)*	236.21 (32.93)*	213.84 (18.59)*	229.58 (25.97)*
	Weekly ZA	153.24 (21.31)	231.07 (42.70)*	299.17 (41.08)*†	265.79 (47.41)*†	288.93 (55.32)*†
Volume (mm3)	*Saline*	197.61 (30.88)	182.48 (24.00)	160.46 (29.70)	139.63 (16.15)	123.89 (18.70)
	Bolus ZA	193.12 (16.42)	257.59 (36.09)*	255.69 (46.05)*	186.03 (22.23)*	200.58 (27.75)*
	Weekly ZA	196.36 (35.05)	260.75 (67.52)*	317.40 (51.75)*†	233.58 (49.21)*†	258.56 (54.51)*†
Moment of Inertia (mm^4)	*Saline*	134.7 (47.10)	104.41 (24.40)	90.68 (33.55)	66.2 (15.00)	55.93 (15.59)
	Bolus ZA	110.31 (42.69)	160.1 (42.28)**	154.22 (55.00)*	83.62 (17.06)**	101.11 (27.48)*
	Weekly ZA	103.06 (23.45)	157.88 (84.39)**	232.09 (69.76)*†	133.82 (54.31)*†	151.33 (58.87)*†

Mean (SD) *p<0.01 when compared to saline, **p<0.05 when compared to saline, † p<0.01 when compared to Bolus ZA

b

Non-operated Femur

Parameter	Treatment Group	2 Weeks	4 Weeks	6 Weeks	12 Weeks	26 Weeks
BMC (mcg)	*Saline*	82.56 (4.98)	90.86 (5.75)	93.88 (6.72)	110.48 (4.87)	126.25 (8.71)
	Bolus ZA	77.05 (3.76)**	90.42 (4.24)	92.59 (6.09)	113.90 (10.40)	168.7 (49.3)*
	Weekly ZA	80.40 (5.91)	86.48 (4.27)**	95.15 (5.74)	114.62 (4.67)	180.64 (62.29)*
Volume (mm3)	*Saline*	94.70 (6.96)	102.39 (7.20)	89.03 (17.48)	86.06 (4.52)	110.83 (13.76)
	Bolus ZA	86.18 (4.76)*	97.19 (5.51)	86.89 (11.91)	87.89 (7.97)	141.79 (46.77)*
	Weekly ZA	89.98 (6.58)	94.96 (9.62)	88.40 (13.44)	87.87 (3.40)	150.07 (49.26)*
Moment of Inertia (mm^4)	*Saline*	19.68 (3.02)	22.62 (2.75)	23.32 (5.31)	26.39 (3.06)	34.58 (5.01)
	Bolus ZA	16.35 (1.68)*	20.73 (2.05)	22.15 (3.41)	26.69 (5.26)	33.38 (6.02)
	Weekly ZA	17.89 (2.39)	19.74 (3.39)**	22.94 (2.89)	26.78 (2.91)	36.62(5.22)†

Mean (SD) *p<0.01 when compared to saline, **p<0.05 when compared to saline, † p<0.01 when compared to Bolus ZA

Units are micrograms (mcg), millimetres cubed (mm3), millimetres to the power of 4 (mm4). In operated femurs, ZA treatment produced significant increases in all parameters compared to saline from 4 weeks onwards. Weekly ZA showed significant increases compared to Bolus ZA in BMC and polar moment of inertia from 12 weeks.

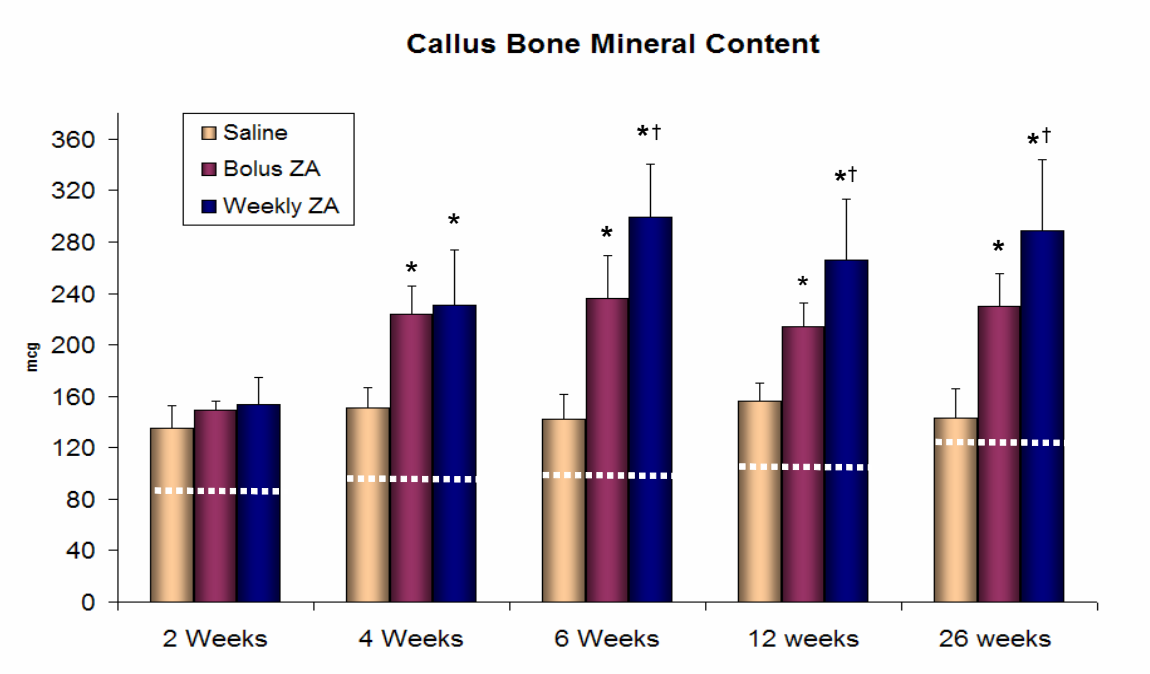

Figure 5.3a. *Bar chart showing mean callus BMC for all treatment groups from 2 – 26 weeks post fracture.* Error bars represent 1 standard deviation, white dashed lines represent mean BMC for Saline control non-operated limbs at each time point examined. Star symbol (*) represents p<0.01 when compared to Saline, cross symbol (†) represents p<0.01 when compared to Bolus ZA. ZA treatment produced increases of up to 2-fold in callus BMC compared to Saline. Weekly ZA produced further increases over Bolus ZA at 6, 12 and 26 weeks

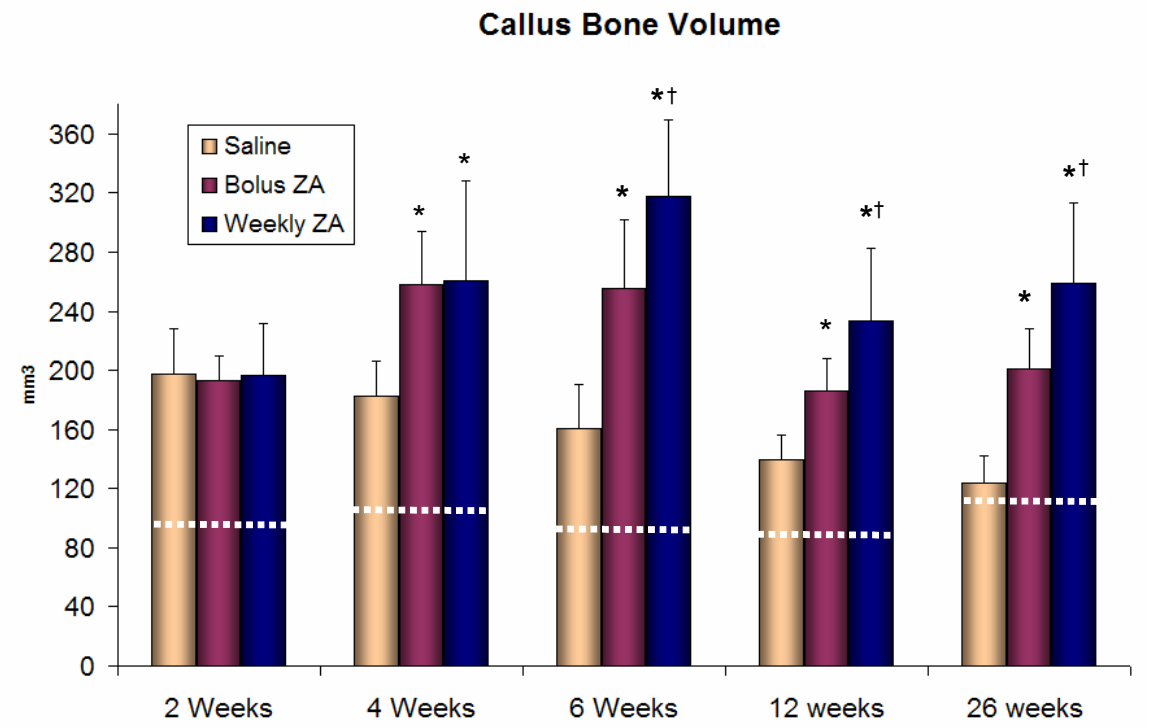

Figure 5.3b. *Bar chart showing mean callus bone volume for all treatment groups from 2 – 26 weeks post fracture.* Error Bars represent standard deviations, white dashed lines represent mean bone volume for Saline control non-operated limbs at each time point examined. Star symbol (*) represents p<0.01 when compared to Saline, cross symbol (†) represents p<0.01 when compared to Bolus ZA. ZA treatment produced increases of up to 2-fold in callus volume compared to Saline. Weekly ZA produced further increases over Bolus ZA at 6, 12 and 26 weeks.

Differences in mineralised callus size and content between the two ZA treatment groups were also evident. At 6, 12 and 26 week time points Weekly ZA administration produced increases of 24% to 32% in mean callus BMC and 2% to 30% in callus volume when compared to Bolus ZA administration ($p<0.01$) (Table 5.3, Figures 5.2 and 5.3a). Furthermore, polar moment of inertia was significantly increased at 6, 12 and 26 weeks in the Weekly ZA group compared to Bolus ZA with changes of 50%, 60% and 50% respectively ($p<0.01$), (Table 5.3).

5.3.2 Mechanical testing at 6 weeks and 26 weeks

At 6 weeks, fracture callus peak torque to failure, an indicator of overall callus strength, was increased in both ZA treatment groups, 20% for Bolus ZA and 31% for Weekly ZA when compared to Saline. When tested for significance these data produced p values of <0.05 and <0.01 respectively. Saline fracture calluses were not significantly stronger than the Saline treated contra-lateral femur in peak torque, suggesting that at the time of initial union, normal limb strength was not yet attained. However, Bolus ZA and Weekly ZA treatment produced fracture calluses that were 33% and 45% stronger than the Saline control contralateral limbs, when tested statistically these increases had a p-value of <0.01. These data are outlined in table 5.4 and the ZA produced changes are illustrated in bar chart format in figure 5.4a. Stiffness of the calluses was not increased with ZA treatment compared to Saline at 6 weeks. The energy absorbed in the fracture calluses was increased by 51% in the Weekly ZA samples compared to Saline, with a statistical significance of $p<0.05$. Energy absorbed was not different with Bolus ZA treatment.

By 26 weeks, callus peak torque to failure showed larger increases with ZA treatment compared to Saline. Bolus ZA and Weekly ZA demonstrated increases of 89% and 96% compared to the Saline fractured femora respectively, showing a statistical significance of $p<0.01$. Again no differences in peak torque were noted between the Saline fracture callus and the contra-lateral femur at 26 weeks. However, Bolus ZA and Weekly ZA treated femurs were 136% and 145% stronger than the normal un-fractured limbs at this time, with a statistical significance of $p<0.01$. Stiffness of the fracture callus was also increased with ZA treatment at 26 weeks with a 74% increase with Bolus ZA and a 70% increase with Weekly ZA compared to Saline calluses. These increases were of a statistical significance of $p<0.01$. In addition the energy absorbed was increased by 69% in the Bolus ZA samples compared to Saline calluses ($p<0.01$), this time there was no change in the Weekly ZA samples. All data outcomes from mechanical testing are listed in table 5.4.

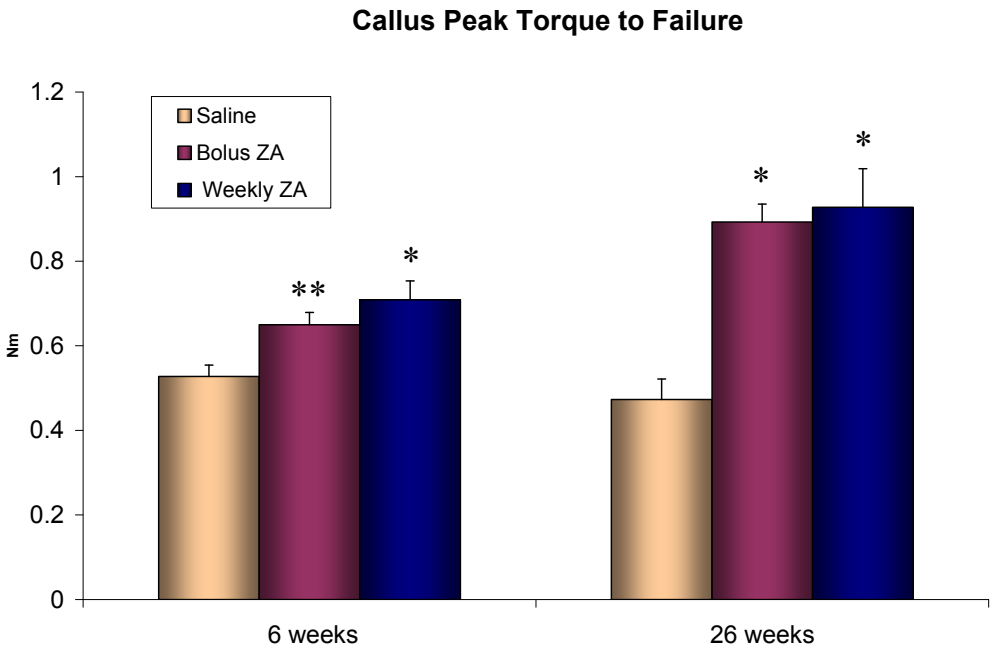

Figure 5.4a *Bar chart of mean fracture callus peak torque to failure for each treatment group at 6 and 26 weeks post fracture*.
Error bars represent standard errors, Two stars (**) represents $p<0.05$, and one star (*) represents $p<0.01$ when compared to Saline. Dashed lines represent data from control un operated limb at each time point. Both Bolus ZA and Weekly ZA produced increases over Saline at 6 and 26 weeks post fracture.

Using the data obtained for the polar moment of inertia, callus circumference, callus stiffness and the peak torque to failure, the intrinsic material properties of the callus tissue were determined as explained in section 2.6.3. At 6 weeks both Bolus ZA and Weekly ZA demonstrated inferior material properties with decreases in both peak stress, a measure of the strength per unit area of callus material, and shear modulus, an assessment of stiffness per unit of material. Peak stress was for reduced 26% for Bolus ZA and 38% for Weekly ZA when compared to Saline. When tested statistically, these reductions were of significance levels of $p<0.05$ for Bolus ZA and $p<0.01$ for Weekly ZA. In addition, shear modulus was decreased 49% in Bolus ZA samples and 58% in Weekly ZA samples compared to Saline at this time, with a significance of $p<0.01$. Data for intrinsic material property measures are outlined in table 5.4 and figure 5.4 illustrates the extensive changes seen with ZA treatment. No differences in callus intrinsic material properties were detected between Bolus and Weekly ZA treatment groups at 6 weeks.

Table 5.4 *Data generated from mechanical testing of both operated and non-operated femurs at 6 and 26 weeks post fracture. Data is presented as mean (standard deviation).*

		Operated Femur		*Non-operated Femur*	
Parameter	***Treatment Group***	**6 weeks**	**26 weeks**	**6 weeks**	**26 weeks**
Peak Torque (Nm)	*Saline*	0.543 (0.030)	0.473 (0.048)	0.489 (0.024)	0.378 (0.075)
	Bolus ZA	0.650 (0.029)**	0.893 (0.042)*	0.475 (0.043)	0.487 (0.069)
	Weekly ZA	0.709 (0.044)*	0.928 (0.091)*	0.501 (0.028)	0.287 (0.029)
Stiffness (Nm/deg)	*Saline*	0.0285 (0.002)	0.075 (0.007)	0.019 (0.001)	0.047 (0.007)
	Bolus ZA	0.030 (0.003)	0.130 (0.006)*	0.021 (0.002)	0.054 (0.006)
	Weekly ZA	0.035 (0.004)	0.127 (0.009)*	0.0173 (0.002)	0.046 (0.005)
Energy Absorbed (Nm.deg)	*Saline*	6.254 (0.771)	4.436 (0.722)	7.445 (0.755)	3.968 (0.569)
	Bolus ZA	8.140 (0.922)	7.518 (0.575)*	6.880 (0.927)	6.983 (0.390)±
	Weekly ZA	9.417 (1.216)**	6.012 (0.687)	9.951 (1.511)	5.736 (0.418)±±
Peak Stress (Mpa)	*Saline*	14.83 (0.94)	29.26 (3.91)	40.81 (2.03)	20.67 (3.48)
	Bolus ZA	11.05 (1.21)**	27.84 (2.85)	39.43 (3.38)	32.88 (5.93)±
	Weekly ZA	9.17 (0.83)*	17.82 (3.12)**†	42.40 (2.85)	17.84 (1.91)
Peak Strain	*Saline*	0.102 (0.007)	0.027 (0.002)	0.0936 (0.007)	0.022 (0.002)
	Bolus ZA	0.151 (0.013)**	0.036 (0.003)**	0.082 (0.007)	0.023 (0.002)
	Weekly ZA	0.164 (0.019)*	0.037 (0.002)*	0.105 (0.008) °	0.019 (0.003)
Shear Modulus (Mpa)	*Saline*	200.22 (17.29)	1256.70 (114.10)	579.93 (36.72)	1054.99 (125.63)
	Bolus ZA	101.82 (17.73)*	1031.65 (61.11)	616.52 (57.56)	1512.75 (201.92)
	Weekly ZA	84.52 (14.24)*	669.60 (118.11)*†	515.84 (47.89)	1194.99 (146.30)

Mean (SE)

*p<0.01 when compared to Saline operated, **p<0.05 when compared to Saline operated, †p<0.05 when compared to Bolus ZA operated

± p<0.01 when compared to Saline non-opertaed, ±±p<0.05 when compared to Saline non-opertaed, °p<0.05 vs Bolus ZA non-operated

Units are Newton meters (Nm), Newton meters per degree (Nm/deg), Newton meters multiplied by degrees (Nm.deg), megapascals (Mpa). In operated femurs, ZA treatment produced significant increases in peak torque at both 6 and 26 weeks. Peak stress and shear modulus were significantly reduced in both ZA treatment groups compared to Saline at 6 weeks. By 26 weeks however, only Weekly ZA treatment showed reductions in peak stress and shear modulus. Only some small changes were observed with ZA treatment in the non-operated femurs.

By 26 weeks, Bolus ZA had equivalent peak stress and shear modulus to Saline samples, whilst Weekly ZA maintained a decrease in peak stress of 36% compared to Bolus ZA and 39% compared to Saline. Both reductions when tested statistically showed significances of $p<0.05$. (Table 5.4, Figure 5.4b). Furthermore, callus shear modulus was also reduced 35% in the Weekly ZA samples compared to Bolus ZA, with a significance of $p<0.05$, and 47% compared to Saline, with $p<0.01$ (Table 5.4, Figure 5.4c).

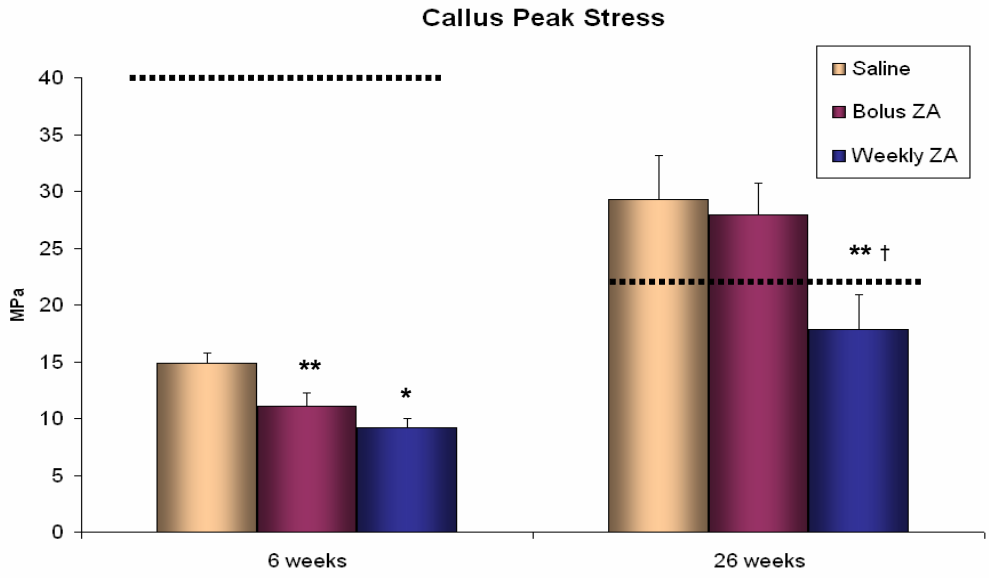

Figure 5.4b *Bar chart of mean values for fracture callus peak stress for each treatment group at 6 and 26 weeks post fracture.*
Error bars represent standard errors, 1 star (*) represents $p<0.01$ when compared to Saline, 2 stars (**) represent $p<0.05$ when compared to Saline, 1 cross (†) represents $p<0.05$ when compared to Bolus ZA. Dashed lines represent data from control non operated limb at each time point. At 6 weeks ZA treatment resulted in reductions in peak stress of 26% (Bolus ZA) and 38% (Weekly ZA) compared to Saline. For Bolus ZA this was reversed by 26 weeks with no difference in Peak Stress to Saline. This was not the case for Weekly ZA which maintained a 39% reduction in peak Stress compared to Saline and a 36% reduction compared to Bolus ZA.

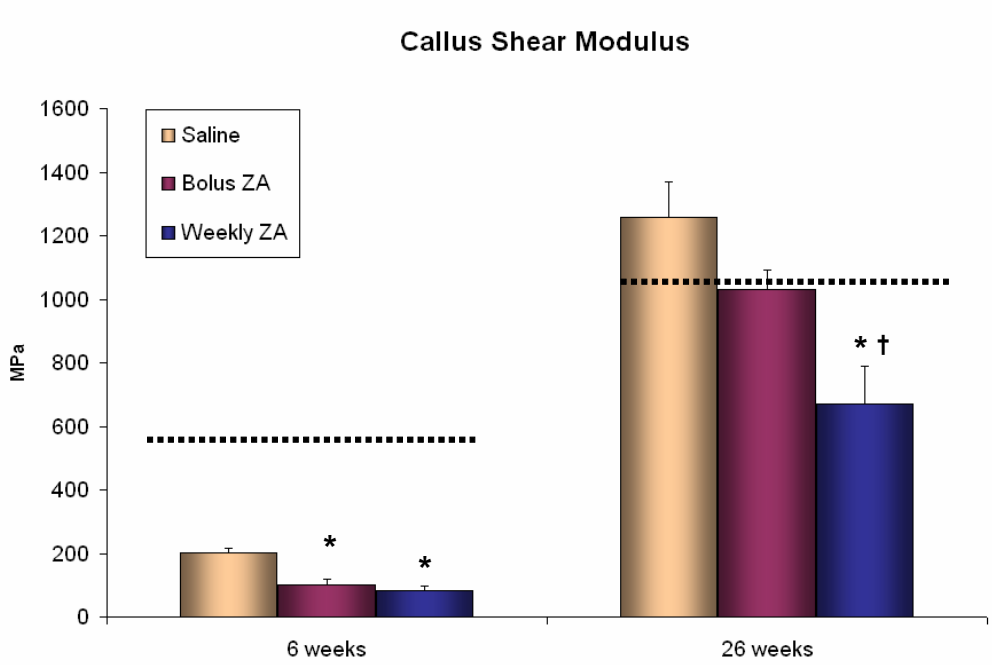

Figure 5.4c *Bar chart of mean values for fracture callus shear modulus for each treatment groups at 6 and 26 weeks post fracture*. Error bars represent Standard Errors, 1 star (*) represents p<0.01 when compared to Saline, 1 cross (†) represents p<0.05 when compared to Bolus ZA. Dashed lines represent data from control non operated limb at each time point. At 6 weeks ZA treatment produced reductions in Shear modulus of 49% (Bolus ZA) and 58% (Weekly ZA) compared to Saline. For Bolus ZA this had recovered by 26 weeks, whereas Weekly ZA maintained a 47% reduction in shear modulus compared to Saline at this time.

5.3.3 Hard callus remodelling with ZA treatment

5.3.3.1 QCT analysis

Hard callus remodelling commenced between 4 and 6 weeks in the Saline group, reducing bone volume such that by 26 weeks it was only 12% greater than the control contralateral limb. When tested statistically this data produced a significance of $p<0.01$. Bolus ZA samples also commenced remodelling after 4 weeks, with a slight reduction in callus volume by 6 weeks. By 26 weeks the mineralised tissue volume of the Bolus ZA femurs was 81% greater than the control contra-lateral limb, with a statistical significance of $p<0.01$. In contrast, such remodelling was delayed until after 6 weeks in the Weekly ZA group, when ZA dosing had ceased, such that the callus volume remained at 133% of that of the control contralateral limb volume at 26 weeks, with a significance of $p<0.01$. Furthermore, by this time Weekly ZA dosed calluses were 29% larger than Bolus ZA dosed calluses, with a significance of $p<0.01$ this confirmed clear differences between the two ZA dosing regimes. Data are outlined in Table 5.3 and changes are illustrated in Figure 5.3).

Cross sectional images of QCT scans revealed additional details on the rate of hard callus remodelling. As seen in Figure 5.2, formation of a peripheral cortical ring or neo-cortex in the fracture callus is visible as early as 4 weeks in the Saline samples.

The Bolus ZA group demonstrated commencement of neo-cortex formation at 6 weeks. Weekly ZA samples showed a further delay in neo-cortical bone formation, this sign of hard callus remodelling not evident until the 12th week, 6 weeks after dosing had ceased (Figure 5.2). These observational differences were supported by quantitative analysis of histology sections.

5.3.3.2 Histology and histomorphometry

The percentage of the fracture callus that was remodelled neo-cortical bone was similar between Saline and Bolus ZA at 6, 12 and 26 weeks. However, the Weekly ZA group showed a significant reduction in the proportion of this remodelled callus at 6 ($p<0.04$), 12 and 26 weeks ($p<0.01$) (Figure 5.5) Similarly, the area of the callus that was retained primary un-remodelled bone was greater in Weekly ZA compared to Bolus ZA and Saline at 6 weeks ($p<0.01$), at 12 weeks ($p<0.03$) and 26 weeks ($p<0.01$). (Figures 5.5 and 5.6).

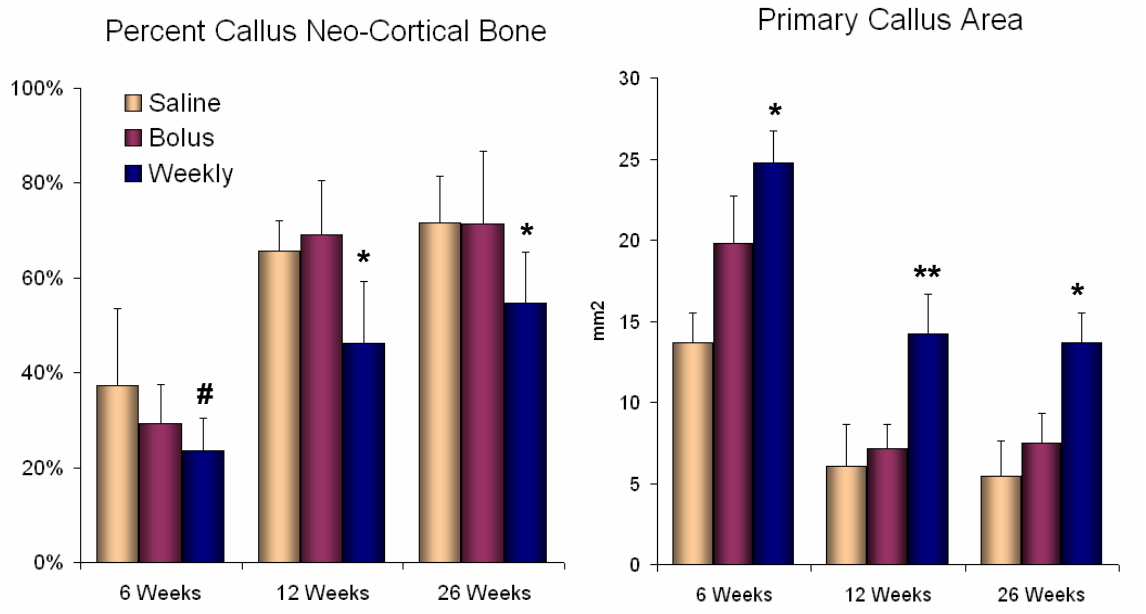

Figure 5.5 *Bar charts of mean values for percentage of callus neo-cortical bone and primary callus area at 6, 12 and 26 weeks post fracture for each treatment group.*

Error bars are 1 standard deviation. 1 star (*) represents $p<0.01$ when compared to Saline, hash (#) represents $p<0.04$ when compared to Saline, 2 stars (**) represents $p<0.03$ when compared to Saline. Weekly ZA showed reduced remodelled neo-cortical bone and increased callus retained primary bone area compared to Saline at all time points. Bolus ZA was not different to Saline at all time points examined.

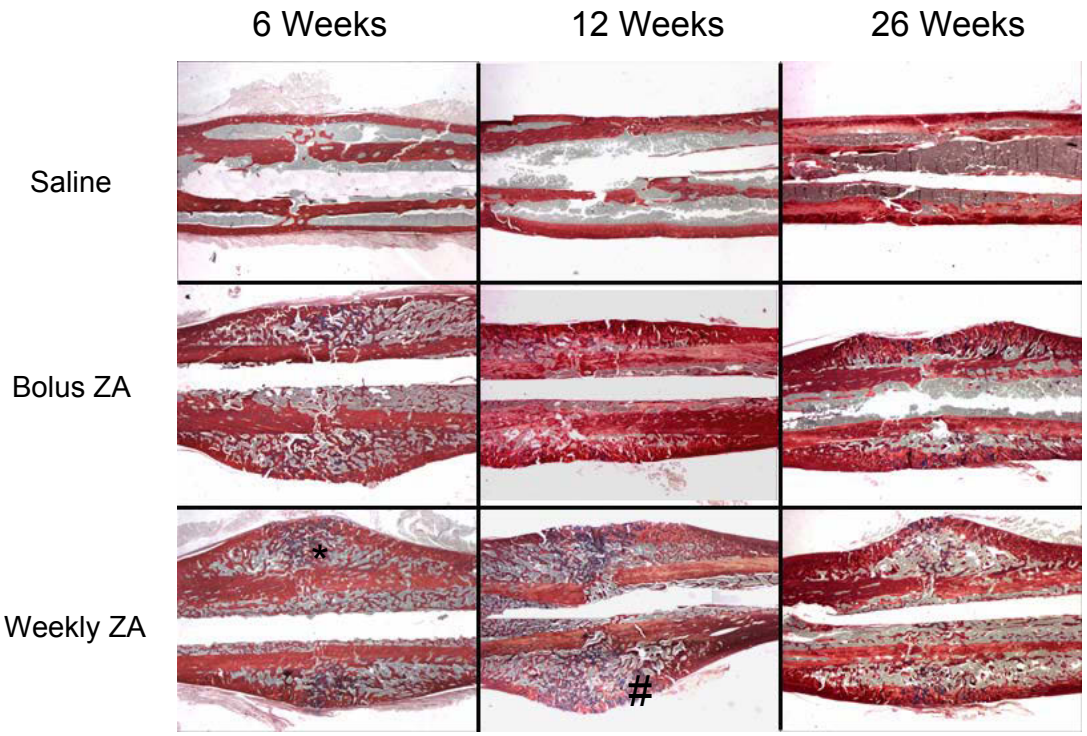

Figure 5.6 *Representative images of sections of samples from each treatment group at 6, 12 and 26 weeks.* Alcian blue/Sirius Red stained sections x 1.0 magnification. Note the extensive retention of primary callus (*) and reduced neo-cortex formation (#) in the Weekly ZA treatment group compared to both Saline and Bolus ZA.

5.3.3.3 Micro CT analysis

Micro computerised tomography (μCT) supported the results for the QCT and histomorphometric analysis. At 26 weeks Bolus ZA showed superior hard callus remodelling on μCT scan images when compared to Weekly ZA. Callus size in the Bolus ZA sample was comparable to Saline treated samples at 26 weeks, whilst it also demonstrated numerous other signs of superior remodelling compared to Weekly ZA. These included a reduction in retention of primary trabecular compared to that of the Weekly ZA sample, corresponding to the histomorphometric data. In addition, these images demonstrated that the percentage of the remaining Bolus ZA callus (excluding the original cortex) that is remodelled neo-cortical bone was notably greater than that seen in the Weekly ZA example (Figures 5.7).

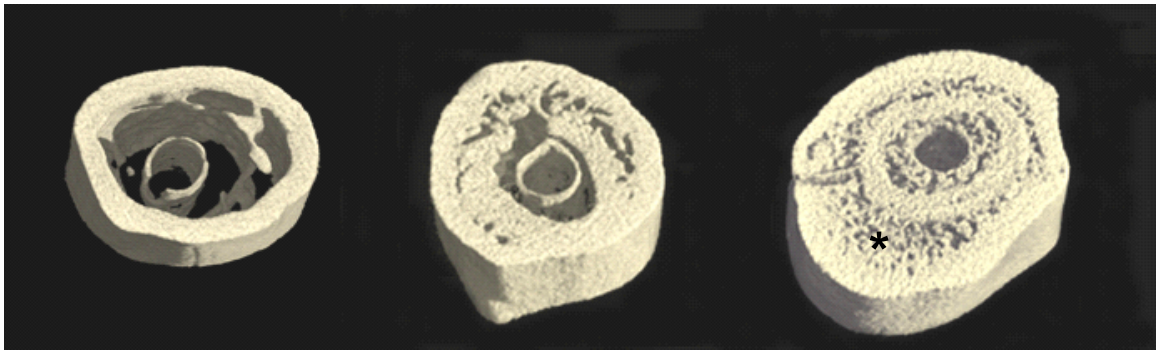

Figure 5.7. *Representative 3D cross sectional reconstruction images from the central fracture region generated from μCT scans at 26 weeks for each treatment group.* Weekly ZA demonstrates extensive retention of un-remodelled primary bone (*) compared to Saline and Bolus ZA. Further, Saline samples show complete removal of the original cortical bone at this stage, this original cortex is still evident in both the Bolus and Weekly ZA samples.

5.4 Discussion

It was hypothesised that bolus ZA administration would be superior to weekly administration, at the same dose level in enhancing fracture callus strength. The results of this study taken as a whole are entirely consistent with this hypothesis. Bolus and Weekly ZA dosing regimens both produced significant increases in callus BMC, volume and strength at 6 and 26 weeks time points. However, important differences between Bolus and Weekly ZA dosing emerged from this analysis, suggesting Weekly ZA produced a callus of inferior material properties due to delayed remodelling.

Firstly, in the BMC, volume and polar moment of inertia of the fractured region at 6 and 26 weeks, Weekly ZA produced significant increases over Bolus dosing. However, these increases were not reflected by further increases in callus strength. This implies that the increases in size of the callus in the Weekly ZA group occurred by the retention of mechanically inferior callus tissue compared to Bolus ZA. Calculated values for the peak stress and shear modulus of the callus material at 6 and 26 weeks vindicated this conclusion. At 6 weeks, both Bolus ZA and Weekly ZA showed significant reductions in peak stress and shear modulus compared to Saline, suggesting reduced resistance to torque and reduced stiffness of the callus material with ZA treatment at this stage. Even so, an increase in peak torque was still achieved at 6 weeks in both ZA treatment groups. This is attributed to increases in polar moment of inertia of 69% in Bolus ZA group and 154% in the Weekly ZA group compared to Saline.

By 26 weeks however, Bolus ZA was equivalent to Saline in both peak stress and shear modulus, Weekly ZA remaining inferior, with these parameters remaining significantly reduced compared to both Saline and Bolus ZA samples. Again, increased overall strength over Saline calluses was still achieved by a 169% increase in polar moment of inertia in the inferior Weekly ZA callus.

The outcome data for the callus material properties confirmed that the continuous Weekly ZA dosing to 6 weeks significantly hindered hard callus remodelling even up to 26 weeks post fracture. The Weekly ZA dosed calluses at 26 weeks clearly exhibited inferior material properties, such that the increased callus size compared to the Bolus ZA group did not account for added increases in overall callus strength.

QCT analysis further confirmed that hard callus remodelling was significantly hindered after Weekly ZA dosing. Between 2 and 4 weeks post fracture in this model, Saline samples showed a slight decrease in callus volume by QCT with both ZA treatment groups significantly increasing in callus volume at this stage. Between 4 and 6 weeks however both the Saline and Bolus ZA groups showed slight but obvious decreases in callus size suggesting remodelling had commenced. In contrast, the continuous dosing in the Weekly ZA group between 4 and 6 weeks, led to a steady increase in callus volume at this point. It was not until the 12 week time point that the Weekly ZA treatment group demonstrated a significant decrease in callus volume suggesting that any hard callus remodelling did not commence in this group until after 6 weeks when ZA dosing had ceased. These structural differences that result from altered hard callus remodelling can be seen clearly in the QCT images in Figure 5.2.

The cross-sectional QCT scans clearly illustrate the effects of delayed remodelling, not only on callus size but also on the critical process of neo-cortex formation. At 6 weeks the normal fracture callus remodelling in the Saline samples lead to the formation of an external ring of neo-cortical bone, evident as a dense ring of bone on the outer perimeter of the callus. Similarly, although less evident, the Bolus ZA dosed samples had commenced production of such neo-cortical rings by 6 weeks. In contrast, the Weekly ZA dosed samples failed to produce evidence of such neo-cortex formation at this time, providing more evidence of delayed hard callus remodelling in this continuous ZA dose group. The delayed appearance of this indicator of remodelling is consistent with the study of continuous Incandronate dosing during fracture repair in the rat (Li *et al.*, 1999). However, by 12 weeks a neo-cortex was evident in the Weekly ZA samples, once more this sign of remodelling was noted after cessation of ZA dosing in this group.

By 26 weeks both ZA treatment groups had shown significant decreases in callus size, although they still remained significantly larger than Saline calluses at this

time. Nevertheless, even 20 weeks after the cessation of dosing, the Weekly ZA dosed samples retained a 29% increase over Bolus ZA in callus volume at 26 weeks. This is a final product of the delay in commencement and reduced rate of hard callus remodelling after continuous ZA dosing during early fracture healing.

Histological evaluation enabled assessment of both primary callus removal and neo-cortex production, providing extra evidence to support these results. At all late time points callus content of remodelled neo-cortical bone was not significantly different between Bolus ZA and Saline, whereas Weekly ZA group calluses remained significantly reduced compared to Saline in its callus neo-cortical bone content even out to the final 26 week time point. In addition, significant retention of the callus area containing un-remodelled primary bone was evident only in the Weekly ZA treatment group compared to Saline at all late time points.

Micro CT scans provided evidence from a 3 dimensional view reinforcing the long term effects of the continuous Weekly ZA dosing compared to Bolus ZA. The marked retention of primary callus between the original cortex and the neo-cortex in the Weekly ZA samples at 26 weeks is clearly observed in these scan images (Figure 5.7). The Bolus ZA dosed sample exhibited a smaller, more mature callus at this time. These images also illustrate the process of removal of the original cortical bone in the Saline callus. The neo-cortex formed during the repair process in the control callus became the new cortical bone structure, as the original cortices were almost completely resorbed and removed by 26 weeks. BP treatment on the other hand prevented the removal of the original cortex in both treatment groups, such that it remained part of the callus structure at 26 weeks. This retention is due to the binding of ZA to the original cortex at the time of drug treatment, such that its removal is inhibited even out to the 26 week time point.

This investigation has shed light on the importance of dosing frequency of BPs during fracture repair. By administering a single bolus dose of ZA at 1 week post fracture, significant enhancements in net callus production were realised, improving the overall strength of the fracture site by the time of initial union. This was at the cost of a small, reversible decrease in material properties. The superior hard callus remodelling noted in the Bolus ZA group resulted in a fracture callus with material properties equivalent to Saline controls by 26 weeks post fracture. Although Weekly ZA produced calluses with equivalent increases in strength to Bolus ZA, the delayed hard callus remodelling and resulting reduced bone quality may be detrimental in the clinical setting. This critical outcome will lead to more knowledgeable decisions regarding the treatment of osteoporotic patients with BPs during periods of fracture healing.

6 Dose finding study for MMI270 MMP inhibitor in Rats

6.1 Introduction

Matrix metalloproteinase's (MMPs) are the main active proteases required for collagen matrix degradation. Many MMPs exist in the body, a number of which are active during bone formation and resorption. During endochondral fracture healing both MMP-9 and MMP-13 are actively associated with the process of cartilage matrix degradation, such that fracture healing in both the MMP-9 and MMP-13 knockout mice is significantly delayed (Colnot *et al.*, 2003, Kosaki *et al.*, 2007). Osteoclasts have been shown to express and secrete MMP-9 during the process of bone resorption thus it could be assumed that osteoclasts active in endochondral bone formation are secreting MMP-9 and thus driving the degradation of the cartilage matrix (Rice *et al.*, 1997). However, MMP-9 knockout mice do not demonstrate limited bone resorption, suggesting that although this metalloproteinase is expressed and active during resorption, it may not be essential to this process (Delaisse *et al.*, 2003). Another role for MMP-9 in bone resorption is permitting migration of osteoclasts, in particular through un-mineralised matrices (Sato *et al.*, 1998).

Other cell types involved in endochondral ossification have also been shown to express and secrete these proteinases. These include the vascular endothelial cell, the chondroclast and the chondrocyte itself (Melton *et al.*, 2006, Colnot *et al.*, 2003). The primary role of MMP-9 has therefore been assumed based on the activities associated with this pattern of expression. Vascular invasion of chondral matrix during endochondral ossification involves all these cell types and since it is significantly delayed in the MMP-9 knockout mouse (Vu *et al.*, 1998) it is most certainly a process this protease is essential for. The resorptive activity of the osteoclast may not be essential to the process of cartilage matrix resorption, as the degrading actions of these other MMP-9 expressing cells may compensate in their absence, or indeed represent the primary mode of matrix removal. In the MMP-9 knockout mouse fracture study, the delayed fracture healing was shown to be a result of reduced vascular invasion and a reduction in the release of the angiogenic agent VEGF from chondrocyte matrix, and not due to reduced bone resorption or osteoclastic function (Colnot *et al.*, 2003). In summary, osteoclasts can participate in tissue remodelling in one of two ways: firstly, a specific role which involves ruffled border formation and acid secretion to resorb bone tissue, secondly a non-specific role involves secretion of proteases such as MMP-9 into differing matrices.

In addition to MMP-9, MMP-13 activity has been demonstrated during fracture healing. At the growth plate MMP-13 is secreted by the hypertrophic chondrocytes that form the terminal end of the cartilage tissue. Since these chondrocytes are the first level of invasion at the base of the growth plate, the MMP-13 secreted by these cells plays an important role in endochondral ossification. MMP-13 knockout mice demonstrate severe growth plate abnormalities, with an extended hypertrophic chondrocyte zone (Stickens *et al.*, 2004). As MMP-13 is capable of type II collagen degradation, it acts in the hypertrophic zone to denature the type II collagen of the proliferating chondrocyte matrix to allow for deposition of type X collagen matrix in these terminal cells. The type X collagen matrix allows for mineralisation of the cartilage matrix and subsequent vascular invasion (Wu *et al.*, 2002). The denatured type II collagen can then be degraded by in growing MMP-9 secreting vascular cells (Yamagiwa *et al.*, 1999).

MMP-9 and MMP-13 expressing cells therefore act in concert to degrade the un-mineralised cartilaginous matrix to allow vascularisation and subsequent ossification of the cartilage matrix. The vacated chondrocyte lacunae become the major site of primary bone formation. It can be concluded from these studies closely examining the role of numerous cell types during endochondral ossification, that their one common characteristic is the expression and/or secretion of MMPs. In conjunction with this knowledge and the delayed fracture healing exhibited by MMP-9 and MMP-13 knockout mice we aimed to investigate the overall contribution of MMPs to fracture healing by inhibiting their actions using the broad spectrum MMP inhibitor MMI270. The hypothesis of this study being that the inhibitor MMI270 would lead to significantly delayed endochondral fracture union. The effects of this MMP inhibitor on bone homeostasis or repair have not been explored. Similar broad spectrum inhibitors have been examined in a culture model of osteoclast migration, demonstrating efficiency against degradation of a type I collagen substrate by osteoclasts (Sato *et al.*, 1998).

6.2 Study design

6.2.1 Fracture repair study

The rat closed femoral fracture model used in chapter 3 was again utilised in this study in 9 week old male Wistar rats to analyse initial endochondral fracture union to 6 weeks. Based on previous work using the MMP inhibitor MMI270 to investigate the effects of inhibition of angiogenesis on cold injury induced brain oedema in rats, we obtained the dose for use in this fracture study (Kawai *et al.*, 2003). The authors of this study used a dose of 40mg/kg per day as a continuous SC injection utilising osmotic

pumps and were able to successfully inhibit angiogenesis in this model. Therefore in the original fracture study in this body of work, MMI270 was administered at a dose of 20mg/kg SC twice daily commencing one week post surgery and delivered in 50% dimethyl sulfoxide (DMSO). Control rats received the vehicle 50% DMSO in Saline subcutaneously. More details on this protocol can be found in section 8.1.3.2. As performed in chapter 3, samples were harvested for radiological and histological examination at 2, 4, and 6 weeks post fracture with 10 rats in each group. Radiological analysis of samples from the fracture study revealed that endochondral ossification was not successfully inhibited in this model using the dose of 20mg/kg twice daily. As a result an additional dose finding study was performed to optimise the dose required to inhibit this process.

6.2.2 Dose finding study

The outcomes of the initial fracture repair study led to the development of an additional dose finding study. This investigation aimed to assess increasing doses of MMI270 in growing rats. As the process of endochondral ossification occurs during longitudinal growth in a manner very similar to that seen during fracture repair (section 1.3.2), three different increased dose levels of MMI270 were given to growing rats over a 4 week period. In addition to increasing the dose levels, a new mode of administration was also added to this study, oral administration by gavage. This was performed to examine whether the compound may be absorbed more readily by oral administration, thereby inducing a stronger effect with a reduced dose.

Oral doses of MMI270 were given at the same dose levels but with the vehicle being 1% carboxymethyl cellulose (CMC), control rats receiving the same volume of 1% CMC only. The final 8 treatment groups for the dose finding study therefore included 40mg/kg, 80mg/kg and 120mg/kg twice daily as either SC injection or oral gavage. The 2 control groups received the same volume of 50% DMSO subcutaneously or 1% CMC by oral gavage. As this study was pilot work and to reduce rat numbers used, only 2 rats were allocated to each treatment group, to a total of 16 rats for the entire study. Analysis of the growth plates from these samples involved simple x-rays and observational histology.

6.3 Results

6.3.1 Fracture study

6.3.1.1 Radiographic union

Union of fractures was assessed radiologically and recorded for each sample. No difference was demonstrated in the rate of union with treatment. At two weeks all fractures had not united regardless of treatment. By 4 and 6 weeks 90% and 100% of fractures were united in the vehicle and MMP inhibitor groups respectively. Data are shown in Table 6.1 and representative x-ray images from each group are shown in Figure 6.1. These images clearly show no differences in the rate of healing with treatment.

Treatment Group		***2 weeks***	***4 weeks***	***6 weeks***
Vehicle	*United*	0	9	9
	Not United	10	1	1
	Total	10	10	10
MMI270	*United*	0	10	10
	Not United	11	0	0
	Total	11	10	10

Table 6.1. *Union rates in the MMP inhibitor (MMI270) and vehicle groups as determined from radiographs.* No differences were seen in the rate of union with MMI270 treatment.

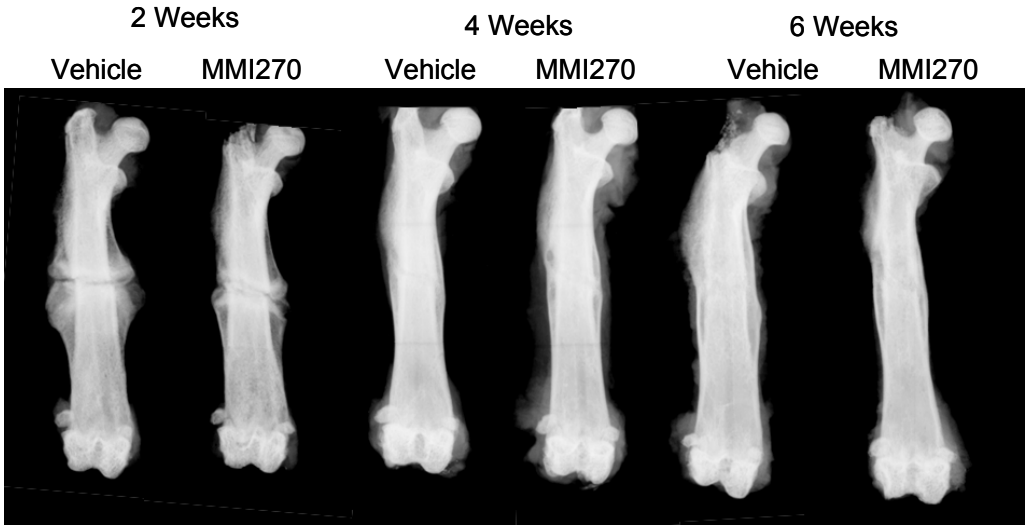

Figure 6.1 *Representative X-ray images of fractured femora from each treatment group (Vehicle or MMI270) at each harvest time point*. Original magnification x 1.5. No radiological differences were noted between the two treatment groups at any time point examined. The fracture line is evident at 2 weeks in both groups, by 4 weeks it is bridged with bony callus in all samples and by 6 weeks calluses are being remodelled and are reducing in size.

6.3.1.2 QCT analysis of fracture callus

QCT scans demonstrated small differences between vehicle and MMP inhibitor doses in fracture callus mineralised tissue properties. At 2 weeks post fracture no differences were seen, by 4 weeks however callus BMC was reduced 11% in the MMP inhibitor group. This result was not significant when tested statistically, with a p-value of 0.07. Callus volume was also decreased at 4 weeks in the MMP inhibitor group by 16%, with a significance of $p<0.05$. As a result of the reduction in callus volume, polar moment of inertia, a theoretical measure of callus strength, was also reduced at 4 weeks by 26%. When tested statistically this outcome produced a p-value of $p=0.05$. By 6 weeks any differences in callus properties were no longer present. No differences were seen in callus BMD (Table 6.2).

	Treatment Group	***2 Weeks***	***4 Weeks***	***6 Weeks***
BMC (mcg)	*Vehicle*	132.46 (9.42)	129.60 (21.87)	149.34 (36.83)
	MMI270	132.49 (8.26)	115.34 (8.42)†	137.949 (26.69)
BMD (mcg/mm3)	*Vehicle*	769.95 (58.45)	868.97 (54.47)	921.22 (70.99)
	MMI270	775.51 (41.26)	913.49 (66.55)	942.66 (79.18)
Volume (mm3)	*Vehicle*	179.20 (20.6)	152.93 (32.49)	166.41 (51.81}
	MMI270	176.14 (14.33)	128.34 (10.88)*	149.61 (42.52)
Polar Moment of Inertia	*Vehicle*	102.22 (27.09)	79.804 (32.99)	97.63 (36.49)
	MMI270	96.00 (17.28)	56.84 (12.77)**	78.24 (49.16)

*† p=0.07 when compared to Vehicle, *p<0.05 when compared to Vehicle, **p=0.05 when compared to Vehicle*

Table 6.2. *Data generated from QCT scans of operated femurs for bone mineral content (BMC), bone mineral density (BMD), bone volume (Volume) and polar moment of inertia of fracture calluses at 2, 4 and 6 weeks.*

6.3.1.3 Dual energy x-ray absorbtiometry (DEXA) scan data of non operated femurs

In order to analyse any systemic effects of the MMP inhibitor, DEXA scans were performed on the left non-operated femora of the rats in this experiment. Table 6.3 outlines the data produced from these scans showing no significant changes between treatment groups at any time point examined. However at 2 weeks there is a trend for a 3% decrease in femoral BMD with MMP inhibition and at 6 weeks a 3% decrease in bone area. Although, when tested statistically these differences were not significant as they produced a p-value of 0.08.

Treatment Group		**2 weeks**	**4 weeks**	**6 weeks**
Vehicle	*BMD*	0.192 (0.01)	0.205 (0.01)	0.220 (0.01)
	BMC	0.171 (0.01)	0.184 (0.01)	0.201 (0.01)
	Bone Area	0.888 (0.05)	0.901 (0.03)	0.915 (0.03)
MMI270	*BMD*	0.186 (0.01)	0.203 (0.01)	0.219 (0.01)
	BMC	0.163 (0.01)	0.181 (0.01)	0.194 (0.01)
	Bone Area	0.882 (0.04)	0.893 (0.04)	0.886 (0.04)

Table 6.3 *Data generated from DEXA scans of non-operated femurs.* Mean (SD)

6.3.1.4 Histological analysis of fracture healing

As the x-ray grading revealed no difference in the rate of union between the treatment groups it was determined that the dose of the MMP inhibitor MMI270 used in the experiment was not high enough to completely inhibit MMP activity and thus delay endochondral fracture healing in these rats. For this reason histological analysis of these samples was not performed.

6.3.2 Results from dose finding study for MMI270

6.3.2.1 Radiographic analysis

X-rays of proximal tibia of samples treated with the increasing doses of MMI270 revealed radiological changes in the growth plate compared to control samples. The growth plate between the epiphysis and metaphysis is normally translucent on x-ray as seen clearly in the control samples in Figure 6.2 below. Both the oral gavage and SC high dose (80mg/kg and 120mg/kg) samples demonstrated an increase in this translucent area when compared to control samples, particularly in the subcutaneous treated group. This difference was more obvious when examining histological sections of the growth plate region.

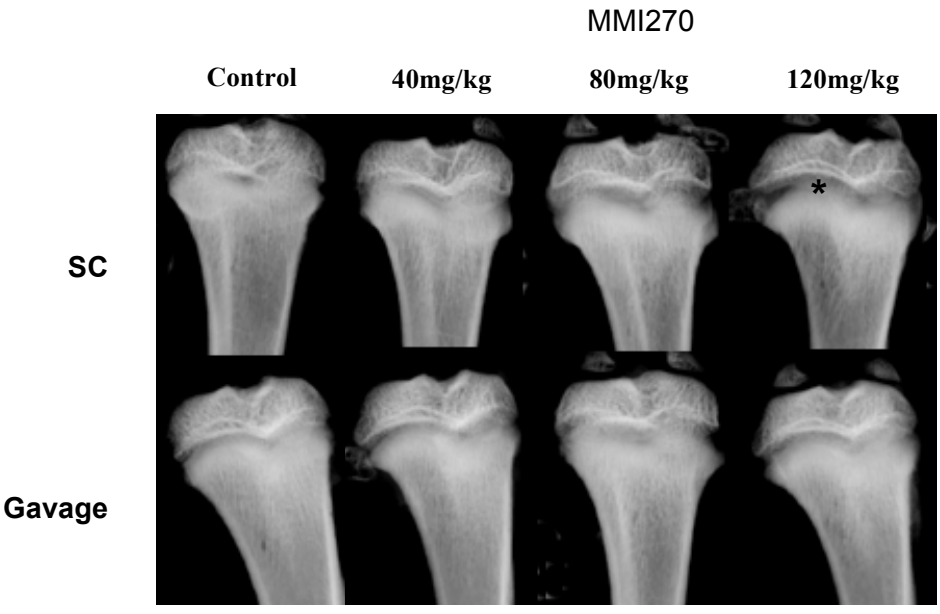

Figure 6.2 *Representative X-ray images of proximal tibia from each treatment group from dose finding study after 4 weeks of dosing with MMI270*. Original magnification x 1.5. An increase in the radiolucent region at the site of the growth plate (*) is evident in the high dose SC MMI270 groups. This suggests expansion of the cartilaginous growth plate.

6.3.2.2 Histological analysis

6.3.2.2.1 Growth plate height

Histology sections of the growth plate region confirmed the findings from x-rays that the high level SC doses of MMI270 produced an increase in the length of the growth plate. The height of the cartilage growth plate as examined observationally was notably increased in the 80mg/kg and 120mg/kg MMI270 SC dosed samples when compared to the control group. Slight increases in growth plate height were seen in the oral treatment group. These changes can be are evident in Figure 6.3 which shows the red stained cartilaginous growth plate widened in the high dose groups. As only two samples were studied for each treatment group only observational qualitative data was obtained from this study.

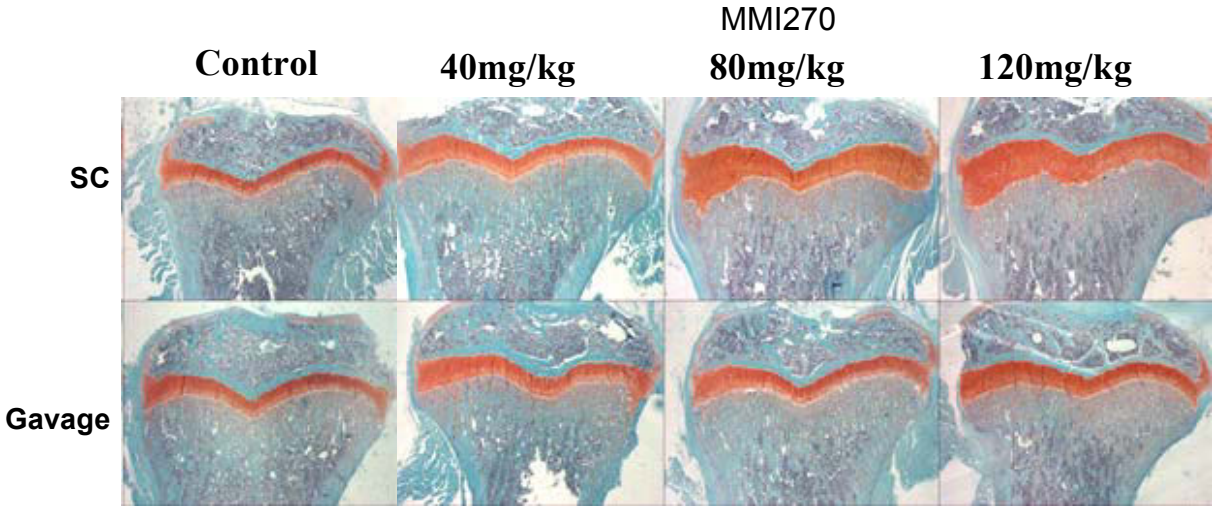

Figure 6.3a *Representative images of histological sections of proximal tibia stained Saffranin O, which stains cartilage matrix red, and light green which stains all other tissue greed, for each control and MMI270 groups*. Original magnification x 1.4. Corresponding to the x-ray images in Figure 6.3, the growth plate regions shown in red in the SC dosed MMI270 80mg/kg and 120mg/kg groups are clearly expanded when compared to control samples.

Examination of histological changes at higher magnifications revealed that the increases seen in growth plate height were due to a lengthening of the hypertrophic chondrocyte zone, as indicated by the asterix (Figure 6.3b). In some regions this zone also appeared less organised and columnar than the control samples, a common finding in models of growth plate disruption (Nagai and Aoki, 2002), (Malemud, 2006).

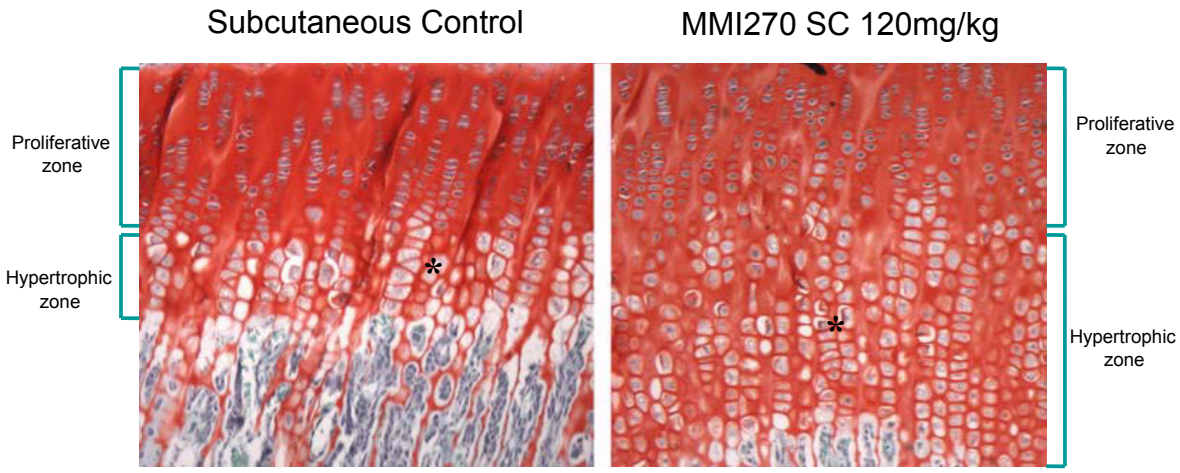

Figure 6.3b. *Representative images of histological sections from the proximal tibia stained with Saffranin O, Light Green for control and high dose (120mg/kg) subcutaneous (SC) samples.* Original magnification x 10. The expanded growth plate in the MMI270 samples is due to an increase in the hypertrophic zone, asterix, with some loss of the columnar organisation. The proliferative zone appears unaffected.

6.3.2.2.2 Chondrocyte mineralisation

Mineralisation of the hypertrophic chondrocyte matrix was assessed using a von Kossa stain which stains mineral deposition black, and using toluidine blue as a counterstain for the cartilage matrix and marrow cells. As shown in Figure 6.3c, in the most affected SC high dose group (120mg/kg) shown in the image on the right, the lengthened hypertrophic zone appears to have mineralised in a relatively normal manner, with black stained mineralised longitudinal septa seen close to the top of the hypertrophic zone and extending to the terminal end of the growth plate, indicated by a red asterix. Transverse septa appear mainly non-mineralised, similar to that seen in the control samples. Although this zone is longer and less organised than the control sample, the mineralisation patterns appear to be identical.

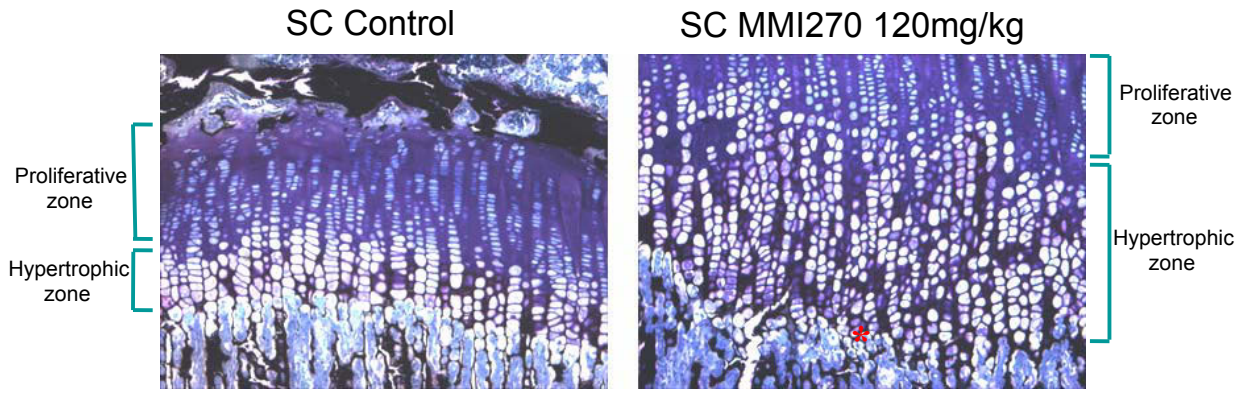

Figure 6.3c. *Representative images of histological sections of proximal tibial growth plates stained with von Kossa and toludine blue for SC Control and SC MMI270 high dose (120mg/kg)*. Original magnification x 10. Von Kossa stained areas are black and show mineralised tissue, Toludine blue stains the chondral matrix purple/blue. The MMI270 dosed sample demonstrates an expanded hypertrophic zone that shows a normal pattern of mineralisation in the longitudinal septa throughout the zone with slightly disorganised columns.

6.3.2.2.3 Adverse events from dose finding study

Overall body weight of the rats over the 4 week experimental period was notably lower in the high dose (120mg/kg) MMI270 groups with a 15% reduction in body weight in the 120mg/kg SC compared to controls and a 19% reduction in the 120mg/kg oral group by the end of the experimental period. With only 2 samples per group, no statistical calculations were preformed.

Throughout the later stages of the study, the SC dose rats began to develop persistent sores and lumps at the sites of injections, some wounds showing considerable breakdown and extensive bleeding subsequent to injections. To reduce the impact on these rats, the injection sites were spread over the skin surface to prevent re-injection into wound sites and further tissue damage.

6.4 Discussion

The initial fracture experiment performed with the MMP inhibitor MMI270 used a dose level of 20mg/kg administered twice daily SC (Medina *et al.*, 2003). This dose although sufficient to impair angiogenesis in a brain injury model, was not enough to delay the process of endochondral fracture healing. Radiological fracture union in these animals was achieved in 95% of all samples by 4 weeks post fracture, regardless of

treatment, as seen in Figure 6.1. Although some small changes were noted on analysis between the treatment group and controls from QCT analysis, it was agreed that histological analysis was not required as the expected outcome was clearly not achieved.

The lack of the anticipated result from the fracture experiments using MMI270 led to a pilot study aiming to optimise the dose of this agent required in these rats to impede endochondral ossification. This pilot study examined only endochondral ossification during long bone growth to assess the efficacy of the doses used because this process closely resembles endochondral fracture healing, as described in detail in section 1.3.2 of this thesis. As this agent has previously been delivered SC at similar dose rates (Kawai *et al.*, 2003), both oral and SC dosing was explored. By increasing the dose level by up to 6-fold the optimal dose level and mode of administration was determined.

Radiological analysis revealed the first evidence of detrimental effects on the growth plates of these rats. An obvious expansion of the radio-translucent region at the tibial growth plate was seen in the 80mg/kg and 120mg/kg SC doses groups. This expansion was not notable in any of the orally dosed rat samples.

Histological analysis confirmed these findings, demonstrating a widened growth plate in the tibia in both the 80mg/kg and 120mg/kg SC groups. Upon close examination it became clear that the expansion of the growth plate lay mainly in the hypertrophic chondrocyte zone with slight but distinct disorganisation of columns, as had been previously seen in MMP-9 and MMP13 knockout mice (Stickens *et al.*, 2004) (Figure 6.3b). Assessment of mineralisation in the hypertrophic zone revealed a normal pattern of longitudinal septal mineralisation throughout the extended area (Figure 6.3c). These results suggest that normal MMP activity is not required for mineralisation of chondrocyte matrix, but it is essential for the degradation of the non-mineralised septa, allowing vascular invasion.

Again the orally dosed group did not show significant changes in the growth plate morphology, confirming that oral dosing with this compound will not produce the desired outcome in this study. This lack of effect in the oral dose group confirms the observation from the initial fracture study, even with a 6 fold increase in dose of the inhibitor. These results together confirm this agent is active in impeding endochondral ossification when administered by SC injection at doses of more than 80mg/kg twice daily.

When administering such undocumented high doses of any agent, adverse effects on the welfare of animals should be taken into account. The reduction in body weight at the end time point suggests a reduction in growth in the high dose

(120mg/kg) group rats. Furthermore, the skin injection site wounds in the high dose SC group were extensive and could potentially impede correct administration of the agent. Thus, from these results and taking into consideration the adverse effects, the SC dose of 80mg/kg twice daily is the optimal dose required to impede endochondral ossification during long bone growth, with minimal adverse side effects

This examination of MMI270 in growing rats has produced evidence to confirm this agent can successfully delay endochondral ossification during long bone growth. These results suggest that this agent could potentially inhibit the process of endochondral fracture union. An examination of this agent at the doses determined through this study will be performed in the future to extend this line of investigation into the role of MMPs during endochondral fracture repair.

7 Discussion and Conclusion

7.1 Endochondral ossification during repair and growth proceeds normally even with bisphosphonate inhibition of osteoclastic resorption

Endochondral ossification is the most critical form of bone formation during healing of a fracture, it stabilises the damaged limb by bridging the fracture site with a bony callus. As the central process of during skeletal development and post-natal growth, and an essential element for bone repair, the biological mechanisms of endochondral ossification have been well described. (Colnot, 2005, Vortkamp *et al.*, 1998). Many similarities between sites of bone growth and endochondral fracture repair have been revealed, such that the biological understandings of both are intertwined. However, the conceptual knowledge of the importance of osteoclastic activity during endochondral ossification remains to be clarified during both bone growth and repair.

The principal focus of this body of work was to clarify the role osteoclasts play throughout endochondral ossification during fracture repair, extending this interest to include their function during long bone growth.

7.1.1 Radiological union was achieved regardless of ZA treatment

Radiologically determined union of fractures in this study was achieved at a similar rate regardless of ZA dosing, suggesting that endochondral union was unaffected by ZA treatment. BPs have been associated with delays in radiological fracture union (Odvina *et al.*, 2005), in particular after osteotomies in chronically treated osteogenesis imperfecta sufferers (Munns *et al.*, 2004). More commonly however, experiments examining BPs in fracture repair suggested no impairment in healing and frequently reported enhanced mineralisation and size of the bridging callus (Goodship *et al.*, 1994, Li *et al.*, 1999, Bauss *et al.*, 2004, Pizones *et al.*, 2005).

Although x-rays are used clinically to assess the progress of a healing bone, they do not provide all the information required to understand the exact stages of repair. The formation of the cartilage soft callus and the process of its ossification cannot be clearly demonstrated radiologically, leading to the requirement for histological examination of fracture healing.

7.1.2 Normal rate of endochondral ossification with ZA treatment

The rate of endochondral repair in this model proceeded normally regardless of ZA treatment, providing the first level of evidence to suggest osteoclastic activity is not rate limiting to this process. In addition, this outcome demonstrated the potential for the safe use of BPs during periods of bone healing. By measuring the tissue types that constitute the fracture callus, quantitative data was obtained for the progression of endochondral union. The percentage of soft cartilaginous callus reduced from 40% at 1 week post fracture (baseline data) to just 10% at 2 weeks, and by 6 weeks it was completely removed. This pattern of cartilage callus removal was seen in all samples examined, therefore was independent of ZA treatment.

In addition, growth plate height, a measure of disturbance of endochondral growth, remained unaffected by ZA treatment in the growing rats used in this study. This confirms the results obtained by Deckers and colleagues in 2002 that low to medium doses of BPs do not interfere with the vital process of endochondral ossification at the growth plate. More importantly, this outcome supports the conclusion from the fracture experiment that osteoclastic involvement is minimal and unnecessary to the process of endochondral ossification.

The outcomes of this study establish a need for a fundamental re-evaluation of both the basic understanding of bone repair and the clinical treatment of fractures. Until recently mature osteoclasts were assumed to be pivotal to the process of all cartilage matrix removal during endochondral ossification (Tabuchi *et al.*, 2005, Wang *et al.*, 2004b). Although a handful of investigators have provided some evidence to suggest this may not be the case, this thesis provides the first confirming evidence in such a model of fracture repair (Deckers *et al.*, 2002, Flick *et al.*, 2003, Kawana and Sasaki, 2003, Yamazaki and Sasaki, 2005). Thereby, these data contribute extremely important evidence to develop a new level of understanding to the role the osteoclast plays during endochondral fracture repair.

However, further consideration of this result is required to completely exclude osteoclastic resorption from endochondral fracture repair. First and foremost, BPs do not bind to un-mineralised cartilage matrix, thus if an osteoclast that has not been effected by ZA proceeds to the junction of the un-mineralised cartilage border, it may in fact proceed to resorb the cartilage matrix normally. Supplementary evidence to suggest that this was not the case was described in chapter 4 when endochondral fracture healing was examined in the incisor absent (*ia/ia*) mutant rat whose osteoclasts are unable to resorb mineralised tissue.

The question remains; “if osteoclasts are not the cell type driving this essential process, which cells are?” It is clear from this and other studies that TRAP positive osteoclast-like cells are often localised at the fore-front of the invasion into the cartilage tissue during endochondral ossification (Figure 7.1), however these cells may not truly be differentiated osteoclasts (Bronckers *et al.*, 2000). It has been suggested that a cell from the osteoclast lineage, the chondroclast, is the phagocytic cell responsible for un-mineralised cartilage matrix degradation (Cole and Wezeman, 1987, Bettex-Galland *et al.*, 1990, Lewinson and Silbermann, 1992). This multi-nucleated cell is positive for TRAP expression and has been shown in contact with un-mineralised cartilage matrix, however it was demonstrated to have different characteristics to that of the osteoclast (Nordahl *et al.*, 1998). These chondroclasts does not polarise in a similar manner to osteoclasts and when in contact with and presumably resorbing cartilage matrix no ruffled border is formed at the resorbing surface (Kawana and Sasaki, 2003, Yamazaki and Sasaki, 2005).

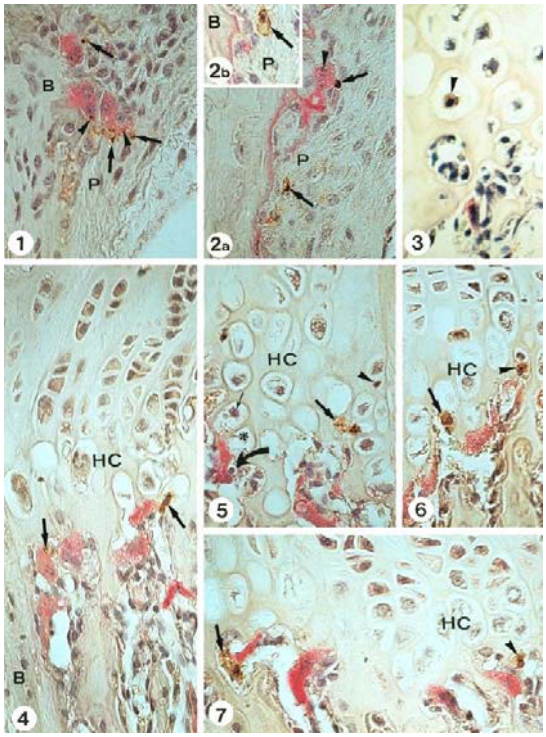

Figure 7.1 *Histological images of TRAP positive cells localised at the chondro-osseous junction*. Reproduced with permission from (Bronckers *et al.*, 2000).
This study examined the phagocytosis of dying chondrocytes in the hypertrophic zone (HC) of the growth plate by red TRAP stained chondroclasts or osteoclasts. Images 1 to 7 show the localisation of TRAP positive phagocytic cells near and engulfing apoptotic annexin V positive (brown) hypertrophic chondrocytes. These authors refer to the TRAP positive cells as osteoclasts, however without confirmation that ruffled borders have formed at resorbing surfaces these cells may be considered as chondroclasts.

It has been demonstrated that without proper ruffled border formation and cell polarisation, osteoclastic bone resorption is not possible (Shimizu-Ishiura *et al.*, 2002). These morphological differences therefore not only distinguish these two cell types by appearance but also their ability to resorb bone, and so their potential for exposure to BPs.

A role for these TRAP positive "chondroclast" cells during endochondral ossification is certainly plausible, however, as is the case for osteoclasts, their outright necessity to this process has been questioned. Recently, using numerous electron microscopic techniques combined with immunohistochemistry, the role of the chondroclast in removal of the un-mineralised cartilage at the chondro-osseous junction was refuted. Close examination of the chondro-osseous junction in new-born rats revealed that although TRAP positive chondroclasts and ED-1 positive macrophages were in the vicinity of the chondro-osseous junction, they were not located at the erosive front of the type-II collagen positive un-mineralised transverse septa of the terminal chondrocytes. Instead, CD34-positive endothelial cells of capillary vessels lined the degrading septal matrix within a row of developing chondrocytes (Figure 7.2) (Sawae *et al.*, 2003).

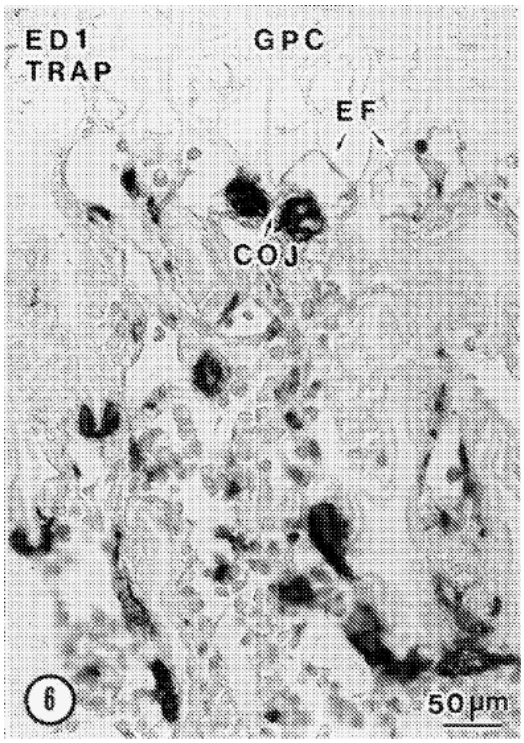

Figure 7.2 *Image of histology section showing localisation of macrophages at the chondro-osseous junction.* Double staining of ED1 and TRAP. ED-1-positive monocytes/macrophages (dark stained cells) are seen at the chondro-osseous junction (COJ), but they are distant from the erosive front (EF) of the transverse septal cartilage. (GPC) growth plate cartilage. Reproduce by permission of Oxford University Press (Sawae *et al.*, 2003).

Confirmation of this observational study came from the osteopetrotic *op/op* mutant mouse. The *op/op* mouse completely lacks macrophage colony stimulating factor (M-CSF) and is therefore entirely devoid of all macrophage populations, encompassing both osteoclasts and chondroclasts (Figure 7.3a) (Nishino *et al.*, 2001). However, endochondral ossification at the growth plate of tibia in growing *op/op* mice proceeded normally when examined by Deckers *et al.* 2002. Although osteoclasts were absent from the region of the chondro-osseous junction, sinusoid-like structures still invaded the chondral growth plate cartilage normally. As expected in these tibia, trabecular bone was increased the *op/op* mice (Figure 7.3b-B) (Deckers *et al.*, 2002). Moreover, endochondral fracture repair has also been shown to occur normally in these mice. Flick's group in 2003, demonstrated that union was achieved in un-fixed fractures at the same rate in *op/op* mice as normal CBAxB6 mice. Figure 7.3c shows radiological union in the *op/op* mice compared to CBAxB6 mice with the same rate of healing. Thus, even though chondroclasts may be actively involved in cartilage invasion during endochondral ossification, similar to osteoclasts, their elimination is not rate limiting to this process.

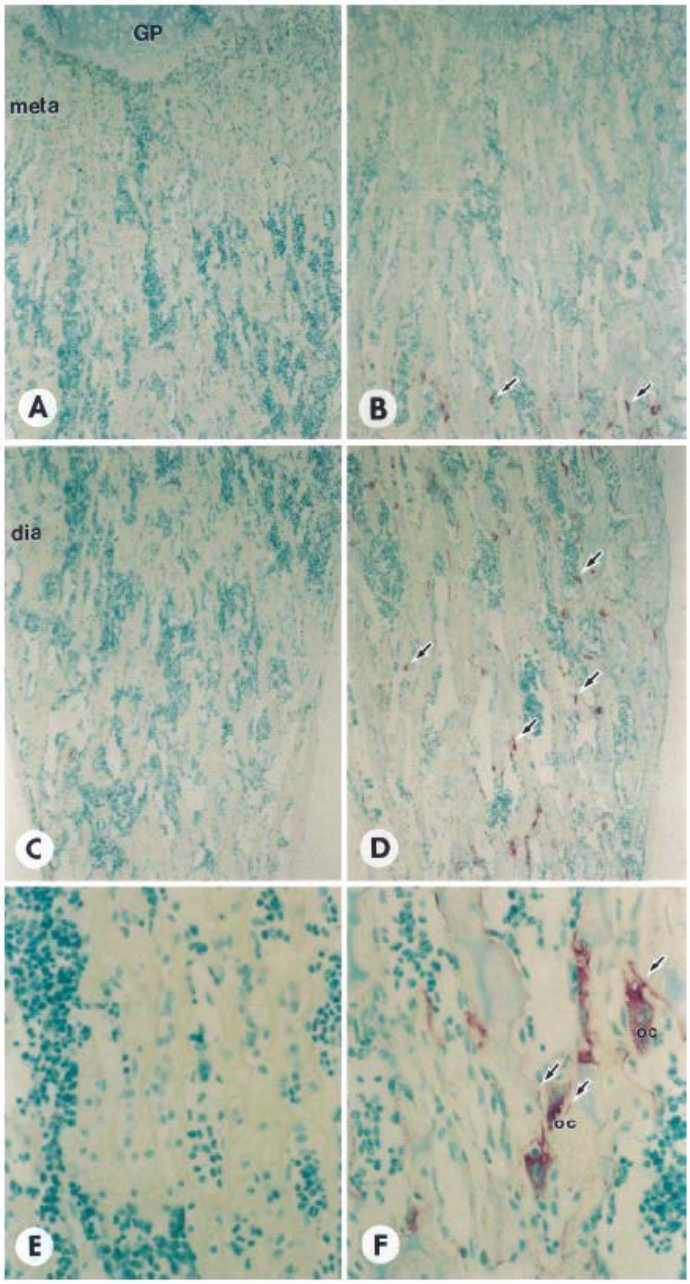

Figure 7.3a. *Histological images showing a lack of TRAP positive cells in op/op mouse metaphyseal bone.* Reproduced with kind permission of Springer Science and Business Media (Nishino *et al.*, 2001)
TRAP enzyme histochemistry of tibiae of op/op mice with (B,D,F) or without (A,C,E) macrophage colony stimulating factor (M-CSF) injection. A, B Metaphyses (*meta*). C-F Diaphyses (*dia*). TRAP-positive osteoclasts (*arrows*) can be seen in the diaphyseal region of the tibiae in the M-CSF injected *op/op* mouse (B,D), whereas no TRAP positive osteoclasts were found in the control *op/op* mouse (A,C,E). At a higher magnification, TRAP-positive reversal lines (*arrows*) were observed continuing resorption of the lacunae on with TRAP-positive osteoclasts (*oc*) were located (F). *GP*, growth plate. X70 (A-D), x320 (E,F).

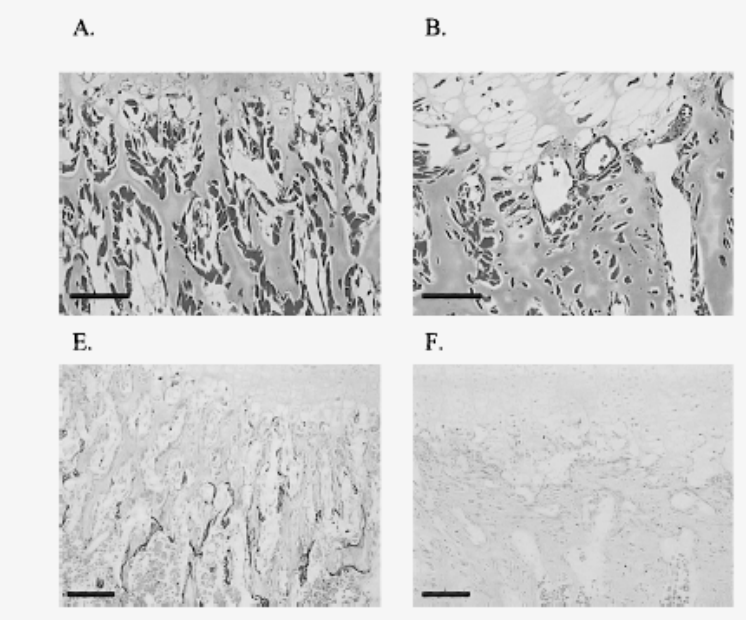

Figure 7.3b. *Histology sections of the chondro-osseous junction of op/op mice (B and F) compared to their normal littler mates (A and E).* Reproduced with permission from (Deckers *et al.*, 2002).
Note the lack of TRAP positive cells in the chondro-osseous junction. Still the cartilage growth plate is being invaded without chondroclasts or osteoclasts present.

General histology and absence of TRAP activity in tibias of 7 day-old *op/op* mice. (A-D) Goldners staining and (E-H) TRAP staining of tibias of 7 day-old (A and E) unaffected littermates, (B and F) *op/op* mice. Trabecular bone was increased in (B) op/op mice as shown by Goldner. Sinusoid-like structures invaded the lacunae of mineralised chondrocytes in the growth plate. (E) Numerous TRAP positive cells were identified at the chondro-osseous junction and at the metaphysis in the unaffected littermates and heterozygotes and absent in (F) the mutants. A-B magnification x400 and E-F magnification x 200.

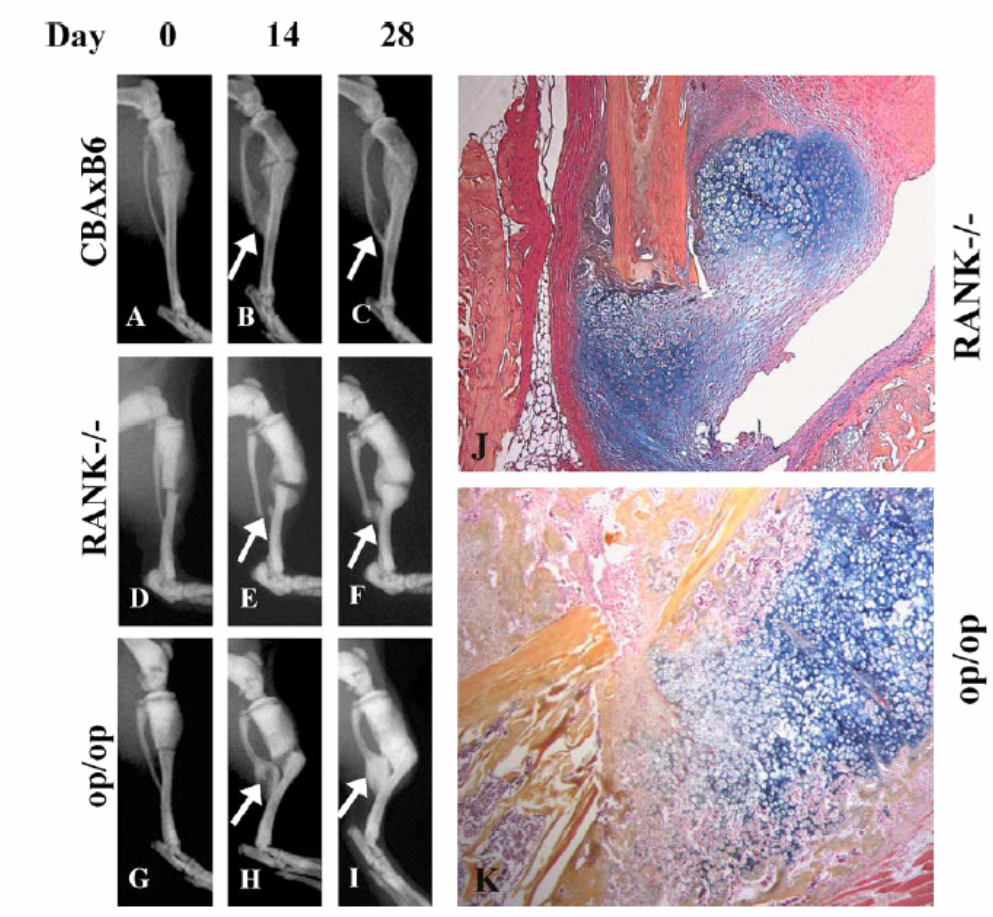

Figure 7.3c. *X-ray images and histology sections of endochondral fracture repair of op/op mice (G,H,I and K)* Note the normal rate of radiological healing and endochondral ossification after fracture. Reproduced with permission from (Flick *et al.*, 2003).

RANK -/- animals exhibit radiographic and histological evidence of callus formation but not union. Representative X-rays taken on day 0 (A,D,G); day 14 (B, E, H); and day 28 (C,F,I) post fracture from CBAxB6 (A,B,C); RANK -/- (D,E,F); and op/op (G,H,I) animals with un-stabilised fractures are shown. Arrows indicate fracture callus surrounding the tibia/fibula junction. Note the absence of bony union in panel (F). Representative alcian blue hematoxylin stained sections of RANK -/- and op/op (K) fracture callus 14 days post-fracture are shown at 50x original magnification.

An alternative hypothesis regarding which cell type is driving cartilage invasion during endochondral ossification was suggested by Sawae and colleagues in 2003, the vascular endothelial cell. It has been extensively demonstrated that angiogenesis, or vascular invasion, is a pivotal requirement for endochondral ossification (Vu *et al.*, 1998, Gerber *et al.*, 1999, Deckers *et al.*, 2002). Therefore, it is conceivable that the migratory cells of the blood vessels are capable of degrading the un-mineralised cartilage matrix, creating a path for vessel propagation (Takahara *et al.*, 2004). The fact that these lining cells have been shown to secrete MMP-9 supports this hypothesis.

As described in detail in section 1.3.2.3, MMP-9 is a protease that has been shown to be essential for degradation of cartilage matrix, in particular the type X collagen fibres that constitute the hypertrophic chondrocyte matrix found at the chondro-osseous junction (Malemud, 2006). In addition, MMP-9 knockout mice demonstrate significant delays in endochondral fracture repair, confirming the crucial role of this protease during this process (Colnot *et al.*, 2003). Thus, the expression of MMP-9 by vascular endothelial cells and their proven migratory function at other tissue sites (Blavier and Delaisse, 1995, Yoshida *et al.*, 2004, Milkiewicz *et al.*, 2006, Melton *et al.*, 2006), demonstrate the potential for a fundamental role for these cells to endochondral ossification during both growth and repair. Chapter 6 of this thesis revealed preliminary data aiming to develop a technique of inhibiting MMP activity during fracture healing in order to perform an examination of the importance of MMPs in this model. The outcomes of which are discussed in section 7.4.

By eliminating osteoclast activity during endochondral fracture union, numerous clinical implications regarding treatment with BPs and other anti-resorptive agents are revealed. By proving these cells are not essential to this process, the safety of BPs and other anti-osteoclastic therapies during initial fracture repair have been upheld. Many recent investigations into the use of anti-resorptives agents to enhance the healing process have increased the importance of these revelations. By preserving the bone callus formed through endochondral ossification, BPs haven been proven to enhance callus size and strength, thereby increasing resistance to re-fracture (Goodship *et al.*, 1994, Li *et al.*, 1999, Bilston *et al.*, 2002, Amanat *et al.*, 2005). Confirming these agents will not interfere with the attainment of initial union enhances their potential to augment fracture healing.

7.1.3 Enhanced net hard callus production with ZA treatment

BP treatment during fracture healing is commonly associated with enhanced content of mineralised or hard callus and improved mechanical properties of the

fracture site. (Goodship *et al.*, 1994, Li *et al.*, 1999, Bilston *et al.*, 2002, Little *et al.*, 2003b, Amanat *et al.*, 2005). Although it has been suggested by some authors that this is due to increased bone formation, little evidence of this exists. In fact, reductions in bone formation parameters such as mineral apposition rate and bone formation rate during BP treatment and bone healing have been demonstrated in rabbits (Smith *et al.*, 2004, Takahashi *et al.*, 2006), and in the presence of the anabolic stimulus BMP-7, no change in bone formation rate was noted with ZA treatment in rats (Little *et al.*, 2005). Therefore, with the understanding of the mechanism of action of BPs, the enhanced hard callus is more likely a result of hard callus retention due to reduced resorption and remodelling. These previous outcomes led to the analysis of hard callus content as well as endochondral union in ZA treated fracture calluses in this study.

As previously demonstrated, ZA treatment led to enhanced net hard callus production in this model. From as early as 2 weeks post fracture, ZA dosing in either Bolus or Weekly form resulted in increases of up to 2-fold in both bone mineral content and volume of mineralised tissue in the fracture calluses.

The normal pattern of hard callus formation and removal in this model was exhibited by the Saline control group. Callus BMC increased slightly between 2 and 4 weeks post fracture, beginning to decrease by 6 weeks. Callus volume in the Saline samples in fact showed a steady decrease from 2 to 6 weeks post fracture (Figure 3.3). These dynamic changes suggest that whilst the fracture site was being bridged by new bone formation, the existing peripheral bony callus was resorbed and remodelled by osteoclasts at a slightly faster rate. In contrast, ZA treatment consistently resulted in steady increases in callus BMC and bone Volume throughout the early healing phase up to 6 weeks. The exception of which being a slight reduction in callus volume in the Bolus ZA HD group between 4 and 6 weeks. Hence, the lack of resorption under BP treatment protects the existing bone callus such that it is progressively added to throughout the healing process, (Figures 3.3). Possible detrimental effects of such delayed hard callus remodelling were examined in chapter 5 and will be discussed further in section 7.2.2.

Further differences were exhibited within the ZA treatment groups with the Weekly ZA dosed animals demonstrating enhanced effects on primary callus retention compared to Bolus ZA. Increases of up to 30% in callus Volume and BMC were evident in the Weekly ZA groups over the Bolus ZA dose groups from as early as 4 weeks post fracture. These outcomes point to an additive effect of the continuous ZA dosing in both Weekly ZA groups. Although the Weekly doses were one fifth the potency of the single bolus doses, as the callus formed the available bone binding sites were increased for every dose, developing an additive effect. At the ZA dosing

commencement time of 1 week post fracture, the amount of callus that was mineralised bone tissue was 60% as determined by the histomorphometric analysis of callus content (Figure 3.4). Thereby, approximately 60% of the callus was bound by the single ZA dose given in both LD and HD Bolus ZA groups. The remaining 40% of the hard callus that formed after this time however was not dosed with ZA, and thus would not have been protected from resorption. On the other hand, when the dose was administered weekly, at 1 week 60% of the callus was only dosed with one fifth of the bolus dose. However 1 week later (2 weeks post fracture), after approximately 91% of the hard callus had formed, the existing 60% was dosed again, along with the new 31% formed. Following from this, at 3 weeks we again dosed all existing callus in addition to the new callus formed and so on until 5 weeks post fracture when approximately 99% of the hard callus had formed. Hence, by continually dosing the existing callus and the newly formed callus on a weekly basis with ZA, the portion of the hard callus bound with ZA would have increased dramatically. This in turn increased the portion of the callus protected from resorption and enhanced the net hard callus production up to 6 weeks.

When the High Dose (HD) groups were compared with the Low Dose (LD) groups within each of the administration modes (Bolus and Weekly) no significant differences were demonstrated. These results suggest that the magnitude of the response to ZA in regard to hard callus retention was not dependent on the actual dose of ZA present in the callus, but more so on the percent of the callus bound by ZA. That is, the mode of administration of ZA produced more impact on the forming callus than the level of ZA dosing used. In contrast to this outcome, cyclical intermittent dosing of ibandronate in ovariectomised (OVX) rats provided equivalent bone preservation to a total single loading dose (Bauss *et al.*, 2002). Thus, although bolus and intermittent treatment had similar effects in osteoporotic animal models, they may have profoundly differing effects in osteoporotic fractures.

A recently published study performed by our group is consistent with the outcome that mode of administration carries more impact on bone than overall dose (Amanat *et al.*, 2007). This study employed the same rat fracture model to examine the timing of a single bolus dose of ZA with doses of 0.1mg/kg administered at 0, 1 and 2 weeks post fracture. At the final 6 week time point, the 1 week and 2 week dosed groups showed superior enhancement of net hard callus production compared to both the groups dosed at the time of surgery. In addition, scintillation counting performed on samples dosed with carbon 14 (^{14}C) tagged ZA showed an increased uptake in the callus in the 1 and 2 week post fractures ZA dose groups compared to dosing at the time of surgery. Thus, when the dose was administered at 1 or 2 weeks post fracture,

the callus mineralised tissue volume was much greater, increasing the bone surfaces available for ZA binding and consequently enhancing callus preservation.

By dividing the ZA dose into Weekly doses, the resulting callus therefore contained more mineralised tissue volume at 6 weeks post fracture, improving mechanical integrity and hence it's resistance to re-fracture. Mechanical strength of ZA treated fracture calluses was enhanced in this study and is discussed in section 7.3. Although, this conclusion is based upon the assumption that the material properties of the retained callus are similar to untreated remodelled bone. Since the primary woven bone callus is normally remodelled into more mature lamellar bone during repair, it has been suggested that the hindrance of such remodelling could be detrimental to the material properties of the callus tissue (Li *et al.*, 1999, Cao *et al.*, 2002, Ulrich-Vinther and Andreassen, 2005). Chapter 5 of this thesis examined this pertinent issue in detail, providing a new level of understanding regarding dosing frequency of BPs and their effects on hard callus remodelling.

7.2 Endochondral fracture union in the osteoclast mutant incisor absent rat.

To expand the examination of the role active osteoclasts play during endochondral fracture repair, the well described osteoclast mutant *ia/ia* rat was utilised. Due to a spontaneous mutation rendering osteoclasts in these rats incapable of active bone resorption (Reinholt *et al.*, 1999, Van Wesenbeeck *et al.*, 2004), the incisor absent (*ia/ia*) rat provided a useful non-pharmacological model to further examine the effects of reduced osteoclast function on endochondral fracture repair and long bone growth.

7.2.1 The *ia/ia* rat demonstrates osteopetrosis due to inactive osteoclasts with recovery commencing by 12 weeks of age.

Previous examinations of the *ia/ia* rat have closely explored their phenotype confirming that their osteopetrosis is a direct result of inactive osteoclast (Marks, Jr., 1976). Therefore, these studies have focused on the morphology and activity of the mutant osteoclasts *in vivo* (Marks, Jr., 1973, Reinholt *et al.*, 1999). Although a large body of work has been published on these rats, the exact age of recovery of osteoclast function has not been discretely characterised. In order to perform analysis of fracture repair under conditions of inactive osteoclastic resorption in these rats, knowledge regarding the exact age of recovery of osteoclast function was necessary. This was determined through a detailed analysis of the phenotype of the *ia/ia* rat, confirming the

extensive osteopetrotic phenotype these mutated rats demonstrate and elucidating a more precise age of recovery. This allows for subsequent fracture repair examinations within the period of reduced osteoclast function. Extensive radiological and histological examination of growing *ia/ia* rats revealed the typical osteopetrotic phenotypic changes, as previously reported (Marks, Jr., 1973). At the tissue level, remarkable increases in metaphyseal bone density in *ia/ia* rats were seen on radiographs and quantified by DEXA scan and histology up to 20 weeks of age.

Previous evaluation of the chemical content of metaphyseal bone matrix in *ia/ia* rats demonstrated an increased hexosamine complex, suggestive of increased calcified cartilage content (Boskey and Marks, Jr., 1985). The matrix of *ia/ia* metaphysis also showed a higher mineral to matrix ratio with increased hydroxyapatite crystal size. However an abnormal ratio of calcium to phosphate in these larger crystals was noted suggesting imperfect or irregular organisation of hydroxyapatite. It was concluded by these investigators that in osteopetrotic bones, mineral deposition continues in the absence of remodelling, leaving an excess of calcified cartilage upon which crystal deposition but not maturing occurs, producing metaphyseal bone with distinctively altered matrix. It could be asserted that such alterations in mineral composition could be behind the extensively increased BMD in the *ia/ia* rats generated from DEXA scans in this study.

It was not until the histology sections were examined more closely that it became evident that recovery from the osteopetrotic bone phenotype had occurred. When the tibial metaphyseal bone was separated into proximal and distal regions, reductions in bone volume were observed from 12 weeks of age in the *ia/ia* rats, suggesting that resorptive function was recovering. At the systemic level, serum c-terminal telopeptide cross-links (CTX), a marker of resorptive activity, began to increase at 9 weeks of age, then normalised to wt/het levels by 12 weeks of age, coinciding with the histological findings (Figure 4.8).

Lastly, examination of osteoclast function at the cellular level demonstrated reduced *in vivo* osteoclast resorption in the *ia/ia* cell population compared to wt/het controls. Again, corresponding to the histological changes, by 12 weeks of age osteoclastic resorption *in vitro* had recovered to a similar level as normal cells. This extensive phenotypic analysis provided not only the information required to ensure subsequent fracture studies were performed prior to phenotype recovery, but also extended the current understanding of the *ia/ia* rat phenotype.

7.2.2 Experimental *ia/ia* rats exhibited inactive resorption throughout fracture repair experiments.

To assess the exact level of resorptive activity during the fracture experiments in the *ia/ia* rat, samples of non-operated tibia were analysed in a similar manner to those used in the phenotype study. DEXA scans showed over a two-fold increase in *ia/ia* rat metaphyseal BMD compared to wt/het rats, which was maintained throughout the experimental period. Furthermore, histology revealed up to a 75% increase in proximal metaphyseal BV/TV and a 6-fold increase in distal metaphyseal BV/TV in the *ia/ia* rats compared to normal controls. Again these differences were maintained throughout the experimental period. More importantly, as expected from the initial phenotype work, the distal metaphyseal BV/TV remained consistent at 50% in the *ia/ia* rats during the experiment, confirming there was no recovery from osteoclast dysfunction to the end 8 week time point of the fracture experiment.

7.2.3 Endochondral fracture repair occurs normally in the absence of functionally resorbing osteoclasts in the *ia/ia* rat.

The main goal of this study was to examine endochondral fracture repair in the absence of actively resorbing osteoclasts, adding to the findings from chapter 3. Fracture repair in the *ia/ia* rat has previously been examined, confirming that the fracture calluses in the *ia/ia* rats are larger and contain more mineralised tissue. It has also been demonstrated that remodelling of the hard callus is significantly delayed in these rats (Schmidt *et al.*, 1977, Marks, Jr. and Schmidt, 1978). Although to date, no mention has been made in regard to the initial process of endochondral fracture union, therefore, mine is the first study to examine endochondral fracture repair in this model.

The rate of endochondral fracture repair in the *ia/ia* rat was equivalent to wt/het control rats up to the 3 week end time point, similar to the results obtained with ZA treatment as described in chapter 3. Since an absence of osteoclast function was confirmed in these rats, this outcome strongly supports the hypothesis that osteoclast function is not a prerequisite for the removal of the cartilage soft callus through endochondral ossification during the healing of fractures.

In addition to the work performed by Flick *et al.* 2003, demonstrating normal endochondral fracture union in both the *op/op* osteopetrotic mouse and RANK:Fc treated mice, along with the more recent work by Ulrich-Vinther et al in 2005, showing no effects on fracture callus formation in OPG treated rats, the outcomes of this body of work have added important knowledge to the understanding of the biology of fracture healing.

7.2.4 Normal Endochondral growth plate height in the *ia/ia* rat

In order to enhance the results obtained during endochondral fracture repair, the growth plates were also examined in the wt/het and *ia/ia* samples to assess the effects of reduced osteoclast resorption on endochondral long bone growth. Yet again, endochondral ossification remained unaffected, with no difference in growth plate height in the *ia/ia* rats compared to those of controls. This outcome supports all the results presented in this thesis, confirming that osteoclast function is not rate limiting to the cartilage resorption phenomenon of endochondral ossification. Furthermore, this result is in contrast to the abnormal widening of growth plates in MMP deficient animals, and as I demonstrated with the MMP inhibitor MMI270 in chapter 6 of this thesis.

7.2.5 Hard callus remodelling is delayed in the *ia/ia* rat fracture callus.

Osteoclast function is essential to hard callus remodelling during fracture healing, such that weekly BP dosing hindered this process up to 6 months after fracture, see section 7.3. Such delays in hard callus remodelling have also been previously shown in the *ia/ia* rats (Schmidt *et al.*, 1977, Marks, Jr. and Schmidt, 1978).

Although analysis of early fracture repair to union was the focus in the present examination of *the ia/ia* rat, differences in early hard callus remodelling were evident. Following the pattern seen in the saline administered Wistar rats in chapter 3, the wt/het control fractures showed a decrease in callus volume between the 2 and 3 week post fracture time points. In contrast, the mutant *ia/ia* rats demonstrated a significant increase in callus size at this stage. Hence, the early remodelling of the primary hard callus evident in the normal samples was completely lacking in those of the *ia/ia* rats.

Callus BMD was also significantly impacted by the reduced resorption in the *ia/ia* rat, with the slight increase in BMD seen at 1 week after fracture in the *ia/ia* samples compared to wt/het, no longer evident by the end 3 week time point. This could be explained by the reduction in hard callus remodelling, because primary woven bone is less dense than remodelled lamellar bone (Ulrich-Vinther and Andreassen, 2005). On the other hand, it could also be considered that this outcome was due to the inclusion of the original cortical bone in the QCT scan data. The non-operated femora demonstrated an 18% decrease in cortical bone BMD in the *ia/ia* rat compared to wt/het controls by the 3 week end time point. Thus, since the original cortical bone is included in the callus data, this decrease in BMD would influence the overall data obtained in the fracture calluses.

The reduced hard callus remodelling clearly demonstrated in the *ia/ia* rats could significantly impact the strength of the callus produced during fracture healing in these rats. It has been suggested that inhibited remodelling of poor quality bone tissue, leads to inferior mechanical properties (Tuukkanen *et al.*, 2000). In line with this, chapter 5 of this thesis demonstrated that reduced hard callus remodelling under the influence of continuous BP dosing produced a callus that exhibited inferior material properties. This will be discussed in section 7.3.

7.2.6 Normal endochondral ossification in the *ia/ia* rat suggests the redundancy of osteoclastic resorption during this initial stage of fracture repair

The *ia/ia* rat provided a useful model of osteoclast dysfunction in order to further examine the role of the osteoclast during fracture repair. By extensively evaluating the level of resorptive activity throughout post-natal growth in these rats, a discrete period of recovery was determined between 63 and 84 days of age, a significant improvement on the approximated 50 to 100 days previously reported (Marks, Jr., 1973). Fracture studies performed prior to this period of recovery confirmed the hypothesis that in the absence of actively resorbing osteoclasts endochondral fracture healing proceeds normally. Thereby this study provides additional evidence for a redundant role of osteoclasts in bringing about the completion of soft callus removal in endochondral ossification. The results of this study may also refute suggestions that normal endochondral ossification under BP treatment was due to the lack of binding of BP to the soft cartilaginous callus. However this hypothesis still requires further confirmation as the TRAP positive cell population that is not resorbing bone tissue is present in both this model and the BP treated animals. Due to their frequent location at the chondro-osseous junction, the TRAP positive pre-osteoclasts or “chondroclasts” may in fact be the active cells driving cartilage matrix removal during endochondral fracture repair.

Shown to secrete MMPs, this cell population may be able to degrade the un-mineralised cartilage matrix and allow for vascular invasion (Cole and Wezeman, 1987, Bettex-Galland *et al.*, 1990, Lewinson and Silbermann, 1992). Furthermore, MMP-9 secreting vascular endothelial cells have also been suggested as pertinent to this process and thus may also make-up this invading cell population, see section 7.1.2. Both these cell types exist and are functional in the *ia/ia* rat, whilst also unaffected by bone tissue bound BPs, thus they may be the cells driving endochondral repair in the fracture experiments outlined in this investigation. In order to confirm the necessity of

these cell populations to this process, a new line of experimental investigation must be performed.

Firstly, MMP inhibition may confirm the suggested role these proteases play in this process. This was examined in chapter 6 of this thesis using and MMP inhibitor in the Wistar rat fracture model. Secondly, the effect of eliminating the TRAP positive pre-osteoclast or chondroclast cell population should be examined to confirm or rule out their necessity. This could be achieved by manipulating the RANKL/RANK pathway of osteoclastogenesis stimulation. The endogenously produced RANKL inhibiting osteoprotegerin (OPG) has been explored as a new agent for anti-resorptive therapy (section 1.4.7.1). Due to its ability to reduce osteoclast populations by inhibiting the RANKL signal to differentiate into osteoclasts, recombinant OPG provides a good model to analyse the effects of eliminating TRAP positive pre-osteoclasts from endochondral fracture repair. Although a substantial study investigating OPG during fracture healing has been performed, (Ulrich-Vinther *et al.*, 2005, Ulrich-Vinther and Andreassen, 2005), the focus of the work performed by these authors has been on radiologically determined union and the later stages of hard callus remodelling and fails to examine closely the process of initial endochondral repair.

Flick and colleagues, in 2003, provide the most relevant evidence regarding the role of TRAP positive cells during endochondral repair. By administering RANK:Fc to mice with tibial fractures, the RANK signalling pathway was blocked, preventing osteoclastogenesis. Fractures in these mice achieved union normally, although they showed signs of delayed hard callus remodelling. In addition to RANK:Fc intervention in this study, fracture healing was examined in osteopetrotic *op/op* mice. Even with a complete absence of TRAP positive cells, these mice still achieved endochondral union at a similar rate to controls. However, this study was limited by the fact that the examination of repair in the *op/op* mice was not completed before their documented age of phenotypic recovery. Moreover, It has been suggested that VEGF may compensate for mCSF in promoting osteoclast fomrmation in these mice and since VEGF expression in a fracture callus is extremely high it may have stimulated local osteoclast formation at the repair site (Niida et al., 1999). Hence, questions still remain; could the complete abolishment of a TRAP positive cell population including osteoclasts and chondroclasts lead to delays in endochondral fracture union? My aim is to perform the examinations required to answer this.

7.3 Effects of Bolus compared to continuous ZA treatment on hard callus remodelling

Clinical applications of the newer more potent BPs in the treatment of osteoporosis have shown increased patient compliance and reduced side effects with reductions in dosing frequency from weekly ALN to monthly ibandronate and more recently, yearly ZA (Thiebaud *et al.*, 1997, Reid *et al.*, 2002, Bone *et al.*, 2004, Black *et al.*, 2007, Lindsay R *et al.*, 2006). What is yet to be determined however is whether these changes in the clinical field may impact on the healing of fractures in these patients. With the aim to model the difference between the new emerging more potent BPs to the previous compounds, this study examined Weekly ZA to a single moderate Bolus ZA dose in a rat fracture model. This examination focused only on the high dose ZA regimes from the study in chapter 3. By examining the later stages of repair, hard callus remodelling, important differences were elucidated between the two dosing regimens.

The concern of long term dosed patients displaying reduced bone turnover and delayed fracture repair (Odvina *et al.*, 2005) was not modelled by the design of this investigation.

7.3.1 Enhanced net hard callus production but not callus strength with Weekly ZA treatment compared to bolus

At 6 weeks post fracture, Weekly ZA dosing at the high dose level produced a larger more mineralised fracture callus than either Saline or Bolus ZA dosing. As discussed in section 7.1.3 this difference between ZA dosing regimes was due to the additive effect of continual ZA dosing on the forming fracture callus, preserving a larger portion of the primary woven bone callus. Interestingly, this difference between Weekly ZA and Bolus ZA dosing was maintained throughout the long term analysis up to 26 weeks post fracture.

As shown previously, BP treatment during fracture healing produces significantly larger calluses which frequently correlate to improvements in overall mechanical strength (Goodship *et al.*, 1994, Li *et al.*, 1999, Bilston *et al.*, 2002, Amanat *et al.*, 2005). This was also the case in the current examination, with both Bolus and Weekly ZA dosing enhancing fracture peak torque to failure by up to 31% and 96% at either 6 or 26 weeks respectively compared to Saline. Of interest, however, is the fact that fracture peak torque to failure was not different between Bolus and Weekly ZA treatments at both 6 and 26 weeks. In light of the fact that Weekly ZA produced larger calluses than Bolus ZA at both these time points, this outcome implies that the larger

callus developed by Weekly ZA treatment is a product of retention of mechanically inferior bone tissue.

Calculated values for the intrinsic material properties of the fracture calluses, peak stress and shear modulus, confirmed this inference. At 6 weeks, similar reductions in peak stress and shear modulus were noted in both ZA groups compared to Saline, inferring the material properties of the tissue components in these un-remodelled calluses were inferior at this stage. However, by 26 weeks, both the callus peak stress and shear modulus in the Bolus ZA group had normalised to Saline levels, whilst these parameters in the Weekly ZA calluses remained significantly reduced compared to both Saline and Bolus ZA treatments. Therefore this final outcome confirmed that the Weekly ZA dosing to 6 weeks post fracture indeed produced a fracture callus of inferior material properties. By 26 weeks post fracture the Bolus ZA calluses exhibited intrinsic material properties comparable to Saline control samples. On the other hand, Weekly ZA calluses retained tissue of evidently reduced quality even as long as 26 weeks post fracture.

It must be pointed out that the measures of callus material properties used in this investigation have been adapted from engineering calculations based on homogenous, isotropic (equivalent when analysed in any direction), regular cylindrical samples (Turner and Burr, 1993). Hence, these parameters are merely a crude indication of the intrinsic material properties of the samples from this study. The rat fracture samples examined in this study are non-homogenous, anisotropic and of irregular geometrical shape. Therefore any interpretation of this data must be made cautiously.

As speculated by numerous authors, the production of a fracture callus inferior in material properties may be a result of reduced hard callus remodelling (Li *et al.*, 1999, Cao *et al.*, 2002, Ulrich-Vinther and Andreassen, 2005). Hard callus remodelling is a process which involves extensive resorption of the primary woven bone callus and its replacement with more compact lamellar bone until the site resembles its original weight bearing cortical bone structure and is essential to completion of fracture healing (section 1.3.4) (Einhorn, 1998, Einhorn, 2005). Retention of the primary woven bone, through reduced remodelling produced a callus which demonstrated inferior intrinsic material properties. Such delayed remodelling and poorer intrinsic material properties have been demonstrated in numerous studies examining fracture repair with high dose or continuous BP therapy (Li *et al.*, 2001, Cao *et al.*, 2002, Mori, 2003, Cao *et al.*, 2006). However, these effects of BP treatment may be limited to sites of bone repair. During normal bone homeostasis, under continuous high level incandronate dosing, native rib cortical bone demonstrated no changes in intrinsic material properties, but it

did show overall increases in BMD and bending strength compared to control samples (Komatsubara *et al.*, 2004). Hence, consideration of the effects of BPs on material properties of bone may only be of importance during high bone turnover situations like bone repair.

7.3.2 Superior hard callus remodelling with Bolus ZA compared to Weekly ZA treatment.

The normal dynamics of hard callus remodelling, established by the Saline treated samples, is represented on QCT scans by a consistent decline in callus BMC and volume from as early as 4 weeks post fracture, as mentioned previously in section 7.1.3 and demonstrated in Figures 5.3a and b. This decline verifies the occurrence of hard callus remodelling at these early stages. Although not of the same magnitude, Bolus ZA also demonstrated a slight trend for a decrease in callus volume between 4 and 6 weeks post fracture. In contrast, Weekly ZA treatment prevented such decline in callus size until after 6 weeks post fracture, suggesting delays in the commencement of hard callus remodelling. This delay led to fracture calluses over twice the size of Saline samples in the Weekly ZA group, even out to the 26 week time point.

In addition to the quantified QCT values, the cross sectional images from these scans revealed a visible difference between Bolus and Weekly ZA calluses. An outer ring of neo-cortical bone, formed by remodelling of the primary hard callus, was noted at 6 weeks in both Saline and Bolus ZA samples (Figure 5.2). However, the formation of this neo-cortex was delayed until the 12 week time point in the Weekly ZA group. This outcome is consistent with that demonstrated by continuous Incandronate treatment (Li *et al.*, 1999) and continuous high dose ALN treatments (Cao *et al.*, 2006) during fracture healing in rats.

Finally, histological evaluation complemented these findings regarding delayed remodelling, with Bolus ZA showing a comparable callus percentage of neo-cortical bone to Saline at 6, 12 and 26 weeks, whilst Weekly ZA showed significantly less remodelled neo-cortical bone and an increased area of retained woven bone callus compared to both Saline and Bolus ZA treatments.

Importantly, at 26 weeks Bolus ZA samples showed superior remodelling to Weekly ZA with closer structural similarities to that of the Saline group. This was illustrated three dimensionally through micro CT scan images (Figure 5.7). What also became apparent from the micro CT scans was the almost complete removal of the old cortex in the Saline samples by 26 weeks. The new outer cortex that was formed through remodelling of the primary woven callus became the primary structure at the

healing site, and eventually formed the cortex of the healed limb. Nevertheless, ZA treatment, in both Bolus and Weekly form, limited such removal of the original cortex. Since this bone was present at the time of initial ZA dosing, it was protected from resorption. In this context, reviewing the histological images at 26 weeks, the same pattern was evident, where Saline samples showed only small remnants of old cortical bone and ZA samples exhibiting clear retention of original cortical bone structures (Figure 5.6). These findings are consistent with those also demonstrated with incandronate (Li *et al.*, 2001) and ALN (Cao *et al.*, 2002) during fracture healing in normal and OVX rats.

7.3.3 Single Bolus dosing of ZA is preferential to Weekly dosing during the late stage fracture healing.

Delays in hard callus remodelling with ZA treatment were confirmed through numerous levels of examination in this study, revealing extensive differences between Bolus and Weekly ZA dosing regimes. Bolus ZA dosing demonstrated superior hard callus remodelling without compromising the increased strength of the callus. It therefore became apparent that hard callus remodelling is necessary to improve the material properties of the callus structure.

Bone strength is in fact determined by three parameters; bone tissue volume, micro-architectural organisation of the bone tissue and the degree of mineralisation of the bone matrix (Boivin and Meunier, 2002b). Delayed bone remodelling due to reduced resorption has been correlated to disorganisation of the bone micro-architecture and thus reduced quality of the tissue (Ulrich-Vinther and Andreassen, 2005). The early primary callus formed of woven bone possesses reduced material properties compared to the later more refined lamellar bone matrix formed through remodelling (Currey, 2003). The retention of the inferior primary callus, as seen clearly at 26 weeks in the Weekly ZA calluses, would therefore greatly influence the material properties of the callus. Moreover, chronic BP treatment has been associated with an increase in the appearance or accumulation of micro cracks which render the bone more susceptible to fractures (Mashiba *et al.*, 2001). Thus provides further evidence that the delays in hard tissue remodelling produced by BP treatment result in callus tissue that is inferior in material properties.

As demonstrated in this study, such a delay in remodelling of primary callus certainly influenced the overall mechanical properties of the fracture callus. Mechanical strength was equivalent in Weekly ZA and Bolus ZA groups at 26 weeks, despite the greater bone volume evident in the Weekly ZA calluses. The lack of correlation between bone volume and strength indicating inferior tissue properties in the Weekly

ZA treated groups. As suggested by previous authors, the increase in bone volume in this group may represent a compensatory response to maintain callus strength in the face of reducing intrinsic tissue properties (Cao *et al.*, 2002). In this case, the delay in remodelling would represent a strength-mediated regulatory response rather than a response to ZA treatment.

We can put forward 3 reasons why this is probably not the case. Firstly, if such compensation existed, it is likely that the increase would return strength to that of control calluses. Strength was in fact increased over control animals with ZA treatment. Secondly, such a response would require an increase in bone formation, which we know is most commonly reduced in these BP treated models. Lastly, if callus strength were the primary regulatory factor, the improvement in intrinsic tissue properties in Bolus ZA samples between 6 and 26 weeks (Table 5.5) would be coincident to a decline in tissue volume, thereby maintaining callus strength. This decline is not evident, with Bolus ZA callus remaining 61% larger and 88% stronger than Saline control samples at 26 weeks. Therefore, even though the Bolus ZA callus demonstrated equivalent material properties to Saline at this time, the increase in tissue volume was maintained, with almost a doubling in overall strength. Thus, it is more likely that the delay in hard callus remodelling is a direct effect of ZA treatment and not a compensatory mechanism for inferior tissue quality.

Initially, it was understood that BPs merely prevented resorption of existing bone tissue, thus preserving the bone architecture. However, more recently it has been revealed that BPs also allow for enhanced secondary mineralisation (Boivin and Meunier, 2002a). Bone maturation occurs in two stages, primary mineralisation and secondary mineralisation. By preserving the primary under-mineralised bone tissue from resorption, more sites are able to obtain a level of secondary mineralisation, enhancing overall bone mineral content. In a study of ALN therapy in post menopausal osteoporotic women, the mean degree of mineralisation of bone was increased up to 11.4% compared to untreated osteoporotic control subjects. These results translating to significant increases in BMD at the measured sites and a significant reduction in the occurrence of fractures (Boivin *et al.*, 2000). Further, chronic, high dose incandronate in a dog model produced further increases in vertebral ultimate torque, over lower doses even though trabecular architecture was comparable, suggesting improved mineralisation of trabecular structures in the high dose group (Komatsubara *et al.*, 2003). However, callus BMD in the current study was equivalent from 6 weeks post fracture regardless of treatment (data not shown). This suggests that the degree of mineralisation of bone was not altered with ZA treatment in this study and therefore

was not a contributing factor to the increased mechanical strength of the fracture calluses.

With further investigations, the key information produced by these studies could also be of relevance to the mode of administration of BPs in treatment of osteoporotic patients who sustain fractures. Fracture healing is delayed in models of osteoporosis without treatment (Namkung-Matthai *et al.*, 2001). A recent study of open fracture healing in OVX rats showed that BP treatment actually increased the rate of union of fractures (Toro J, 2005). These results combined with the outcomes from this study suggest that if optimised, BP dosing during osteoporotic fracture healing may not only enhance the healing process but also improve the callus resistance to re-fracture. In concert with other studies, which suggest less frequent BP dosing is optimal in the treatment of osteoporosis (Monier-Faugere *et al.*, 1999, Schimmer and Bauss, 2003, Lindsay R *et al.*, 2006), this work implies that such optimisation will include reduced dosing frequency of the more potent BPs. Further investigation is required to ascertain if this reduction in dosing frequency, combined with a decrease in duration of administration, can resolve the potential delay in fracture repair in patients already on BPs when they sustain a fracture.

Of additional interest are the clinical situations where patients are already on long term BP treatment and sustain a fracture. Many concerns have been raised that complications including delayed healing or non-union may occur in these patients. This has been demonstrated in osteogenesis imperfecta (OI) sufferers who undergo chronic treatment with high dose BPs (Munns *et al.*, 2004). Open osteotomy fractures in these patients resulted in delayed healing or non-union in many cases, whereas non-surgical closed fractures healed without such complications. This outcome suggests that in situations where the anabolic stimulus to injury may be impaired, such as after an open surgical osteotomy, chronic pre-dosing with BPs may have a detrimental effect. Hence a new line of investigation examining high dose, long-term pre-dosing with BPs in the rat fracture model used in this investigation will be performed.

Osteoporotic patients commonly demonstrate high bone turnover with an imbalance between formation and resorption, the net result of which being reduced bone volume. In animal models of this disease, delayed fracture repair has been demonstrated with reduced maturity of callus bone (Namkung-Matthai *et al.*, 2001). This may be due to a decreased anabolic response to injury in these animals. Thus, in light of the evidence presented in BP treated OI patients, pre-dosing of BPs in osteoporotic patients may also be detrimental to bone repair. Although in an open fracture study in ovariectomised (OVX) rats, ALN increased the rate of union over controls even with pre-dosing (Toro J, 2005). One further line of investigation from this

work is the comparison of much longer term pre-dosing with post surgical only doses in an OVX rat fracture model.

7.4 High dose levels of the MMP inhibitor MMI270 interferes with normal growth plate endochondral ossification

7.4.1 Anti-inflammatory dose levels of MMI270 do not interfere with endochondral fracture union.

Based on previous studies using MMI270 to block MMP driven tissue damage and inflammation in a rat model of induced colitis (Medina *et al.*, 2003), a dose level of 20mg/kg twice daily of MMI270 was administered during the 6 week period of endochondral fracture healing. As this agent had not previously been used to examine endochondral ossification the effects of this dosing regime were unknown at the beginning of the experiment. When no evidence of the hypothesised delay in endochondral repair was realised, a dose finding study was implemented, increasing the dose level and altering the mode of administration of MMI270, with the aim to alter the growth plates in young rats.

7.4.2 High dose MMI270 interferes with normal endochondral growth, lengthening the growth plate of long bones.

Dose levels of MMI270 up to 6 times of that used in the initial fracture experiment were explored in growing rats and side effects monitored closely throughout the 4 week experimental period. As this agent had previously been administered orally (Kawai *et al.*, 2003), both SC and oral administration were explored. Radiographs and histology demonstrated extensive effects of MMI270 at dose levels of 80 mg/kg and 120mg/kg twice daily by SC mode on growth plate morphology. The height of the growth plate was considerably increased in these high dose SC groups as seen in figure 6.3a. This increased height was mainly due to an increase in the hypertrophic chondrocyte zone, as previously demonstrated in MMP-9 and MMP-13 knockout mice (Stickens *et al.*, 2004) (Figure 6.3b). These changes in the hypertrophic chondrocyte zone did not result in alterations in mineralisation of chondrocyte matrix, suggesting MMP activity is not vital to this stage of endochondral

ossification. The process of mineralisation of chondrocyte matrix has not been mentioned in examinations of the relevant MMP knockout models to date, suggesting these authors also noted no differences here.

However, what has been documented in the MMP-13 knockout mouse is an increase in metaphyseal primary trabecular bone that persists until adulthood, unlike the growth plate phenotype which resolves itself during post natal growth (Stickens *et al.*, 2004). The authors of this work suggest that other MMPs are able to compensate for MMP-13 at the growth plate leading to resolution here, but evidently MMP-13 is pertinent to the removal of the excessive trabecular bone formed in the metaphysis. If similar changes in metaphyseal trabecular bone are realised with the optimised dose of MMI270, then one would expect that any bone formed in the healing fracture would not be removed. In addition to MMP-9 and MMP-13 mice knockouts this study also examined a double knockout of both MMP-13 and MMP-9 in mice. The growth plate phenotype was further enhanced in the double knockout animal model, with extensive increases in the hypertrophic chondrocyte zone at the growth plate.

Taking into consideration the extensive damage to the skin at the administration sites in the SC groups with the highest MMI270 dose of 120mg/kg, the suggested dose to be used in future experiments using this agent would be 80mg/kg twice daily by SC injections.

7.4.3 MMI270 can be utilised to inhibit MMP activity and thus elucidate its activities during endochondral ossification

The results seen in this pilot study at the growth plate would be expected to translate closely to fracture healing under the influence of this agent. Thus an extensive cartilage callus, rich in hypertrophic chondrocytes, would be expected to persist in the calluses of MMI270 treated rats, delaying union. If this hypothesis is confirmed, the impending fracture studies using MMI270 will provide new and exciting knowledge regarding the dissociated roles of osteoclasts and MMP secreting cells during both endochondral growth and repair.

7.5 Conclusion

Osteoclasts can participate in endochondral ossification through secretion of MMPs, although this is a non-specific role of these cells. In contrast, it is only when osteoclasts are remodelling mineralised tissue that they attach to the surface and form a ruffled border. It is this process that is specific to osteoclast function.

As chondrocytes and vascular endothelial cells secrete MMP-13 and MMP-9 respectively, they are capable of resorption of the un-mineralised transverse septa at the chondro-osseous junction without osteoclast function. Hence, osteoclast function is not rate limiting during the degradation and penetration of chondral matrix during endochondral ossification. Remodelling of mineralised tissue on the other hand is limited by osteoclast function. Thereby, osteoclast function is redundant to the attainment of initial union during endochondral fracture repair, whereas it is essential to the subsequent phase of hard callus remodelling.

Whilst in osteopetrotic animals hard callus remodelling is grossly deficient, BP treatment can allow slow remodelling to occur, depending on the dose regime. A single bolus dose of ZA delays remodelling in the early weeks, but primary callus retention increases strength with only a small and reversible negative impact on the material properties of the callus. Weekly ZA dosing on the other hand had a more severe and prolonged effect on remodelling, this adversely effected the material properties of the callus in both the short term and long term. Bolus or yearly intermittent dosing is thus likely to be preferable over weekly dosing in terms of long term fracture callus remodelling.

Therefore, this detailed investigation has revealed important findings leading to the re-evaluation of the fundamental role osteoclasts play during fracture repair. In doing so, this study has led to the considerations that the application of BPs to clinical situations of bone repair is safe. Finally, this examination has revealed novel findings regarding the effects of BP dosing frequency on fracture repair, which may strongly influence the clinical treatment of osteoporotic patients.

8 Appendix

8.1 Animal Handling and Surgery

8.1.1 Basic Animal Care

Four hundred and seven male Wistar rats were obtained from the Animal Resource Centre (ARC) in Western Australia at 8 weeks of age. A colony of incisor absent (*ia/ia*) rats with a Wistar rat lineage was developed from a small breeding population kindly donated to our group by Neucom Northeastern Ohio Universities College of Medicine. Twenty five male mutant homozygous *ia/ia* rats and 25 male wild type/heterozygous (wt/het) rats were used for the phenotype analysis study. In addition, 33 male *ia/ia* and 33 male wt/het rats were used for fracture repair studies in this rat population. All rats were housed in high lid cages and with free access to standard rat food pellets and water over the total period of breeding and experiments.

At the time of surgical intervention rats were anaesthetised with 75mg/kg Ketamine and 10mg/kg Xylazine both as intraperitoneal injections. Post surgery pain relief was given in the form of buprenorphine (Temgesic) SC at a dose of 0.01mg/kg. All rats were mobile and regained normal movement within 2 days of surgery. All experimental procedures were approved by the Westmead Hospital Animal Ethics Committee (WHAEC) under approval numbers 4024.06-06 and 1002.06-06.

8.1.2 The Einhorn closed rat fracture model

The technique involves insertion of a 1.1mm Kirschner wire (k-wire) into the medullary canal of the right femur through a small incision over the patellar of the knee (Figure 8.1). The wire was driven into the canal using a Stryker TPS irrigation console and driver (Stryker, Australia) until it penetrated the cortical bone of the greater trochanter (Figure 8.1). The k-wire was left protruding from the knee to allow easy placement of the femur for the process of fracture production.

Figure 8.1. *Surgical insertion of the Kirschner wire.*
A small incision is made anterior to the distal femur. The patellar is moved slightly to the lateral side and the k-wire is driven into the canal through the distal femur until the proximal trochanter is reached.

Once the k-wire was correctly positioned the right femur was placed lateral side up in the 3-point device (Figure 2.2). Under sterile conditions using the excess wire the femur was aligned in a medial lateral position perpendicular to the 2 base wedges on the 3-point weight drop fracture apparatus. The lateral proximal femoral protuberance was used as an anatomical point to align the femur correctly for a mid-diaphyseal fracture. Once positioned correctly the top of the 3-point apparatus was released onto the femur and pressure applied so the femur was tightly positioned in the 3-point device. The 500g weight was then dropped from a height of 55cm to create a clean transverse mid diaphyseal fracture.

Radiographs were obtained using a Faxitron radiology system MX20 (Faxitron X-ray Corporation, Illinois, USA) to visualise the quality of fracture produced, (Figure 8.2). Fractures in animals that lay outside the criteria for exclusion were immediately sacrificed in a CO_2 chamber their before recovery from anaesthesia. The exclusion criteria included fractures that showed obvious radiographic signs of fragmentation or fractures that were metaphyseal, either distally or proximally. Approximately 5% of all fractures were excluded from the study at surgery following these guidelines.

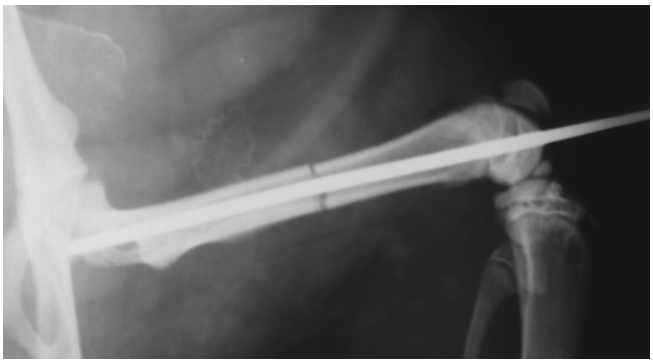

Figure 8.2. *Post surgery x-ray demonstrating correct placement of intramedullary Kirschner wire and creation of a clean transverse mid diaphyseal fracture using the apparatus.* The k-wire is trimmed flush to the knee and the wound sutured once x-ray confirmation of fracture is complete.

When the fracture was accepted the k-wire was trimmed flush with the knee and the incision sutured as required. All fractures that were not excluded at the time of surgery were further graded according to the grading system in Table 8.1. Approximately 20% of all the fractures produced using this technique were not perfectly clean transverse fractures. The fractures that were not perfect were assigned to treatment groups such that each group contained a similar number of imperfect fractures.

Description	***Grading ID***
Centre, transverse and clean	1
Distal, transverse and clean	2
Centre but slightly oblique	3
Distal and slightly oblique	4
Centred but not obviously clean	5
Proximal, transverse and clean	6

Table 8.1 *Post operative grading by radiographs*

8.1.3 Optimisation of the closed rat fracture technique in the incisor absent rat.

8.1.3.1 Surgical techniques and modifications

The same procedure used for the 9 week old Wistar rats was used for the *ia/ia* rat fracture examination however with slight modifications.

Incisor absent rats demonstrate extensive retention of metaphyseal spongiosa due to reduced resorption, described in detail in section 4.3.1. This dense metaphyseal bone made insertion of the intramedullary k-wire difficult. The surgeons found they were less confident of correct placement of the wire, thus x-rays were performed after wire positioning to ensure correct insertion prior to fracture. This allowed for re-positioning of the wire if required and at times lead to exclusion of rats due to penetration of the bone cortex by the pin.

In addition to pin placement, the 3-point weight drop fracture apparatus also required optimisation. Due to the early age of phenotype reversal in the *ia/ia* rats, they were just 5 weeks old at the time of surgery, thus the apparatus underwent considerable modifications. Firstly the weight required to produce a fracture on impact was reduced to from 500g to 300g. Further, the height from which the weight was dropped was also reduced by 7cm. The apparatus itself underwent the following changes: the height between the top plastic platform and the platform below the spring

was reduced from 13cm to 11cm, and the height from the platform below the spring to the base of the apparatus was reduced from 7cm to 6cm. These changes were required to reduce the travel distance of the 3-point supports and blade, reducing the impact created by the weight on the smaller bones. Finally the thickness of the 3-point support and blade were reduced by the attachment of additional thinner pieces of metal to the existing set up. This meant that the wedges were not only thinner but also closer together, reducing the impact area and creating a cleaner fracture line. As a result of these changes to the 3-point weight drop fracture apparatus, the quality of closed fractures produced in the younger *ia/ia* rats was improved, reducing the number of exclusions.

8.1.3.2 Exclusion criteria

The same exclusion criteria used for the Wistar rats was employed for the *ia/ia* fracture studies. However the exclusion rate in this rat study was slightly higher than the Wistar rats, particularly so in the mutant *ia/ia* rats. Although the technique was optimised for the younger bones, the dense metaphyseal bone and the brittleness of the cortical bone of *ia/ia* rats, commonly associated with osteopetrosis, meant an increased chance of poor pin placement and fragmentation during fracture. An exclusion rate of approximately 10% of fractures was noted in the *ia/ia* rat studies.

8.1.4 Dosing Regimes

8.1.4.1 Bisphosphonate

The BP zoledronic acid (ZA) (Novartis Pharma) was administered SC at the doses outlined in Table 8.2. Four milligram vials of Zometa® (zoledronic acid), were reconstituted in 4 ml of sterile saline and diluted accordingly to produce concentrations of: 0.1mg/ml, 0.02mg/ml, 0.025mg/ml and 0.005mg/ml for each dose level, see Figure 8.3 for inactive ingredients. Dosing commenced 1 week post surgery as either a single bolus dose or weekly doses up until the time of harvest. The Weekly ZA groups were administered the same total dose as the Bolus ZA groups divided over the 5 week dosing period. The doses of ZA utilised were within clinically relevant doses used for the treatment of human osteoporosis.

Treatment Group	*ZA Dose concentration mg/kg*	*Number of doses*
Saline	0.000	5
Bolus Low Dose ZA	0.025	1
Weekly Low Dose ZA	0.005	5
Bolus High Dose ZA	0.100	1
Weekly High Dose ZA	0.020	5

Table 8.2. Zoledronic acid (*ZA) treatment groups*

Zometa®

(zoledronic acid) Injection

Concentrate for Intravenous Infusion

Rx only

Prescribing Information

DESCRIPTION

Zometa® contains zoledronic acid, a bisphosphonic acid which is an inhibitor of osteoclastic bone resorption. Zoledronic acid is designated chemically as (1-Hydroxy-2-imidazol-1-yl-phosphonoethyl) phosphonic acid monohydrate and its structural formula is

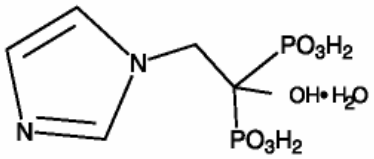

Zoledronic acid is a white crystalline powder. Its molecular formula is $C_5H_{10}N_2O_7P_2 \cdot H_2O$ and its molar mass is 290.1g/Mol. Zoledronic acid is highly soluble in 0.1N sodium hydroxide solution, sparingly soluble in water and 0.1N hydrochloric acid, and practically insoluble in organic solvents. The pH of a 0.7% solution of zoledronic acid in water is approximately 2.0.

Zometa® (zoledronic acid) Injection is available in vials as a sterile liquid concentrate solution for intravenous infusion. Each 5-mL vial contains 4.264 mg of zoledronic acid monohydrate, corresponding to 4 mg zoledronic acid on an anhydrous basis.

Inactive Ingredients: mannitol, USP, as bulking agent, water for injection and sodium citrate, USP, as buffering agent.

Figure 8.3 *Chemical formula and supplier details for zoledronic acid as used in this investigation*. Obtained from the Novartis website.
http://www.pharma.us.novartis.com/product/pi/pdf/Zometa.pdf

8.1.4.2 Matrix metalloproteinase inhibitor

The matrix metalloproteinase (MMP) inhibitor MMI270 (CGS27023A) is a broad spectrum MMP inhibitor. It was supplied by Novartis Pharma for use in this project and has been widely utilised in animal experiments investigating its effects on angiogenesis (Tamura *et al.*, 2004). Figure 8.4 shows the chemical structure of the molecule. The

MMP inhibitor MMI270 dose used in the fracture study was obtained from a study in rats investigating the effects of inhibition of angiogenesis on brain oedema in cold injury in rats (Kawai *et al.*, 2003). A dose of 40mg/kg as a continuous SC injection utilising osmotic pumps was delivered daily. In this study, MMI270 was administered at a dose of 20mg/kg SC twice daily commencing one week post surgery. The molecule was stored at 4°C in powder form and then dissolved at a concentration of 20mg/ml in a solution of 50% dimethlysulfoxide (DMSO) and sterile water for injection. Thus, each rat was dosed with a volume of MMI270 solution equivalent to their weight in kilograms i.e. a 0.5Kg rat received 0.5mls of MMI270 solution. Control rats received the same volume/weight ratio of 50% DMSO in sterile water. The drug was prepared fresh before each injection time and injections were performed between 9 and 10am in the morning and then again between 4 and 5pm in the afternoon. Fifty percent DMSO was used as a vehicle to deliver this agent as it is not water soluble.

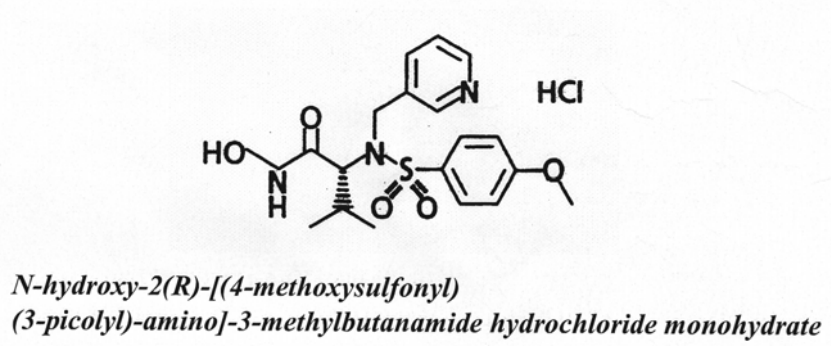

Figure 8.4 *Chemical formula for the MMP inhibitor MMI270 used in this investigation.*

8.1.5 Sample harvest

Fracture experiment rats were euthanased at each outcome time point in a CO_2 gas chamber and both right and left femora were excised from all rats. Rats used for the *ia/ia* rat phenotype analysis were also euthanased in a CO_2 gas chamber before removal of both right and left tibia and femora. All removed bones were stripped of soft tissue and fixed in diethylpolycarbonate (DEPC, Sigma-Aldrich, Steinhein, Germany) treated 4% paraformaldehyde (Merck, USA) at 4°C for 24 hours at a tissue to solution ratio of at least 1:20. After fixation all femora were place in 70% alcohol and stored at 4°C for further analysis.

Fixative Solution: 4% Paraformaldehyde

The aim of fixation is the coagulation or precipitation of the substances making up the protoplasm eg. proteins, lipids, carbohydrates, & inorganic salts. This process renders the cells, tissues and their elements resistant to further changes prior to microscopic examination. An appropriate fixative will therefore; penetrate tissues and

cross-link cells quickly, preserve all tissue elements and harden the tissues so that the subsequent processing will not affect them.

Procedure

Forty grams of paraformaldehyde (PFA) was added to a mixture of 100mls of a 1x solution of phosphate buffered saline (PBS) and 800mls of DEPC treated water. The DEPC was used to ensure the solution was Ribonucleotidase (RNase) free. This solution was stirred on magnetic stirrer at 55°C for approximately 1-2hrs until dissolved. It was ensured that the solution did not reach a higher temperature than 55°C as above these temperatures the fixative is inactivated. A small amount of sodium hydroxide pellets was added to increase the pH and enhance the dissolving rate of the PFA. After cooling the solutions, the pH was adjusted to 7.4 by adding drops of a 20% hydrochloric acid solution, before being topped up to 1 litre with DEPC treated water. The solution was then filtered using a 500ml Nalgene Bottle-top filter with 0.2um pore size into a RNase free bottle. This solution was then stored at 4°C until required.

8.2 Radiological Analysis:

8.2.1 Radiographs

Radiographs were performed on a digital Faxitron MX-20 with 14-Bit digital camera (Faxitron X-ray Corporation, Illinois, USA) for 60 seconds at 27Kv at 1.5 x magnification. Digital images were saved as 24 bit TIFF images for later analysis. See Figure 8.5 for an example of a radiograph of a harvested femora.

X-rays were used to determine the accuracy of the fractures produced with the employed closed fracture method, as described in section 8.1.2. Further, the x-rays were also used to assess the union rates of fractures at the time of harvest. A fracture was considered united if radio-dense tissue bridged both sides of the fracture site.

Figure 8.5. *Radiograph examples of fracture calluses*
(a) Representative x-ray of post harvest sample at 1 week post fracture with pin still in medullary canal. (b) Representative x-ray of post harvest fracture samples at 6 weeks with pin removed.

8.2.2 DEXA

ia/ia rat phenotype analysis (chapter 5)

Proximal tibia were scanned on a GE Lunar Piximus2 (Lunar, Madison, WI) research Dual Energy X-ray Absorbtiometry (DEXA) scanner for analysis of metaphyseal bone. Four tibia were scanned simultaneously and a consistent region of interest (ROI), 23 pixels in length and 14 pixels wide, was positioned immediately under the growth plate of each sample. Measurements were made for each ROI producing data for BMC and BMD.

8.2.3 Quantitative Computerised Tomography (QCT) analysis

Quantitative computerised tomography (QCT) scans were performed using a Stratec xQCT research SA+ scanner (Norland Stratec, Durlacher, Germany)

Wistar rat fracture studies, used in chapters 3, 4 and 6.

Both right and left femora were scanned from all experimental animals. In all the right femora, 9 consecutive cross sectional slices of 1mm thickness with a slice distance of 1mm were taken in the fracture callus, with the centre slice being in the line of fracture. The data from these slices were added together to produce data for the entire fracture callus. Two, 1mm, cross sectional slices were taken in all left femora. One slice was taken in the metaphyseal region (trabecular bone) 8mm from the tip of the distal femur, and the other slice was in the mid shaft (cortical bone) 16mm from the metaphyseal slice. Data from the single central slice was extrapolated to a 9mm distance to provide contralateral limb data for comparison to fractured limb data and to allow for monitoring of systemic effects of the ZA. All scans were performed at the highest resolution of 70μm and a scan speed of 5μm/s. Analysis was performed on slices using a threshold of 250 to obtain data on the effects of ZA treatment on both trabecular and cortical BMC, Area, BMD and polar moment of inertia. Data obtained from CT scans for periosteal circumference were used to calculate values for Stress data by combination with the fracture callus peak torque obtained from mechanical testing determined by a formula, see section 8.5.4.

ia/ia rat fracture study

As the fracture experiments in *ia/ia* rats were performed at a younger age of 5 weeks and harvested at an end time point of 8 weeks of age, the formed fracture callus covered a shorter length of the femora so CT scans were performed over a 5 mm region instead of 10 mm. Five slices 1 mm apart and of 1 mm thickness were scanned in the fracture callus with the middle slice in the centre of the fracture site. Again, total callus BMC, mineralised tissue volume, BMD, and polar moment of inertia data were generated for each fracture callus.

Left whole femora were scanned with 3 slices of 1 mm thickness placed 2 mm apart to cover an equivalent 5 mm region. The same total values were produced as for the callus region in the fractured limbs however the measurements for BMC and volume were multiplied by 2.5 to produce data comparable for the 5 mm region scanned. Data for BMD and Polar moment of inertia were averaged for the 3 slices.

Images from all femoral QCT scans were obtained using Scion image for Windows (Scion Incorporated, USA) imaging software from the centre of the scanned region for observational analysis of callus remodelling and bone architecture. See figure 8.6 for an example of a cross sectional image produced using this technique.

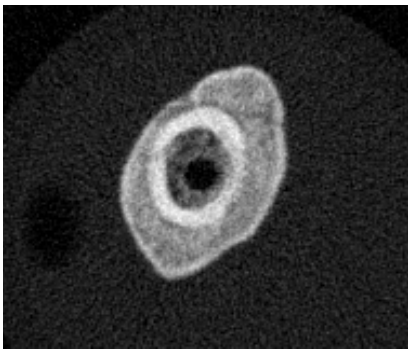

Figure 8.6. *Example of a cross sectional CT scan slice image generated from Stratec QCT scan data using Scion image.*

8.2.4 Micro Computerised Tomography (µCT)

Micro CT scans were performed using a desk top micro-tomographic imaging system (Skyscan 1172, Skyscan NV, Belgium) on the operated femur of one sample from each treatment group at 26 weeks. Samples selected for scanning were those that demonstrated QCT data similar to mean values for each group. Scans were performed of the entire fracture callus and corresponding area on the contra-lateral limbs at a resolution of 15µm and a 10µm slice increment. Images were converted from TIFF format to bitmap format using NRecon Software (Version 1.4.4, Skyscan, Belgium).

Three-dimensional imaging and rendering was performed using VGStudio Max (Version 1.2, Volume Graphics, Germany).

8.3 Histology

8.3.1 Sample preparation

The distal half of the left femora were bisected in the sagittal plane, the anterior half was placed in 70% alcohol and processed for un-decalcified histological analysis (section 8.4.2) and the posterior half was decalcified in 12.5% ethylenediaminetetra acetic acid (EDTA), 0.5% PFA (see below for details) at a pH of 8.0 at room temperature for 4 - 6 weeks with weekly solution changes before being processed to paraffin, section 8.4.3.

Right femora were bisected in the sagittal plane and proximal and distal ends were removed. The distal end of fracture area was marked red with mercurochrome to allow for orientation when creating sections. Both halves were decalcified in a 12.5% EDTA, 0.5% PFA solution at a pH of 8.0 at room temperature for 4 to 6 weeks. The volume to tissue ratio was at least 20:1 and weekly solution changes were made before the samples were checked for proper decalcification and processed to paraffin, section 8.4.3.

Decalcifying solution for paraffin samples - 12.5% EDTA 0.5% PFA solution

This solution is used to remove the calcium from bone samples prior to embedding in paraffin wax. Other decalcification solutions use acids, which can destroy the bone morphology in paraffin sections and make quantitation difficult. Acid based decalcifying solutions can also degrade RNA vital for *in situ* hybridisations. This solution is kept in the fridge but once used with the specimens, is left to warm to room temperature for the decalcification process.

Procedure

0.5M EDTA

Forty six grams of sodium hydroxide and 372g of EDTA were added to 1500ml of sterile water (Baxter, Australia), and stirred without heat until dissolved. The pH of the solution was adjusted to 8.0 by adding drops of a 20% hydrochloric acid solution, before topping up to 2L with sterile water. The solution was then filtered with a Nalgene bottle-top filter with 0.2 μm pore size (Nalgene, NY, USA) into RNase free bottle. After filtering the solution is treated with DEPC (2mls in 2L) and left overnight in a fume hood before being autoclaved the next day before use. Autoclaving of DEPC treated solutions is essential to deactivate the carcinogenic potential of the solution.

One hundred millilitres of 1 x PBS and 5g of PFA were added to 800 mls of the 0.5M EDTA solution and stirred on a magnetic stirrer at 55°C (no higher) for 1-2 hours or until dissolved. The pH of the solution was again adjusted to 8.0 before being topped up to 1 litre with DEPC treated water. The solution was then stored at 4°C until use.

8.3.2 Un-decalcified histological processing into resin blocks and sectioning: *ia/ia* rat phenotype samples only

After fixation in 4% PFA for 24hrs at 4°C samples were transferred to 70% alcohol for approximately 1 week. Samples were then processed for resin embedding.

Procedure

The tissue samples were processed through three main steps prior to embedding in resin. Firstly they were dehydrated through 24 hour incubations at 4°C in graded acetones, 70%, 90%, 100% and then 2 further 100% acetones under vacuum for 1 hour at each solution change. Secondly, infiltration of the samples was performed by a 3 day incubation in a 50% methylmethacrylate (MMA) (Merck, USA), and 50% acetone solution under vacuum daily for 1 hour. This was followed by a 4 day incubation after a 4 hour vacuum at 4°C in an infiltration solution containing 94.75% MMA, 5% Dibutyl Phthylate (Sigma-Aldrich, Steinheim, Germany) and 0.25% Perkadox 16 (Swift & Co, Australia). Finally the samples were embedded in 25 ml glass vials in an embedding solution containing 94.5% MMA, 5% Dibutyl Phthylate (Sigma-Aldrich, Steinheim, Germnay) and 0.5% Perkadox 16 (Swift & Co, Australia). Embedded samples were vacuum impregnated for 3-4 hours before the lids were placed on tightly and the vials were transferred to a water bath set at 28°C for polymerisation. Once polymerization was complete the glass vials were shattered and resin blocks removed. The resin block was then trimmed to size and mounted to an aluminium chuck using super strength Araldite (Araldite, Selleys Pty Ltd, Sydney, Australia) (Aluminium Assignments, Sydney, Australia) The chuck was of specified size to fit into the mount holder in the Leica RM2155 semi- motorised microtome (Leica, Germany) used for sectioning. The processed resin blocks were then sectioned on the Leica RM2155 microtome.

Procedure

Five micron thick sections were created using a Leica D file tungsten carbide blade after trimming of the blocks to obtain a full face of the tissue. Seventy precent alcohol was used to lubricate the block and sections during the sectioning process. 10 sections were taken and assessed for quality under low power with a light microscope at very low light to protect fluorescent labels. Sections were then placed in consecutive

order on numbered slides coated with gelatin solution, see below. Sections were then slowly dipped three times in a special spreading solution (60ml ethylene glycol mono-ethyl ether, 100ml ethanol and 40ml sterile water) heated to 65°C. A piece of clear thin plastic was carefully placed over the section and pressed tightly. Then a piece of absorbent paper was placed on top of plastic and this process was repeated for all sections. Sections were then clipped together with bulldog clips and baked at 47°C overnight to adhere sections to slide.

Gel coating of slides:

The solution for coating slides involved dissolving 7.5g of gelatin in 500mls of distilled water which was heated to 60°C on a heat plate. Once dissolved the solution was removed from heat and allowed to cool. Then 0.25g of potassium chromate was added to the solution and dissolved.

Slides were washed in warm water with detergent and rinsed in distilled water before being dried overnight. Slides were then dipped in gelatin solution for 30 seconds and drained, then allowed to dry overnight in oven at 47 °C.

8.3.3 Decalcified histology sample processing into paraffin and sectioning: Right and posterior left distal femora

After decalcification was complete, as confirmed through pin testing and x-rays, samples were processed overnight in a Leica TP1020 automatic tissue processor (Leica, Germany) set with the following program.

Procedure

The samples are processed through three main stages all under vacuum, before embedding in wax blocks. Firstly, the samples are dehydrated through two changes of 70% alcohol for 1 hour each then 1 change of 95% alcohol for 1 hour followed by three changes of 100% alcohol for 1 ½ hours each. Secondly the samples are cleared in three changes of 100% xylene for 1 ½ hours each followed by infiltration in 2 changes of paraffin wax (Paraplast tissue embedding medium, SPI supplies, PA, USA) at 60°C for 2 hours each. Finally the samples were embedded using metal moulds and a Tissuetek embedding station (Tissuetek, Sydney Australia) at 60°C and set hard on a cold plate at -4°C. Once embedded the paraffin blocks are sectioned on the Leica RM2155 microtome.

Procedure

Blocks were placed on a holder (chuck) of the microtome and trimmed at 15µm increments until a complete face of the tissue was reached at the surface of the block.

Next the block was placed in water on top of a Medite cold plate at 4°C (HD Scientific, Australia) for approximately 10 minutes (it was important not to leave the trimmed sample in the water for longer than 20 minutes as the cells would absorb the water and swell out of the block). After sufficient soaking the face of the block was lightly dried and placed on the cold plate surface for approximately 10 seconds. Then the block was re-positioned in the chuck (same orientation as before) and sections were taken at 5µm thickness. Ribbons of sections were floated on a water bath at 42 °C and allowed to float for 10-20 second to partly melt the wax to remove compression of the section created by the sectioning process. Then sections were picked up one section at a time on a labelled FOL's* coated slide. After draining for a few minutes, sections were placed in an oven at 47 °C overnight. This was repeated for all paraffin blocks. It was ensured that each section was placed on the correctly labelled slide and that sections were picked up in consecutive order on numbered slides.

** FOL's coating of slides*

Nine grams of gelatin was dissolved in 432mls of water heated to 50°C. The solution was then cooled and 180mls of 95% alcohol was added. Next, 6g of potassium chromate was dissolved in 30mls of water and added to the mixture. Slides were washed in warm water with detergent and rinsed in distilled water before being dried overnight. They were then dipped in the gelatin solution for 30 seconds and drained. Then allowed to dry overnight in oven at 47 °C before use.

8.3.4 Histological Staining Methods

8.3.4.1 Paraffin sections:

Haematoxylin and Eosin stain

Haematoxylin stains basophilic and nucleic acid cellular elements including nuclei blue/purple. Eosin is used as a contrasting counterstain for the haematoxylin and stains all other tissue and cellular elements shades of pink to red. Nuclei of cells stain blue/purple, the cytoplasm stains varying shades of red-pink, muscle fibres and bone matrix stain deeply pinky red and red blood cells stain orange/red. Cartilage matrix stains blue/purple (Figure 8.7a).

Procedure

Sections were warmed in an oven at 60°C until the wax had melted and then deparaffinised in two changes of xylene for 5 mins each. Slides were then re-hydrated through two changes of 100% alcohol and then 70% alcohol for 3 minutes each before being rinsed in distilled water. Next, sections were stained with haematoxylin* for 5

minutes then rinsed in distilled water for 15 secs followed by 'bluing' (neutralising) in saturated lithium carbonate for 10 seconds. After another rinse in distilled water sections were counterstained with eosin for 1 minute and then rinsed in 3 changes of 100% ethanol for 3 minutes each. Clearing of sections was performed using 3 changes of xylene for 3 minutes each before being cover slipped using Ultramount (Fronine, NSW, Australia).

Haematoxylin stain

Five grams of haematoxylin was dissolved in a few millilitres of absolute alcohol. Then 50g of aluminium ammonium sulfate was dissolved in 50 ml water by gently heating. These two solutions were mixed before 1g of sodium iodate (for chemical ripening, 300 ml of glycerol, 700 ml of distilled water and 20 ml of glacial acetic acid were added.

Bluing solution

2.5g of lithium carbonate was dissolved in 100mL distilled water.

Eosin counterstain

Five hundred milligrams of aqueous eosin Y and 50mg of phloxine was added to 75 ml of distilled water, 370 ml of 100% ethanol and 2 ml of glacial acetic acid.

Saffranin O, Light Green Stain

This stain is an excellent basic stain for highlighting cartilaginous tissue and was employed in this study to determine the cartilage content in fracture calluses. It resulted in red staining of cartilage with the dye saffranin O binding to proteoglycans in the cartilage matrix, the nuclei staining purple/black with the haematoxylin and the bone and soft tissue stained green using light green.

See Figure 8.7b for example of this staining method. Derived from O'Driscoll et al (O'Driscoll *et al.*, 1999).

Procedure

Sections were deparaffinised as before for haematoxylin and eosin staining and stained with the dye haematoxylin as described in that section. Next the slides were stained with 0.4% aqueous light green for 6 mins followed by 2 rinses in aqueous 1% acetic acid for 3 mins each. Subsequently staining with a 0.1% aqueous Saffranin O solution for 5 mins and then sections were quickly rinsed in 95% alcohol three times and then dipped in three changes of 100% alcohol for 3 seconds each. They were then cleared with three changes (1 minute each) of 100% xylene and mounted using Ultramount (Fronine, NSW, Australia).

Alcian Blue/ Picro-sirius Red Stain

This staining technique was employed both for its specific staining of cartilage matrix blue with Alcian blue and the bone matrix with the picro-sirius red. With this stain, nuclei stained black and bone, see Figure 8.7c for example of stain, derived from Scammel et al 1996.

Procedure

Sections were deparaffinised as before for haematoxylin and eosin staining and stained with the dye haematoxylin as described in that section. The slides were then stained with Wiegerts Haematoxylin for 15 mins. After being washed under running tap water for 5 mins sections were then stained with Alcian Blue solution (1% in 3% acetic acid) for 10 mins. This was followed by a rinse with distilled water before being stained with a 1% aqueous phosphomolybdic acid for 2 mins. After again being rinsed in distilled water they were stained with a 0.1% Sirius Red in saturated picric acid for 90 mins.

Dehydration was then performed with 70% ethanol for 3 mins, followed by 95% ethanol for 3 mins and two changes of absolute ethanol for 3 mins each. Sections were then cleared in three changes (3 minutes each) of 100% xylene before being mounted using Ultramount (Fronine, NSW, Australia).

Weigerts haematoxylin

1.0g haematoxylin was dissolved in 100 ml of 95% alcohol and 1.16g of ferric chloride ($FeCL_3.6H_2O$) was dissolved in 100 ml of 1% aqueous hydrochloric acid. Equal volumes of each of these solutions were then mixed together before use. This stain was not stored for longer than 8 days when solutions had been mixed. However the separate solutions could be stored separately for longer periods of time.

8.3.4.2 Resin Section Stains:

Von Kossa stain

This staining technique allows for clear observation and analysis of mineralised tissue in sections. The silver substitution reaction depends on the presence of phosphate and carbonate salts and not on the presence of calcium. The principle involved in this stain is the conversion of either salt into its silver equivalent (e.g. silver carbonate) with the subsequent reduction of this by ultraviolet light or a reducing agent to metallic silver. The silver nitrate needs to be stored at 4°C in either a dark bottle or a

bottle wrapped in aluminium foil. Phosphate and carbonate (Ca^{2+}) groups stain black and nuclei stain red. See Figure 8.8d for example of stain.

Procedure

The resin was removed from the sections using two changes of 100% acetone for 10 minutes each. Sections were then placed in a 1% aqueous silver nitrate solution freshly prepared from a 10% stock. This was exposed to ultraviolet light in a Stratagene UV stratalinker 1800 (California, USA) which produces UV light in s closed cabinet for 9 minutes. After a rinse in running distilled water for 10 minutes sections were fixed in 5% aqueous sodium thiosulphate for 30 seconds and then rinsed in distilled water before two rinses in 100% alcohol and cleared in 3 changes of 100% xylene and mounted using Ultramount (Fronine, NSW, Australia).

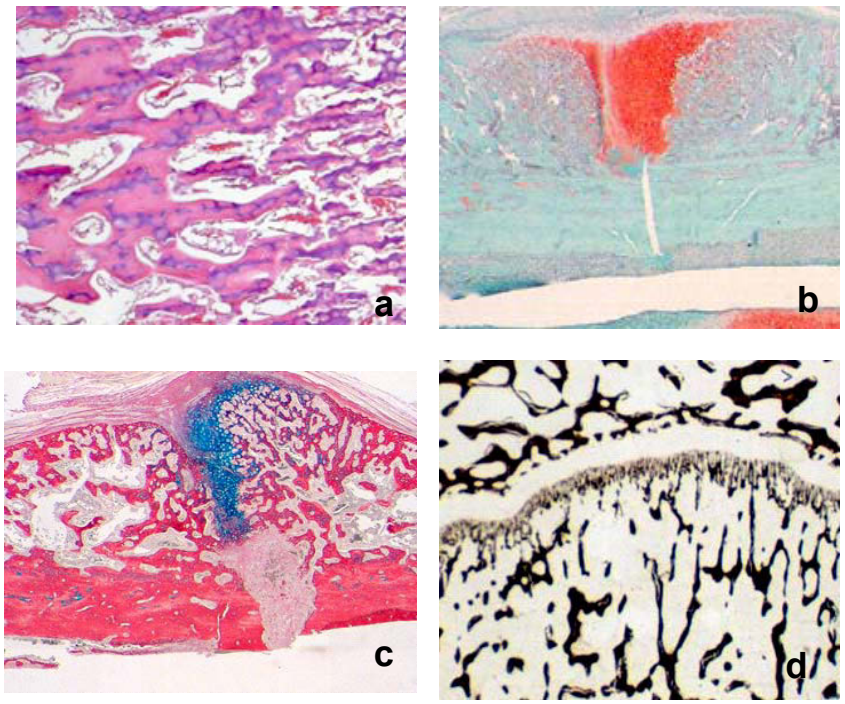

Figure 8.7 *Images of bone tissue sections stained with a) H&E, b) Saffranin O/Light Green, c) Alcian Blue/Sirius Red, and d) Von Kossa.* Original magnifications: a) x20, b)x1.0, c) x1.0, d) x 2.5, e) x20

8.3.5 Histomorphometric Analysis

Histological sections were analysed and quantified using a Leica DMLA CTRMC microscope (Leica, Germany) and a QICAM Fast 1394 colour 12 bit camera with QCapture software version 2.6.8.2 (Quantitative Imaging Corporation, Canada). Images were analysed using the BIOQUANT measure 32 Nova prime (Nashville, Texas). The following methods describe the procedures used to quantify histological observations.

8.3.5.1 Bioquant software setup for sample group analysis

Procedure

1. Turn on QICAM camera
2. Open Bioquant software package
3. Create new data volume for set of samples to be measure:
   - Select new data volume
   - Choose from existing data volumes if you are using an existing set up as a template. Or choose create new data volume to set up a new one.
   - Enter data volume name (i.e. rat fracture) and enter first sample number
4. Select edit data set and modify names of arrays to be measured. eg bone volume, cartilage volume etc.
5. Ensure the data set for the first sample contains ALL data arrays to be measured so it can be copied for all other samples.
6. Exporting data from software
   - Select "create data tree"
   - Select c drive and select bioquant and then the data folder.
   - Select create data volume
   - Highlight data sets to be copied and select enhanced export and add data files to command box.
   - Select save to file and save as a text file
   - Text file can then be opened with excel to allow data analysis and manipulation.

Examples of arrays include; Area (A1) as bone area or total area of cartilage area, and Length (L1) as osteoclast surface or bone surface

8.3.5.2 Fracture callus analysis

Portion as percent of avascular cartilage tissue content in a callus

Using centrally sliced fracture sections stained with Saffranin O for cartilage, the percentage of the entire fracture callus that was avascular cartilage tissue was calculated on Bioquant Image analysis software as set out above.

Procedure

This analysis was performed at a magnification of x2.5 on both anterior and posterior halves of the callus section, each half segregated into 3 fields of view. Firstly using the irregular ROI tool the total callus area excluding the original cortical bone was traced around, Figure 8.8a. Then by setting the green threshold tool to a maximum, this area was filled with red pixels and by selecting preview and measure, data for this area was generated, Figure 8.8b.

To then calculate the area that is not vascularised bone tissue i.e. the avascular fibrous and cartilage tissue, this area was traced around carefully using the irregular ROI tool ensuring all invaded and mineralised tissue was excluded. Again this area was measured using the threshold tool, Figure 8.8c. By repeating this process for the total of 6 fields of view, data for the total callus area and total avascular non-mineralised callus area was generated. By subtracting the avascular area from the total callus area, the area that was vascularised bone tissue was calculated and expressed as a percentage of the total callus area.

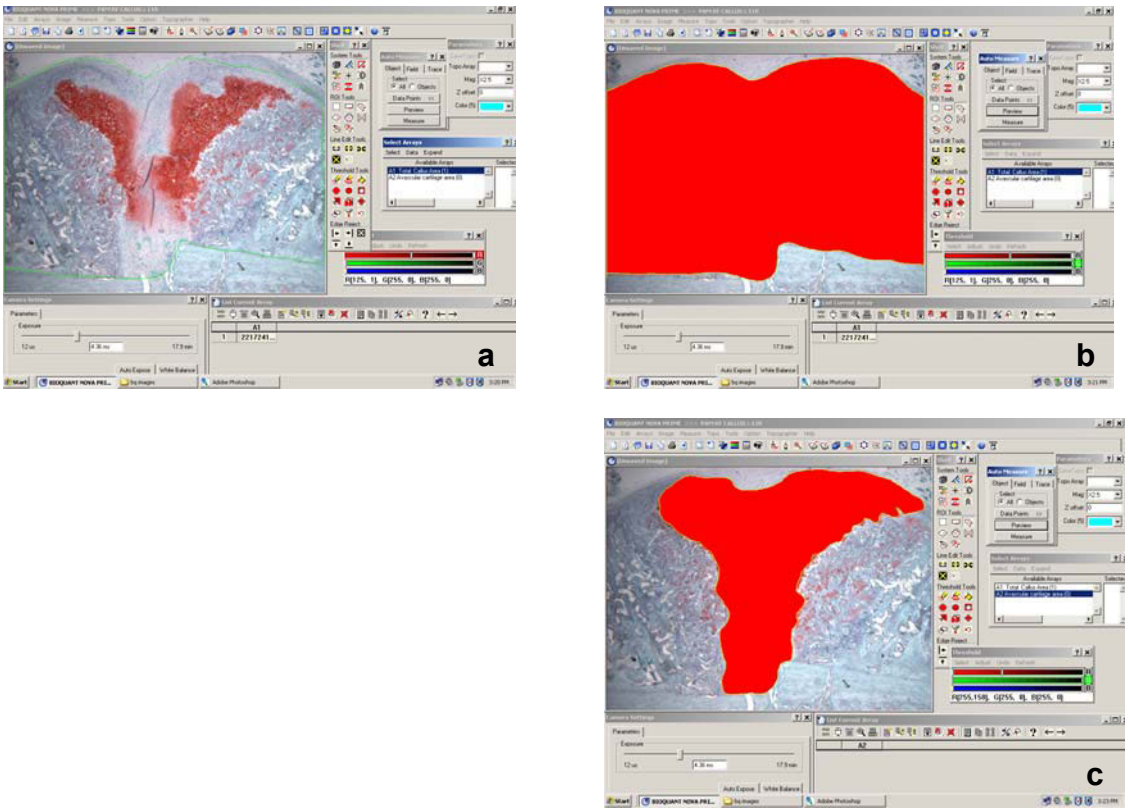

Figure 8.8. *Example of image analysis using Bioquant to determine the area of each callus containing vascular bone tissue.*

a) Selection of the region of interest (ROI) around the total callus area in field
b) Measuring total callus area
c) Selection of and measuring the area of the callus that is not vascularised bone tissue.

Percent lamellar bone content of callus

This analysis is performed on Alcian Blue/ Sirius Red stained tissue sections.

Procedure

Using a similar technique outlined for the callus cartilage percentage data, using Bioquant image analysis, sections were analysed one side of the fracture at a time with 3 fields of view per side. At x2.5 magnification the entire area of the callus was measured, Figure 8.9a-b, then the area of callus that was not remodelled neo-cortical bone as shown in Figure 8.9c, was measured. In the case of ZA treated samples, this

area contained retained primary bone callus. Saline samples on the other hand demonstrate no retained bone in this region, and was seen as empty marrow space due to resorption of the primary bone.

Data were expressed as either percentage callus neo-cortical bone or callus area of retained primary bone.

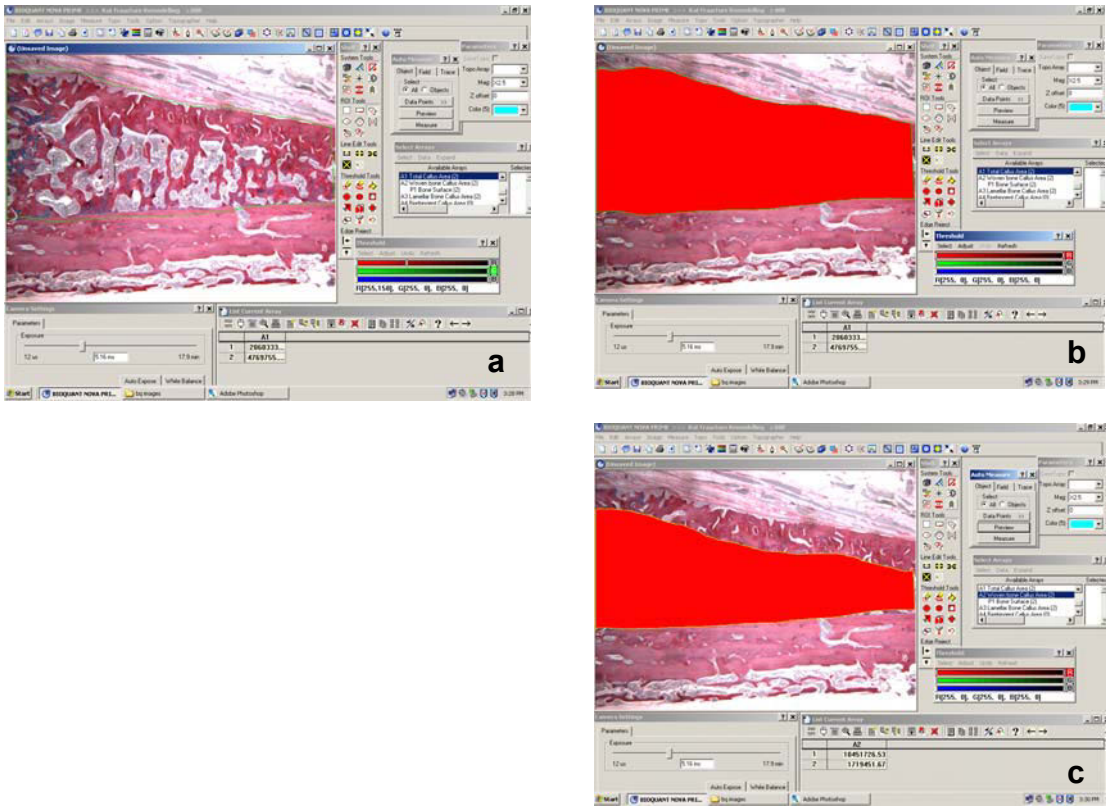

Figure 8.9 *Example of image analysis using Bioquant to determine the area of each callus containing remodelled neo-cortical bone*

a) Selection of the ROI around the total callus area in field
b) Measuring total callus area
c) Selection of and measuring the area of the callus that is not remodelled neo-cortical bone, i.e. the area that is retained primary callus

8.3.5.3 Growth plate

Analysis of growth plate height was performed on saffranin O stained sections of the left distal femora for the Wistar rat samples and the left proximal tibia for the *ia/ia* rat fracture samples.

Procedure

Using Bioquant software the growth plate height was determined for each sample from an average of 15 individual thickness measurements spread evenly across the entire section. An array called individual height was used to measure the individual values taken at a magnification of x5. Each measurement was taken from the

top of the red stained resting zone directly down along the axis of the chondrocyte columns to meet the last intact transverse septum of the terminal chondrocyte of that column. With 3 fields of view each producing 5 height values, 15 measures were taken for each sample and averaged, Figure 8.10.

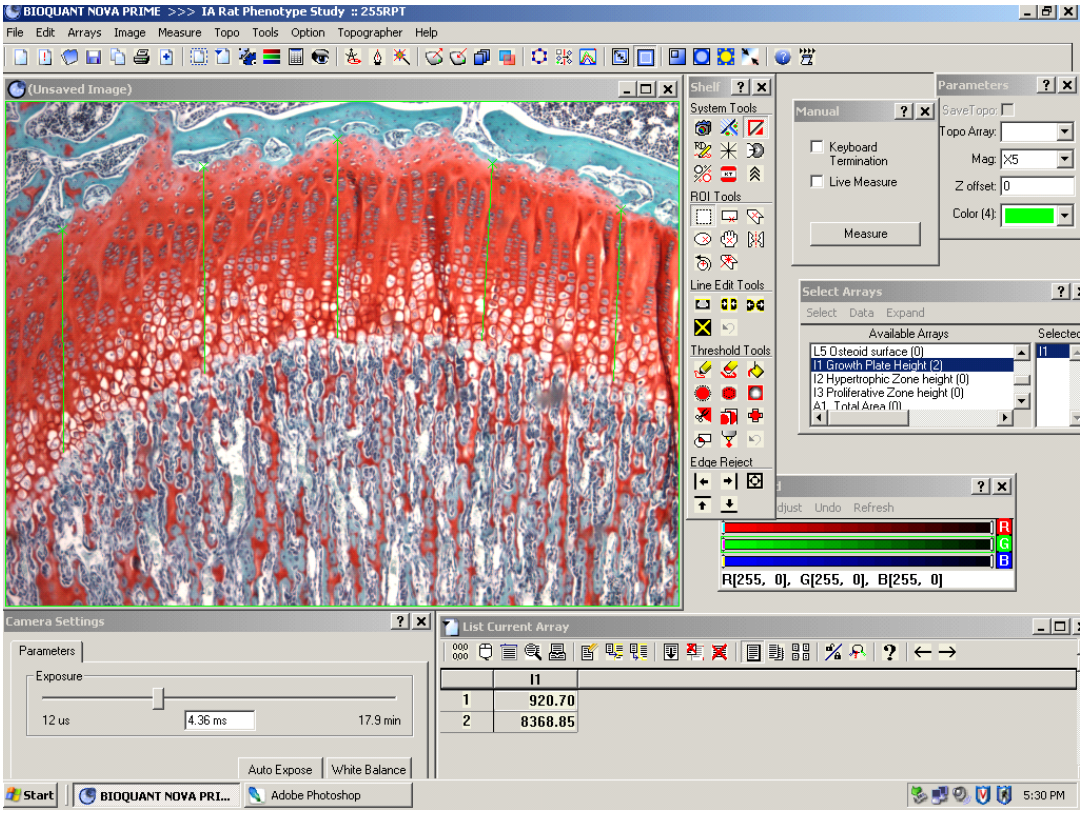

Figure 8.10. *Example of image analysis using Bioquant to determine the average growth plate height for ZA treated Wistar and ia/ia phenotype samples.*
The green lines along the axis of the red stained growth plate measured the height at each of those points. Three fields of view each with 5 measurements were performed for each sample and averaged. This was performed at x5 magnification.

8.3.5.4 Metaphyseal BV/TV analysis

Using Bioquant image analysis software and the Leica microscope and QICAM camera set up, bone volume to tissue volume ratio (BV/TV) data was generated for the proximal tibial metaphysis of all samples from the *ia/ia* rat fracture and phenotype studies.

Procedure

For the phenotype analysis, two regions of interest were analysed at x2.5 magnification. The proximal metaphysis is localised to directly under the growth plate, and the distal metaphysis directly under the proximal region.

Using the red threshold tool the entire region of interest was selected, being careful to not include the growth plate or cortical bone, and measured for total area

(Figure 8.11a-b). Then the red threshold was reduced to approximately (0, 125) such that only the black stained mineralised tissue was selected and the spaces were empty. This selection was measured to produce data for bone area in the region as well as bone surface (a perimeter array grouped to the area array), Figure 8.11c. This technique was performed on both proximal and distal regions and the data were presented as bone area/total area (%). The same procedure was used for the *ia/ia* fracture samples, however only the proximal metaphyseal area was measured.

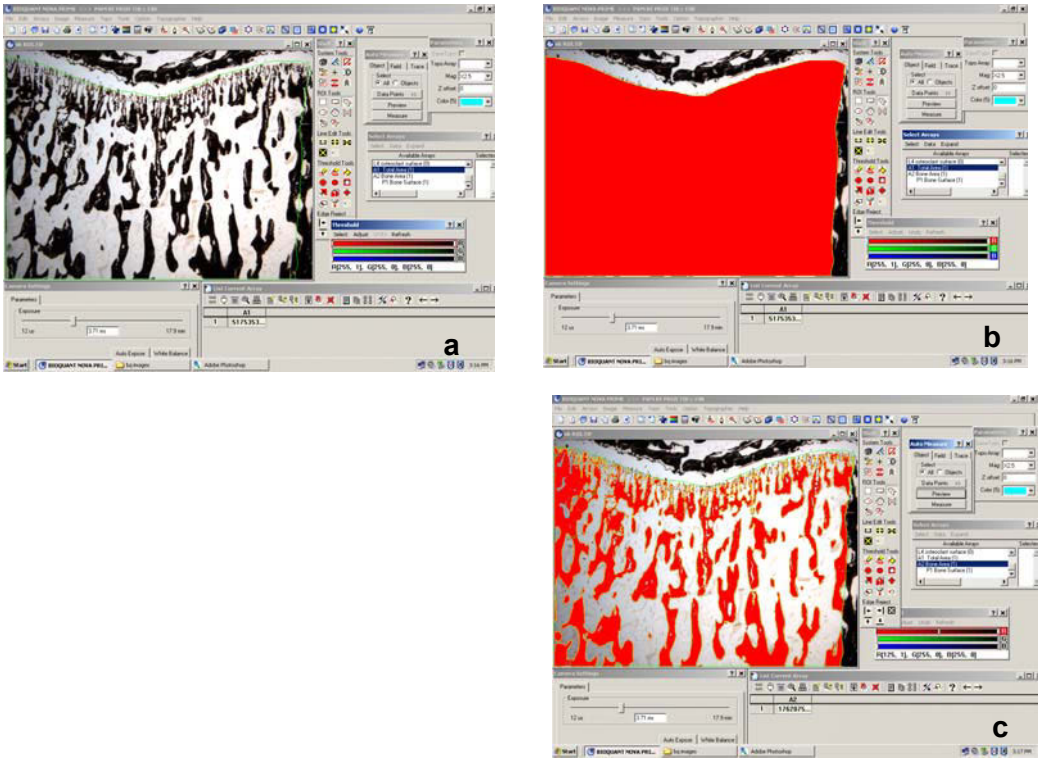

Figure 8.11 *Example of image analysis using Bioquant to determine the metaphyseal BV/TV in ia/ia samples.*

a) Selection of the ROI around the region of interest excluding the growth plate and cortical bone
b) Measuring total area
c) Selection of and measuring the bone area and surface within the region of interest using the threshold technique

8.4 Biomechanical testing

8.4.1 Sample harvest and preparation

Left and right femora were harvested from animals assigned to mechanical testing experiment and wrapped in saline soaked gauze before being stored at -80°C.

Procedure

Frozen samples were then thawed and kept moist with 0.9% saline until testing. Femora from 6 and 26 weeks time points were trimmed of all soft tissue remnants and bone ends were embedded in the centre of 5/8 zinc plated hexagonal nuts (James Glenn, Tempe, Australia) using two-part 5 minute epoxy resin (Araldite, Selleys Pty Ltd, Sydney, Australia), for the 6 week samples. By the stage of harvesting the 26 week time point samples this embedding technique had optimised and changed to a two part epoxy resin mix (Ebalta SG 130/PUR 11, Ebalta Kunststoff GmbH, Germany). This new technique improved the rate at which the bones could be potted without altering the quality of embedding.

The distance between the embedded ends of the femora was not exactly the same for all samples but it was ensured the entire callus remained exposed. This distance, known as gage, was measured prior to testing for use in the analysis of the data produced. Once the resin had set the remaining exposed specimen was wrapped once again in saline soaked gauze and re-frozen until testing.

8.4.2 Testing apparatus

The materials tester ELF 3400 (EnduraTEC, USA) was used to test right and left femora in torsion. (Figure 8.12)

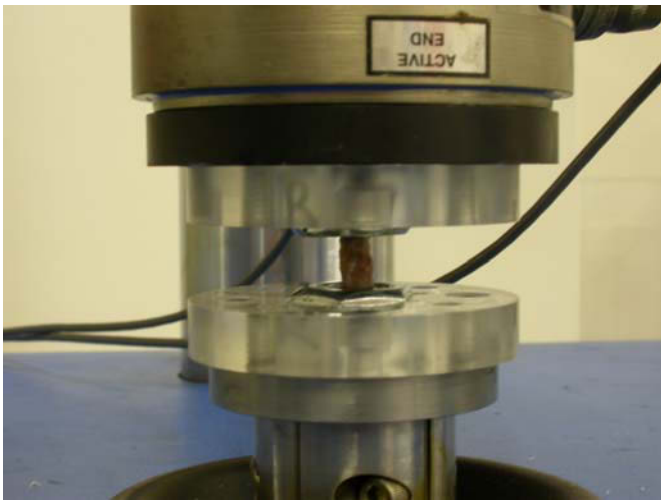

Figure 8.12 *A close up photograph of the ELF testing apparatus testing a fracture sample in torsion.* The image shows the top and bottom jigs attached to the Elf and holding a test bone between them.

8.4.3 Testing procedure

Procedure

Bones were thawed and kept moist 0.9% saline until testing. Left and right femora at both 6 and 26 week time points were tested in torsion using a previously published protocol (Amanat *et al.*, 2005). Bones were tested to failure by external rotation at an angular displacement of 6 degrees/second. Torque and angular displacement were recorded and the software generated data text files for each sample.

8.4.4 Analysis of data

Peak torque (Nm), the energy absorbed (Nm.deg) and stiffness were generated by the analysis method and compared between groups.

Peak torque or fracture torque is a measure of the maximum torque at which the bone breaks, therefore it is referred to as the strength of the bone. The energy absorbed is the amount of energy required to split the bone and is a measurement of the toughness of the fracture callus or bone. It is a quantification of the materials ability to resist a brittle fracture. Energy absorbed was calculated by the area under the torque vs. rotation curve using the trapezoidal rule.

Lastly the stiffness of the bone was calculated by the slope of the linear region of the torque against the angular displacement curve. This is a measure of the bones resistance to torsion and is commonly referred to as the rigidity of the structure.

In order to expand on the properties of the bones tested, further calculations were performed to determine the intrinsic material properties of the samples. The peak torque and rotation were converted into peak stress and strain using calculations based on formulae for a circular shaft subjected to torsion (Turner and Burr, 1993).

Procedure

Peak stress was calculated as a measure of the peak torque per unit of bone in each sample using the following formula and expressed as Mega Pascals (MPa).

$$\text{Stress} = \frac{\text{Peak Torque to failure (Nm)} \times \text{radius (m)}}{\text{Polar Moment of Inertia (m}^4\text{)}}$$

Where the radius was calculated from periosteal circumference as determined from the central slice of the QCT scans of each fracture sample. The polar moment of inertia was

determined by the QCT scan analysis software and averaged over the 9 slices in each fracture callus.

Shear strain was calculated as a measure of the angular displacement per unit of bone for each samples based on the following formula:

$$\text{Strain} = \frac{\text{Angular displacement } (\theta) \text{ x radius (m)}}{\text{Gage length (m)}}$$

Where the radius was calculated from the periosteal circumference as determined from the central slice of the QCT scans for each fracture sample. The gage length was measured as the distance between the two hexagonal nuts in which each end of the bone was embedded.

Finally, the shear modulus was determined for each sample as a measure of the stiffness per unit area of the material using the following formula and expressed as Mega Pascals (MPa)

$$\text{Strain} = \frac{\text{Peak Torque to failure (Nm) x gage length (m)}}{\text{Angular displacement } (\theta) \text{ x Polar Moment of Inertia } (m^4)}$$

8.5 In vitro primary osteoclast culture experiments

8.5.1 RANKL-induce culture in plastic wells

8.5.1.1 Bone marrow collection

Primary osteoclast cultures were prepared from harvested diaphyseal bone marrow. Right femora were removed from each experimental animal and stripped of all soft tissue. Bone specimens were then dipped in 70% alcohol to sterilise them and transferred to sterile Petri dishes. Under sterile conditions in a class II biosafety cabinet, both the proximal and distal ends of the femora were removed. The marrow cavity was flushed with approximately 3 ml of sterile PBS using a sterile 19 gauge needle and 3 ml syringe. Once flushed clean the femora were disposed of and the PBS solution containing the marrow contents was transferred to a sterile 15 ml Falcon tube (Falcon, USA). Marrow cells were dispersed by trituration using a 1ml pipette tip. Next PBS was added to each marrow sample to make a total volume of 10mls. Samples were mixed

and centrifuged in an Eppendorf centrifuge 5804R (Hamburg, Germany) at 300 RCF/1299 rpm for 5 minutes at 20°C. After removing the PBS from the cell pellet formed, the pellet was resuspended in 5 mls of alpha minimum essential media (α-MEM), (Gibco Laboratories, CA, USA) supplemented with 10% foetal bovine serum (FBS, Invitrogen) and 2mM L-glutamine antibiotics (100units/me penicillin and 0.1mg/ml streptomycin).

In order to separate the white blood cell population from the sample the cells are run through a gradient medium Histopaque-1077 (Sigma-Alrdich, Steinhein, Germany). One millilitre of Histopaque-1077 was carefully underlaid beneath the media/cell suspension and the cells were separated by centrifugation in an Eppendorf centrifuge 5804R (Hamburg, Germany) at 300RCF/1299RPM for 21 minutes at 4 °C with the brake off. The cloudy layer that formed underneath the media layer was carefully removed using a 1 ml pipette and placed in a fresh tube. The cell sample was then rinsed to remove any remaining Histopaque-1077 by adding PBS to a total of 10 mls and centrifuged for a further 3 minutes at 300RFC/1299RPM for 3 minutes at 20 °C with braking on. The supernatant was aspirated once again and the pellet was resuspended in 2mls of the supplemented α-MEM media.

Finally a cell count was performed in a haemato cytometer using 10µl of the resuspended cells in media. Samples were then diluted appropriately to generate a final concentration of 1 x 10^6 cells/ml for cell culture seeding.

8.5.1.2 Cell proliferation and differentiation

Cells were plated in 48 well plates (Falcon) at a seeding density of 5 x 10^5 created by adding 0.125mls of the cell suspension (1x10^6 cells/ml) and 0.125ml of α-MEM, containing 2ng/ml RANKL (R&D Systems) and 0.4ng/ml of macrophage colony stimulating factor (M-CSF) (R&D Systems). Multiwell plates were placed in a Steri-cycle CO_2 incubator (Thermo Electron Corporation, Ohio USA) and grown at 37 °C in the presence of 5% CO_2.

The supplemented α-MEM media containing 1ng/ml RANKL and 0.2ng/ml M-CSF was replaced every three days. At days 6 and 9 images of cultured cells were captured using an Olympus CKX41 microscope and Olympus DP12 digital camera (Olympus Corporation, Tokyo, Japan) at10x magnification.

After 10 days of culture the media was removed and the cell populations fixed and stained for TRAP expression.

8.5.1.3 TRAP staining of osteoclasts

Once the media was removed from all culture wells and each rinsed twice with 0.5mls PBS, the cells were then fixed with 0.5mls/well of 4% PFA at room temperature for 15 minutes and then re-rinsed twice more with 0.5ml PBS. Cells were then pre-treated with 0.3 ml of 1M Tris-HCL buffer (pH 9.4) at RT for 15 minutes followed by 0.3 ml 1M sodium acetate buffer (pH 5.0). After this re-treatment, cells were stained with the TRAP stain*, at 37°C for 30-45 minutes until cells were coloured red. Finally cells were fixed with 0.5ml/well of 4% PFA at room temperature (RT) for 15 minutes before 2 rinses in distilled water and air dried for imaging.

** TRAP stain solution preparation:*

Basic fuschin solution was pre-prepared by adding 1 g of basic fuschin to 20ml distilled water and 5ml concentrated hydrochloric acid, which was warmed gently whilst mixing. To make 17.5mls of stain solution, 50µl of 40mg/ml sodium nitrite was first added to 50µl of basic fuschin solution. This produced small bubbles and a brown discolouration. The reacted sodium nitrite/basic fuschin was then added to 17.5mg of tartaric acid dissolved in 17.5ml 1M sodium acetate buffer. Next, 20mg of Napthol ASBI Phosphate dissolved in 1ml dimethylformamide was added. The solution was mixed well and filtered through a Millex GV 0.22µm syringe filter unit (Millipore, Cork, Ireland). Staining solution was used immediately.

8.5.1.4 Analysis of osteoclast differentiation.

Analysis of TRAP positive (TRAP +) cells in cultures was performed using a Leica MZ8 dissecting microscope (Leica, Germany) attached to the same QICAM camera and BIOQUANT image analysis set-up used for the histomorphometric analysis (see section 8.4.5).

At 2.5x magnification, six separate fields of view, ROI's, were analysed in each well and the number of TRAP positive cells counted in each field. This was performed using BIOQUANT software using the manual measure option and an array measure for object count. The average number of osteoclasts per field of view or ROI was then calculated for each well.

8.5.2 RANKL-induce osteoclast culture on calcium phosphate discs

8.5.2.1 Bone marrow collection – was performed as per section 8.5.1.1

8.5.2.2 Cell proliferation and differentiation

Bone marrow cells were plated in 12 well plates containing calcium phosphate coated Osteologic discs (BD BioCoat, Bone cell Culture System, BD Biosciences, Ontario, Canada) at a seeding density of 5 x 10^5 by adding 0.25 ml of the cells suspended in media to each well. Then 0.25 ml of α-MEM, containing 2ng/ml RANKL (R&D Systems) and 0.4ng/ml of macrophage colony stimulating factor (M-CSF) (R&D Systems), was added to each well so that a total volume of 0.5 ml per well was achieved. Plated cells were grown in a CO_2 incubator under identical conditions as cells grown on plastic (see section 8.6.1.2).

The supplemented α-MEM media containing 1ng/ml RANKL and 0.2ng/ml M-CSF was replaced every three days in each well and samples returned to the incubator. Cells were again photographed at days 6 and 9.

At day 10 of culture the media was removed and the cells were detached from the plates using 1ml of bleach per well for 3 minutes at room temperature. After bleaching, wells were rinsed twice with 1ml of distilled water and stored in fresh distilled water at 4°C until von Kossa staining was performed.

8.5.2.3 Von Kossa stain on calcium phosphate discs.

After removal of the distilled water 1ml of 1% aqueous silver nitrate solution was added to each well. The plates were then placed under UV light in a Stratagene UV stratalinker 1800 (California, USA). The stain solution was then removed and wells rinsed with distilled water twice before being air-dried for imaging.

8.5.2.4 Analysis of resorption pit formation

Resorption pit formation was quantified using the Leica MZ8 microscope, QICAM camera and BIOQUANT image analysis system (see section 8.6.1.4). At a magnification of 0.8x, ROIs located around the centre of the well, incorporating 90% of the calcium phosphate surface were measured. Using a red threshold of (0,112,) and using the auto measure: area function setting, the area of each plate coloured in black/brown from the Von Kossa staining was measured. The inverse of this value, i.e. the area of resorbed calcium phosphate, was expressed as a percentage of the total ROI.

8.5.3 RANKL-induce osteoclast cultures on human bone discs

8.5.3.1 Bone marrow collection – was performed as per section 8.5.1.1

8.5.3.2 Cell proliferation and differentiation

Plating of cells for human bone disc resorption analysis was done at a seeding density of 5 x 10^5 in the OsteoAssay human bone plate containing 96 wells (Cambrex Biosceinces, Walkersville, USA). Again, 0.125 ml of the cell suspension and 0.125 ml of α-MEM, containing 2ng/ml RANKL (R&D Systems) and 0.4ng/ml of macrophage colony stimulating factor (M-CSF) (R&D Systems), was added to each well to achieve a total volume of 0.25mls per well. Plated cells were grown as described in section 8.6.1.2.

In addition to plating cells from the day of harvest (day 0) a duplicate set of cells were also plated in standard plastic 48 well plate wells. After a media change at day 3, these cells were removed from the plastic wells at day 6 using trypsin/EDTA (invitrogen). Firstly the cells were rinsed with two changes of 100 µl of PBS before adding 30 µl of trypsin for 15 minutes at 37°C. Cells were then washed off the surface using vigorous pippetting and added to the OsteoAssay plates with an extra 220 µl of the osteoclast differentiation media.

Cells grown in the human bone disc plates were allowed to differentiate and resorb the bone discs to release collagen degradation products into their media. Media samples of 100µl were obtained from each well every 4 days prior to replacement of the culturing solution. Each sample was individually stored in Eppendorf tubes and placed at -20 °C until analysis of collagen degradation products was performed. The final day of media harvest for each sample was day 14.

8.5.3.3 Analysis of collagen breakdown products by ELISA

Upon completion of the culture experiments involving the human bone discs all samples collected were processed using an enzyme-linked immunosorbent assay kit (ELISA) for the quantitation of Helical Peptide 620-633 from the α1 chain of Type I collagen, (Metra, Quidel Corporation, San Diego, CA). Each sample was measured in duplicate using the following procedure based on the instructions included with the ELISA kit:

All ELISA strips required were warmed to room temperature whilst media samples were thawed. Twenty µl of each of the standards, controls or samples were added to each allocated well in duplicate, a further 150µl of the enzyme conjugate was then added to each well and incubated at 2-8°C for 18 hours. After incubation the strips were manually inverted to remove all excess enzyme conjugate and each well was

rinsed with 275µl of 1x wash buffer for a total of three washes, manually inverting between washes. After the final wash, the strips were blotted vigorously on paper towel and the bottom of the strips wiped clean of any lint or contaminants. One hundred and fifty µl of working substrate solution was added to each well and incubated for 60 minutes at room temperature. The reaction was terminated with 100µl of Stop solution per well. The absorbance was read on a Multiskan Ascent plate reader (MTX Lab Systems Inc, USA), at 405nm within 30 minutes of the addition of the stop solution.

Calibration standards were plotted from the known control samples (averaged) using Microsoft Excel. From this curve, a line of best fit using the logarithmic decay function was generated. The resultant equation was then used to calculate the concentrations in µg/ml for each sample and then averaged.

8.6 Serum analysis of resorption markers

8.6.1 ELISA assay for CTX

8.6.1.1 Sample harvest

Serum samples were obtained from growing rats in the *ia/ia* rat phenotype study to determine concentrations of serum C-terminal telopeptide cross-links (CTX), a degradation product of type I collagen. Blood samples of approximately 1-2mls were collected from each allocated rat via cardiac puncture during euthanasia by CO_2 gas. After 30-60 minutes at RT samples were spun at a speed of 1300 rpm for 5 minutes at RT in a Biofuge Pico centrifuge (Kendro Kab Products, Germany) to pellet the cells to the bottom of the tubes. Serum was collected from the spun samples and stored at -20°C until analysis was performed.

8.6.1.2 ELISA method

The RatLaps CTX ELISA kit (Nordic Bioscience Diagnostics, Denmark) was used for this analysis of CTX concentration in the serum samples collected using the following protocol as outlined by the kit instructions.

All solutions and samples were equilibrated to RT before proceeding. One hundred µl of the biotinylated antibody was added to each well to be used and covered with sealing tape before incubating at RT for 30 minutes. After removal of the tape the wells were rinsed in washing solution 5 times then 20µl of each standard, control and sample was added to their respective well followed by 100µl of primary antibody, all samples and standards were analysed in duplicate. The plate was then incubated for 18 hours at 2-8°C after sealing with tape. Plates were unsealed and rinsed with washing

solution 5 times then 100µl of peroxidase conjugated goat anti-rabbit IgG antibody was added to each well and covered with sealing tape for further incubation at RT for 60 minutes. Following the same wash procedure as before, the wells were rinsed and then 100µl of the substrate solution was added for 15 minutes at RT after resealing with tape. The reaction was stopped by the addition of 100 µl of stopping solution and the absorbance read with a Multiskan Ascent plate reader (MTX Lab Systems Inc, USA) at 450nm. A reference reading was performed at 650nm.

8.6.1.3 Data analysis

Using Microsoft Excel, as for the human bone disc ELISA reading, the calibration standards were plotted from the known control samples (averaged). From this curve a line of best fit using the logarithmic decay function was generated. The resultant equation was then used to calculate the concentrations in µg/ml for each sample and a mean was calculated.

8.7 Statistical analysis of data

SPSS (SPSS Inc, Chicago, USA) statistics program was used for all data analysis in this thesis. All numerical data from the ZA studies were analysed using a one-way analysis of variance (ANOVA) with post hoc t-tests by the least squares differences (LSD) method, as there were always at least three treatment groups to compare. All numerical data for *ia/ia* rat and MMI270 studies was analysed using Independent samples t-test assuming equal variances. When p-values were less than 0.05, results were considered different with statistical significance. P-values were reported as $p<0.01$, $p<0.02$ or $p<0.05$ to demonstrate the level of significance with $p<0.01$ being the highest.

Where data was categorical such as when determining union or non-unions from radiographs, standard t tests could not be applied, therefore chi squared analysis was used to test statistical significance.

Reference List

Abad, V., Meyers, J.L., Weise, M., Gafni, R.I., Barnes, K.M., Nilsson, O., Bacher, J.D., and Baron, J., 2002. The role of the resting zone in growth plate chondrogenesis. Endocrinology 143, 1851-1857.

Adolphson, P., Abbaszadegan, H., Boden, H., Salemyr, M., and Henriques, T., 2000. Clodronate increases mineralization of callus after Colles' fracture: a randomized, double-blind, placebo-controlled, prospective trial in 32 patients. Acta Orthop. Scand. 71, 195-200.

Aharinejad, S., Marks, S.C., Jr., Bock, P., Mason-Savas, A., MacKay, C.A., Larson, E.K., Jackson, M.E., Luftensteiner, M., and Wiesbauer, E., 1995. CSF-1 treatment promotes angiogenesis in the metaphysis of osteopetrotic (toothless, tl) rats. Bone 16, 315-324.

Aitken, C.J., Hodge, J.M., and Nicholson, G.C., 2004. Adenoviral down-regulation of osteopontin inhibits human osteoclast differentiation in vitro. J. Cell Biochem. 93, 896-903.

Alini, M., Matsui, Y., Dodge, G.R., and Poole, A.R., 1992. The extracellular matrix of cartilage in the growth plate before and during calcification: changes in composition and degradation of type II collagen. Calcif. Tissue Int. 50, 327-335.

Allen, M. and Burr, D., 2007. Mineralisation, Microdamage, and matrix: How Bisphosphonates influence Material proerties of bone. BoneKey. Osteovision. 4:49-60., 49-60.

Amanat, N., Brown, R., Bilston, L.E., and Little, D.G., 2005. A single systemic dose of pamidronate improves bone mineral content and accelerates restoration of strength in a rat model of fracture repair. J. Orthop. Res. 23, 1029-1034.

Amanat, N., McDonald, M., Godfrey, C., Bilston, L., and Little, D., 2007. Optimal timing of a single dose of zoledronic acid to increasestrength in rat fracture repair. J. Bone and Min Res. In press.

An, Y., Friedman, R.J., Parent, T., and Draughn, R.A., 1994. Production of a standard closed fracture in the rat tibia. J. Orthop. Trauma 8, 111-115.

Angel, N.Z., Walsh, N., Forwood, M.R., Ostrowski, M.C., Cassady, A.I., and Hume, D.A., 2000. Transgenic mice overexpressing tartrate-resistant acid phosphatase exhibit an increased rate of bone turnover. J. Bone Miner. Res. 15, 103-110.

Arsenault, A.L., 1987. Microvascular organization at the epiphyseal-metaphyseal junction of growing rats. J. Bone Miner. Res. 2, 143-149.

Asou, Y., Rittling, S.R., Yoshitake, H., Tsuji, K., Shinomiya, K., Nifuji, A., Denhardt, D.T., and Noda, M., 2001. Osteopontin facilitates angiogenesis, accumulation of osteoclasts, and resorption in ectopic bone. Endocrinology 142, 1325-1332.

Augat, P., Merk, J., Genant, H.K., and Claes, L., 1997. Quantitative assessment of experimental fracture repair by peripheral computed tomography. Calcif. Tissue Int. 60, 194-199.

Bauss, F., Schenk, R.K., Hort, S., Muller-Beckmann, B., and Sponer, G., 2004. New model for simulation of fracture repair in full-grown beagle dogs: model characterization and results from a long-term study with ibandronate. J. Pharmacol. Toxicol. Methods 50, 25-34.

Bauss, F., Wagner, M., and Hothorn, L.H., 2002. Total administered dose of ibandronate determines its effects on bone mass and architecture in ovariectomized aged rats. J. Rheumatol. 29, 990-998.

Bekker, P.J., Holloway, D., Nakanishi, A., Arrighi, M., Leese, P.T., and Dunstan, C.R., 2001. The effect of a single dose of osteoprotegerin in postmenopausal women. J. Bone Miner. Res. 16, 348-360.

Bekker, P.J., Holloway, D.L., Rasmussen, A.S., Murphy, R., Martin, S.W., Leese, P.T., Holmes, G.B., Dunstan, C.R., and DePaoli, A.M., 2004. A single-dose placebo-controlled study of AMG 162, a fully human monoclonal antibody to RANKL, in postmenopausal women. J. Bone Miner. Res. 19, 1059-1066.

Bettex-Galland, M., Boillat, C., and Bettex, M., 1990. Chondroclasts in osteoneogenesis. Tissue Cell 22, 93-100.

Bilston, L.E., Little, D.G., Smith, N.C., Williams, P., and Briody, J., 2002. Zoledronic acid improves the mechanical properties of normal and healing bone. Clin. Biomech. (Bristol. , Avon.) 17, 716-718.

Black, D.M., Cummings, S.R., Karpf, D.B., Cauley, J.A., Thompson, D.E., Nevitt, M.C., Bauer, D.C., Genant, H.K., Haskell, W.L., Marcus, R., Ott, S.M., Torner, J.C., Quandt, S.A., Reiss, T.F., and Ensrud, K.E., 1996. Randomised trial of effect of alendronate on risk of fracture in women with existing vertebral fractures. Fracture Intervention Trial Research Group. Lancet 348, 1535-1541.

Black, D.M., Delmas, P.D., Eastell, R., Reid, I.R., Boonen, S., Cauley, J.A., Cosman, F., Lakatos, P., Leung, P.C., Man, Z., Mautalen, C., Mesenbrink, P., Hu, H., Caminis, J., Tong, K., Rosario-Jansen, T., Krasnow, J., Hue, T.F., Sellmeyer, D., Eriksen, E.F., and Cummings, S.R., 2007. Once-yearly zoledronic acid for treatment of postmenopausal osteoporosis. N. Engl. J. Med. 356, 1809-1822.

Blair, H.C., Zaidi, M., and Schlesinger, P.H., 2002. Mechanisms balancing skeletal matrix synthesis and degradation. Biochem. J. 364, 329-341.

Blavier, L. and Delaisse, J.M., 1995. Matrix metalloproteinases are obligatory for the migration of preosteoclasts to the developing marrow cavity of primitive long bones. J. Cell Sci. 108, 3649-3659.

Boissier, S., Ferreras, M., Peyruchaud, O., Magnetto, S., Ebetino, F.H., Colombel, M., Delmas, P., Delaisse, J.M., and Clezardin, P., 2000. Bisphosphonates inhibit breast and prostate carcinoma cell invasion, an early event in the formation of bone metastases. Cancer Res. 60, 2949-2954.

Boivin, G. and Meunier, P.J., 2002a. Effects of bisphosphonates on matrix mineralization. J. Musculoskelet. Neuronal. Interact. 2, 538-543.

Boivin, G. and Meunier, P.J., 2002b. The degree of mineralization of bone tissue measured by computerized quantitative contact microradiography. Calcif. Tissue Int. 70, 503-511.

Boivin, G.Y., Chavassieux, P.M., Santora, A.C., Yates, J., and Meunier, P.J., 2000. Alendronate increases bone strength by increasing the mean degree of mineralization of bone tissue in osteoporotic women. Bone. 27, 687-694.

Bolander, M.E., 1992. Regulation of fracture repair by growth factors. Proc Soc Exp Biol Med 200, 165-170.

Bone, H.G., Hosking, D., Devogelaer, J.P., Tucci, J.R., Emkey, R.D., Tonino, R.P., Rodriguez-Portales, J.A., Downs, R.W., Gupta, J., Santora, A.C., and Liberman,

U.A., 2004. Ten years' experience with alendronate for osteoporosis in postmenopausal women. N. Engl. J. Med. 350, 1189-1199.

Bonnarens, F. and Einhorn, T.A., 1984. Production of a standard closed fracture in laboratory animal bone. J. Orthop. Res. 2, 97-101.

Bosch, P., Musgrave, D.S., Lee, J.Y., Cummins, J., Shuler, T., Ghivizzani, T.C., Evans, T., Robbins, T.D., and Huard, 2000. Osteoprogenitor cells within skeletal muscle. J. Orthop. Res. 18, 933-944.

Boskey, A.L. and Marks, S.C., Jr., 1985. Mineral and matrix alterations in the bones of incisors-absent (*ia/ia*) osteopetrotic rats. Calcif. Tissue Int. 37, 287-292.

Boskey, A.L., Spevak, L., Paschalis, E., Doty, S.B., and McKee, M.D., 2002. Osteopontin deficiency increases mineral content and mineral crystallinity in mouse bone. Calcif. Tissue Int. 71, 145-154.

Bouxsein, M.L., Myers, K.S., Shultz, K.L., Donahue, L.R., Rosen, C.J., and Beamer, W.G., 2005. Ovariectomy-induced bone loss varies among inbred strains of mice. J. Bone Miner. Res. 20, 1085-1092.

Boyle, W.J., Simonet, W.S., and Lacey, D.L., 2003. Osteoclast differentiation and activation. Nature 423, 337-342.

Bronckers, A.L., Goei, W., van Heerde, W.L., Dumont, E.A., Reutelingsperger, C.P., and van den Eijnde, S.M., 2000. Phagocytosis of dying chondrocytes by osteoclasts in the mouse growth plate as demonstrated by annexin-V labelling. Cell Tissue Res. 301, 267-272.

Bruder, S.P., Fink, D.J., and Caplan, A.I., 1994. Mesenchymal stem cells in bone development, bone repair, and skeletal regeneration therapy. J. Cell Biochem. 56, 283-294.

Brumsen, C., Hamdy, N.A., and Papapoulos, S.E., 1997. Long-term effects of bisphosphonates on the growing skeleton. Studies of young patients with severe osteoporosis. Medicine (Baltimore) 76, 266-283.

Camacho, N.P., Raggio, C.L., Doty, S.B., Root, L., Zraick, V., Ilg, W.A., Toledano, T.R., and Boskey, A.L., 2001. A controlled study of the effects of alendronate in a growing mouse model of osteogenesis imperfecta. Calcif. Tissue Int. 69, 94-101.

Cao, Y., Mori, S., Mashiba, T., Kaji, Y., Manabe, T., Iwata, K., Miyamoto, K., Komatsubara, S., and Yamamoto, T., 2006. 1alpha,25-Dihydroxy-2beta(3-hydroxypropoxy)vitamin D(3) (ED-71) suppressed callus remodeling but did not interfere with fracture healing in rat femora. Bone. ..

Cao, Y., Mori, S., Mashiba, T., Westmore, M.S., Ma, L., Sato, M., Akiyama, T., Shi, L., Komatsubara, S., Miyamoto, K., and Norimatsu, H., 2002. Raloxifene, estrogen, and alendronate affect the processes of fracture repair differently in ovariectomized rats. J. Bone Miner. Res. 17, 2237-2246.

Chen, T., Berenson, J., Vescio, R., Swift, R., Gilchick, A., Goodin, S., LoRusso, P., Ma, P., Ravera, C., Deckert, F., Schran, H., Seaman, J., and Skerjanec, A., 2002. Pharmacokinetics and pharmacodynamics of zoledronic acid in cancer patients with bone metastases. J. Clin. Pharmacol. 42, 1228-1236.

Choi, J.Y., Kim, H.J., Lee, Y.C., Cho, B.O., Seong, H.S., Cho, M., and Kim, S.G., 2007. Inhibition of bone healing by pamidronate in calvarial bony defects. Oral Surg. Oral Med. Oral Pathol. Oral Radiol. Endod. 103, 321-328.

Chung, U.I., Schipani, E., McMahon, A.P., and Kronenberg, H.M., 2001. Indian hedgehog couples chondrogenesis to osteogenesis in endochondral bone development. J. Clin. Invest 107, 295-304.

Cimaz, R. and Biggioggero, M., 2001. Osteoporosis. Curr. Rheumatol. Rep. 3, 365-370.

Cole, A.A. and Wezeman, F.H., 1987. Cytochemical localization of tartrate-resistant acid phosphatase, alkaline phosphatase, and nonspecific esterase in perivascular cells of cartilage canals in the developing mouse epiphysis. Am. J. Anat. 180, 237-242.

Colnot, C., 2005. Cellular and molecular interactions regulating skeletogenesis. J. Cell Biochem. 95, 688-697.

Colnot, C., Thompson, Z., Miclau, T., Werb, Z., and Helms, J.A., 2003. Altered fracture repair in the absence of MMP9. Development 130, 4123-4133.

Corey, E., Brown, L.G., Quinn, J.E., Poot, M., Roudier, M.P., Higano, C.S., and Vessella, R.L., 2003. Zoledronic acid exhibits inhibitory effects on osteoblastic and osteolytic metastases of prostate cancer. Clin. Cancer Res. 9, 295-306.

Currey, J.D., 2003. The many adaptations of bone. J. Biomech. 36, 1487-1495.

Dai, X.M., Zong, X.H., Akhter, M.P., and Stanley, E.R., 2004. Osteoclast deficiency results in disorganized matrix, reduced mineralization, and abnormal osteoblast behavior in developing bone. J. Bone Miner. Res. 19, 1441-1451.

de Palma, L., Tulli, A., Maccauro, G., Sabetta, S.P., and del Torto, M., 1994. Fracture callus in osteopetrosis. Clin. Orthop. 85-89.

Deckers, M.M., Van Beek, E.R., Van Der, P.G., Wetterwald, A., Wee-Pals, L., Cecchini, M.G., Papapoulos, S.E., and Lowik, C.W., 2002. Dissociation of angiogenesis and osteoclastogenesis during endochondral bone formation in neonatal mice. J. Bone Miner. Res. 17, 998-1007.

Delaisse, J.M., Andersen, T.L., Engsig, M.T., Henriksen, K., Troen, T., and Blavier, L., 2003. Matrix metalloproteinases (MMP) and cathepsin K contribute differently to osteoclastic activities. Microsc. Res. Tech. 61, 504-513.

Duvall, C.L., Taylor, W.R., Weiss, D., Wojtowicz, A.M., and Guldberg, R.E., 2006. Impaired Angiogenesis, Early Callus Formation, and Late Stage Remodeling In Fracture Healing of Osteopontin Deficient Mice. J. Bone Miner. Res. ..

Einhorn, T.A., 1998. The cell and molecular biology of fracture healing. Clin Orthop S7-21.

Einhorn, T.A., 2005. The science of fracture healing. J. Orthop. Trauma. 19, S4-S6.

Ek-Rylander, B., Flores, M., Wendel, M., Heinegard, D., and Andersson, G., 1994. Dephosphorylation of osteopontin and bone sialoprotein by osteoclastic tartrate-resistant acid phosphatase. Modulation of osteoclast adhesion in vitro. J. Biol. Chem. 269, 14853-14856.

Engsig, M.T., Chen, Q.J., Vu, T.H., Pedersen, A.C., Therkidsen, B., Lund, L.R., Henriksen, K., Lenhard, T., Foged, N.T., Werb, Z., and Delaisse, J.M., 2000. Matrix metalloproteinase 9 and vascular endothelial growth factor are essential for osteoclast recruitment into developing long bones. J. Cell Biol. 151, 879-889.

Evans, K.D., Lau, S.T., Oberbauer, A.M., and Martin, R.B., 2003. Alendronate affects long bone length and growth plate morphology in the oim mouse model for Osteogenesis Imperfecta. Bone 32, 268-274.

Everts, V., Delaisse, J.M., Korper, W., and Beertsen, W., 1998. Cysteine proteinases and matrix metalloproteinases play distinct roles in the subosteoclastic resorption zone. J. Bone Miner. Res. 13, 1420-1430.

Everts, V., Delaisse, J.M., Korper, W., Jansen, D.C., Tigchelaar-Gutter, W., Saftig, P., and Beertsen, W., 2002. The bone lining cell: its role in cleaning Howship's lacunae and initiating bone formation. J. Bone Miner. Res. 17, 77-90.

Eyres, K.S., Bell, M.J., and Kanis, J.A., 1993. New bone formation during leg lengthening. Evaluated by dual energy X-ray absorptiometry. J Bone Joint Surg Br 75, 96-106.

Farina, C. and Gagliardi, S., 1999. Selective inhibitors of the osteoclast vacuolar proton ATPase as novel bone antiresorptive agents. Drug Discov. Today 4, 163-172.

Ferguson, C., Alpern, E., Miclau, T., and Helms, J.A., 1999. Does adult fracture repair recapitulate embryonic skeletal formation? Mech. Dev. 87, 57-66.

Ferretti, J.L., Capozza, R.F., and Zanchetta, J.R., 1996. Mechanical validation of a tomographic (pQCT) index for noninvasive estimation of rat femur bending strength. Bone 18, 97-102.

Ferretti, M., Palumbo, C., Bertoni, L., Cavani, F., and Marotti, G., 2006. Does static precede dynamic osteogenesis in endochondral ossification as occurs in intramembranous ossification? Anat. Rec. A Discov. Mol. Cell Evol. Biol. 288, 1158-1162.

Fleisch, H., 1999. From polyphosphates to bisphosphonates and their role in bone and calcium metabolism. Prog Mol Subcell Biol 23, 197-216.

Fleisch, H., 2001. Can bisphosphonates be given to patients with fractures? J Bone Miner Res 16, 437-440.

Flick, L.M., Weaver, J.M., Ulrich-Vinther, M., Abuzzahab, F., Zhang, X., Dougall, W.C., Anderson, D., O'Keefe, R.J., and Schwarz, E.M., 2003. Effects of receptor activator of NFkappaB (RANK) signaling blockade on fracture healing. J. Orthop. Res. 21, 676-684.

Gardner, T.N., Evans, M., Simpson, H., and Kenwright, J., 1998. Force-displacement behaviour of biological tissue during distraction osteogenesis. Med. Eng Phys. 20, 708-715.

Garnero, P., Borel, O., Byrjalsen, I., Ferreras, M., Drake, F.H., McQueney, M.S., Foged, N.T., Delmas, P.D., and Delaisse, J.M., 1998. The collagenolytic activity of cathepsin K is unique among mammalian proteinases. J. Biol. Chem. 273, 32347-32352.

Garnero, P., Ferreras, M., Karsdal, M.A., NicAmhlaoibh, R., Risteli, J., Borel, O., Qvist, P., Delmas, P.D., Foged, N.T., and Delaisse, J.M., 2003. The type I collagen fragments ICTP and CTX reveal distinct enzymatic pathways of bone collagen degradation. J. Bone Miner. Res. 18, 859-867.

Gasser, J.A., 1995. Assessing bone quantity by pQCT. Bone. 17, 145S-154S.

Gerber, H.P. and Ferrara, N., 2000. Angiogenesis and bone growth. Trends Cardiovasc. Med. 10, 223-228.

Gerber, H.P., Vu, T.H., Ryan, A.M., Kowalski, J., Werb, Z., and Ferrara, N., 1999. VEGF couples hypertrophic cartilage remodeling, ossification and angiogenesis during endochondral bone formation. Nat. Med. 5, 623-628.

Gerstenfeld, L.C., Cho, T.J., Kon, T., Aizawa, T., Tsay, A., Fitch, J., Barnes, G.L., Graves, D.T., and Einhorn, T.A., 2003. Impaired fracture healing in the absence of TNF-alpha signaling: the role of TNF-alpha in endochondral cartilage resorption. J. Bone Miner. Res. 18, 1584-1592.

Giuliani, N., Pedrazzoni, M., Negri, G., Passeri, G., Impicciatore, M., and Girasole, G., 1998a. Bisphosphonates stimulate formation of osteoblast precursors and mineralized nodules in murine and human bone marrow cultures in vitro and promote early osteoblastogenesis in young and aged mice in vivo. Bone 22, 455-461.

Giuliani, N., Pedrazzoni, M., Passeri, G., Negri, G., Impicciatore, M., and Girasole, G., 1998b. [Bisphosphonates stimulate the production of basic fibroblast growth factor and the formation of bone marrow precursors of osteoblasts. New findings about their mechanism of action]. Minerva Med 89, 249-258.

Glatt, M., Pataki, A., Evans, G.P., Hornby, S.B., and Green, J.R., 2004. Loss of vertebral bone and mechanical strength in estrogen-deficient rats is prevented by long-term administration of zoledronic acid. Osteoporos. Int. 15, 707-715.

Goodship, A.E., Walker, P.C., McNally, D., Chambers, T., and Green, J.R., 1994. Use of a bisphosphonate (pamidronate) to modulate fracture repair in ovine bone. Ann Oncol 5 Suppl 7, S53-S55.

Goodship, A.E., Watkins, P.E., Rigby, H.S., and Kenwright, J., 1993. The role of fixator frame stiffness in the control of fracture healing. An experimental study. J. Biomech. 26, 1027-1035.

Greiner, S., Kadow-Romacker, A., Lubberstedt, M., Schmidmaier, G., and Wildemann, B., 2006. The effect of zoledronic acid incorporated in a poly(D,L-lactide) implant coating on osteoblasts in vitro. J. Biomed. Mater. Res. A. ..

Hadjiargyrou, M., Ahrens, W., and Rubin, C.T., 2000. Temporal expression of the chondrogenic and angiogenic growth factor CYR61 during fracture repair. J Bone Miner Res 15, 1014-1023.

Hak, D.J., Makino, T., Niikura, T., Hazelwood, S.J., Curtiss, S., and Reddi, A.H., 2006. Recombinant human BMP-7 effectively prevents non-union in both young and old rats. J. Orthop. Res. 24, 11-20.

Hamma-Kourbali, Y., Di, B.M., Ledoux, D., Oudar, O., Leroux, Y., Lecouvey, M., and Kraemer, M., 2003. A novel non-containing-nitrogen bisphosphonate inhibits both in vitro and in vivo angiogenesis. Biochem. Biophys. Res. Commun. 310, 816-823.

Hausman, M.R., Schaffler, M.B., and Majeska, R.J., 2001. Prevention of fracture healing in rats by an inhibitor of angiogenesis. Bone 29, 560-564.

Hayman, A.R., Jones, S.J., Boyde, A., Foster, D., Colledge, W.H., Carlton, M.B., Evans, M.J., and Cox, T.M., 1996. Mice lacking tartrate-resistant acid phosphatase (Acp 5) have disrupted endochondral ossification and mild osteopetrosis. Development 122, 3151-3162.

Helfrich, M.H., 2003. Osteoclast diseases. Microsc. Res. Tech. 61, 514-532.

Helfrich, M.H., Nesbitt, S.A., Lakkakorpi, P.T., Barnes, M.J., Bodary, S.C., Shankar, G., Mason, W.T., Mendrick, D.L., Vaananen, H.K., and Horton, M.A., 1996. Beta 1 integrins and osteoclast function: involvement in collagen recognition and bone resorption. Bone. 19, 317-328.

Henriksen, K., Sorensen, M.G., Nielsen, R.H., Gram, J., Schaller, S., Dziegiel, M.H., Everts, V., Bollerslev, J., and Karsdal, M.A., 2006. Degradation of the organic phase of bone by osteoclasts: a secondary role for lysosomal acidification. J. Bone Miner. Res. 21, 58-66.

Hofbauer, L.C., Khosla, S., Dunstan, C.R., Lacey, D.L., Boyle, W.J., and Riggs, B.L., 2000. The roles of osteoprotegerin and osteoprotegerin ligand in the paracrine regulation of bone resorption. J. Bone Miner. Res. 15, 2-12.

Hollberg, K., Hultenby, K., Hayman, A., Cox, T., and Andersson, G., 2002. Osteoclasts from mice deficient in tartrate-resistant acid phosphatase have altered ruffled borders and disturbed intracellular vesicular transport. Exp. Cell Res. 279, 227-238.

Hollberg, K., Nordahl, J., Hultenby, K., Mengarelli-Widholm, S., Andersson, G., and Reinholt, F.P., 2005. Polarization and secretion of cathepsin K precede tartrate-resistant acid phosphatase secretion to the ruffled border area during the activation of matrix-resorbing clasts. J. Bone Miner. Metab. 23, 441-449.

Holliday, L.S., Welgus, H.G., Fliszar, C.J., Veith, G.M., Jeffrey, J.J., and Gluck, S.L., 1997. Initiation of osteoclast bone resorption by interstitial collagenase. J. Biol. Chem. 272, 22053-22058.

Hollinger, J. and Wong, M.E., 1996. The integrated processes of hard tissue regeneration with special emphasis on fracture healing. Oral Surg. Oral Med. Oral Pathol. Oral Radiol. Endod. 82, 594-606.

Holstein, J.H., Menger, M.D., Scheuer, C., Meier, C., Culemann, U., Wirbel, R.J., Garcia, P., and Pohlemann, T., 2006. Erythropoietin (EPO) - EPO-receptor signaling improves early endochondral ossification and mechanical strength in fracture healing. Life Sci. ..

Hordon, L.D., Itoda, M., Shore, P.A., Shore, R.C., Heald, M., Brown, M., Kanis, J.A., Rodan, G.A., and Aaron, J.E., 2006. Preservation of thoracic spine

microarchitecture by alendronate: comparison of histology and microCT. Bone. 38, 444-449.

Hosking, D., Lyles, K., Brown, J.P., Fraser, W.D., Miller, P., Diaz, C.M., Devogelaer, J.P., Hooper, M., Su, G., Zelenakas, K., Pak, J., Fashola, T., Saidi, Y., Fink, E.E., and Reid, I.R., 2006. Long Term Control of Bone Turnover in Pagets Disease with Zoledronic Acid and Risedronate. J. Bone Miner. Res. ..

Hou, P., Troen, T., Ovejero, M.C., Kirkegaard, T., Andersen, T.L., Byrjalsen, I., Ferreras, M., Sato, T., Shapiro, S.D., Foged, N.T., and Delaisse, J.M., 2004. Matrix metalloproteinase-12 (MMP-12) in osteoclasts: new lesson on the involvement of MMPs in bone resorption. Bone. 34, 37-47.

Huk, O.L., Zukor, D.J., Antoniou, J., and Petit, A., 2003. Effect of pamidronate on the stimulation of macrophage TNF-alpha release by ultra-high-molecular-weight polyethylene particles: a role for apoptosis. J. Orthop. Res. 21, 81-87.

Hunter, W.L. and Arsenault, A.L., 1990. Vascular invasion of the epiphyseal growth plate: analysis of metaphyseal capillary ultrastructure and growth dynamics. Anat. Rec. 227, 223-231.

Hutchinson, J.H., Halczenko, W., Brashear, K.M., Breslin, M.J., Coleman, P.J., Duong, l.T., Fernandez-Metzler, C., Gentile, M.A., Fisher, J.E., Hartman, G.D., Huff, J.R., Kimmel, D.B., Leu, C.T., Meissner, R.S., Merkle, K., Nagy, R., Pennypacker, B., Perkins, J.J., Prueksaritanont, T., Rodan, G.A., Varga, S.L., Wesolowski, G.A., Zartman, A.E., Rodan, S.B., and Duggan, M.E., 2003. Nonpeptide alphavbeta3 antagonists. 8. In vitro and in vivo evaluation of a potent alphavbeta3 antagonist for the prevention and treatment of osteoporosis. J. Med. Chem. 46, 4790-4798.

Hyvonen, P.M., Karhi, T., Kosma, V.M., Liimola-Luoma, L., and Hanhijarvi, H., 1994. The influence of dichloromethylene bisphosphonate on the healing of a long bone fracture, composition of bone mineral and histology of bone in the rat. Pharmacol. Toxicol. 75, 384-390.

Inada, M., Wang, Y., Byrne, M.H., Rahman, M.U., Miyaura, C., Lopez-Otin, C., and Krane, S.M., 2004. Critical roles for collagenase-3 (Mmp13) in development of growth plate cartilage and in endochondral ossification. Proc. Natl. Acad. Sci. U. S. A 101, 17192-17197.

Inui, T., Ishibashi, O., Inaoka, T., Origane, Y., Kumegawa, M., Kokubo, T., and Yamamura, T., 1997. Cathepsin K antisense oligodeoxynucleotide inhibits osteoclastic bone resorption. J. Biol. Chem. 272, 8109-8112.

Irving, M.H., 1964. THE BLOOD SUPPLY OF THE GROWTH CARTILAGE IN YOUNG RATS. J. Anat. 98:631-9., 631-639.

Ishibashi, O., Niwa, S., Kadoyama, K., and Inui, T., 2006. MMP-9 antisense oligodeoxynucleotide exerts an inhibitory effect on osteoclastic bone resorption by suppressing cell migration. Life Sci. ..

Jackson, R.A., McDonald, M.M., Nurcombe, V., Little, D.G., and Cool, S.M., 2006. The use of heparan sulfate to augment fracture repair in a rat fracture model. J. Orthop. Res. 24, 636-644.

Jamsa, T., Rho, J.Y., Fan, Z., MacKay, C.A., Marks, S.C., Jr., and Tuukkanen, J., 2002. Mechanical properties in long bones of rat osteopetrotic mutations. J. Biomech. 35, 161-165.

Jemtland, R., Lee, K., and Segre, G.V., 1998. Heterogeneity among cells that express osteoclast-associated genes in developing bone. Endocrinology. 139, 340-349.

Jiang, Y., Zhao, J., White, D.L., and Genant, H.K., 2000. Micro CT and Micro MR imaging of 3D architecture of animal skeleton. J. Musculoskelet. Neuronal. Interact. 1, 45-51.

Johansson, M., Jansson, L., Ehinger, M., Fasth, A., Karlsson, S., and Richter, J., 2006. Neonatal hematopoietic stem cell transplantation cures oc/oc mice from osteopetrosis. Exp. Hematol. 34, 242-249.

Johansson, N., Saarialho-Kere, U., Airola, K., Herva, R., Nissinen, L., Westermarck, J., Vuorio, E., Heino, J., and Kahari, V.M., 1997. Collagenase-3 (MMP-13) is expressed by hypertrophic chondrocytes, periosteal cells, and osteoblasts during human fetal bone development. Dev. Dyn. 208, 387-397.

Juppner, H., 2000. Role of parathyroid hormone-related peptide and Indian hedgehog in skeletal development. Pediatr. Nephrol. 14, 606-611.

Kanis, J.A., Gertz, B.J., Singer, F., and Ortolani, S., 1995. Rationale for the use of alendronate in osteoporosis. Osteoporos. Int. 5, 1-13.

Kawai, N., Kawanishi, M., and Nagao, S., 2003. Treatment of cold injury-induced brain edema with a nonspecific matrix metalloproteinase inhibitor MMI270 in rats. Acta Neurochir. Suppl 86:291-5., 291-295.

Kawana, F. and Sasaki, T., 2003. Osteoclast differentiation and characteristic trabecular bone formation during growth plate destruction in osteoprotegerin-deficient mice. J. Electron Microsc. (Tokyo). 52, 515-525.

Kimble, R.B., Bain, S., and Pacifici, R., 1997. The functional block of TNF but not of IL-6 prevents bone loss in ovariectomized mice. J. Bone Miner. Res. 12, 935-941.

Kirsch, T., Nah, H.D., Shapiro, I.M., and Pacifici, M., 1997. Regulated production of mineralization-competent matrix vesicles in hypertrophic chondrocytes. J. Cell Biol. 137, 1149-1160.

Kiviranta, R., Morko, J., Uusitalo, H., Aro, H.T., Vuorio, E., and Rantakokko, J., 2001. Accelerated turnover of metaphyseal trabecular bone in mice overexpressing cathepsin K. J. Bone Miner. Res. 16, 1444-1452.

Kleerekoper, M. and Schein, J.R., 2001. Comparative safety of bone remodeling agents with a focus on osteoporosis therapies. J. Clin. Pharmacol. 41, 239-250.

Knauper, V., Lopez-Otin, C., Smith, B., Knight, G., and Murphy, G., 1996. Biochemical characterization of human collagenase-3. J. Biol. Chem. %19;271, 1544-1550.

Knothe Tate, M.L., Adamson, J.R., Tami, A.E., and Bauer, T.W., 2004. The osteocyte. Int. J. Biochem. Cell Biol. 36, 1-8.

Kobayashi, T., Chung, U.I., Schipani, E., Starbuck, M., Karsenty, G., Katagiri, T., Goad, D.L., Lanske, B., and Kronenberg, H.M., 2002. PTHrP and Indian hedgehog control differentiation of growth plate chondrocytes at multiple steps. Development 129, 2977-2986.

Kodama, H., Yamasaki, A., Abe, M., Niida, S., Hakeda, Y., and Kawashima, H., 1993. Transient recruitment of osteoclasts and expression of their function in osteopetrotic (op/op) mice by a single injection of macrophage colony-stimulating factor. J. Bone Miner. Res. 8, 45-50.

Koivukangas, A., Tuukkanen, J., Kippo, K., Jamsa, T., Hannuniemi, R., Pasanen, I., Vaananen, K., and Jalovaara, P., 2003. Long-term administration of clodronate does not prevent fracture healing in rats. Clin. Orthop. 268-278.

Kokubu, T., Hak, D.J., Hazelwood, S.J., and Reddi, A.H., 2003. Development of an atrophic nonunion model and comparison to a closed healing fracture in rat femur. J. Orthop. Res. 21, 503-510.

Komatsubara, S., Mori, S., Mashiba, T., Ito, M., Li, J., Kaji, Y., Akiyama, T., Miyamoto, K., Cao, Y., Kawanishi, J., and Norimatsu, H., 2003. Long-term treatment of incadronate disodium accumulates microdamage but improves the trabecular bone microarchitecture in dog vertebra. J. Bone Miner. Res. 18, 512-520.

Komatsubara, S., Mori, S., Mashiba, T., Li, J., Nonaka, K., Kaji, Y., Akiyama, T., Miyamoto, K., Cao, Y., Kawanishi, J., and Norimatsu, H., 2004. Suppressed bone turnover by long-term bisphosphonate treatment accumulates microdamage but maintains intrinsic material properties in cortical bone of dog rib. J. Bone Miner. Res. 19, 999-1005.

Kong, Y.Y., Yoshida, H., Sarosi, I., Tan, H.L., Timms, E., Capparelli, C., Morony, S., Oliveira, d.S.A., Van, G., Itie, A., Khoo, W., Wakeham, A., Dunstan, C.R., Lacey, D.L., Mak, T.W., Boyle, W.J., and Penninger, J.M., 1999. OPGL is a key regulator of osteoclastogenesis, lymphocyte development and lymph-node organogenesis. Nature 397, 315-323.

Kornak, U., Kasper, D., Bosl, M.R., Kaiser, E., Schweizer, M., Schulz, A., Friedrich, W., Delling, G., and Jentsch, T.J., 2001. Loss of the ClC-7 chloride channel leads to osteopetrosis in mice and man. Cell 104, 205-215.

Kosaki, N., Takaishi, H., Kamekura, S., Kimura, T., Okada, Y., Minqi, L., Amizuka, N., Chung, U.I., Nakamura, K., Kawaguchi, H., Toyama, Y., and D'Armiento, J., 2007. Impaired bone fracture healing in matrix metalloproteinase-13 deficient mice. Biochem. Biophys. Res. Commun. 354, 846-851.

Kostenuik, P.J., 2005. Osteoprotegerin and RANKL regulate bone resorption, density, geometry and strength. Curr. Opin. Pharmacol. 5, 618-625.

Kronenberg, H.M., 2003. Developmental regulation of the growth plate. Nature 423, 332-336.

Kronenberg, H.M., Lanske, B., Kovacs, C.S., Chung, U.I., Lee, K., Segre, G.V., Schipani, E., and Juppner, H., 1998. Functional analysis of the PTH/PTHrP network of ligands and receptors. Recent Prog. Horm. Res. 53, 283-301.

Kumar, S., Dare, L., Vasko-Moser, J.A., James, I.E., Blake, S.M., Rickard, D.J., Hwang, S.M., Tomaszek, T., Yamashita, D.S., Marquis, R.W., Oh, H., Jeong, J.U., Veber, D.F., Gowen, M., Lark, M.W., and Stroup, G., 2007. A highly potent inhibitor of cathepsin K (relacatib) reduces biomarkers of bone resorption both in vitro and in an acute model of elevated bone turnover in vivo in monkeys. Bone. 40, 122-131.

Lacey, D.L., Timms, E., Tan, H.L., Kelley, M.J., Dunstan, C.R., Burgess, T., Elliott, R., Colombero, A., Elliott, G., Scully, S., Hsu, H., Sullivan, J., Hawkins, N., Davy, E., Capparelli, C., Eli, A., Qian, Y.X., Kaufman, S., Sarosi, I., Shalhoub, V., Senaldi, G., Guo, J., Delaney, J., and Boyle, W.J., 1998. Osteoprotegerin ligand is a cytokine that regulates osteoclast differentiation and activation. Cell. 93, 165-176.

Lark, M.W., Stroup, G.B., James, I.E., Dodds, R.A., Hwang, S.M., Blake, S.M., Lechowska, B.A., Hoffman, S.J., Smith, B.R., Kapadia, R., Liang, X., Erhard, K., Ru, Y., Dong, X., Marquis, R.W., Veber, D., and Gowen, M., 2002. A potent small molecule, nonpeptide inhibitor of cathepsin K (SB 331750) prevents bone matrix resorption in the ovariectomized rat. Bone 30, 746-753.

Lazner, F., Gowen, M., Pavasovic, D., and Kola, I., 1999. Osteopetrosis and osteoporosis: two sides of the same coin. Hum. Mol. Genet. 8, 1839-1846.

Lee, E.R., Murphy, G., El Alfy, M., Davoli, M.A., Lamplugh, L., Docherty, A.J., and Leblond, C.P., 1999. Active gelatinase B is identified by histozymography in the cartilage resorption sites of developing long bones. Dev. Dyn. 215, 190-205.

Lenehan, T.M., Balligand, M., Nunamaker, D.M., and Wood, F.E., Jr., 1985. Effect of EHDP on fracture healing in dogs. J. Orthop. Res. 3, 499-507.

Levitt, N.C., Eskens, F.A., O'Byrne, K.J., Propper, D.J., Denis, L.J., Owen, S.J., Choi, L., Foekens, J.A., Wilner, S., Wood, J.M., Nakajima, M., Talbot, D.C., Steward, W.P., Harris, A.L., and Verweij, J., 2001. Phase I and pharmacological study of the oral matrix metalloproteinase inhibitor, MMI270 (CGS27023A), in patients with advanced solid cancer. Clin. Cancer Res. 7, 1912-1922.

Lewinson, D. and Silbermann, M., 1992. Chondroclasts and endothelial cells collaborate in the process of cartilage resorption. Anat. Rec. 233, 504-514.

Li, C., Mori, S., Li, J., Kaji, Y., Akiyama, T., Kawanishi, J., and Norimatsu, H., 2001. Long-term effect of incadronate disodium (YM-175) on fracture healing of femoral shaft in growing rats. J. Bone Miner. Res. 16, 429-436.

Li, J., Mori, S., Kaji, Y., Kawanishi, J., Akiyama, T., and Norimatsu, H., 2000a. Concentration of bisphosphonate (incadronate) in callus area and its effects on fracture healing in rats. J Bone Miner Res 15, 2042-2051.

Li, J., Mori, S., Kaji, Y., Mashiba, T., Kawanishi, J., and Norimatsu, H., 1999. Effect of bisphosphonate (incadronate) on fracture healing of long bones in rats. J Bone Miner Res 14, 969-979.

Li, J., Sarosi, I., Yan, X.Q., Morony, S., Capparelli, C., Tan, H.L., McCabe, S., Elliott, R., Scully, S., Van, G., Kaufman, S., Juan, S.C., Sun, Y., Tarpley, J., Martin, L., Christensen, K., McCabe, J., Kostenuik, P., Hsu, H., Fletcher, F., Dunstan, C.R., Lacey, D.L., and Boyle, W.J., 2000b. RANK is the intrinsic hematopoietic cell surface receptor that controls osteoclastogenesis and regulation of bone mass and calcium metabolism. Proc. Natl. Acad. Sci. U. S. A 97, 1566-1571.

Li, Z., Kong, K., and Qi, W., 2006. Osteoclast and its roles in calcium metabolism and bone development and remodeling. Biochem. Biophys. Res. Commun. 343, 345-350.

Licata, A.A., 1997. Bisphosphonate therapy. Am. J. Med. Sci. 313, 17-22.

Lin, R., Amizuka, N., Sasaki, T., Aarts, M.M., Ozawa, H., Goltzman, D., Henderson, J.E., and White, J.H., 2002. 1Alpha,25-dihydroxyvitamin D3 promotes vascularization of the chondro-osseous junction by stimulating expression of vascular endothelial growth factor and matrix metalloproteinase 9. J. Bone Miner. Res. 17, 1604-1612.

Lindsay R, Saag K, Kriegman A, Davis J, Beamer E, and Zhou W. A single Zoledronic Acid 5mg Infusion is preferred over weekly 70mg oral Alendronate in a clinical trial of postmenopausal women with osteoporosis/opsteopenia. Osteoporos.Int. 17[Suppl 1], S43. 2006.
Ref Type: Abstract

Lipton, A., Small, E., Saad, F., Gleason, D., Gordon, D., Smith, M., Rosen, L., Kowalski, M.O., Reitsma, D., and Seaman, J., 2002. The new bisphosphonate, Zometa (zoledronic acid), decreases skeletal complications in both osteolytic and osteoblastic lesions: a comparison to pamidronate. Cancer Invest. 20 Suppl 2:45-54., 45-54.

Little, D.G., Cornell, M.S., Briody, J., Cowell, C.T., Arbuckle, S., and Cooke-Yarborough, C.M., 2001b. Intravenous pamidronate reduces osteoporosis and improves formation of the regenerate during distraction osteogenesis. A study in immature rabbits. J. Bone Joint Surg. Br. 83, 1069-1074.

Little, D.G., Cornell, M.S., Briody, J., Cowell, C.T., Arbuckle, S., and Cooke-Yarborough, C.M., 2001a. Intravenous pamidronate reduces osteoporosis and improves formation of the regenerate during distraction osteogenesis. A study in immature rabbits. J. Bone Joint Surg. Br. 83, 1069-1074.

Little, D.G., Cornell, M.S., Hile, M.S., Briody, J., Cowell, C.T., and Bilston, L., 2001c. Effect of pamidronate on distraction osteogenesis and fixator-related osteoporosis. Injury 32 Suppl 4, SD14-SD20.

Little, D.G., McDonald, M., Bransford, R., Godfrey, C.B., and Amanat, N., 2005. Manipulation of the anabolic and catabolic responses with OP-1 and zoledronic acid in a rat critical defect model. J. Bone Miner. Res. 20, 2044-2052.

Little, D.G., Peat, R.A., Mcevoy, A., Williams, P.R., Smith, E.J., and Baldock, P.A., 2003a. Zoledronic acid treatment results in retention of femoral head structure after traumatic osteonecrosis in young Wistar rats. J. Bone Miner. Res. 18, 2016-2022.

Little, D.G., Smith, N.C., Williams, P., Briody, J., Bilston, L.E., Smith, E., Gardiner, E.M., and Cowell, C.T., 2003b. Zoledronic Acid Prevents Osteopenia and Increases Bone Strength in a Rabbit Model of Distraction Osteogenesis. J. Bone Miner. Res. 18, 1300-1307.

Lowery, G.L., Kulkarni, S., and Pennisi, A.E., 1999. Use of autologous growth factors in lumbar spinal fusion. Bone. 25, 47S-50S.

Lu, X.M., Yang, Q.M., and Deng, L.F., 2004. [Mechanism of the WNT family in vertebrate skeleton development]. Yi Chuan 26, 947-952.

Madsen, J.E., Berg-Larsen, T., Kirkeby, O.J., Falch, J.A., and Nordsletten, L., 1998. No adverse effects of clodronate on fracture healing in rats. Acta Orthop. Scand. 69, 532-536.

Maes, C., Carmeliet, P., Moermans, K., Stockmans, I., Smets, N., Collen, D., Bouillon, R., and Carmeliet, G., 2002. Impaired angiogenesis and endochondral bone formation in mice lacking the vascular endothelial growth factor isoforms VEGF164 and VEGF188. Mech. Dev. 111, 61-73.

Maffulli, N., Cheng, J.C., Sher, A., and Lam, T.P., 1997. Dual-energy X-ray absorptiometry predicts bone formation in lower limb callotasis lengthening. Ann. R. Coll. Surg. Engl. 79, 250-256.

Makino, T., Hak, D.J., Hazelwood, S.J., Curtiss, S., and Reddi, A.H., 2005. Prevention of atrophic nonunion development by recombinant human bone morphogenetic protein-7. J. Orthop. Res. 23, 632-638.

Malemud, C.J., 2006. Matrix metalloproteinases: role in skeletal development and growth plate disorders. Front Biosci. 11:1702-15., 1702-1715.

Mao, J.J. and Nah, H.D., 2004. Growth and development: Hereditary and mechanical modulations. Am. J. Orthod. Dentofacial Orthop. 125, 676-689.

Mark, H., Nilsson, A., Nannmark, U., and Rydevik, B., 2004a. Effects of fracture fixation stability on ossification in healing fractures. Clin. Orthop. 245-250.

Mark, H., Penington, A., Nannmark, U., Morrison, W., and Messina, A., 2004b. Microvascular invasion during endochondral ossification in experimental fractures in rats. Bone 35, 535-542.

Mark, H. and Rydevik, B., 2005. Torsional stiffness in healing fractures: influence of ossification: an experimental study in rats. Acta Orthop. 76, 428-433.

Marks, S.C., Jr., 1973. Pathogenesis of osteopetrosis in the ia rat: reduced bone resorption due to reduced osteoclast function. Am. J. Anat. 138, 165-189.

Marks, S.C., Jr., 1976. Osteopetrosis in the IA rat cured by spleen cells from a normal littermate. Am. J. Anat. 146, 331-338.

Marks, S.C., Jr. and Schmidt, C.J., 1978. Bone remodeling as an expression of altered phenotype: studies of fracture healing in untreated and cured osteopetrotic rats. Clin. Orthop. 259-264.

Marks, S.C., Jr. and Schneider, G.B., 1982. Transformations of osteoclast phenotype in ia rats cured of congenital osteopetrosis. J. Morphol. 174, 141-147.

Mashiba, T., Hirano, T., Turner, C.H., Forwood, M.R., Johnston, C.C., and Burr, D.B., 2000. Suppressed bone turnover by bisphosphonates increases microdamage accumulation and reduces some biomechanical properties in dog rib. J. Bone Miner. Res. 15, 613-620.

Mashiba, T., Turner, C.H., Hirano, T., Forwood, M.R., Jacob, D.S., Johnston, C.C., and Burr, D.B., 2001. Effects of high-dose etidronate treatment on microdamage accumulation and biomechanical properties in beagle bone before occurrence of spontaneous fractures. Bone 29, 271-278.

McCarthy, E.A., Raggio, C.L., Hossack, M.D., Miller, E.A., Jain, S., Boskey, A.L., and Camacho, N.P., 2002. Alendronate treatment for infants with osteogenesis imperfecta: demonstration of efficacy in a mouse model. Pediatr. Res. 52, 660-670.

McDonald MM, Dulai SK, Godfrey C, Sztynda T, Little DG. 2006. Osteoclasts are functionally redundant in initial endochondral fracture union but not callus remodeling: Insights into optimal bisphosphonate dosing. J Bone Miner Res 21[Suppl 1], S398.

McHugh, K.P., Hodivala-Dilke, K., Zheng, M.H., Namba, N., Lam, J., Novack, D., Feng, X., Ross, F.P., Hynes, R.O., and Teitelbaum, S.L., 2000. Mice lacking beta3 integrins are osteosclerotic because of dysfunctional osteoclasts. J. Clin. Invest 105, 433-440.

McLean, W. and Olsen, B.R., 2001. Mouse models of abnormal skeletal development and homeostasis. Trends Genet. 17, S38-S43.

Medina, C., Videla, S., Radomski, A., Radomski, M.W., Antolin, M., Guarner, F., Vilaseca, J., Salas, A., and Malagelada, J.R., 2003. Increased activity and expression of matrix metalloproteinase-9 in a rat model of distal colitis. Am. J. Physiol Gastrointest. Liver Physiol 284, G116-G122.

Melton, J.T., Clarke, N.M., and Roach, H.I., 2006. Matrix metalloproteinase-9 induces the formation of cartilage canals in the chondroepiphysis of the neonatal rabbit. J. Bone Joint Surg. Am. 88 Suppl 3:155-61., 155-161.

Meyer, R.A., Jr., Tsahakis, P.J., Martin, D.F., Banks, D.M., Harrow, M.E., and Kiebzak, G.M., 2001. Age and ovariectomy impair both the normalization of mechanical properties and the accretion of mineral by the fracture callus in rats. J. Orthop. Res. 19, 428-435.

Milkiewicz, M., Kelland, C., Colgan, S., and Haas, T.L., 2006. Nitric oxide and p38 MAP kinase mediate shear stress-dependent inhibition of MMP-2 production in microvascular endothelial cells. J. Cell Physiol. 208, 229-237.

Miller, B.S., Bronk, J.T., Nishiyama, T., Yamagiwa, H., Srivastava, A., Bolander, M.E., and Conover, C.A., 2007. Pregnancy associated plasma protein-A is necessary for expeditious fracture healing in mice. J. Endocrinol. 192, 505-513.

Misof, B.M., Roschger, P., Baldini, T., Raggio, C.L., Zraick, V., Root, L., Boskey, A.L., Klaushofer, K., Fratzl, P., and Camacho, N.P., 2005. Differential effects of alendronate treatment on bone from growing osteogenesis imperfecta and wild-type mouse. Bone. 36, 150-158.

Monier-Faugere, M.C., Geng, Z., Paschalis, E.P., Qi, Q., Arnala, I., Bauss, F., Boskey, A.L., and Malluche, H.H., 1999. Intermittent and continuous administration of the bisphosphonate ibandronate in ovariohysterectomized beagle dogs: effects on bone morphometry and mineral properties. J. Bone Miner. Res. 14, 1768-1778.

Monkkonen, J., Koponen, H.M., and Ylitalo, P., 1990. Comparison of the distribution of three bisphosphonates in mice. Pharmacol. Toxicol. 66, 294-298.

Mori, S., 2003. Fracture healing with anti-resorptive agents. J. Musculoskelet. Neuronal. Interact. 3, 314-316.

Mori, S., Sawai, T., Teshima, T., and Kyogoku, M., 1988. A new decalcifying technique for immunohistochemical studies of calcified tissue, especially applicable to cell surface marker demonstration. J. Histochem. Cytochem. 36, 111-114.

Mulari, M., Vaaraniemi, J., and Vaananen, H.K., 2003. Intracellular membrane trafficking in bone resorbing osteoclasts. Microsc. Res. Tech. 61, 496-503.

Mulari, M.T., Qu, Q., Harkonen, P.L., and Vaananen, H.K., 2004. Osteoblast-like Cells Complete Osteoclastic Bone Resorption and Form New Mineralized Bone Matrix In Vitro. Calcif. Tissue Int. ..

Munns, C.F., Rauch, F., Zeitlin, L., Fassier, F., and Glorieux, F.H., 2004. Delayed osteotomy but not fracture healing in pediatric osteogenesis imperfecta patients receiving pamidronate. J. Bone Miner. Res. 19, 1779-1786.

Murakami, H., Nakamura, T., Tsurukami, H., Abe, M., Barbier, A., and Suzuki, K., 1994. Effects of tiludronate on bone mass, structure, and turnover at the epiphyseal, primary, and secondary spongiosa in the proximal tibia of growing rats after sciatic neurectomy. J. Bone Miner. Res. 9, 1355-1364.

Murakami, S. and Noda, M., 2000. Expression of Indian hedgehog during fracture healing in adult rat femora. Calcif. Tissue Int. 66, 272-276.

Murphy, M.G., Cerchio, K., Stoch, S.A., Gottesdiener, K., Wu, M., and Recker, R., 2005. Effect of L-000845704, an alphaVbeta3 integrin antagonist, on markers of bone turnover and bone mineral density in postmenopausal osteoporotic women. J. Clin. Endocrinol. Metab 90, 2022-2028.

Nagai, H. and Aoki, M., 2002. Inhibition of growth plate angiogenesis and endochondral ossification with diminished expression of MMP-13 in hypertrophic chondrocytes in FGF-2-treated rats. J. Bone Miner. Metab 20, 142-147.

Nakamura, H., Sato, G., Hirata, A., and Yamamoto, T., 2004. Immunolocalization of matrix metalloproteinase-13 on bone surface under osteoclasts in rat tibia. Bone. 34, 48-56.

Namkung-Matthai, H., Appleyard, R., Jansen, J., Hao, L.J., Maastricht, S., Swain, M., Mason, R.S., Murrell, G.A., Diwan, A.D., and Diamond, T., 2001. Osteoporosis influences the early period of fracture healing in a rat osteoporotic model. Bone 28, 80-86.

Niida, S., Kaku, M., Amano, H., Yoshida, H., Kataoka, H., Nishikawa, S., Tanne, K., Maeda, N., Nishikawa, S., and Kodama, H., 1999. Vascular endothelial growth factor can substitute for macrophage colony-stimulating factor in the support of osteoclastic bone resorption. J. Exp. Med. 19;190, 293-298.

Nishino, I., Amizuka, N., and Ozawa, H., 2001. Histochemical examination of osteoblastic activity in op/op mice with or without injection of recombinant M-CSF. J. Bone Miner. Metab 19, 267-276.

Nordahl, J., Andersson, G., and Reinholt, F.P., 1998. Chondroclasts and osteoclasts in bones of young rats: comparison of ultrastructural and functional features. Calcif. Tissue Int. 63, 401-408.

Nunamaker, D.M., 1998. Experimental models of fracture repair. Clin. Orthop. S56-S65.

Nyman, J.S., Yeh, O.C., Hazelwood, S.J., and Martin, R.B., 2004. A theoretical analysis of long-term bisphosphonate effects on trabecular bone volume and microdamage. Bone. 35, 296-305.

Nyman, M.T., Gao, T., Lindholm, T.C., and Lindholm, T.S., 1996. Healing of a tibial double osteotomy is modified by clodronate administration. Arch. Orthop. Trauma Surg. 115, 111-114.

Nyman, M.T., Paavolainen, P., Holmstrom, T., Penttinen, R., and Verkasalo, M., 1993a. Clodronate reduces plate osteopenia in the rabbit. Acta Orthop. Scand. 64, 50-54.

Nyman, M.T., Paavolainen, P., and Lindholm, T.S., 1993b. Clodronate increases the calcium content in fracture callus. An experimental study in rats. Arch. Orthop. Trauma Surg. 112, 228-231.

O'Driscoll, S.W., Marx, R.G., Fitzsimmons, J.S., and Beaton, D.E., 1999. Method for automated cartilage histomorphometry. Tissue Eng 5, 13-23.

Odgren, P.R., Kim, N., MacKay, C.A., Mason-Savas, A., Choi, Y., and Marks, S.C., Jr., 2003a. The role of RANKL (TRANCE/TNFSF11), a tumor necrosis factor family member, in skeletal development: effects of gene knockout and transgenic rescue. Connect. Tissue Res. 44 Suppl 1:264-71.

Odgren, P.R., Philbrick, W.M., and Gartland, A., 2003b. Perspective. Osteoclastogenesis and growth plate chondrocyte differentiation: emergence of convergence. Crit Rev. Eukaryot. Gene Expr. 13, 181-193.

Odvina, C.V., Zerwekh, J.E., Rao, D.S., Maalouf, N., Gottschalk, F.A., and Pak, C.Y., 2005. Severely suppressed bone turnover: a potential complication of alendronate therapy. J. Clin. Endocrinol. Metab. 90, 1294-1301.

Parfitt, A.M., 2002. Targeted and nontargeted bone remodeling: relationship to basic multicellular unit origination and progression. Bone 30, 5-7.

Park, S.H., O'Connor, K., Sung, R., McKellop, H., and Sarmiento, A., 1999. Comparison of healing process in open osteotomy model and closed fracture model. J. Orthop. Trauma 13, 114-120.

Park, S.H., Silva, M., Bahk, W.J., McKellop, H., and Lieberman, J.R., 2002. Effect of repeated irrigation and debridement on fracture healing in an animal model. J. Orthop. Res. 20, 1197-1204.

Pataki, A., Muller, K., Green, J.R., Ma, Y.F., Li, Q.N., and Jee, W.S., 1997. Effects of short-term treatment with the bisphosphonates zoledronate and pamidronate on rat bone: a comparative histomorphometric study on the cancellous bone formed before, during, and after treatment. Anat. Rec. 249, 458-468.

Peter, C.P., Cook, W.O., Nunamaker, D.M., Provost, M.T., Seedor, J.G., and Rodan, G.A., 1996. Effect of alendronate on fracture healing and bone remodeling in dogs. J. Orthop. Res. 14, 74-79.

Phillips, C.L., Bradley, D.A., Schlotzhauer, C.L., Bergfeld, M., Libreros-Minotta, C., Gawenis, L.R., Morris, J.S., Clarke, L.L., and Hillman, L.S., 2000. Oim mice exhibit altered femur and incisor mineral composition and decreased bone mineral density. Bone 27, 219-226.

Pizones, J., Plotkin, H., Parra-Garcia, J.I., Alvarez, P., Gutierrez, P., Bueno, A., and Fernandez-Arroyo, A., 2005. Bone healing in children with osteogenesis imperfecta treated with bisphosphonates. J. Pediatr. Orthop. 25, 332-335.

Plotkin, H., Rauch, F., Zeitlin, L., Munns, C., Travers, R., and Glorieux, F.H., 2003. Effect of pamidronate treatment in children with polyostotic fibrous dysplasia of bone. J. Clin. Endocrinol. Metab. 88, 4569-4575.

Pufe, T., Wildemann, B., Petersen, W., Mentlein, R., Raschke, M., and Schmidmaier, G., 2002. Quantitative measurement of the splice variants 120 and 164 of the

angiogenic peptide vascular endothelial growth factor in the time flow of fracture healing: a study in the rat. Cell Tissue Res. 309, 387-392.

Reid, I.R., Brown, J.P., Burckhardt, P., Horowitz, Z., Richardson, P., Trechsel, U., Widmer, A., Devogelaer, J.P., Kaufman, J.M., Jaeger, P., Body, J.J., Brandi, M.L., Broell, J., Di Micco, R., Genazzani, A.R., Felsenberg, D., Happ, J., Hooper, M.J., Ittner, J., Leb, G., Mallmin, H., Murray, T., Ortolani, S., Rubinacci, A., Saaf, M., Samsioe, G., Verbruggen, L., and Meunier, P.J., 2002. Intravenous zoledronic acid in postmenopausal women with low bone mineral density. N. Engl. J. Med. 346, 653-661.

Reinholt, F.P., Hultenby, K., Heinegard, D., Marks, S.C., Jr., Norgard, M., and Anderson, G., 1999. Extensive clear zone and defective ruffled border formation in osteoclasts of osteopetrotic (*ia/ia*) rats: implications for secretory function. Exp. Cell Res. 251, 477-491.

Reinholt, F.P., Hultenby, K., Oldberg, A., and Heinegard, D., 1990. Osteopontin--a possible anchor of osteoclasts to bone. Proc. Natl. Acad. Sci. U. S. A 87, 4473-4475.

Reinholz, G.G., Getz, B., Pederson, L., Sanders, E.S., Subramaniam, M., Ingle, J.N., and Spelsberg, T.C., 2000. Bisphosphonates directly regulate cell proliferation, differentiation, and gene expression in human osteoblasts. Cancer Res 60, 6001-6007.

Reinholz, G.G., Getz, B., Sanders, E.S., Karpeisky, M.Y., Padyukova, N.S., Mikhailov, S.N., Ingle, J.N., and Spelsberg, T.C., 2002. Distinct mechanisms of bisphosphonate action between osteoblasts and breast cancer cells: identity of a potent new bisphosphonate analogue. Breast Cancer Res. Treat. 71, 257-268.

Rice, D.P., Kim, H.J., and Thesleff, I., 1997. Detection of gelatinase B expression reveals osteoclastic bone resorption as a feature of early calvarial bone development. Bone 21, 479-486.

Rittling, S.R., Matsumoto, H.N., McKee, M.D., Nanci, A., An, X.R., Novick, K.E., Kowalski, A.J., Noda, M., and Denhardt, D.T., 1998. Mice lacking osteopontin show normal development and bone structure but display altered osteoclast formation in vitro. J. Bone Miner. Res. 13, 1101-1111.

Roach, H.I. and Clarke, N.M., 1999. "Cell paralysis" as an intermediate stage in the programmed cell death of epiphyseal chondrocytes during development. J. Bone Miner. Res. 14, 1367-1378.

Roach, H.I. and Clarke, N.M., 2000. Physiological cell death of chondrocytes in vivo is not confined to apoptosis. New observations on the mammalian growth plate. J. Bone Joint Surg. Br. 82, 601-613.

Rodan, G.A., 1997. Bone mass homeostasis and bisphosphonate action. Bone 20, 1-4.

Rogers, M.J., Gordon, S., Benford, H.L., Coxon, F.P., Luckman, S.P., Monkkonen, J., and Frith, J.C., 2000. Cellular and molecular mechanisms of action of bisphosphonates. Cancer 88, 2961-2978.

Roth, V.G., 1976. Pycnodysostosis presenting with bilateral subtrachanteric fractures: case report. Clin. Orthop. 247-253.

Rundhaug, J.E., 2003. Matrix metalloproteinases, angiogenesis, and cancer: commentary re: A. C. Lockhart *et al.*, Reduction of wound angiogenesis in patients treated with BMS-275291, a broad spectrum matrix metalloproteinase inhibitor. Clin. Cancer Res., 9: 00-00, 2003. Clin. Cancer Res. 9, 551-554.

Saftig, P., Hunziker, E., Wehmeyer, O., Jones, S., Boyde, A., Rommerskirch, W., Moritz, J.D., Schu, P., and von Figura, K., 1998. Impaired osteoclastic bone resorption leads to osteopetrosis in cathepsin-K-deficient mice. Proc. Natl. Acad. Sci. U. S. A. 95, 13453-13458.

Sahni, M., Guenther, H.L., Fleisch, H., Collin, P., and Martin, T.J., 1993. Bisphosphonates act on rat bone resorption through the mediation of osteoblasts. J Clin Invest 91, 2004-2011.

Sato, M., Grasser, W., Endo, N., Akins, R., Simmons, H., Thompson, D.D., Golub, E., and Rodan, G.A., 1991. Bisphosphonate action. Alendronate localization in rat bone and effects on osteoclast ultrastructure. J. Clin. Invest. 88, 2095-2105.

Sato, T., Foged, N.T., and Delaisse, J.M., 1998. The migration of purified osteoclasts through collagen is inhibited by matrix metalloproteinase inhibitors. J. Bone Miner. Res. 13, 59-66.

Sawae, Y., Sahara, T., and Sasaki, T., 2003. Osteoclast differentiation at growth plate cartilage-trabecular bone junction in newborn rat femur. J. Electron Microsc. (Tokyo). 52, 493-502.

Scammell, B.E. and Roach, H.I., 1996. A new role for the chondrocyte in fracture repair: endochondral ossification includes direct bone formation by former chondrocytes. J. Bone Miner. Res. 11, 737-745.

Schaller, S., Henriksen, K., Sveigaard, C., Heegaard, A.M., Helix, N., Stahlhut, M., Ovejero, M.C., Johansen, J.V., Solberg, H., Andersen, T.L., Hougaard, D., Berryman, M., Shiodt, C.B., Sorensen, B.H., Lichtenberg, J., Christophersen, P., Foged, N.T., Delaisse, J.M., Engsig, M.T., and Karsdal, M.A., 2004. The chloride channel inhibitor n53736 prevents bone resorption in ovariectomized rats without changing bone formation. J. Bone Miner. Res. 19, 1144-1153.

Schell, H., Lienau, J., Epari, D.R., Seebeck, P., Exner, C., Muchow, S., Bragulla, H., Haas, N.P., and Duda, G.N., 2006. Osteoclastic activity begins early and increases over the course of bone healing. Bone. 38, 547-554.

Schenk, R.K., Spiro, D., and Wiener, J., 1967. Cartilage resorption in the tibial epiphyseal plate of growing rats. J. Cell Biol. 34, 275-291.

Schenk, R.K., Wiener, J., and Spiro, D., 1968. Fine structural aspects of vascular invasion of the tibial epiphyseal plate of growing rats. Acta Anat. (Basel) 69, 1-17.

Schimmer, R.C. and Bauss, F., 2003. Effect of daily and intermittent use of ibandronate on bone mass and bone turnover in postmenopausal osteoporosis: a review of three phase II studies. Clin. Ther. 25, 19-34.

Schindeler, A. and Little, D.G., 2005. Osteoclasts but not osteoblasts are affected by a calcified surface treated with zoledronic acid in vitro. Biochem. Biophys. Res. Commun. 338, 710-716.

Schmidmaier, G., Wildemann, B., Cromme, F., Kandziora, F., Haas, N.P., and Raschke, M., 2002. Bone morphogenetic protein-2 coating of titanium implants increases biomechanical strength and accelerates bone remodeling in fracture treatment: a biomechanical and histological study in rats. Bone 30, 816-822.

Schmidt, C.J., Marks, S.C., Jr., Jordan, C.A., and Hawes, L.E., 1977. A radiographic and histologic study of fracture healing in osteopetrotic rats. Radiology 122, 517-519.

Seifert, M.F., 1996. Abnormalities in bone cell function and endochondral ossification in the osteopetrotic toothless rat. Bone 19, 329-338.

Seifert, M.F., Popoff, S.N., Jackson, M.E., MacKay, C.A., Cielinski, M., and Marks, S.C., Jr., 1993. Experimental studies of osteopetrosis in laboratory animals. Clin. Orthop. Relat Res. 23-33.

Shapses, S.A., Cifuentes, M., Spevak, L., Chowdhury, H., Brittingham, J., Boskey, A.L., and Denhardt, D.T., 2003. Osteopontin facilitates bone resorption, decreasing bone mineral crystallinity and content during calcium deficiency. Calcif. Tissue Int. 73, 86-92.

Shimizu-Ishiura, M., Kawana, F., and Sasaki, T., 2002. Osteoprotegerin administration reduces femural bone loss in ovariectomized mice via impairment of osteoclast structure and function. J. Electron Microsc. (Tokyo). 51, 315-325.

Simon, A.M., Manigrasso, M.B., and O'Connor, J.P., 2002. Cyclo-oxygenase 2 function is essential for bone fracture healing. J. Bone Miner. Res. 17, 963-976.

Simonet, W.S., Lacey, D.L., Dunstan, C.R., Kelley, M., Chang, M.S., Luthy, R., Nguyen, H.Q., Wooden, S., Bennett, L., Boone, T., Shimamoto, G., DeRose, M., Elliott, R., Colombero, A., Tan, H.L., Trail, G., Sullivan, J., Davy, E., Bucay, N., Renshaw-Gegg, L., Hughes, T.M., Hill, D., Pattison, W., Campbell, P., Sander, S., Van, G., Tarpley, J., Derby, P., Lee, R., and Boyle, W.J., 1997. Osteoprotegerin: a novel secreted protein involved in the regulation of bone density. Cell. 89, 309-319.

Singh, I.J., Tonna, E.A., and Gandel, C.P., 1974. A comparative histological study of mammalian bone. J. Morphol. 144, 421-437.

Smith, E.J., Little, D.G., Briody, J.N., Mcevoy, A., Smith, N.C., Eisman, J.A., and Gardiner, E.M., 2005. Transient Disturbance in Physeal Morphology Is Associated With Long-Term Effects of Nitrogen-Containing Bisphosphonates in Growing Rabbits. J. Bone Miner. Res. 20, 1731-1741.

Smith, E.J., Mcevoy, A., Little, D.G., Baldock, P.A., Eisman, J.A., and Gardiner, E.M., 2004. Transient retention of endochondral cartilaginous matrix with bisphosphonate treatment in a long-term rabbit model of distraction osteogenesis. J. Bone Miner. Res. 19, 1698-1705.

Soon, G., Quintin, A., Scalfo, F., Antille, N., Williamson, G., Offord, E., and Ginty, F., 2006. PIXImus bone densitometer and associated technical measurement issues of skeletal growth in the young rat. Calcif. Tissue Int. 78, 186-192.

St Jacques, B., Hammerschmidt, M., and McMahon, A.P., 1999. Indian hedgehog signaling regulates proliferation and differentiation of chondrocytes and is essential for bone formation. Genes Dev. 13, 2072-2086.

Stepan, J.J., Alenfeld, F., Boivin, G., Feyen, J.H., and Lakatos, P., 2003. Mechanisms of action of antiresorptive therapies of postmenopausal osteoporosis. Endocr. Regul. 37, 225-238.

Stevens, D.A. and Williams, G.R., 1999. Hormone regulation of chondrocyte differentiation and endochondral bone formation. Mol. Cell Endocrinol. 151, 195-204.

Stickens, D., Behonick, D.J., Ortega, N., Heyer, B., Hartenstein, B., Yu, Y., Fosang, A.J., Schorpp-Kistner, M., Angel, P., and Werb, Z., 2004. Altered endochondral bone development in matrix metalloproteinase 13-deficient mice. Development 131, 5883-5895.

Street, J., Bao, M., Deguzman, L., Bunting, S., Peale, F.V., Jr., Ferrara, N., Steinmetz, H., Hoeffel, J., Cleland, J.L., Daugherty, A., van Bruggen, N., Redmond, H.P., Carano, R.A., and Filvaroff, E.H., 2002. Vascular endothelial growth factor stimulates bone repair by promoting angiogenesis and bone turnover. Proc. Natl. Acad. Sci. U. S. A 99, 9656-9661.

Street, J., Winter, D., Wang, J.H., Wakai, A., McGuinness, A., and Redmond, H.P., 2000. Is human fracture hematoma inherently angiogenic? Clin. Orthop. 224-237.

Sundquist, K.T., Cecchini, M.G., and Marks, S.C., Jr., 1995. Colony-stimulating factor-1 injections improve but do not cure skeletal sclerosis in osteopetrotic (op) mice. Bone 16, 39.

Symons, A.L., 2003. Reduced growth hormone receptor immunoreactivity in osteoclasts adjacent to the erupting molar in the incisor-absent (osteopetrotic) rat. Eur. J. Oral Sci. 111, 503-509.

Tabuchi, M., Miyazawa, K., Kimura, M., Maeda, H., Kawai, T., Kameyama, Y., and Goto, S., 2005. Enhancement of crude bone morphogenetic protein-induced new bone formation and normalization of endochondral ossification by bisphosphonate treatment in osteoprotegerin-deficient mice. Calcif. Tissue Int. 77, 239-249.

Takahara, M., Naruse, T., Takagi, M., Orui, H., and Ogino, T., 2004. Matrix metalloproteinase-9 expression, tartrate-resistant acid phosphatase activity, and DNA fragmentation in vascular and cellular invasion into cartilage preceding primary endochondral ossification in long bones. J. Orthop. Res. 22, 1050-1057.

Takahashi, M., Yukata, K., Matsui, Y., Abbaspour, A., Takata, S., and Yasui, N., 2006. Bisphosphonate modulates morphological and mechanical properties in distraction osteogenesis through inhibition of bone resorption. Bone. 39, 573-581.

Tamura, M., Unno, K., Yonezawa, S., Hattori, K., Nakashima, E., Tsukada, H., Nakajima, M., and Oku, N., 2004. In vivo trafficking of endothelial progenitor cells their possible involvement in the tumor neovascularization. Life Sci. 75, 575-584.

Tarvainen, R., Olkkonen, H., Nevalainen, T., Hyvonen, P., Arnala, I., and Alhava, E., 1994. Effect of clodronate on fracture healing in denervated rats. Bone 15, 701-705.

Tatsuyama, K., Maezawa, Y., Baba, H., Imamura, Y., and Fukuda, M., 2000. Expression of various growth factors for cell proliferation and cytodifferentiation during fracture repair of bone. Eur. J. Histochem. 44, 269-278.

Teronen, O., Heikkila, P., Konttinen, Y.T., Laitinen, M., Salo, T., Hanemaaijer, R., Teronen, A., Maisi, P., and Sorsa, T., 1999. MMP inhibition and downregulation by bisphosphonates. Ann. N. Y. Acad. Sci. 878:453-65., 453-465.

Thiebaud, D., Burckhardt, P., Kriegbaum, H., Huss, H., Mulder, H., Juttmann, J.R., and Schoter, K.H., 1997. Three monthly intravenous injections of ibandronate in the treatment of postmenopausal osteoporosis. Am. J. Med. 103, 298-307.

Thomsen, J.S., Laib, A., Koller, B., Prohaska, S., Mosekilde, L., and Gowin, W., 2005. Stereological measures of trabecular bone structure: comparison of 3D micro computed tomography with 2D histological sections in human proximal tibial bone biopsies. J. Microsc. 218, 171-179.

Toro J, Tomin E, Shore B, Sull A, Morr S, Meyers E, Lane JM. 2005. PTH and Alendronate improve osteotomy healing in an osteoporotic rat model. 52nd annual Meeting of The Orthopaedic Research Society , Abstract 1810.

Turner, C.H. and Burr, D.B., 1993. Basic biomechanical measurements of bone: a tutorial. Bone. 14, 595-608.

Tuukkanen, J., Koivukangas, A., Jamsa, T., Sundquist, K., MacKay, C.A., and Marks, S.C., Jr., 2000. Mineral density and bone strength are dissociated in long bones of rat osteopetrotic mutations. J. Bone Miner. Res. 15, 1905-1911.

Ulrich-Vinther, M. and Andreassen, T.T., 2005. Osteoprotegerin Treatment Impairs Remodeling and Apparent Material Properties of Callus Tissue without Influencing Structural Fracture Strength. Calcif. Tissue Int. ..

Ulrich-Vinther, M., Schwarz, E.M., Pedersen, F.S., Soballe, K., and Andreassen, T.T., 2005. Gene therapy with human osteoprotegerin decreases callus remodeling with limited effects on biomechanical properties. Bone. 37, 751-758.

Uusitalo, H., Hiltunen, A., Soderstrom, M., Aro, H.T., and Vuorio, E., 2000. Expression of cathepsins B, H, K, L, and S and matrix metalloproteinases 9 and 13 during chondrocyte hypertrophy and endochondral ossification in mouse fracture callus. Calcif. Tissue Int. 67, 382-390.

Van Wesenbeeck, L., Odgren, P.R., MacKay, C.A., D'Angelo, M., Safadi, F.F., Popoff, S.N., Van Hul, W., and Marks, S.C., Jr., 2002. The osteopetrotic mutation toothless (tl) is a loss-of-function frameshift mutation in the rat Csf1 gene: Evidence of a crucial role for CSF-1 in osteoclastogenesis and endochondral ossification. Proc. Natl. Acad. Sci. U. S. A 99, 14303-14308.

Van Wesenbeeck, L., Odgren, P.R., MacKay, C.A., and Van Hul, W., 2004. Localization of the gene causing the osteopetrotic phenotype in the incisors absent (ia) rat on chromosome 10q32.1. J. Bone Miner. Res. 19, 183-189.

Vortkamp, A., Lee, K., Lanske, B., Segre, G.V., Kronenberg, H.M., and Tabin, C.J., 1996. Regulation of rate of cartilage differentiation by Indian hedgehog and PTH-related protein. Science 273, 613-622.

Vortkamp, A., Pathi, S., Peretti, G.M., Caruso, E.M., Zaleske, D.J., and Tabin, C.J., 1998. Recapitulation of signals regulating embryonic bone formation during postnatal growth and in fracture repair. Mech. Dev. 71, 65-76.

Vu, T.H., Shipley, J.M., Bergers, G., Berger, J.E., Helms, J.A., Hanahan, D., Shapiro, S.D., Senior, R.M., and Werb, Z., 1998. MMP-9/gelatinase B is a key regulator of growth plate angiogenesis and apoptosis of hypertrophic chondrocytes. Cell 93, 411-422.

Wallis, G.A., 1996. Bone growth: coordinating chondrocyte differentiation. Curr. Biol. 6, 1577-1580.

Wang, D., Li, W., Pechar, M., Kopeckova, P., Bromme, D., and Kopecek, J., 2004a. Cathepsin K inhibitor-polymer conjugates: potential drugs for the treatment of osteoporosis and rheumatoid arthritis. Int. J. Pharm. 277, 73-79.

Wang, K., Yamamoto, H., Chin, J.R., Werb, Z., and Vu, T.H., 2004b. EGFR-deficient mice have delayed primary endochondral ossification due to defective osteoclast recruitment. J. Biol. Chem. ..

Wang, T.M., Hsu, J.F., Jee, W.S., and Matthews, J.L., 1993. Evidence for reduced cancellous bone mass in the spontaneously hypertensive rat. Bone Miner. 20, 251-264.

Weinstein, R.S. and Manolagas, S.C., 2000. Apoptosis and osteoporosis. Am. J. Med. 108, 153-164.

Wiktor-Jedrzejczak, W., Bartocci, A., Ferrante, A.W., Jr., Ahmed-Ansari, A., Sell, K.W., Pollard, J.W., and Stanley, E.R., 1990. Total absence of colony-stimulating factor 1 in the macrophage-deficient osteopetrotic (op/op) mouse. Proc. Natl. Acad. Sci. U. S. A. 87, 4828-4832.

Winding, B., NicAmhlaoibh, R., Misander, H., Hoegh-Andersen, P., Andersen, T.L., Holst-Hansen, C., Heegaard, A.M., Foged, N.T., Brunner, N., and Delaisse, J.M., 2002. Synthetic matrix metalloproteinase inhibitors inhibit growth of established

breast cancer osteolytic lesions and prolong survival in mice. Clin. Cancer Res. 8, 1932-1939.

Wood, J., Bonjean, K., Ruetz, S., Bellahcene, A., Devy, L., Foidart, J.M., Castronovo, V., and Green, J.R., 2002. Novel antiangiogenic effects of the bisphosphonate compound zoledronic acid. J. Pharmacol. Exp. Ther. 302, 1055-1061.

Wu, C.W., Tchetina, E.V., Mwale, F., Hasty, K., Pidoux, I., Reiner, A., Chen, J., Van Wart, H.E., and Poole, A.R., 2002. Proteolysis involving matrix metalloproteinase 13 (collagenase-3) is required for chondrocyte differentiation that is associated with matrix mineralization. J. Bone Miner. Res. 17, 639-651.

Xia, L., Kilb, J., Wex, H., Li, Z., Lipyansky, A., Breuil, V., Stein, L., Palmer, J.T., Dempster, D.W., and Bromme, D., 1999. Localization of rat cathepsin K in osteoclasts and resorption pits: inhibition of bone resorption and cathepsin K-activity by peptidyl vinyl sulfones. Biol. Chem. 380, 679-687.

Yamagiwa, H., Tokunaga, K., Hayami, T., Hatano, H., Uchida, M., Endo, N., and Takahashi, H.E., 1999. Expression of metalloproteinase-13 (Collagenase-3) is induced during fracture healing in mice. Bone 25, 197-203.

Yamasaki, A., Itabashi, M., Sakai, Y., Ito, H., Ishiwari, Y., Nagatsuka, H., and Nagai, N., 2001. Expression of type I, type II, and type X collagen genes during altered endochondral ossification in the femoral epiphysis of osteosclerotic (oc/oc) mice. Calcif. Tissue Int. 68, 53-60.

Yamashita, D.S. and Dodds, R.A., 2000. Cathepsin K and the design of inhibitors of cathepsin K. Curr. Pharm. Des. 6, 1-24.

Yamazaki, H. and Sasaki, T., 2005. Effects of osteoprotegerin administration on osteoclast differentiation and trabecular bone structure in osteoprotegerin-deficient mice. J. Electron Microsc. (Tokyo). 54, 467-477.

Yang, L.C., Majeska, R.J., Laudier, D.M., Mann, R., and Schaffler, M.B., 2005. High-dose risedronate treatment partially preserves cancellous bone mass and microarchitecture during long-term disuse. Bone. 37, 287-295.

Yoshida, D., Takahashi, H., and Teramoto, A., 2004. Inhibition of glioma angiogenesis and invasion by SI-27, an anti-matrix metalloproteinase agent in a rat brain tumor model. Neurosurgery. 54, 1213-1220.

Zhou, Z., Apte, S.S., Soininen, R., Cao, R., Baaklini, G.Y., Rauser, R.W., Wang, J., Cao, Y., and Tryggvason, K., 2000. Impaired endochondral ossification and angiogenesis in mice deficient in membrane-type matrix metalloproteinase I. Proc. Natl. Acad. Sci. U. S. A 97, 4052-4057.